



## INTEGRATION OF STRATEGIES FOR REAL-TIME OPTIMIZATION AND SUPERVISORY CONTROL

Rafael Brandão Demuner

Tese de Doutorado apresentada ao Programa de Pós-graduação em Engenharia Química, COPPE, da Universidade Federal do Rio de Janeiro, como parte dos requisitos necessários à obtenção do título de Doutor em Engenharia Química.

Orientador: Argimiro Resende Secchi

Rio de Janeiro  
Dezembro de 2022

INTEGRATION OF STRATEGIES FOR REAL-TIME OPTIMIZATION AND  
SUPERVISORY CONTROL

Rafael Brandão Demuner

TESE SUBMETIDA AO CORPO DOCENTE DO INSTITUTO ALBERTO LUIZ  
COIMBRA DE PÓS-GRADUAÇÃO E PESQUISA DE ENGENHARIA DA  
UNIVERSIDADE FEDERAL DO RIO DE JANEIRO COMO PARTE DOS  
REQUISITOS NECESSÁRIOS PARA A OBTENÇÃO DO GRAU DE DOUTOR  
EM CIÊNCIAS EM ENGENHARIA QUÍMICA.

Orientador: Argimiro Resende Secchi

Aprovada por: Prof. Argimiro Resende Secchi

Prof. Príamo Albuquerque Melo Jr

Prof. Márcio André Fernandes Martins

Prof. Marcelo Farenzena

Prof. Ardson dos Santos Vianna Junior

RIO DE JANEIRO, RJ – BRASIL

DEZEMBRO DE 2022

Demuner, Rafael Brandão

Integration of Strategies for Real-Time Optimization and Supervisory Control/Rafael Brandão Demuner. – Rio de Janeiro: UFRJ/COPPE, 2022.

XXIX, 198 p.: il.; 29,7cm.

Orientador: Argimiro Resende Secchi

Tese (doutorado) – UFRJ/COPPE/Programa de Engenharia Química, 2022.

Referências Bibliográficas: p. 174 – 198.

1. Otimização em Tempo Real. 2. Controle Preditivo Baseado em Modelo. 3. Sistemas Não-Lineares. 4. Identificação On-line. I. Secchi, Argimiro Resende. II. Universidade Federal do Rio de Janeiro, COPPE, Programa de Engenharia Química. III. Título.

*Ninguém ignora tudo. Ninguém  
sabe tudo. Todos nós sabemos  
alguma coisa. Todos nós ignoramos  
alguma coisa. Por isso aprendemos  
sempre.*  
*Paulo Freire*

# Agradecimentos

Primeiramente, gostaria de agradecer ao Professor Argimiro, o qual tive o privilégio de ter sido seu orientado desde o mestrado. Agradeço por todos os ensinamentos, pela sabedoria, pela paciência, pelo incentivo e pelas oportunidades concedidas.

Aos demais professores do PEQ, aos quais contribuíram para minha formação e educação. Ao Professor Príamo, que foi meu orientador no mestrado, pelas discussões sobre modelagem de processos e pelas contribuições para minha formação. Aos funcionários do PEQ, em especial, a Vera Cruz, por sempre estar disponível em ajudar.

À minha família, Braz, Tania e Gabriela, por todo o apoio e incentivo e pela oportunidade de estudo e educação. Obrigado pelo amor e carinho, mesmo que distante.

À minha esposa, Mariele, a qual faz parte da minha vida e das conquistas. Obrigado por me incentivar a ser um profissional e pessoa melhor. Agradeço pela paciência, compreensão e apoio.

Ao Aldo, Lucilene, Verena, Poline, Lucas e Tadeu, obrigado pelo apoio e incentivo ao longo desses anos.

Aos colegas do LADES, LASAP e G-130, pela amizade, pelas discussões filosóficas e troca de conhecimento e pelas boas risadas.

Ao CNPq, CAPES e FAPERJ, que ao longo desses anos, contribuíram com o suporte financeiro para o desenvolvimento deste trabalho.

Resumo da Tese apresentada à COPPE/UFRJ como parte dos requisitos necessários para a obtenção do grau de Doutor em Ciências (D.Sc.)

## INTEGRAÇÃO DE ESTRATÉGIAS DE OTIMIZAÇÃO EM TEMPO REAL E CONTROLE SUPERVISÓRIO

Rafael Brandão Demuner

Dezembro/2022

Orientador: Argimiro Resende Secchi

Programa: Engenharia Química

Uma das dificuldades nas implementações práticas da estratégia de Otimização em Tempo Real (RTO) é a integração entre as camadas de otimização e controle, principalmente devido às diferenças entre os modelos utilizados em cada camada, o que pode resultar em objetivos inalcançáveis provenientes da camada de otimização para a camada de controle. Nesse contexto, o Controle Preditivo Econômico baseado em Modelo (EMPC) é uma estratégia em que problemas de otimização e controle são resolvidos simultaneamente. O presente trabalho apresenta uma estratégia de RTO baseado em EMPC considerando uma abordagem baseada em dados para obtenção do modelo dinâmico do processo. Para isso, é considerada a estrutura de um modelo de Hammerstein, em que a função estática não-linear é um modelo em estado estacionário da planta identificado utilizando Processos Gaussianos. O EMPC proposto considera a minimização da norma do gradiente da função objetivo econômica, sendo calculado através do modelo baseado em Processos Gaussianos. É considerada uma estratégia de estimação dinâmica de estados e parâmetros, baseado no Filtro de Kalman Estendido (EKF), para estimação de distúrbios. Essa estratégia foi aplicada ao problema benchmark do Reator de Willians-Otto e apresentou resultados superiores às abordagens clássicas de RTO e RTO Híbrida (H-RTO) em termos econômicos, além de menor tempo médio de iteração.

Abstract of Thesis presented to COPPE/UFRJ as a partial fulfillment of the requirements for the degree of Doctor of Science (D.Sc.)

## INTEGRATION OF STRATEGIES FOR REAL-TIME OPTIMIZATION AND SUPERVISORY CONTROL

Rafael Brandão Demuner

December/2022

Advisor: Argimiro Resende Secchi

Department: Chemical Engineering

One of the difficulties in the practical implementations of the Real-Time Optimization (RTO) strategy is the integration between the optimization and control layers, mainly due to the differences between the models used in each layer, which may result in unreachable setpoints coming from optimization to the control layer. In this context, Economic Model Predictive Control (EMPC) is a strategy where optimization and control problems are solved simultaneously. The present work presents an RTO framework based on an EMPC structure considering a data-driven approach to obtain the dynamic model of the process. For this, a Hammerstein model structure is considered, in which its nonlinear static function is the steady-state model of the plant identified using a Gaussian Process model. The proposed EMPC considers the minimization of the norm of the gradient of the economic objective function, being calculated through the Gaussian Process model. It is also considered a dynamic state and parameter estimation based on the Extended Kalman Filter (EKF) in order to estimate the disturbances. This strategy was applied to the Williams-Otto Reactor benchmark and presented superior results to the classic RTO and Hybrid RTO (H-RTO) in terms of economic benefit, besides a lower average iteration time.

# Contents

<b>List of Figures</b>	<b>xi</b>
<b>List of Tables</b>	<b>xviii</b>
<b>List of Symbols</b>	<b>xix</b>
<b>List of Abbreviations</b>	<b>xxviii</b>
<b>1 Introduction</b>	<b>1</b>
1.1 Motivation and Contextualization . . . . .	1
1.2 Objectives . . . . .	8
1.3 Thesis Outline . . . . .	9
<b>2 Literature Review</b>	<b>11</b>
2.1 Real-Time Optimization Problem Formulation . . . . .	11
2.1.1 RTO Formulation . . . . .	11
2.2 Real-Time Optimization Strategies . . . . .	12
2.2.1 The Two-Step Approach . . . . .	13
2.2.2 ISOPE . . . . .	17
2.2.3 Modifier Adaptation . . . . .	25
2.2.4 Optimization by Regulation . . . . .	36
2.2.5 Hybrid RTO . . . . .	43
2.3 Model Predictive Control (MPC) . . . . .	47
2.4 Strategies for Integration of RTO and Supervisory Control Layer . .	51
2.4.1 Two-stage MPC: LP-MPC and QP-MPC . . . . .	52
2.4.2 Economic Model Predictive Control (EMPC) and the One- layer Approach . . . . .	54
<b>3 Surrogate Model-Based Optimization</b>	<b>61</b>
3.1 Gaussian Process Models . . . . .	64
3.1.1 Covariance Functions . . . . .	66
3.2 Sequential Approximation Optimization Methods (SAO) . . . . .	67

3.3	Bayesian Optimization . . . . .	69
3.4	Data Generation for Surrogate Models Building . . . . .	74
<b>4</b>	<b>A Comparison of Strategies based on Gaussian Process for RTO purposes</b>	<b>79</b>
4.1	Introduction . . . . .	79
4.2	Gaussian Processes Model Structure . . . . .	82
4.3	Modifier Adaptation based on GP models and Bayesian Optimization . . . . .	83
4.4	Proposed Methodology . . . . .	85
4.5	Case Studies . . . . .	91
4.5.1	Case Study: Exothermic CSTR Reactor . . . . .	92
4.5.2	Case Study: The Willians-Otto Reactor . . . . .	93
4.5.3	Optimization Solver . . . . .	97
4.6	Results and Discussion . . . . .	97
4.6.1	Exothermic CSTR . . . . .	97
4.6.2	Williams-Otto Reactor . . . . .	106
4.7	Partial Conclusions . . . . .	115
<b>5</b>	<b>Tracking Necessary Condition of Optimality by a Data-driven solution combining Steady-State and Transient data</b>	<b>117</b>
5.1	Introduction . . . . .	117
5.2	Model Structures . . . . .	122
5.2.1	Gaussian Processes Model Structure . . . . .	122
5.2.2	Hammerstein Model Structure . . . . .	122
5.3	Proposed Methodology . . . . .	125
5.3.1	RTO and MPC integration framework . . . . .	125
5.3.2	Classic RTO Framework - RTO + QP-MPC . . . . .	134
5.4	Case Study: The Willians-Otto Reactor . . . . .	137
5.4.1	Model Equations . . . . .	137
5.4.2	Economical Optimization Problem . . . . .	137
5.4.3	Controlled and Manipulated Variables . . . . .	138
5.4.4	Model Identification . . . . .	139
5.4.5	Dynamic and Steady-State Characterization . . . . .	140
5.5	Results and Discussion . . . . .	142
5.5.1	Willians-Otto Reactor Characterization . . . . .	142
5.5.2	Nonlinear Model Identification . . . . .	147
5.5.3	RTO Strategies Applied to Willians-Otto Reactor . . . . .	155
5.5.4	Comparison of the Proposed Strategies in the Presence of Noise . . . . .	162

5.6	Partial Conclusions . . . . .	169
<b>6</b>	<b>Conclusion</b>	<b>171</b>
6.1	Future Research . . . . .	173
	<b>References</b>	<b>174</b>

# List of Figures

1.1	Hierarchical control structure (adapted from MENDOZA <i>et al.</i> (2016)). . . . .	2
2.1	Graphical interpretation of the modifiers applied to a given constraint function. The real constraint function is given by $G_p(u) = -3u^2 + 4u + 1$ and the model constraint function is given by $G(u) = -1.7u^2 + 2.6u + 0.1$ . At $u = 0.5$ , applying the modifier adaptation approach, the modified constraint function is given by $G_{mod} = -1.7u^2 + 2.7u + 1.325$ . Therefore, at $u = 0.5$ , $G_p(0.5) = G_{mod}(0.5) = 2.25$ , and $\nabla G_p(0.5) = \nabla G_{mod}(0.5) = 1$ . . . . .	26
2.2	NCO tracking structure. Adapted from JÄSCHKE and SKOGESTAD (2011). . . . .	40
2.3	Comparison of (a) Classic RTO, (b) D-RTO and (c) H-RTO structures. Adapted from KRISHNAMOORTHY <i>et al.</i> (2018). . . . .	44
3.1	First five iterations of Bayesian Optimization applied to the function $\phi_{ec} = -\sin(3u) - u^2 - 0.7u$ inside the domain $-1 \leq u \leq 2$ . The function maximum occurs at $u^* = -0.3593$ and $\phi_{ec}(u^*) = 0.50$ . . . . .	73
3.2	Latin Hypercube Sampling applied to the two-dimensional domain ( $n = 2$ ) with $m = 4$ sampling points. . . . .	75
3.3	Latin Hypercube Sampling Technique applied to a three-dimension ( $n = 3$ ) with $m = 10$ sampling points. . . . .	76
4.1	Summary of Modeling strategies and comparison to be studied in this work. . . . .	89
4.2	Willians-Otto Reactor. . . . .	94

4.3	Economic objective function at RTO last iteration for 20 noise realization and for each acquisition function (PI, EI and LCB) using: (a) Strategy 1 (objective function and constraints modeling via GP), (b) Strategy 2 (measured variables ( $y$ ) modeling via GP), (c) Strategy 3 (MA-GP), and (d) Strategy 4 (MAy-GP). Black diamonds represent the average of 20 realizations. Green triangle represents the plant optimum. . . . .	98
4.4	Relative average deviation from the plant optimum of the economic objective function values at RTO last iteration for 20 noise realization and for each acquisition function (PI, EI and LCB) using: (a) Strategy 1 (objective function and constraints modeling via GP), (b) Strategy 2 (measured variables ( $y$ ) modeling via GP), (c) Strategy 3 (MA-GP), and (d) Strategy 4 (MAy-GP). Black diamonds represent the average of 20 realizations. . . . .	99
4.5	Relative average deviation from the plant optimum of the decision variables at RTO last iteration for 20 noise realization and for each acquisition function (PI, EI and LCB) using: (a) Strategy 1 (objective function and constraints modeling via GP), (b) Strategy 2 (measured variables ( $y$ ) modeling via GP), (c) Strategy 3 (MA-GP), and (d) Strategy 4 (MAy-GP). Black diamonds represent the average of 20 realizations. . . . .	100
4.6	RTO iterations using Strategy 1 (objective function and constraints modeling via GP) and comparing different acquisition functions: (a) <i>PI</i> , (b) <i>EI</i> and (c) <i>LCB</i> . (d) The cost evolution for acquisition functions <i>PI</i> , <i>EI</i> , <i>LCB</i> during the 20 iterations. Red dots represent the initial GP training points. Green triangles represent the last iterate of each RTO run. The blue continuous line represents the objective function and input variable relationship and the pink star represents plant optimum. . . . .	101
4.7	RTO iterations using the GP models for Strategy 2 (measured variables ( $y$ ) modeling via GP) and comparing different acquisition functions: (a) <i>PI</i> , (b) <i>EI</i> and (c) <i>LCB</i> . (d) The cost evolution for acquisition functions <i>PI</i> , <i>EI</i> , <i>LCB</i> during the 20 iterations. Red dots represent the initial GP training points. Green triangles represent the last iterate of each RTO run. The blue continuous line represents the objective function and input variable relationship and the pink star represents plant optimum. . . . .	102

4.8	RTO iterations using the GP models for Strategy 3 (MA-GP) and comparing different acquisition functions: (a) <i>PI</i> , (b) <i>EI</i> and (c) <i>LCB</i> . (d) The cost evolution for acquisition functions <i>PI</i> , <i>EI</i> , <i>LCB</i> during the 20 iterations. Red dots represent the initial GP training points. Green triangles represent the last iterate of each RTO run. The blue continuous line represents the objective function and input variable relationship and the pink star represents plant optimum.	103
4.9	RTO iterations using Strategy 4 (MAy-GP) and comparing different acquisition functions: (a) <i>PI</i> , (b) <i>EI</i> and (c) <i>LCB</i> . (d) The cost evolution for acquisition functions <i>PI</i> , <i>EI</i> , <i>LCB</i> during the 20 iterations. Red dots represent the initial GP training points. Green triangles represent the last iterate of each RTO run. The blue continuous line represents the objective function and input variable relationship and the pink star represents plant optimum. . . . .	104
4.10	Average Iteration Time for each acquisition function ( <i>PI</i> , <i>EI</i> and <i>LCB</i> ) using: (a) Strategy 1 (objective function and constraints modeling via GP), (b) Strategy 2 (measured variables ( $\mathbf{y}$ ) modeling via GP), (c) Strategy 3 (MA-GP), and (d) Strategy 4 (MAy-GP). Black diamonds represent the average of the 20 RTO iterations considering 20 realizations. . . . .	105
4.11	Economic objective function at RTO last iteration for 20 noise realization and for each acquisition function ( <i>PI</i> , <i>EI</i> , <i>LCB</i> ) using: (a) Strategy 1 (objective function and constraints modeling via GP), (b) Strategy 2 (measured variables ( $\mathbf{y}$ ) modeling via GP), (c) Strategy 3 (MA-GP), and (d) Strategy 4 (MAy-GP). Black diamonds represent the average of 20 realizations. Green triangle represents the plant optimum. . . . .	107
4.12	Relative average deviation from the plant optimum of the economic objective function values at RTO last iteration for 20 noise realization and for each acquisition function ( <i>PI</i> , <i>EI</i> and <i>LCB</i> ) using: (a) Strategy 1 (objective function and constraints modeling via GP), (b) Strategy 2 (measured variables ( $\mathbf{y}$ ) modeling via GP), (c) Strategy 3 (MA-GP), and (d) Strategy 4 (MAy-GP). Black diamonds represent the average of 20 realizations. . . . .	108

4.13	Relative average deviation from the plant optimum of the decision variables at RTO last iteration for 20 noise realization and for each acquisition function (PI, EI and LCB) using: (a) Strategy 1 (objective function and constraints modeling via GP), (b) Strategy 2 (measured variables ( $y$ ) modeling via GP), (c) Strategy 3 (MA-GP), and (d) Strategy 4 (MAy-GP). Black diamonds represent the average of 20 realizations. . . . .	109
4.14	RTO iterations using Strategy 1 (objective function and constraints modeling via GP) and comparing different acquisition functions: (a) PI, (b) EI and (c) LCB. (d) The cost evolution for acquisition functions PI, EI, LCB during the 20 iterations. Red dots represent the initial GP training points. Green triangles represent the last iterate of each RTO run. Black continuous lines represents the constraint limits and the pink star represents plant optimum. . . . .	110
4.15	RTO iterations using Strategy 2 (measured variables ( $y$ ) modeling via GP) and comparing different acquisition functions: (a) PI, (b) EI and (c) LCB. (d) The cost evolution for acquisition functions PI, EI, LCB during the 20 iterations. Red dots represent the initial GP training points. Green triangles represent the last iterate of each RTO run. Black continuous lines represent the constraint limits and the pink star represents plant optimum. . . . .	111
4.16	RTO iterations using Strategy 3 (MA-GP) and comparing different acquisition functions: (a) PI, (b) EI and (c) LCB. (d) The cost evolution for acquisition functions PI, EI, LCB during the 20 iterations. Red dots represent the initial GP training points. Green triangles represent the last iterate of each RTO run. Black continuous lines represent the constraint limits and the pink star represents plant optimum. . . . .	112
4.17	RTO iterations using Strategy 4 (MAy-GP) and comparing different acquisition functions: (a) PI, (b) EI and (c) LCB. (d) The cost evolution for acquisition functions PI, EI, LCB during the 20 iterations. Red dots represent the initial GP training points. Green triangles represent the last iterate of each RTO run. Black continuous lines represent the constraint limits and the pink star represents plant optimum. . . . .	113

4.18	Average Iteration Time for each acquisition function (PI, EI and LCB) using: (a) Strategy 1 (objective function and constraints modeling via GP), (b) Strategy 2 (measured variables ( $y$ ) modeling via GP), (c) Strategy 3 (MA-GP), and (d) Strategy 4 (MAy-GP). Black diamonds represent the average of the 20 RTO iterations considering 20 realizations. . . . .	114
5.1	Schematic representation of the Hammerstein model. The input $u(t)$ is transformed by the nonlinear function $NL(\cdot)$ , which has as output the variable $v(t)$ . This variable is applied as input for the linear dynamic operator $L(\cdot)$ , yielding the output variable $y(t)$ . . .	123
5.2	Schematic representation of the Wiener model. The input $u(t)$ is transformed by a linear operator $L(\cdot)$ , yielding an intermediate response $v(t)$ . This variable is then transformed by a nonlinear transformation $NL_1(\cdot)$ , yielding the model output response $y(t)$ . . . . .	123
5.3	Schematic representation of the Hammerstein-Wiener model. The input $u(t)$ is transformed by a nonlinear function $NL_1(\cdot)$ , yielding as output the variable $v(t)$ . This signal is then transformed by a linear operator $L(\cdot)$ , yielding a new intermediate response $w(t)$ . This signal is finally transformed by a nonlinear function $NL_2(\cdot)$ , which yield the model output $y(t)$ . . . . .	123
5.4	Schematic representation of the MISO Hammerstein model structure proposed by BILLINGS (1980). . . . .	124
5.5	Schematic representation of the Hammerstein model proposed by KORTMANN and UNBEHAUEN (1987). . . . .	124
5.6	Schematic representation of Hammerstein model proposed by ES-KINAT <i>et al.</i> (1991). . . . .	125
5.7	Comparative of the proposed frameworks. . . . .	127
5.8	Proposed structure of Hammerstein nonlinear model (Structure 2). . . . .	129
5.9	Classic RTO framework in two layers considering an intermediate QP-MPC. . . . .	135
5.10	Steady-state gain of $w_A$ . . . . .	143
5.11	Steady-state gain of $w_B$ . . . . .	143
5.12	Steady-state gain of $w_C$ . . . . .	144
5.13	Steady-Gain of $w_E$ . . . . .	144
5.14	Steady-state gain of $w_P$ . . . . .	145
5.15	Steady-state gain of $w_G$ . . . . .	145
5.16	Steady-state Gain of $w_P$ - filled region represents the positive gain region. . . . .	146

5.17	Dominant time constant of the system. . . . .	146
5.18	$w_A$ predicted and actual values in three scenarios of measured disturbance ( $F_A$ ): (a) Basis case, (b) +10% and (c)-10%. . . . .	149
5.19	$w_B$ predicted and actual values in three scenarios of measured disturbance ( $F_A$ ): (a) Basis case, (b) +10% and (c)-10%. . . . .	149
5.20	$w_C$ predicted and actual values in three scenarios of measured disturbance ( $F_A$ ): (a) Basis case, (b) +10% and (c)-10%. . . . .	150
5.21	$w_E$ predicted and actual values in three scenarios of measured disturbance ( $F_A$ ): (a) Base case, (b) +10% and (c)-10%. . . . .	150
5.22	$w_P$ predicted and actual values in three scenarios of measured disturbance ( $F_A$ ): (a) Base case, (b) +10%, (c)-10% and (d) the maximum value of $w_P$ as a function of $F_A$ . . . . .	151
5.23	$w_G$ predicted and actual values in three scenarios of measured disturbance ( $F_A$ ): (a) Basis case, (b) +10% and (c)-10%. . . . .	151
5.24	Nonlinear model prediction in deviation variables $w_A, w_B, w_C, w_E, w_P$ and $w_G$ using Hammerstein Model - Structure 1 with the training data set. . . . .	153
5.25	Nonlinear model prediction in deviation variable of $w_E$ and $w_P$ using Hammerstein Model - Structure 2 with the training data set. . . . .	154
5.26	Nonlinear model prediction in deviation variable of $w_E$ and $w_P$ using Hammerstein Model - Structure 2 with the validation data set. . . . .	155
5.27	Closed-loop dynamic trajectories of controlled variables in using different RTO strategies: (a), (c), (e), (g), (i), (k) $w_E$ and (b), (d), (f), (h), (j), (l) $w_P$ . . . . .	157
5.28	Closed-loop dynamic trajectories of manipulated variables: (a), (c), (e), (g), (i), (k) $F_B$ and (b), (d), (f), (h), (j), (l) $T_R$ . . . . .	158
5.29	Closed-loop dynamic trajectories of disturbance estimation. . . . .	159
5.30	Closed-loop dynamic trajectory of economic objective function and the accumulated loss function: (a), (c), (e), (g), (i), (k) Objective function $\phi_{eco}$ and (b), (d), (f), (h), (j), (l) Accumulated Loss Function (\$). . . . .	160
5.31	Closed-loop dynamic trajectory of economic output variables in the presence of 1% measurement noise: (a), (c), (e), (g) $w_E$ and (b), (d), (f), (h) $w_P$ . Dots represent the measurements with noise, solid lines represent the estimated output variables by EKF, dotted lines represent the calculated optimal setpoints of output variables and dashed lines represent the plant optimum value. . . . .	163

5.32	Closed-loop dynamic trajectories of manipulated variables in the presence of 1% measurement noise: (a), (c), (e), (g) $F_B$ and (b), (d), (f), (h) $T_R$ . Solid lines represent the optimal output variables determined by the RTO strategies and dashed lines represent the plant optimum value. . . . .	163
5.33	Closed-loop dynamic trajectories of disturbance estimation in the presence of 1% measurement noise. Solid lines represent disturbance estimated by EKF and dashed lines represent the disturbance plant value. . . . .	164
5.34	Closed-loop dynamic trajectory of output variables in the presence of 5% measurement noise: (a), (c), (e), (g) $w_E$ and (b), (d), (f), (h) $w_P$ . Dots represent the measurements with noise, solid lines represent the estimated output variables by EKF, dotted lines represent the calculated optimal setpoints of output variables and dashed lines represent the plant optimum value. . . . .	165
5.35	Closed-loop dynamic trajectories of manipulated variables in the presence of 5% measurement noise: (a), (c), (e), (g) $F_B$ and (b), (d), (f), (h) $T_R$ . Solid lines represent the optimal output variables determined by the RTO strategies and dashed lines represent the plant optimum value. . . . .	166
5.36	Closed-loop dynamic trajectories of disturbance estimation in the presence of 5% measurement noise. Solid lines represent the disturbance estimated by EKF and dashed lines represent the plant value. . . . .	167
5.37	Closed-loop dynamic trajectory of economic objective function and the accumulated loss function in the presence of 1% measurement noise: (a), (c), (e), (g) Objective function $\phi_{eco}$ (\$/s) and (b), (d), (f), (h) Accumulated Loss Function (\$). Dots represent the measured values, solid lines represent the calculated value using estimated quantity by EKF, and dashed lines represents the plant optimum value. . . . .	168
5.38	Closed-loop dynamic trajectory of economic objective function and the accumulated loss function in the presence of 5% measurement noise: (a), (c), (e), (g) Objective function $\phi_{eco}$ and (b), (d), (f), (h) Accumulated Loss Function (\$). Dots represent the measured values, solid lines represent the calculated value using estimated quantity by EKF, and dashed lines represents the plant optimum value. . . .	169

# List of Tables

1.1	Main disturbances and its frequencies (Adapted from BAILEY <i>et al.</i> (1993)) . . . . .	3
4.1	Exothermic CSTR model parameters. . . . .	92
4.2	CSTR Exothermic Reactor initial training points . . . . .	93
4.3	Williams-Otto Reactor Parameters (MARCHETTI, 2009). . . . .	95
4.4	Williams-Otto Reactor initial points. . . . .	96
4.5	RMSE of the objective function predictions in the strategies evaluated. . . . .	99
4.6	Average iteration time obtained in each strategy. . . . .	106
4.7	RMSE of the objective function predictions in the strategies evaluated. . . . .	109
4.8	Average iteration time obtained in each strategy. . . . .	115
5.1	Economic optimal problem solution. . . . .	138
5.2	Mean Squared Error (MSE) of GP model for each reactor outlet mass fraction at steady state. . . . .	147
5.3	Mean Squared Error (MSE) of linear model for each reactor outlet mass fraction in relation to a perturbation in $F_B$ , $T_R$ and disturbance $F_A$ . . . . .	152
5.4	Disturbance values of $F_A$ and steady-state optimal solution for the economical problem. . . . .	156
5.5	Accumulated loss function at the end of simulation. . . . .	161
5.6	Computational cost of each RTO strategy. . . . .	161
5.7	Accumulated loss function at the end of simulation considering noisy measurements. . . . .	168

# List of Symbols

$AccLoss$	Accumulated Loss [-], p. 159
$D$	Set of sampling points [-], p. 77
$E$	Expected value operator [-], p. 64
$E_{a,j}$	Energy of activation of the $j$ -th reaction [-], p. 95
$F_A$	Mass flowrate of $A$ [kg/s], p. 94
$F_B$	Mass flowrate of $B$ [kg/s], p. 94
$G$	Constraints vector of the model [-], p. 12
$GP$	Gaussian Process [-], p. 33
$G_p$	Constraints vector of the plant [-], p. 11
$Loss$	Economic Loss [-], p. 36
$M$	Control horizon of MPC [-], p. 49
$MSE$	Mean Squared Error [-], p. 140
$M_i$	Molar mass of the $i$ -th species [-], p. 94
$P$	Prediction horizon of MPC [-], p. 49
$RMSE$	Root Mean Squared Error [-], p. 91
$T_R$	Reactor temperature [°], p. 94
$W$	Reactor holdup [-], p. 94
$W_{\nabla\phi_{ec}}$	Weighting factor related to the norm of the gradient of this economic objective function [-], p. 134
$W_{\phi_{NMPC}}$	Weighting factor related to the classical NMPC objective function [-], p. 134

$W_{\phi_{ec}}^{(P)}$	Weighting factor related to the final value of the economic objective function [–], p. 134
$W_{\phi_{ec}}$	Weighting factor related to the objective function of the economic optimization problem [–], p. 134
$\Delta_k$	Trust region radius [–], p. 35
$\mathcal{F}$	Regression function [–], p. 65
$\Omega$	Input variables domain [–], p. 123
$\Phi$	Economical performance index calculated using plant model data [–], p. 12
$\Phi_p$	Economical performance index of the plant [–], p. 11
$\bar{\mathbf{a}}$	Hammerstein model extended vector of parameters [–], p. 130
$\bar{\mathbf{a}}_{dyn}$	Hammerstein model linear operator extended vector of parameters [–], p. 130
$\bar{\mathbf{a}}_{ss}$	Gaussian Process extended vector of parameters [–], p. 130
$\cdot^+$	<i>a posteriori</i> information [–], p. 131
$\cdot^-$	<i>a priori</i> information [–], p. 131
$\delta$	Tolerance [–], p. 24
$A$	Linearized system matrix [–], p. 141
$B_d$	Linearized system matrix [–], p. 141
$B$	Gaussian Process prior covariance matrix of the regression parameters [–], p. 65
$B$	Linearized system matrix [–], p. 141
$C$	Linearized system matrix [–], p. 141
$C$	Vector of constraints functions, constraints gradients and objective function gradient [–], p. 26
$D_d$	Linearized system matrix [–], p. 141
$D$	Linearized system matrix [–], p. 141

$F$	Sensitivity matrix [–], p. 38
$G_{mod}$	Modified constraints [–], p. 23, 25
$H_{xy}$	Second-order derivative matrix in relation to $x$ and $y$ [–], p. 19
$H_{SO}$	Selection matrix [–], p. 38
$I$	Identity matrix [–], p. 27
$I$	Identity matrix [–], p. 142
$K_d$	Linearized system gain matrix [–], p. 141
$K_u$	Linearized system gain matrix [–], p. 141
$K$	Kalman Filter gain matrix [–], p. 131
$K$	Matrix of gains [–], p. 27
$K_{LMPC}$	Static-gain obtained from LMPC dynamic model [–], p. 135
$M_f$	Gaussian Process posterior mean function [–], p. 65
$Psi$	Gaussian Process hyperparameters [–], p. 82
$P$	Measured covariance matrix in Kalman Filter [–], p. 131
$Q$	Upper bounding matrix [–], p. 32
$Q$	covariance matrix of variable $\cdot$ [–], p. 131
$S_f$	Gaussian Process posterior covariance function matrix [–], p. 65
$S_{f,zm}$	Gaussian Process posterior covariance function matrix for zero mean regression function [–], p. 65
$S_k$	Matrix of differences of input variables [–], p. 24
$U^*$	Test data set [–], p. 65
$U$	Training data set [–], p. 65
$W_u$	Weight Matrix of MPC [–], p. 48
$W_y$	Weight Matrix of MPC [–], p. 48
$W_{\Delta u}$	Weight Matrix of MPC [–], p. 48

$W_u$	Positive semi-definite diagonal matrix of manipulated variables weighting factors [–], p. 133
$W_y$	Positive semi-definite diagonal matrix of controlled variables weighting factors [–], p. 133
$W_{\Delta u}$	Positive semi-definite diagonal matrix of manipulated variables movement suppression factors [–], p. 133
$\Delta \mathbf{u}_{k+1}$	Decision variable increment defined as the differences of input variables at each iteration [–], p. 32
$\Delta$	Search region limit [–], p. 24
$\Lambda$	Modifiers vector [–], p. 26
$\Phi_{mod}$	Modified objective function [–], p. 26
$\Theta^{(0)}$	Measured variables training set [–], p. 70
$\alpha$	Model parameters vector [–], p. 12
$\alpha_{dyn}$	Hammerstein model dynamic linear operator parameters [–], p. 128
$\beta$	Gaussian Process prior regression parameters [–], p. 65
$\eta$	Lagrange multiplier [–], p. 19
$\hat{z}$	Augmented state vector [–], p. 131
$\lambda^G$	First-order modifiers vector of constraints [–], p. 25
$\lambda^\Phi$	First-Order modifier of objective function [–], p. 26
$\lambda$	Eigenvalues vector [–], p. 142
$\lambda$	Lagrange multiplier or modifier [–], p. 19
$\lambda_k$	Lagrange multipliers or modifiers [–], p. 22
$\mathcal{C}$	Kalman Filter observability vector [–], p. 131
$\mathcal{U}^{(0)}$	Input variables training set [–], p. 70
$\mu$	Lagrange multiplier [–], p. 19
$\sigma$	Additional vector of optimization problem [–], p. 18

$\theta$	Dynamic Model Parameters [–], p. 48
$\varepsilon^G$	Zero-order modifiers vector of constraints [–], p. 25
$\omega$	Weight vector [–], p. 78
$\zeta$	first-order approximation of the economic objective function gradient [–], p. 57
$a_k$	Differences of plant measurement and model predicted value [–], p. 23
$c_u$	weights related to the $u$ variables in the economic optimization objective function [–], p. 53
$c_y$	weights related to the $y$ variables in the economic optimization objective function [–], p. 53
$c$	Controlled variable vector [–], p. 38
$e_j$	Unit vector in the direction $j$ [–], p. 29
$f_{MPC}$	MPC Process Model [–], p. 48
$f_{ss}$	Mathematical model of the process [–], p. 12
$f_{EMPC}$	EMPC process model [–], p. 55
$f_{OL}$	Process model of the one-layer approach [–], p. 55
$n_k$	Vector normal to the hyperplane [–], p. 31
$u_p^*$	Plant optimum [–], p. 15
$u_{LP-PC}$	Manipulated variables setpoints in LP-MPC [–], p. 53
$u_{QP-PC}$	Manipulated variables setpoints in QP-MPC [–], p. 53
$u$	RTO decision variables [–], p. 11
$u_{LB}$	Decision variable Lower bound [–], p. 68
$u_{SP}$	model-based optimization optimal solution [–], p. 12
$u_{SP}^*$	plant true optimal solution [–], p. 11
$u_{UB}$	Decision variable Upper bound [–], p. 68
$u_{cand}$	Candidate Solution [–], p. 70

$\mathbf{u}_{inac}$	Decision variables which are inactive [–], p. 41
$\mathbf{u}_{k+1}^{neg}$	Optimization solution in one half subspace [–], p. 31
$\mathbf{u}_{k+1}^{pos}$	Optimization solution in one half subspace [–], p. 31
$\mathbf{u}_{max}$	Decision or input variable upper bound [–], p. 23
$\mathbf{u}_{min}$	Decision or input variable lower bound [–], p. 23
$\mathbf{u}_{ref}$	Reference value of variable $\mathbf{u}$ [–], p. 135
$\mathbf{u}_s$	Steady-state solution in one-layer approach [–], p. 55
$\mathbf{v}$	Additional vector of optimization problem [–], p. 18
$\mathbf{y}_p$	Plant measured or output variables [–], p. 11
$\mathbf{y}_{LP-PC}$	Output variables setpoints in LP-MPC [–], p. 53
$\mathbf{y}_{QP-PC}$	Output variables setpoints in QP-MPC [–], p. 53
$\mathbf{y}_{ref}$	Reference value of variable $\mathbf{y}$ [–], p. 135
$\nabla_x f$	Gradient of the function $f$ with respect to $\mathbf{x}$ [–], p. 15
$\nabla_r f$	Reduced gradient of the function $f$ with respect to $\mathbf{x}$ [–], p. 15
$\nabla_x^2 f$	Hessian of the function $f$ with respect to $\mathbf{x}$ [–], p. 15
$\nabla_r^2 f$	Reduced gradient of the function $f$ with respect to $\mathbf{x}$ [–], p. 15
$\epsilon$	Arbitrary positive scalar [–], p. 32
$\eta_1$	Trust-region metrics threshold value [–], p. 69
$\eta_2$	Trust-region metrics threshold value [–], p. 69
$\gamma_{inc}$	Trust-region radius increase factor [–], p. 69
$\gamma_{red}$	Trust-region radius reduction factor [–], p. 69
$\hat{\mathbf{g}}$	Constaints function approximation [–], p. 68
$\hat{\mathcal{L}}$	Approximated problem Lagrangian function [–], p. 68
$\hat{\phi}_{ec}$	Objective function approximation [–], p. 68

$\kappa$	Condition Number [–], p. 24
$t_{min}$	Shortest distance between complement affine subspaces [–], p. 30
$\mathcal{AF}$	Acquisition Function [–], p. 70
$\mathcal{AF}_{EIC}$	Constrained Expected Improvement acquisition function [–], p. 72
$\mathcal{AF}_{EI}$	Expected Improvement acquisition function [–], p. 71
$\mathcal{AF}_{LCB}$	Lower confidence bound acquisition function [–], p. 72
$\mathcal{AF}_{PIC}$	Constrained Probability of Improvement acquisition function [–], p. 74
$\mathcal{AF}_{PI}$	Probability of Improvement acquisition function [–], p. 71
$\mathcal{A}_\epsilon$	Set of active constraints [–], p. 32
$\mathcal{G}$	Gain in Bayesian Optimization [–], p. 70
$\mathcal{L}$	Lagrangian function [–], p. 19, 68
$\mu(\mathbf{u})$	Mean function in Gaussian Process [–], p. 64
$\phi_c$	Controller objective function general expression [–], p. 134
$\phi_{EMPC}$	EMPC objective function [–], p. 55
$\phi_{LP-PC}$	Objective function of LP-MPC [–], p. 53
$\phi_{OL}$	Objective function of one-layer approach [–], p. 55
$\phi_{OL}$	One-layer economic objective function [–], p. 57
$\phi_{QP-MPC}$	QP-MPC Controller objective function [–], p. 135
$\phi_{QP-PC}$	Objective function of QP-MPC [–], p. 53
$\phi_{ec}$	Economical performance index [–], p. 11
$\phi_{id}$	Objective Function of the Identification Problem [–], p. 14
$\psi$	Distance Metric [–], p. 76
$\psi$	Distance metric [–], p. 78
$\psi_{max}$	Maximum Distance [–], p. 78

$\psi_{max}$	Maximum distance metric [–], p. 77
$\rho_{\phi,k}$	Trust-region actual change in objective function [–], p. 68
$\rho_{g_i,k}$	Trust-region actual change in constraints functions [–], p. 68
$\rho_k$	Trust-region update metric [–], p. 68
$\sigma$	Singular value of a matrix [–], p. 24
$\sigma(\cdot)$	standard deviation operator [–], p. 35
$\sigma_{f,zm}^2$	Gaussian Process posterior covariance function for zero mean regression function [–], p. 65
$\sigma_f^2$	Gaussian Process posterior covariance function [–], p. 65
$\sigma_{max}$	Upper bound on spectral radial of Hessian matrix [–], p. 30
$\sigma_{noise}$	Measurement noise [–], p. 30
$\tau_j$	Time constant of the dynamic system in relation to the $j$ -th eigenvalue [–], p. 142
$\epsilon_{UB}$	Upper bound of the gradient error norm [–], p. 30
$a$	Transfer function denominator coefficients [–], p. 130
$b$	Transfer function numerator coefficients [–], p. 130
$c_u$	weights related to the $u$ variables in the economic optimization objective function [–], p. 53
$c_y$	weights related to the $y$ variables in the economic optimization objective function [–], p. 53
$h$	Amplitude of the perturbation [–], p. 29
$k(\mathbf{u}, \mathbf{u}')$	Covariance function in Gaussian Process [–], p. 64
$k_j$	Specific reaction rate of the $j$ -th reaction [–], p. 95
$k_M$	Matérn covariance function matrix [–], p. 67
$k_P$	Polynomial covariance function matrix [–], p. 66
$k_{SE}$	Squared exponential covariance function matrix [–], p. 67
$k_{const}$	Constant covariance function matrix [–], p. 66

$k_{j,0}$	Specific reaction rate of the $j$ -th reaction at reference temperature [-], p. 95
$k_{linear}$	Linear covariance function matrix [-], p. 66
$n_{\alpha}$	Parameters vector dimension [-], p. 16
$n_g$	Dimension of constraints vector [-], p. 11
$n_p$	Number of poles in transfer function [-], p. 130
$n_u$	Dimension of decision variables vector [-], p. 11
$n_y$	Dimension of output variables vector [-], p. 11
$n_z$	Number of zeros in transfer function [-], p. 130
$n_{\alpha,dyn}$	Hammerstein model dynamic linear operator parameter vector dimension [-], p. 128
$r$	Packing radius [-], p. 78
$r_j$	Reaction rate [-], p. 94
$v$	Hammerstein model intermediate variable [-], p. 128
$w_i$	Mass fraction of $i$ -th species [-], p. 94
$y_j^{ss}$	Steady-state model of variable $y_j$ [-], p. 130
$z$	$z$ operator [-], p. 130

# List of Abbreviations

<i>MSE</i>	Mean Squared Error, p. 140
<i>RMSE</i>	Root Mean Squared Error [–], p. 91
ARMAX	Autoregressive model with moving average and exogenous variables, p. 51
ARX	Autoregressive model with exogenous variables, p. 51
AsROPA	Asynchronous Real-time Optimization with Persistent Parameter Adaptation, p. 46
CSTR	Continuous stirred tank reactor, p. 94
D-RTO	Dynamic Real-Time Optimization, p. 5
EKF	Extended Kalman Filter, p. 43, 126
EMPC	Economic Model Predictive Control, p. 7, 54
FIR	Finite Impulse Response, p. 51
GP	Gaussian Process, p. 4
H-RTO	Hybrid Real-Time Optimization, p. 6, 43, 127
ISOPE	Integrated System Optimization and Parameter Estimation, p. 4, 18
KKT	Karush-Kuhn-Tucker, p. 15
LHD	Latin Hypercube Design, p. 75
LHS	Latin Hypercube Sampling, p. 75
LMPC	Linear Model Predictive Control, p. 135
LP-MPC	Linear Programming based Model Predictive Control, p. 6

LP	Linear Programming, p. 53
MA	Modifier-Adaptation, p. 4
MIMO	Multiple-Input Multiple-Output, p. 3
MPC	Model Predictive Control, p. 3
NCO	Necessary Condition of Optimality, p. 4
NMPC	Nonlinear Model Predictive Control, p. 7
QDMC	Quadratic Dynamic Matrix Control, p. 135
QP-MPC	Quadratic Programming based Model Predictive Control, p. 6
QP	Quadratic Programming, p. 50, 53
ROPA	Real-time Optimization with Persistent Parameter Adaptation, p. 45
RTO	Real Time Optimization, p. 3
SAO	Sequential Approximation Optimization, p. 64
SOC	Self Optimizing Control, p. 5
SQP	Sequential Quadratic Programming, p. 50
SSD	Steady-State Detection, p. 13

# Chapter 1

## Introduction

### 1.1 Motivation and Contextualization

Industrial process plants are characterized by several unit operations aiming to convert raw materials into products. In the current fierce economic competitiveness, chemical processes have become increasingly integrated, showing more significant interactions and dependence among the process variables, justified by an increase in energy efficiency and an intensification of mass and heat transfer phenomena (YUAN *et al.*, 2012). Consequently, this increase in process complexity also challenges defining the control and optimization structures.

One of the challenges in designing control and optimization structures is how to guarantee at the same time a safe operation, meeting process constraints and product specifications, as well as ensuring that the operation is as profitable as possible. Additionally, the dynamic characteristics, such as fluctuations in raw material and product costs, the different specifications and grades of the products, and unmeasured and unexpected disturbances, impose robustness requirements for the designed solutions (ARKUN and STEPHANOPOULOS, 1980).

In modern process plants, the control structure is typically hierarchical, where each level has a specific function in this structure and operates at different frequencies. Decision-making actions interconnect the structure layers. The output action of a higher-level layer is a setpoint or reference for a lower-level layer to execute an action. The lower-level layers' feedback to a higher-level layer is also essential to continue the cycle. Figure 1.1 illustrates the hierarchy between layers in a conventional control structure.

The time scale of each layer is related to its objective. The upper layers are related to management and business strategy activities, while the lower layers are related to the operational activities of an industrial plant. In general, the upper layers (strategic decisions) occur in the long term, while the lower layers (opera-

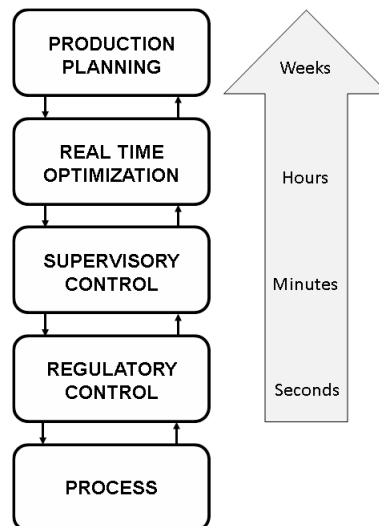


Figure 1.1: Hierarchical control structure (adapted from MENDOZA *et al.* (2016)).

tional decisions) occur in the medium and short term.

At the upper levels, the production planning layer is related to the economic objectives of the plant regarding the evaluation and allocation of materials, production rates, product grades, and sales. This layer can also be disturbed by fluctuations in the market, demand, and prices (MARCHETTI, 2009).

At the lowest level, the regulatory control layer is responsible for executing the cycles of the PID controllers, following the setpoints given by the immediately above control layer, the supervisory control (ELLIS *et al.*, 2014). The regulatory control layer is responsible for maintaining the stability of the plant by controlling the variables involving, for example, flow rates in the pipes, gas pressure, temperatures, and reservoir levels, which suffer high-frequency disturbances in the shortest time scale of the control structure.

In the supervisory control layer, advanced control algorithms are applied, such as model-based predictive control (MPC). MPC is an optimization-based and multivariate control strategy well suited for leading with constraints, being a well-accepted strategy for industrial applications (ELLIS *et al.*, 2014). Indeed, one of the main reasons for the MPC's success in the industry is dealing with input variables coupling in multiple-input multiple-output (MIMO) systems.

Regarding the MPC optimization problem, its objective function is typically defined considering three main contributions. The first one represents the deviation of the controlled variables from their setpoints. A second term represents the magnitude of the control action, mainly used to avoid aggressive control policies. Finally, a third contribution can be considered in the formulation, which describes the difference between the manipulated variables to a reference trajectory or a target value.

The controlled variables' setpoints and the manipulated variables' reference values could be determined by an upper layer named Real-Time Optimization (RTO). This layer represents a centralization of information from higher levels, which are strategic. Thus, the optimization level consolidates this strategic information and sends decisions to lower levels associated with operational questions. This layer aims to maximize some performance index oriented to operational profit, satisfying process constraints, such as operational, safety, and environmental limits (NAYSMITH and DOUGLAS, 1995). For this, one of the ways to obtain the optimal operating conditions and respect these constraints is through a model-based optimization problem, typically nonlinear (ELLIS *et al.*, 2014).

Additionally, the RTO layer plays a fundamental role when disturbances occur. Due to disturbances (operational or strategic), the economic optimum operating point of the process could change, needing to be updated. The RTO layer does this last task by updating the setpoints of the supervisory control layer. The prominent disturbances examples and frequencies are presented in Table 1.1. According to ARKUN and STEPHANOPOULOS (1980), the disturbances classification in terms of frequency and its impact on the economic index of the plant is an essential criterion for determining RTO cycle frequency.

Table 1.1: Main disturbances and its frequencies (Adapted from BAILEY *et al.* (1993))

Main disturbances	Examples	Time Scale
Utility limitations	cooling water, electricity and steam	hours/days
Feedstock variation	composition and availability	hours/days
Product demand	desired production	days/weeks
Equipment limitation	lower heat exchange due to fouling	days/weeks
Market changes	product price and raw material costs	weeks
Product specification changes	product purity	weeks/months
Catalyst deactivation	activity loss due to coke deposition	weeks/months

Among the benefits of the RTO structure is the increase in the yield and purity of the products, the reduction of energy consumption and operational costs, and the reduction of maintenance costs. It means that the RTO structure leads the plant to a most profitable point (LEE and WEEKMAN, 1976).

The most widespread RTO strategy is called a two-step approach, which was proposed by SHI-SHANG *et al.* (1987). In this strategy, sequential steps of identification and optimization are carried out in an RTO cycle. The identification step uses the reconciled process data to update the process model parameters and increase model prediction accuracy. An optimization step is then carried out based

on the updated model to determine the optimum solution to be applied to the plant.

Despite being the most popular strategy, the limitations of the two-step approach have also been discussed. The main disadvantage of this strategy is that it does not guarantee convergence to the plant optimum, which may even lead to process instability (MARCHETTI, 2009). Previous work of FORBES *et al.* (1994) and FORBES and MARLIN (1996) proposed adequacy criteria of the model, which are sufficient conditions that the model should present to guarantee the convergence to the plant optimum point.

Other strategies have been developed, focusing on optimality and feasibility whenever the model does not meet the model adequacy criteria. Those strategies are based on adding terms to the objective function and constraints, called modifiers. These modifiers depend on the plant measured variables gradients (MARCHETTI, 2009). ROBERTS (1979) proposed the Integrated System Optimization and Parameter Estimation (ISOPE) strategy, which considers a modified optimization problem with a step of identification. TATJEWSKI (2002) proposed a variant of this strategy considering a shift term in the objective function, such that an identification step is no longer necessary. MARCHETTI (2009) proposed the Modifier-Adaptation (MA) approach, such that correction terms are added to the optimization problem objective function and the constraints, eliminating the identification step. These modifiers are intended to meet the Necessary Condition of Optimality (NCO) upon convergence.

However, calculating the gradients based on measurements could also lead to other issues. First, in the case of uncertainties and noise in the process' measured variables, such fluctuations also affect the calculation of gradients, often estimated from finite difference formulas. Moreover, gradient estimation also implies the need for additional perturbations applied to the process at each iteration of the RTO system to update the modifiers. In order to overcome the gradient estimation and its drawbacks, FERREIRA *et al.* (2018) proposed a Modifier Adaptation strategy based on Gaussian Process (GP) models. In this approach, the GP is applied to model the plant-model mismatch. This approach can be interpreted as a higher-order correction term. DEL RIO CHANONA *et al.* (2021) expanded the methodology by introducing Bayesian Optimization concepts, such as using acquisition functions in the RTO approach. DELOU *et al.* (2022) expanded the original work of FERREIRA *et al.* (2018) and proposed a modifier-adaptation strategy such that the correction terms are applied to the output variables instead of the objective function and constraints, also using GP.

Another drawback of the classical RTO structures is related to the low frequency of the optimization cycles. Since RTO is based on a steady-state model,

optimization and identification steps can only be carried out if the process is at a steady-state. This condition is verified by an steady-state detection step (SSD) (DARBY *et al.*, 2011). However, due to changes in input variables or disturbances, the optimization step can be delayed until the plant reaches a new steady-state (SCHULTZ, 2015). Thus, the RTO strategy can present a low frequency of optimization cycles, especially in processes with slow dynamics and frequent disturbances. Consequently, the plant operates suboptimally until a new steady-state is reached, and the optimum point can be updated (GRACIANO *et al.*, 2015).

In order to increase the frequency of optimization cycles, optimization strategies based on regulation have been proposed. In this scenario, the optimization problem is rewritten as a control problem, as in the Self Optimizing Control (SOC) strategy (SKOGESTAD, 2000b) or the NCO Tracking (SRINIVASAN *et al.*, 2003a,b). Thus, the control objective is to keep the objective function gradient null or, at least, a minimum acceptable deviation from the true optimum of the process, ensuring optimality. However, feasibility guarantee is one limitation of this formulation, such that the constraints are satisfied within a typical range of operation of the process. It is important to highlight that these methods are based on the knowledge of the active constraint regions, which are often assumed to be fixed, regardless of disturbances, which is not necessarily true.

Another possible strategy to overcome the low frequency of the RTO strategy is to apply a dynamic model for optimization purposes. This strategy is called dynamic RTO (D-RTO). However, D-RTO also requires accurate dynamic models, which can be a limitation (GRACIANO *et al.*, 2015). Also, there are still open numerical issues associated with D-RTO to be addressed before practical implementations, especially for large-scale systems (KRISHNAMOORTHY *et al.*, 2018). Additionally, accordingly to BINETTE and SRINIVASAN (2016), another difficulty associated to the D-RTO is the dynamic model update, mainly related to the persistence of the excitation.

An intermediate approach between RTO and D-RTO is called Hybrid RTO (H-RTO). VALLURU *et al.* (2015) proposed a strategy considering a dynamic model and a parameter estimation step through a dynamic observer, such as Extended Kalman Filter (EKF). In this strategy, the dynamic model parameters are updated iteratively using a dynamic observer, so an SSD is not needed. The updated model is applied in a steady-state optimization step, considering the steady-state model version of the dynamic model. This approach was also discussed by KRISHNAMOORTHY *et al.* (2018) and MATIAS and LE ROUX (2018), which showed that the economic performance obtained in H-RTO strategy was between RTO and D-RTO approaches, with the benefit of lower computational cost when compared to D-RTO. Again, the H-RTO presupposes a dynamic model is available,

which may not be true. In this sense, DELOU *et al.* (2021) recently developed an H-RTO framework considering that only a steady-state model is available and an approximate dynamic model is obtained using a Hammerstein model structure.

The classic RTO structure has another significant drawback related to model compatibility between steady-state and dynamic layers. Indeed, the MPC and RTO layers apply different mathematical models to achieve their objectives. While, typically, the models of the RTO layer are rigorous, the models used in the MPC layer are usually linear and obtained from identification strategies around an operating point. Thus, the steady-state predicted by each model is not expected to be the same, which can generate unachievable operating points from the RTO layer to the control layer. Therefore, one crucial aspect is the mismatch between optimization and supervisory control layers.

Some strategies have been proposed to mitigate the model mismatch between RTO and MPC layers. One possibility is using an intermediate optimization layer between the RTO and supervisory control layers to adjust the setpoints determined by the RTO layer. This step considers the steady-state version of the dynamic model used in the control layer to satisfy the MPC constraints (MORSHEDI *et al.*, 1985; YING *et al.*, 1998; YOUSFI and TOURNIER, 1991). In this approach, the intermediate optimization problem is written as Linear or Quadratic Programming and, therefore, is called LP-MPC (Linear Programming MPC) or QP-MPC (Quadratic Programming MPC). In this approach, the setpoints for the MPC layer are updated based on minimizing the deviations between the MPC setpoint and the optimum point provided by the RTO layer under the MPC constraints. The execution of this intermediate layer occurs at the same frequency as the MPC (YING *et al.*, 1998). As a drawback, since this approach still depends on the optimal setpoints, it can operate at a suboptimal point until the plant reaches a new steady-state.

The one-layer optimization approach, latterly called Economic Model Predictive Control (EMPC) (HEIDERINEJAD *et al.*, 2012), is another strategy aiming to deal with the model mismatch between MPC and RTO layers. It consists of simultaneously solving the economic optimization and control problem, incorporating economic aspects in the MPC formulation. DE GOUVÊA and ODLOAK (1996) proposed to include linearized terms of the economic objective function in the MPC objective function. Despite the simple formulation, this strategy may not represent the economic problem of the real process since this optimization problem may be nonlinear. In addition, according to DE GOUVÊA and ODLOAK (1998), these formulations can lead to instability of the closed-loop. ENGELL (2007) presented a strategy consisting of a Nonlinear Model Predictive Control (NMPC) by considering a rigorous nonlinear rigorous dynamic model of a sim-

ulated moving bed (SMB) separation system. In the proposed formulation, the controller's objective function was replaced by an economic objective function aiming to minimize the solvent consumption for a constant feed flow rate and a given purity requirement, in the presence of plant-model mismatch.

DE SOUZA *et al.* (2010) proposed the integration of MPC and RTO layers by including the gradient of the economic objective function in the MPC controller objective function. As a drawback of the strategy, the penalty term associated with economic performance requires the objective function to be convex. In order to address this issue, ALVAREZ and ODLOAK (2012) replaced the gradient of the economic objective function with a weighted norm of its linear approximation around the RTO optimal solution. Thus, the modified problem is convex, and the gradient of the economic objective function is null when the control actions are equal to the values provided by the RTO layer.

Regarding the one-layer optimization or EMPC approaches, as only one model is used for optimization and supervisory control, there is no risk of inconsistencies between the different models used in each layer (ENGELL, 2007). However, the use of nonlinear predictive models requires the solution of an optimal control problem in real time. Additionally, computational complexities, the requirement for online identification techniques for nonlinear processes, the robustness of the solution, and the stability for nonlinear systems are important issues for the practical implementation of the EMPC for large problems.

In summary, based on the previous works, the RTO methodologies present issues and opportunities, which are considered as the base for the development of the present thesis and are highlighted as follows:

- Issue 01 (I1): A steady-state detection step (SSD) in the RTO strategy is necessary before optimization. It leads to an RTO low frequency depending on the frequency of disturbances and suboptimal operation.
- Issue 02 (I2): The model-based optimization problem converges to the model optimum, which may not coincide with the plant optimum. This issue is known as the model adequacy problem.
- Issue 03 (I3): Typically, rigorous models are applied to describe the plant in the RTO layer, while identified models around a reference point are applied in the Supervisory Control layer. This issue leads to incompatibility between RTO and MPC layers.
- Opportunity 01 (Op1): Since rigorous models are applied to describe the plant in the RTO layer when considering large-scale problems require high

computational demand. Therefore, using the surrogate and identified models for optimization is a research opportunity.

- Opportunity 02 (Op2): when dealing with nonlinear models to be applied to NMPC or EMPC frameworks, the computational cost may be an issue, depending on the model structure. Thus, applying dynamic model identification and updating strategies through data-driven approaches represent a research opportunity.

## 1.2 Objectives

Based on the issues and opportunities presented before, the hypothesis of this thesis is the study of a real-time optimization (RTO) strategy that enables the integration between the optimization and supervisory control layers, minimizing the effects of the divergence between the models used in each of the layers. The strategy to be developed must seek to guarantee convergence and lower computational cost when compared to the use of rigorous models in the real-time optimization layer. Furthermore, the proposed methodology must include, in addition to the integration between the layers, the use of process measurements to update the process model, also enabling the use of identified surrogate models.

Therefore, the main objective of this thesis is the development of an EMPC framework that can be applied in the absence of any first-principles model.

In order to achieve the general objectives, the following specific objectives of this work were outlined:

1. Apply Gaussian process for RTO purposes, such that a model could be iteratively built in a scenario in which a steady-state model is not available;
2. Combine steady-state and dynamic data for model development using a Hammerstein model structure, enabling a data-driven modeling strategy;
3. Develop a Multiple-Input-Single-Output Hammerstein model structure to deal with input variables coupling by considering the system's state variables interactions;
4. Develop a complete control framework for RTO and NMPC integration based on a data-driven modeling approach, which presents:
  - An EMPC framework that can be applied in the absence of any first-principles model (dynamic or steady-state models);
  - The tracking of the first-order NCO of the plant optimization problem;

- full compatibility between the models used in optimization and control layers;
- Disturbance and model updating for both optimization and control layers through an Extended Kalman Filter.

## 1.3 Thesis Outline

This thesis is organized into 06 chapters, such that Chapters 1 and 2 contain the Introduction and Literature Review, respectively. Chapter 3 presents the background of Gaussian Process models, Chapters 4 and 5 contain the main contributions and results of the present thesis, and Chapter 6 contains the conclusions about the thesis. A brief description of the content of each chapter is presented below.

Chapter 1 presents a brief contextualization of the theme, showing the scenario in which real-time optimization strategies are presented and the difficulties encountered in the methodologies found in the literature. In addition, the objectives of this work are also presented.

Chapter 2 presents the literature review on the subject, showing the typical formulation of model-based real-time optimization problems, as well as the main strategies found in the literature, discussing the advantages and disadvantages of each of these. Next, the model-based predictive control strategy is presented, and how real-time optimization and predictive control strategies are integrated into a hierarchical control structure. Finally, still in that chapter, it is discussed the use of alternative models to the rigorous model of the process and the applications in optimization and control formulations.

Chapter 3 presents the fundamentals of surrogate-model based optimization strategies, such as Sequential Approximation Optimization and Bayesian Optimization, and introduces surrogate model classes, such as the Gaussian Process, which are an important tool for the development of the present thesis.

Chapter 4 presents the usage of Gaussian Process models applied in RTO strategies. The Gaussian Process is applied to model the plant instead of using it to model the plant-model mismatch, as in modifier-adaptation strategies. The proposed methodology is applied to benchmark problems, such as an exothermic continuous stirred-tank reactor and the Williams-Otto reactor, and compared to strategies present in the literature.

Chapter 5 presents an RTO framework based on an EMPC structure based on a data-driven modeling strategy based on a Gaussian Process and Hammerstein models. The proposed approach presents full compatibility since the optimiza-

tion and control problems are solved simultaneously. The proposed methodology is applied to the Williams-Otto reactor benchmark problem and compared to the strategies in the literature.

Finally, in Chapter 6, the final comments and future research suggestions are presented.

# Chapter 2

## Literature Review

### 2.1 Real-Time Optimization Problem Formulation

#### 2.1.1 RTO Formulation

Real-time optimization consists of solving an optimization problem oriented from an economic point of view, which can be minimizing costs, maximizing profit, or maximizing the production of a product, satisfying the process constraints.

The notation adopted in this work uses the subscript  $p$  when referring to the variables associated with the plant and is exempt from this subscript when dealing with the model. Thus, the plant optimization problem can be written according to Equation 2.1.

$$\begin{aligned} \mathbf{u}_{SP} = \arg \min_{\mathbf{u}} \quad & \Phi_p := \phi_{ec}(\mathbf{y}_p, \mathbf{u}) \\ \text{s.t.} \quad & \mathbf{G}_p := \mathbf{g}(\mathbf{y}_p, \mathbf{u}) \leq \mathbf{0} \end{aligned} \quad (2.1)$$

where  $\mathbf{u}_{SP} \in \mathbb{R}^{n_u}$  is the optimal solution of the problem,  $\mathbf{u} \in \mathbb{R}^{n_u}$  represents decision variables of the optimization problem,  $\mathbf{y}_p \in \mathbb{R}^{n_y}$  are the measured (output) variables,  $\phi_{ec} : \mathbb{R}^{n_y} \times \mathbb{R}^{n_u} \rightarrow \mathbb{R}$  is the economic objective function and  $\mathbf{g} : \mathbb{R}^{n_y} \times \mathbb{R}^{n_u} \rightarrow \mathbb{R}^{n_g}$  is the vector of inequality constraints.

However, the mapping of the process outputs, which is a function of input variables, is not necessarily known. Thus, this mapping is obtained and described by a steady-state model, implicitly written as follows:

$$\mathbf{f}_{ss}(\mathbf{y}, \mathbf{u}, \boldsymbol{\alpha}) = \mathbf{0} \quad (2.2)$$

where  $\boldsymbol{\alpha} \in \mathbb{R}^{n_\alpha}$  are model parameters,  $\mathbf{f}_{ss} : \mathbb{R}^{n_y} \times \mathbb{R}^{n_u} \times \mathbb{R}^{n_\alpha} \rightarrow \mathbb{R}^{n_y}$  represent the relationship between input and output variables.

Therefore, the model-based optimization problem of the plant is described as follows:

$$\begin{aligned}
\mathbf{u}_{SP} = \arg \min_{\mathbf{u}} \quad & \Phi := \phi_{ec}(\mathbf{y}, \mathbf{u}) \\
\text{s.t.} \quad & \mathbf{f}_{ss}(\mathbf{y}, \mathbf{u}, \boldsymbol{\alpha}) = \mathbf{0}, \\
& \mathbf{G} := \mathbf{g}(\mathbf{y}, \mathbf{u}, \boldsymbol{\alpha}) \leq \mathbf{0}
\end{aligned} \tag{2.3}$$

As presented before, it is assumed that the RTO is executed in an upper layer, based on the problem described by Equation 2.3. The solution of this layer determines optimal targets for the process, giving rise to the setpoints for the controlled variables and the reference values for the manipulated variables of the supervisory control, which are denoted as  $\mathbf{y}_{SP} \in \mathbb{R}^{n_y}$  and  $\mathbf{u}_{SP} \in \mathbb{R}^{n_u}$ , respectively, such that  $\mathbf{y}_{SP}$  is obtained by solving  $\mathbf{f}_{ss}(\mathbf{y}, \mathbf{u}_{SP}, \boldsymbol{\alpha}) = \mathbf{0}$ .

## 2.2 Real-Time Optimization Strategies

The optimization layer also called the real-time optimization layer or online optimization layer, is responsible for calculating operational conditions of the process in order to optimize a performance index related to economic objectives, subject to process constraints (NAYSMITH and DOUGLAS, 1995). This goal is achieved by employing a steady-state model of the process typically described by a first-principles, rigorous and nonlinear model (ELLIS *et al.*, 2014).

The RTO layer in a hierarchical control structure is justified by common disturbances, which could have operational or strategic nature. Typically, this last one is related to strategic decisions made on layers above the RTO layer.

Given disturbances, measurement uncertainties, and noise, updating the RTO model or structure is necessary. This step is carried out by considering the information available through process measurements. The RTO strategies can be grouped according to which variables are updated, being a way to distinguish the different existing strategies (CHACHUAT *et al.*, 2009; GARCIA and MORARI, 1981).

In this grouping approach, the methods are divided into three main categories, being this represented by:

- Adaptation model schemes, where the plant measurements are used for model updating, which is achieved by an identification step;
- Modifiers adaptation schemes, where modifiers terms are added to the original optimization problem. In this strategy, the modifiers terms are updated instead of the model parameters, which are considered to be fixed;

- Regulation adaptation, where the manipulated variables are directly modified by a control law, following a feedback control strategy.

The above classification is not unique. However, in the present work, preference will be given to this one, as it is considered the easiest to understand and based on structural issues of RTO strategies.

### 2.2.1 The Two-Step Approach

The two-step approach is classified as a model adaptation strategy. Simply, this approach aims to keep or improve the model's accuracy in a step before the optimization, which is done through an identification step (data reconciliation and parameter estimation), once the process is at steady-state condition, which is achieved by a steady-state detection (SSD) step.

Therefore, in this strategy, two main problems need to be considered, the identification step and the economic optimization itself (HAIMES and WISMER, 1972), which are solved in a sequential way.

The identification step aims to update the model parameters, minimizing the model's prediction errors compared to process measurements. Many factors are essential for this procedure to be effective, including the computational complexity of the model, the number of parameters, the quality and the quantity of available data, and the number of degrees of freedom for the identification problem.

An important step that occurs before or concurrently the parameter estimation step is the data reconciliation, which are part of a comprehensive methodology for reducing measurement errors known as data rectification (JOHNSTON and KRAMER, 1995). According to JOHNSTON and KRAMER (1995), data rectification aims to remove both the random and non-random errors from measurements. The data reconciliation technique applies the process model equations as constraints and obtains estimates of process variables by adjusting process measurements so that the estimates satisfy the constraints. Thus, it is expected the reconciled estimates to be more accurate than the measurements, besides satisfying the model equations (NARASIMHAN and JORDACHE, 1999). The identification step uses the last reconciled measurements to update the model parameters. Another option is to consider the unmeasured variables or model parameters as part of the data reconciliation problem (KIM *et al.*, 1990; VALKÓ and VAJDA, 1987), such that data reconciliation and parameter estimation occur simultaneously.

Based on the updated model, the second step corresponding to the economic optimization problem is solved. In this way, the identification and optimization problems are posed as follows:

Identification:

$$\begin{aligned} \bar{\alpha} &= \arg \min_{\alpha} \phi_{id}(\mathbf{u}, \alpha) \\ \text{s.t.} \quad & f_{ss}(\mathbf{y}, \mathbf{u}, \alpha) = \mathbf{0} \end{aligned} \quad (2.4)$$

Economical Optimization

$$\begin{aligned} \mathbf{u}_{SP} &= \arg \min_{\mathbf{u}} \phi_{ec}(\mathbf{u}, \bar{\alpha}) \\ \text{s.t.} \quad & f_{ss}(\mathbf{y}, \mathbf{u}, \bar{\alpha}) = \mathbf{0}, \\ & \mathbf{g}(\mathbf{y}, \mathbf{u}, \bar{\alpha}) \leq \mathbf{0} \end{aligned} \quad (2.5)$$

It is important to emphasize that the performance of the RTO and control layers are also related to the accuracy of the applied models. Thus, the relationship between the optimal solution and the cost involved in developing the model is a necessary trade-off to be considered (CHEN and JOSEPH, 1987; HAIMES and WISMER, 1972).

Despite the two-step approach being simple to understand, which also justifies the widespread dissemination of this technique, this strategy may have limitations from the point of view of optimality (MARCHETTI *et al.*, 2009). Many previous works in the literature used this approach as the central focus of study (BIEGLER *et al.*, 1985; FORBES *et al.*, 1994; FORBES and MARLIN, 1996; ROBERTS, 1979), aiming to better understand and address the limitations of the classical approach. Next, aspects of convergence and stability of this method are discussed.

### 2.2.1.1 Model Adequacy in Two-Step Approach

One of the relevant questions about RTO systems is the strategy's ability to drive the process to its true optimum. This issue is relevant to model-based systems because, *a priori*, there is no guarantee that the optimum point of the model and the plant are identical. In order to check and ensure that the optimum predicted by the model coincides with the true process optimum, model adequacy criteria were developed for model-based optimization systems.

BIEGLER *et al.* (1985) proposed model adequacy criteria based on the Karush-Kuhn-Tucker (KKT) optimality conditions, considering an optimization problem based on a rigorous model and a simple model. Accordingly to the authors, the first criterion to be verified is that both problems have the same optimum point based on the KKT optimality conditions. In practice, this verification is challenging since the optimum point of an industrial plant is not known *a priori*. Another

necessary criterion is that the gradients of the rigorous and simplified models are the same at the optimum point, which means that the gradient of the plant is equal to the model's gradient at the optimum point. The difficulty in verifying this criterion is determining the plant's gradient from the experimental data.

In the work of FORBES *et al.* (1994), the authors proposed a methodology for verifying the model adequacy using the concept of reduced optimization space. The advantage of using the reduced space is that only the manipulated variables, *i.e.*, the actual degrees of freedom or problem decision variables, are used. Additionally, in the works of FORBES *et al.* (1994) and FORBES and MARLIN (1995), the concept of local adequacy of the model was established.

**Definition 2.2.1** *Point-Wise Model Adequacy Criterion.* (FORBES *et al.*, 1994) and (FORBES and MARLIN, 1995) For the manipulated variables  $\mathbf{u}_p^*$  that represent a single optimum point of the plant, there must be a set of parameters to be adjusted ( $\bar{\alpha}$ ) such that the model-based optimization problem also has an optimum  $\mathbf{u}_{SP} = \mathbf{u}_p^*$ , and the model is considered point-wise adequate. Furthermore, if this optimum point obtained by the model-based problem is unique, the model is said to be strongly point-wise adequate.

In subsequent work, FORBES and MARLIN (1996) proposed a criterion for checking the local adequacy of the model. In mathematical terms, the criterion for verifying Definition 2.2.1 is:

**Criterion 2.2.1** *Point-Wise Model Adequacy Criterion.* According to FORBES and MARLIN (1996), If  $\mathbf{u}_p^*$  is unique (local) optimum point and exists at least one set of values for the adjustable parameters  $\bar{\alpha}$  such that:

$$\nabla_{\alpha} \phi_{id}(\mathbf{u}_p^*, \bar{\alpha}) = \mathbf{0} \quad (2.6)$$

$$\nabla_{\alpha}^2 \phi_{id}(\mathbf{u}_p^*, \bar{\alpha}) > \mathbf{0} \quad (2.7)$$

$$\nabla_u \phi_{ec}(\mathbf{u}_p^*, \bar{\alpha}) = \mathbf{0} \quad (2.8)$$

$$\nabla_u^2 \phi_{ec}(\mathbf{u}_p^*, \bar{\alpha}) > \mathbf{0} \quad (2.9)$$

$$\mathbf{g}(\mathbf{y}_p, \mathbf{u}_p^*, \bar{\alpha}) \leq \mathbf{0} \quad (2.10)$$

then, the combined identification and model-based optimization problems are adequate for use in an RTO strategy.

and  $\nabla_u \phi_{ec}$  and  $\nabla_u^2 \phi_{ec}$  represent the reduced gradient and the reduced Hessian matrix of the objective function, respectively, and  $\nabla_{\alpha} \phi_{id}$  and  $\nabla_{\alpha}^2 \phi_{id}$  represent the reduced gradient and the reduced Hessian matrix of the identification objective function.

It is important to notice that the criteria represented by Equations 2.6 and 2.7 are the sufficient conditions to  $\bar{\mathbf{a}}$  be the strict local minimum point of the identification problem represented by Equation 2.4 at the plant operation point  $\mathbf{u}_p^*$ . Additionally, the criteria given by Equations 2.8 to 2.10 represent the sufficient conditions to  $\mathbf{u}_p^*$  be a strict local minimum of the optimization problem given by Equation 2.5.

Therefore, if all the criteria described by Equations 2.6 to 2.10 are satisfied, the plant optimum point  $\mathbf{u}_p^*$  is also the optimum point of the model based optimization problem with model parameters  $\bar{\mathbf{a}}$ . Additionally, those conditions are also sufficient to say that the model is point-wise adequate.

Accordingly to MARCHETTI *et al.* (2009), those equations are sufficient but not necessary for the model to be adequate. For instance, in the case of  $\mathbf{u}_p^*$  being an optimal point, but the criterion of Equation 2.9 is not satisfied due to the reduced Hessian matrix being positive semidefinite. It is also noticed that the condition represented by Equation 2.6 has  $n_\alpha$  equations, so that satisfying all the criteria of Equations 2.6 to 2.10, generally, is not possible, especially for the cases where there are differences between predicted and observed values due to degrees of freedom (FRANCOIS and BONVIN, 2013; MARCHETTI, 2009).

Finally, the criteria represented by Equations 2.6 to 2.10 are based on the knowledge of  $\mathbf{u}_p^*$ . However, as this value is not known *a priori*, the utilization of Criterion 2.2.1 become difficult to be applied in practice for model selection in the RTO structures.

### 2.2.1.2 Stability of Two-Step Approach

Another important contribution of the work of FORBES and MARLIN (1996) for the Two-Step Approach of RTO schemes is related to stability, which is described by Criterion 2.2.2, based on the concept of stability proposed by WIGGINS (2003).

**Criterion 2.2.2** *Point-Wise Stability.* A system of recursive algebraic equations  $\mathbf{u}_{k+1} = \Gamma(\mathbf{u}_k)$  is said to be asymptotically stable at a fixed point  $\mathbf{u}_p^*$  if it is Lyapunov stable and exists a constant  $\epsilon > 0$ , such that:

$$\|\mathbf{u}_p^* - \mathbf{u}_k\| < \epsilon \quad (2.11)$$

then:

$$\lim_{k \rightarrow \infty} \|\mathbf{u}_p^* - \mathbf{u}_k\| = 0 \quad (2.12)$$

where  $k$  is the iteration index.

Applying nonlinear maps to represent the relation between plant measured variables ( $\mathbf{y}_p$ ), model parameters ( $\boldsymbol{\alpha}$ ) and model output variables ( $\mathbf{y}$ ), and for arbitrarily small deviation from the plant optimum  $\mathbf{u}_p^*$ , FORBES and MARLIN (1996) have shown that:

$$\left\| \left. \frac{\partial \mathbf{u}}{\partial \boldsymbol{\alpha}} \right|_{\bar{\boldsymbol{\alpha}}} \left. \frac{\partial \boldsymbol{\alpha}}{\partial \mathbf{y}_p} \right|_{\mathbf{y}_p(\mathbf{u}_p^*)} \left. \frac{\partial \mathbf{y}_p}{\partial \mathbf{u}} \right|_{\mathbf{u}_p^*} \right\| < 1 \quad (2.13)$$

Equation 2.13 has three useful terms on the left-hand side, as described below:

- $\left. \frac{\partial \mathbf{u}}{\partial \boldsymbol{\alpha}} \right|_{\bar{\boldsymbol{\alpha}}}$  is the parametric sensitivity matrix of the model-based optimization problem solution;
- $\left. \frac{\partial \boldsymbol{\alpha}}{\partial \mathbf{y}_p} \right|_{\mathbf{y}_p(\mathbf{u}_p^*)}$  is the sensitivity of the model parameters to changes in the plant measurements ( $\mathbf{y}_p$ ).
- $\left. \frac{\partial \mathbf{y}_p}{\partial \mathbf{u}} \right|_{\mathbf{u}_p^*}$  is the sensitivity of the process measurements ( $\mathbf{y}_p$ ) with respect to the manipulated variables ( $\mathbf{u}$ ).

The criterion presented in Equation 2.13 is a point-wise stability criterion, focusing on the stability properties in the neighborhood of the plant optimum  $\mathbf{u}_p^*$ , which is not useful for ensuring global stability. One of the difficulties in applying this last criterion is the *a priori* knowledge of  $\mathbf{u}_p^*$ . Additionally, the criterion also needs the calculation of the sensitivity gradients, which can be affected by noise and uncertainties, being the sensitivity  $\left. \frac{\partial \mathbf{y}_p}{\partial \mathbf{u}} \right|_{\mathbf{u}_p^*}$  the term which is more affected, as it is mainly associated to measurements.

## 2.2.2 ISOPE

In order to guarantee the optimality of the solution, ROBERTS (1979) introduced the modifier-based RTO strategies, which essentially aimed to guarantee the first-order KKT condition. As previously stated, the main advantage of the developed strategy is the guarantee of convergence to the optimum, even when the process model used in the optimization is not adequate, which does not happen in the classic two-step approach.

The work of ROBERTS (1979) is an extension of the previous work of HAIMES and WISMER (1972), which solved the steps of optimization and parameter estimation through a multi-objective optimization, introducing two new extra variable vectors in the optimization problem, creating a so-called integrated strategy.

From this premise, the name of the strategy, Integrated System Optimization and Parameter Estimation (ISOPE), arises. The formulation of this strategy is presented below:

Optimization

$$\begin{aligned}
 \mathbf{u}^* &= \arg \min_{\mathbf{u}} \phi_{ec}(\mathbf{u}, \boldsymbol{\sigma}) \\
 \text{s.t.} \quad & \mathbf{f}(\mathbf{y}, \mathbf{u}, \boldsymbol{\sigma}) = \mathbf{0}, \\
 & \mathbf{g}(\mathbf{y}, \mathbf{u}, \boldsymbol{\sigma}) \leq \mathbf{0}
 \end{aligned} \tag{2.14}$$

Parameter Estimation:

$$\begin{aligned}
 \bar{\boldsymbol{\alpha}} &= \arg \min_{\boldsymbol{\alpha}} \phi_{id}(\mathbf{v}, \boldsymbol{\alpha}) \\
 \text{s.t.} \quad & \mathbf{f}(\mathbf{y}, \mathbf{v}, \boldsymbol{\alpha}) = \mathbf{0}, \\
 & \mathbf{g}(\mathbf{y}, \mathbf{v}, \boldsymbol{\alpha}) \leq \mathbf{0}
 \end{aligned} \tag{2.15}$$

where  $\mathbf{u}$  and  $\boldsymbol{\alpha}$  are the model manipulated variables and model parameters, respectively, and  $\mathbf{v}$  and  $\boldsymbol{\sigma}$  are new variables vectors added to the original problem, subjected to the following equality constraints:

$$\begin{aligned}
 \mathbf{u} &= \mathbf{v} \\
 \boldsymbol{\alpha} &= \boldsymbol{\sigma}
 \end{aligned} \tag{2.16}$$

It is interesting to notice that the equality constraints imposed by Equation 2.16 are only satisfied when the convergence of the problem is reached, which is a characteristic of an unfeasible path method.

It is common to distinguish between ISOPE algorithms with and without constraints in output variables (BRDYŚ *et al.*, 1986; LIN *et al.*, 1988). The problem was unconstrained in the original work of ROBERTS (1979). In this case, the theoretical development for obtaining the proposed modifiers is relatively simple. Assuming that the estimated parameters are within a feasible region of the problem, the model parameters can be obtained by solving the following equation:

$$\nabla_{\boldsymbol{\alpha}} \phi_{id}(\mathbf{v}, \boldsymbol{\alpha}) = \mathbf{0} \tag{2.17}$$

In addition, as it is assumed that the solution is within a feasible region, then using Equation 2.17 as an equality constraint in the integrated parameter opti-

mization and estimation problem, it is possible to write:

$$\begin{aligned}
\mathbf{u}^* &= \arg \min_{\mathbf{u}} \phi_{ec}(\mathbf{u}, \boldsymbol{\sigma}) \\
\text{s.t.} \quad & \mathbf{u} = \mathbf{v}, \\
& \boldsymbol{\alpha} = \boldsymbol{\sigma}, \\
& \nabla_{\boldsymbol{\alpha}} \phi_{id}(\mathbf{v}, \boldsymbol{\alpha}) = \mathbf{0}
\end{aligned} \tag{2.18}$$

Thus, the Lagrangian function of the problem in Equation 2.18 is written as follows:

$$\mathcal{L}(\mathbf{u}, \boldsymbol{\alpha}, \mathbf{v}, \boldsymbol{\sigma}, \boldsymbol{\mu}, \boldsymbol{\lambda}, \boldsymbol{\eta}) = \phi_{ec}(\mathbf{u}, \boldsymbol{\sigma}) + \boldsymbol{\lambda}^T(\mathbf{v} - \mathbf{u}) + \boldsymbol{\mu}^T(\boldsymbol{\sigma} - \boldsymbol{\alpha}) + \boldsymbol{\eta}^T \nabla_{\boldsymbol{\alpha}} \phi_{id}(\mathbf{v}, \boldsymbol{\alpha}) \tag{2.19}$$

So that the first-order KKT conditions require that:

$$\nabla_{\mathbf{u}} \mathcal{L} = \nabla_{\mathbf{u}} \phi_{ec} - \boldsymbol{\lambda} = \mathbf{0} \tag{2.20}$$

$$\nabla_{\boldsymbol{\alpha}} \mathcal{L} = \mathbf{H}_{\boldsymbol{\alpha}\boldsymbol{\alpha}} \boldsymbol{\eta} - \boldsymbol{\mu} = \mathbf{0} \tag{2.21}$$

$$\nabla_{\mathbf{v}} \mathcal{L} = \mathbf{H}_{\mathbf{v}\boldsymbol{\alpha}} \boldsymbol{\eta} + \boldsymbol{\lambda} = \mathbf{0} \tag{2.22}$$

$$\nabla_{\boldsymbol{\sigma}} \mathcal{L} = \nabla_{\boldsymbol{\sigma}} \phi_{ec} + \boldsymbol{\mu} = \mathbf{0} \tag{2.23}$$

where:

$$[H_{\boldsymbol{\alpha}\boldsymbol{\alpha}}]_{ij} = \frac{\partial^2 \phi_{id}}{\partial \alpha_i \partial \alpha_j} \tag{2.24}$$

$$[H_{\mathbf{v}\boldsymbol{\alpha}}]_{ij} = \frac{\partial^2 \phi_{id}}{\partial v_i \partial \alpha_j} \tag{2.25}$$

The introduction of the modifiers proposed by ROBERTS (1979) consists in satisfying the optimality condition described by Equation 2.20, which would be equivalent to solving the optimization problem below, introducing equality and inequality constraints to the problem in Equation 2.14, for given values of  $\boldsymbol{\lambda}$  and  $\boldsymbol{\sigma}$ .

$$\begin{aligned}
\mathbf{u}^* &= \arg \min_{\mathbf{u}} \phi_{ec}(\mathbf{u}, \boldsymbol{\sigma}) - \boldsymbol{\lambda}^T \mathbf{u} \\
\text{s.t.} \quad & \mathbf{f}(\mathbf{y}, \mathbf{u}, \boldsymbol{\sigma}) = \mathbf{0}, \\
& \mathbf{g}(\mathbf{y}, \mathbf{u}, \boldsymbol{\sigma}) \leq \mathbf{0}
\end{aligned} \tag{2.26}$$

Using Equations 2.21 to 2.23, it is possible to arrive at the following expression

for calculating the modifiers:

$$\lambda = H_{v\alpha} H_{\alpha\alpha}^{-1} \nabla_{\sigma} \phi_{ec} \quad (2.27)$$

In the particular case in which the number of parameters to be estimated is equal to the number of available measurements, the identification problem can be rewritten as:

$$\mathbf{y}(v, \alpha) - \mathbf{y}_p(v) = \mathbf{0} \quad (2.28)$$

In this case, assuming that the solution is within a feasible region, then using Equation 2.28 as an equality constraint in the integrated parameter optimization and estimation problem, it is possible to write:

$$\begin{aligned} \mathbf{u}^* &= \arg \min_{\mathbf{u}} \phi_{ec}(\mathbf{u}, \sigma) \\ \text{s.t.} \quad &\mathbf{u} = \mathbf{v}, \\ &\alpha = \sigma, \\ &\mathbf{y}(v, \alpha) - \mathbf{y}_p(v) = \mathbf{0} \end{aligned} \quad (2.29)$$

Thus, the Lagrangian function of the problem in Equation 2.29 is written as follows:

$$\mathcal{L}(\mathbf{u}, \alpha, v, \sigma, \boldsymbol{\mu}, \boldsymbol{\lambda}, \boldsymbol{\eta}) = \phi_{ec}(\mathbf{u}, \sigma) + \boldsymbol{\lambda}^T (\mathbf{v} - \mathbf{u}) + \boldsymbol{\mu}^T (\sigma - \alpha) + \boldsymbol{\eta}^T (\mathbf{y}(v, \alpha) - \mathbf{y}_p(v)) \quad (2.30)$$

So that the first-order KKT conditions require that:

$$\nabla_{\mathbf{u}} \mathcal{L} = \nabla_{\mathbf{u}} \phi_{ec} - \boldsymbol{\lambda} = \mathbf{0} \quad (2.31)$$

$$\nabla_{\alpha} \mathcal{L} = \left[ \frac{\partial \mathbf{y}}{\partial \alpha} \right] \boldsymbol{\eta} - \boldsymbol{\mu} = \mathbf{0} \quad (2.32)$$

$$\nabla_v \mathcal{L} = \left[ \frac{\partial \mathbf{y}}{\partial v} - \frac{\partial \mathbf{y}_p}{\partial v} \right] \boldsymbol{\eta} + \boldsymbol{\lambda} = \mathbf{0} \quad (2.33)$$

$$\nabla_{\sigma} \mathcal{L} = \nabla_{\sigma} \phi_{ec} + \boldsymbol{\mu} = \mathbf{0} \quad (2.34)$$

Combining Equations 2.32 to 2.34, it is possible to show that the modifiers are calculated by:

$$\boldsymbol{\lambda} = \left[ \frac{\partial \mathbf{y}}{\partial v} - \frac{\partial \mathbf{y}_p}{\partial v} \right]^T \left[ \frac{\partial \mathbf{y}}{\partial \alpha} \right]^{-1} \nabla_{\sigma} \phi_{ec} \quad (2.35)$$

It is interesting to notice that the modifier  $\lambda$ , in fact, the Lagrange multiplier of the Lagrangian function written accordingly to Equation 2.19.

As said before, the methodology presented above does not include constraints in output variables, so the work of BRDYŚ *et al.* (1986) is an extension of the original work of ROBERTS (1979), addressing the optimization problem with constraints in output variables. The optimization problem to be solved, in this case, is the following one:

$$\begin{aligned}
\mathbf{u}^* &= \arg \min_{\mathbf{u}} \phi_{ec}(\mathbf{u}, \boldsymbol{\alpha}) \\
\text{s.t.} \quad & \mathbf{u} - \mathbf{v} = \mathbf{0}, \\
& \mathbf{g}(\mathbf{y}, \mathbf{u}, \boldsymbol{\alpha}) \leq \mathbf{0}, \\
& \mathbf{y}(\mathbf{v}, \boldsymbol{\alpha}) - \mathbf{y}_p(\mathbf{v}) = \mathbf{0}
\end{aligned} \tag{2.36}$$

where the parameter estimation problem was added to the optimization problem through an equality constraint, which represents the relationship between the model output variable ( $\mathbf{y}$ ) and plant measurements ( $\mathbf{y}_p$ ). It is also important to mention that in Equation 2.36, the number of estimated parameters and the number of plant measurements are equal.

The Lagrangian function of the problem in Equation 2.36 is written as follows:

$$\begin{aligned}
\mathcal{L}(\mathbf{u}, \boldsymbol{\alpha}, \mathbf{v}, \boldsymbol{\mu}, \boldsymbol{\lambda}, \boldsymbol{\eta}) &= \phi_{ec}(\mathbf{u}, \boldsymbol{\alpha}) + \boldsymbol{\lambda}^T(\mathbf{v} - \mathbf{u}) + \boldsymbol{\mu}^T \mathbf{g}(\mathbf{y}, \mathbf{u}, \boldsymbol{\alpha}) + \\
& \boldsymbol{\eta}^T [\mathbf{y}(\mathbf{v}, \boldsymbol{\alpha}) - \mathbf{y}_p(\mathbf{v})]
\end{aligned} \tag{2.37}$$

where  $\boldsymbol{\lambda}$ ,  $\boldsymbol{\mu}$  e  $\boldsymbol{\eta}$  are Lagrange multipliers.

Applying the first-order necessary conditions of optimization to the problem, it follows that:

$$\nabla_{\mathbf{u}} \mathcal{L} = \nabla_{\mathbf{u}} \phi_{ec} - \boldsymbol{\lambda} + \nabla_{\mathbf{u}}^T \mathbf{g} \boldsymbol{\mu} = \mathbf{0} \tag{2.38}$$

$$\nabla_{\boldsymbol{\alpha}} \mathcal{L} = \nabla_{\boldsymbol{\alpha}} \phi_{ec} + \nabla_{\boldsymbol{\alpha}}^T \mathbf{g} \boldsymbol{\mu} + \nabla_{\boldsymbol{\alpha}}^T \mathbf{y} \boldsymbol{\eta} = \mathbf{0} \tag{2.39}$$

$$\nabla_{\mathbf{v}} \mathcal{L} = \boldsymbol{\lambda} + [\nabla_{\mathbf{v}}^T \mathbf{y} - \nabla_{\mathbf{v}}^T \mathbf{y}_p] \boldsymbol{\eta} = \mathbf{0} \tag{2.40}$$

$$\nabla_{\boldsymbol{\lambda}} \mathcal{L} = \mathbf{u} - \mathbf{v} = \mathbf{0} \tag{2.41}$$

$$\nabla_{\boldsymbol{\eta}} \mathcal{L} = \mathbf{y} - \mathbf{y}_p = \mathbf{0} \tag{2.42}$$

$$\nabla_{\boldsymbol{\mu}} \mathcal{L} = \mathbf{g}(\mathbf{y}, \mathbf{u}, \boldsymbol{\alpha}) \leq \mathbf{0} \tag{2.43}$$

$$\boldsymbol{\mu}^T \mathbf{g} = 0 \tag{2.44}$$

Combining Equations 2.39 and 2.40, gives:

$$\lambda = \lambda(\mathbf{u}, \mathbf{v}, \boldsymbol{\alpha}, \boldsymbol{\mu}) = \left[ \nabla_{\mathbf{v}}^T \mathbf{y} - \nabla_{\mathbf{v}}^T \mathbf{y}_p \right] \left[ \nabla_{\boldsymbol{\alpha}}^T \mathbf{y} \right]^{-1} \left[ \nabla_{\boldsymbol{\alpha}}^T \mathbf{g} \boldsymbol{\mu} + \nabla_{\boldsymbol{\alpha}} \phi_{ec} \right] \quad (2.45)$$

Comparing Equations 2.35 and 2.45, it is possible to notice that the difference between these equations is given by the term  $\nabla_{\boldsymbol{\alpha}}^T \mathbf{g} \boldsymbol{\mu}$ , which refers to the constraints  $\mathbf{g}$ . Additionally, it is important to verify that, in the situation where the constraints are imposed only on the control variables  $\mathbf{u}$ , that is, not dependent on the output variables ( $\mathbf{y}$ ) and therefore not dependent on the  $\boldsymbol{\alpha}$  parameters, it follows that Equations 2.35 and 2.45 are identical, because:

$$\nabla_{\boldsymbol{\alpha}}^T \mathbf{g} = \mathbf{0} \quad (2.46)$$

In addition to the case mentioned before, there is another situation where Equations 2.35 and 2.45 are equivalent. It happens when all constraints are inactive, in such a way that the complementarity conditions enforce that:

$$\boldsymbol{\mu}^T \mathbf{g} = 0, \text{ because } \boldsymbol{\mu} = \mathbf{0} \quad (2.47)$$

The modified problem to be solved by the methodology proposed by BRDYŚ *et al.* (1986) consists of the following minimization problem, which aims to satisfy the KKT conditions represented by Equations 2.38, 2.43, and 2.44:

$$\begin{aligned} \mathbf{u}^* &= \arg \min_{\mathbf{u}} \quad \phi_{ec}(\mathbf{u}, \boldsymbol{\alpha}) - \boldsymbol{\lambda}^T \mathbf{u} \\ \text{s.t.} \quad & \mathbf{g}(\mathbf{y}(\mathbf{u}, \boldsymbol{\alpha}), \mathbf{u}, \boldsymbol{\alpha}) \leq \mathbf{0} \end{aligned} \quad (2.48)$$

Subsequently, ZHANG and ROBERTS (1991) proposed a modification of the algorithm proposed by BRDYŚ *et al.* (1986), where a penalty term related to the constraints is added to the objective function of the problem, as described by Equation 2.48, so that the modified problem becomes an unconstrained optimization, as follows:

$$\mathbf{u}^* = \arg \min_{\mathbf{u}} \quad \phi_{ec}(\mathbf{u}, \boldsymbol{\alpha}) - \boldsymbol{\lambda}^T \mathbf{u} + \left[ \nabla_{\mathbf{v}}^T \mathbf{g} \boldsymbol{\mu} \right]^T \mathbf{u} \quad (2.49)$$

Although the problem represented by Equation 2.49 is more straightforward than the problem represented by Equation 2.48, it does not guarantee that the optimization path is feasible, satisfying the constraints in the process variables, except in the convergence of the algorithm.

TATJEWSKI (2002) proposed an optimization strategy such that the parameter estimation step is not considered, which means that the model parameters are

not updated. Also, a term referring to the difference between the process measurements and model predicted values is added to the objective function, written as follows:

$$\mathbf{a}_k = \mathbf{y}_p(\mathbf{u}_k) - \mathbf{y}(\mathbf{u}_k, \boldsymbol{\alpha}) \quad (2.50)$$

Thus, the modified optimization problem proposed by TATJEWSKI (2002) is written as follows:

$$\begin{aligned} \mathbf{u}^* &= \arg \min_{\mathbf{u}} \quad \phi_{ec}(\mathbf{u}, \mathbf{y}(\mathbf{u}, \boldsymbol{\alpha}) + \mathbf{a}_k) - \boldsymbol{\lambda}_k^T \mathbf{u} \\ \text{s.t.} \quad & \mathbf{u}_{min} \leq \mathbf{u} \leq \mathbf{u}_{max} \end{aligned} \quad (2.51)$$

where  $\mathbf{u}_{min}$  and  $\mathbf{u}_{max}$  are the decision variable lower and upper bounds, respectively.

The modifiers are calculated as follows:

$$\boldsymbol{\lambda}_k^T = \frac{\partial \phi_{ec}}{\partial \mathbf{y}}(\mathbf{u}_k, \mathbf{y}_k + \mathbf{a}_k) \left[ \frac{\partial \mathbf{y}_p}{\partial \mathbf{u}}(\mathbf{u}_k) - \frac{\partial \mathbf{y}}{\partial \mathbf{u}}(\mathbf{u}_k, \boldsymbol{\alpha}) \right] \quad (2.52)$$

GAO and ENGELL (2005) proposed a modification of the original ISOPE algorithm, based on the previous work of TATJEWSKI (2002). In this approach, the model parameters also remain constant during all optimization iterations and it was also able to deal with the inequality constraints on the output variables ( $\mathbf{y}$ ). The formulation also deals with plant-model mismatch regarding the constraints by modifying them as follow:

$$\mathbf{G}_{mod}(\mathbf{u}) = \mathbf{G}(\mathbf{u}) + \mathbf{G}_p(\mathbf{u}_k) - \mathbf{G}(\mathbf{u}_k) + [\nabla_{\mathbf{u}} \mathbf{G}_p(\mathbf{u}_k) - \nabla_{\mathbf{u}} \mathbf{G}(\mathbf{u}_k)] (\mathbf{u} - \mathbf{u}_k) \quad (2.53)$$

where  $\mathbf{G}_{mod}$  represents the modified constraints of the model-based optimization problem. Also, for the sake of notation, the dependence of  $\mathbf{G}$  and  $\mathbf{G}_p$  on the output variable were omitted in the above equation.

It is important to notice that, at  $\mathbf{u} = \mathbf{u}_k$ , the modified constraint value is equal to the plant constraint value, as so its gradients. Therefore, the feasibility conditions of the process are satisfied. In addition to the modified constraints, the decision variables ( $\mathbf{u}$ ) search region is bounded so that the modified problem is

written as follows:

$$\begin{aligned}
\mathbf{u}^* &= \arg \min_{\mathbf{u}} \quad \phi_{ec}(\mathbf{u}, \mathbf{y}(\mathbf{u}, \boldsymbol{\alpha} + \mathbf{a})) - \boldsymbol{\lambda}^T \mathbf{u} \\
\text{s.t.} \quad & \mathbf{G}_{mod}(\mathbf{u}) \leq \mathbf{0}, \\
& \mathbf{u}_k - \Delta \leq \mathbf{u} \leq \mathbf{u}_k + \Delta, \\
& \mathbf{u}_{min} \leq \mathbf{u} \leq \mathbf{u}_{max}
\end{aligned} \tag{2.54}$$

where  $\Delta$  represents a bound on the search region.

In addition, the work of GAO and ENGELL (2005) also contributed to a new strategy for obtaining plant gradients, based on the methodology of BRDYŚ and TATJEWSKI (1994), which uses measurements from past iterations to estimate the gradients in the  $k$ -th iteration. In order to ensure a good approximation of the estimated gradients, the condition number of the matrix of differences of the input variables in past iterations is added to the optimization problem as an inequality constraint, ensuring that the condition number does not exceed a pre-established value.

The matrix of differences of input variables is defined as follows:

$$\mathbf{S}_k = [\mathbf{u}_k - \mathbf{u}_{k-1} \cdots \mathbf{u}_k - \mathbf{u}_{k-m}]^T \tag{2.55}$$

The reciprocal of the condition number of the matrix  $\mathbf{S}$  is calculated as follows:

$$\frac{1}{\kappa(\mathbf{S}_k)} = \frac{\sigma_{\min}(\mathbf{S}_k)}{\sigma_{\max}(\mathbf{S}_k)} \geq \delta \tag{2.56}$$

where  $\kappa$  is the condition number,  $\sigma_{\min}$  e  $\sigma_{\max}$  are the maximum and minimum singular values of the matrix  $\mathbf{S}$ , respectively, and  $\delta$  is a pre-established tolerance in the range of  $(0, 1)$ .

Thus, the value of the decision variable in the  $k$ -th optimization iteration ( $\mathbf{u}_k$ ) is obtained taking into account the condition number of the matrix  $\mathbf{S}_k$ , improving the approximation of the obtained gradients. On the other hand, the feasible region of the problem may be reduced, possibly generating a suboptimal point.

Thus, the methodology proposed by GAO and ENGELL (2005) consists of using the condition number as an indicator to verify if a new perturbation point is needed. If the reciprocal of the condition number is below the tolerance, a new perturbation is added to the plant. The new point is obtained through an optimization problem aiming to maximize the condition number, subject to the same domain constraints of the economic optimization problem. Thus, this strategy

does not compromise the feasible region of the problem. The main disadvantage is the need to solve a new optimization problem and the application of a new perturbation to the plant.

### 2.2.3 Modifier Adaptation

A real-time optimization system solution converges to the plant optimum if it iterates to the point that satisfies the plant optimization problem's NCO. To guarantee that convergence, the concept of the modifiers is introduced, representing the difference between the true and predicted NCO values. The modifiers act as correction terms in the model-based optimization problem and are updated at each iteration.

In this type of formulation, unlike two-step optimization and classic ISOPE methods, the idea is to use the process measurements to update the modifiers and not the model parameters. The modifiers consist of affine terms added to the objective function and constraints.

The modified process constraints can be rewritten as (MARCHETTI, 2009; MARCHETTI *et al.*, 2009):

$$\mathbf{G}_{mod}(\mathbf{u}, \boldsymbol{\alpha}) = \mathbf{G}(\mathbf{u}, \boldsymbol{\alpha}) + \boldsymbol{\varepsilon}^G + \left(\boldsymbol{\lambda}^G\right)^T (\mathbf{u} - \mathbf{u}_k) \quad (2.57)$$

where  $\mathbf{G}_{mod} : \mathbb{R}^{n_u} \times \mathbb{R}^{n_\alpha} \rightarrow \mathbb{R}^{n_g}$  is the vector of modified constraints,  $\boldsymbol{\varepsilon}^G \in \mathbb{R}^{n_g}$  is the vector of zeroth-order modifiers of the constraints,  $\boldsymbol{\lambda}^G \in \mathbb{R}^{n_u \times n_g}$  is the matrix of first-order modifiers of the constraints and  $\mathbf{u}_k$  is the plant operational point at iteration  $k$ .

The zeroth-order and first-order modifiers are given by:

$$\begin{aligned} \boldsymbol{\varepsilon}^G &= \mathbf{G}_p(\mathbf{u}_k) - \mathbf{G}(\mathbf{u}_k, \boldsymbol{\alpha}) \\ \boldsymbol{\lambda}^{GT} &= \nabla_{\mathbf{u}} \mathbf{G}_p(\mathbf{u}_k) - \nabla_{\mathbf{u}} \mathbf{G}(\mathbf{u}_k, \boldsymbol{\alpha}) \end{aligned} \quad (2.58)$$

where the modifiers are calculated based on constraints values and its gradients at the current operation point ( $\mathbf{u}_k$ ). A graphical interpretation of the modifiers is presented in Figure 2.1.

In Figure 2.1, the zeroth-order modifier is the difference between the constraint value predicted by the model and the constraint value calculated at  $\mathbf{u}_k$ . The first-order modifier is the difference between the predicted constraint slope and the plant constraint slope.

Additionally, first-order modifiers are also added to the objective function, as

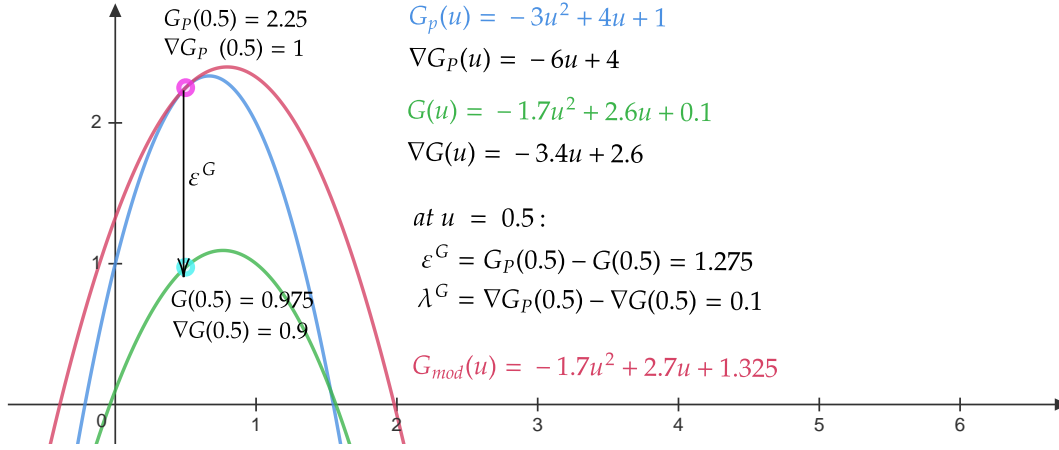


Figure 2.1: Graphical interpretation of the modifiers applied to a given constraint function. The real constraint function is given by  $G_p(u) = -3u^2 + 4u + 1$  and the model constraint function is given by  $G(u) = -1.7u^2 + 2.6u + 0.1$ . At  $u = 0.5$ , applying the modifier adaptation approach, the modified constraint function is given by  $G_{mod} = -1.7u^2 + 2.7u + 1.325$ . Therefore, at  $u = 0.5$ ,  $G_p(0.5) = G_{mod}(0.5) = 2.25$ , and  $\nabla G_p(0.5) = \nabla G_{mod}(0.5) = 1$ .

presented in Equation 2.59.

$$\Phi_{mod}(\mathbf{u}, \boldsymbol{\alpha}) = \Phi(\mathbf{u}, \boldsymbol{\alpha}) + \left(\lambda^\Phi\right)^T \mathbf{u} \quad (2.59)$$

where  $\Phi_{mod}$  is the modified objective function and  $\lambda^\Phi$  is the first-order modifier of the objective function, given by:

$$\lambda^\Phi = \nabla_{\mathbf{u}} \Phi_p(\mathbf{u}_k) - \nabla_{\mathbf{u}} \Phi(\mathbf{u}_k, \boldsymbol{\alpha}) \quad (2.60)$$

So that the following vectors of modifiers and constraints can be written:

$$\boldsymbol{\Lambda} = \left[ \varepsilon^{G_1}, \dots, \varepsilon^{G_{n_g}}, \lambda^{G_1 T}, \dots, \lambda^{G_{n_g} T}, \lambda^{\Phi T} \right]^T \quad (2.61)$$

$$\mathbf{C} = \left[ G_1, \dots, G_{n_g}, \nabla_{\mathbf{u}}^T G_1, \dots, \nabla_{\mathbf{u}}^T G_{n_g}, \nabla_{\mathbf{u}}^T \Phi \right]^T \quad (2.62)$$

Such that:

$$\boldsymbol{\Lambda}(\mathbf{u}_k) = \mathbf{C}_p(\mathbf{u}_k) - \mathbf{C}(\mathbf{u}_k) \quad (2.63)$$

where  $\boldsymbol{\Lambda}$  is the vector that encompasses all the modifiers,  $\mathbf{C}$  and  $\mathbf{C}_p$  are vectors that have information of constraints, its gradients and the objective function gradient from the model based problem and the plant information, respectively. Ad-

ditionally,  $\mathbf{C}, \mathbf{C}_p, \mathbf{\Lambda} \in \mathbb{R}^{n_{mod}}$ , where  $n_{mod} = n_g + n_u(n_g + 1)$ .

Thus, with the values of the objective function and the constraints based on the plant information (corresponding to the vector  $\mathbf{C}_p$ ) and the same information predicted by the model, *i.e.*,  $\mathbf{C}$ , it is possible to calculate the value of the modifiers  $\mathbf{\Lambda}$ . Therefore, with the definitions presented above, the optimization problem for the adaptation method is posed as follows:

$$\begin{aligned} \mathbf{u}^* = \arg \min_{\mathbf{u}} \quad & \Phi_{mod}(\mathbf{u}, \boldsymbol{\alpha}) = \Phi(\mathbf{u}, \boldsymbol{\alpha}) + \left(\lambda^\Phi\right)_k^T \mathbf{u} \\ \text{s.t.} \quad & \mathbf{G}_{mod}(\mathbf{u}, \boldsymbol{\alpha}) = \mathbf{G}(\mathbf{u}, \boldsymbol{\alpha}) + (\boldsymbol{\varepsilon}^G)_k + \left(\lambda^G\right)_k^T (\mathbf{u} - \mathbf{u}_k) \leq \mathbf{0}, \\ & \mathbf{u}_{min} \leq \mathbf{u} \leq \mathbf{u}_{max} \end{aligned} \quad (2.64)$$

where the subscript  $k$  refers to the  $k$ -th iteration.

Typically, to avoid sudden changes in the value of the modifiers for the next iteration, the information is updated using a first-order filter:

$$\mathbf{\Lambda}(\mathbf{u}_k) = (\mathbf{I} - \mathbf{K})\mathbf{\Lambda}(\mathbf{u}_k) + \mathbf{K}\mathbf{\Lambda}(\mathbf{u}_{k-1}) \quad (2.65)$$

where  $\mathbf{I} \in \mathbb{R}^{n_{mod} \times n_{mod}}$  is the identity matrix and  $\mathbf{K} \in \mathbb{R}^{n_{mod} \times n_{mod}}$  is a diagonal matrix which contains the gains  $K_i$ , such that  $0 \leq K_i \leq 1$ , which are tuning parameters of the method.

In terms of implementing the method, the information from  $\mathbf{C}_p$  can be inferred from the measurements  $\mathbf{y}_p$  and its respective gradients. Indeed:

$$\nabla_{\mathbf{u}} \Phi_p(\mathbf{u}_k) = \nabla_{\mathbf{u}} \phi_{ec}(\mathbf{u}_k, \mathbf{y}_{p_k}) + \nabla_{\mathbf{y}} \phi_{ec}(\mathbf{u}_k, \mathbf{y}_{p_k}) \nabla_{\mathbf{u}} \mathbf{y}_p(\mathbf{u}_k) \quad (2.66)$$

$$\nabla_{\mathbf{u}} \mathbf{G}_p(\mathbf{u}_k) = \nabla_{\mathbf{u}} \mathbf{g}(\mathbf{u}_k, \mathbf{y}_{p_k}) + \nabla_{\mathbf{y}} \mathbf{g}(\mathbf{u}_k, \mathbf{y}_{p_k}) \nabla_{\mathbf{u}} \mathbf{y}_p(\mathbf{u}_k) \quad (2.67)$$

where  $\mathbf{y}_{p_k} = \mathbf{y}_p(\mathbf{u}_k)$  are process measurements in the current operating point.

It is worth mentioning that calculating the gradient of the measured variables of the plant ( $\nabla_{\mathbf{u}} \mathbf{y}_p(\mathbf{u}_k)$ ), as well as in other methods that depend on this information, consists of the most significant difficulty of the formulation, not being a closed problem in the literature (MARCHETTI *et al.*, 2016).

As previously presented, the modifier adaptation methodology does not need to estimate the model parameters. Additionally, the question of model adequacy also becomes a more straightforward criterion in this methodology. In the same way as in the two-step RTO approach, theoretically, this criterion is met if there are values  $\bar{\mathbf{\Lambda}}$  that lead to the optimum point of the plant  $\mathbf{u}_p^*$ . Since the parameters are not estimated, Equations 2.6 and 2.7 do not apply. The Equations 2.8 and 2.9 are automatically satisfied as a result of the introduction of modifiers in the

problem. Indeed:

$$\mathbf{G}_{mod}(\mathbf{u}_p^*, \boldsymbol{\alpha}) = \mathbf{G}(\mathbf{u}_p^*, \boldsymbol{\alpha}) + \varepsilon^G + \left(\lambda^G\right)^T (\mathbf{u}_p^* - \mathbf{u}_k) = \mathbf{G}_p(\mathbf{u}_p^*) \leq 0 \quad (2.68)$$

because  $\mathbf{u}_k = \mathbf{u}_p^*$  and, since  $\mathbf{u}_p^*$  being a optimal point of the plant, which is necessarily feasible.

In the same way, for the modified objective function, calculating the derivative of Equation 2.59 with respect to  $\mathbf{u}$ , it follows that:

$$\nabla_{\mathbf{u}} \Phi_{mod}(\mathbf{u}_k) = \nabla_{\mathbf{u}} \Phi(\mathbf{u}_k) + \lambda^{\Phi} \quad (2.69)$$

Thus, calculating  $\nabla_{\mathbf{u}} \Phi_{mod}(\mathbf{u}_k)$  at  $\mathbf{u}_p^*$ , it follows that:

$$\nabla_{\mathbf{u}} \Phi_{mod}(\mathbf{u}_p^*) = \nabla_{\mathbf{u}} \Phi_p(\mathbf{u}_p^*) = \mathbf{0} \quad (2.70)$$

Therefore, the model adequacy criteria for the modifier adaptation method are based on ensuring that the reduced Hessian matrix of the original objective function (without modifiers) of the model-based problem is positive definite.

**Definition 2.2.2** *Point-Wise Model Adequacy Criterion for Modifier-Adaptation Method (MARCHETTI, 2009).* Let  $\mathbf{u}_p^*$  be a unique optimum point of the plant and considered a regular point for the constraints. If the process model is such that the reduced Hessian matrix of the objective function  $\Phi$  is positive definite at  $\mathbf{u}_p^*$

$$\nabla_{\mathbf{u}}^2 \phi_{ec}(\mathbf{u}_p^*, \boldsymbol{\alpha}) > \mathbf{0}$$

then, the process model is adequate for use in the modifier-adaptation RTO Scheme.

Although this criterion is simpler than in the case of the two-step formulation, again, the difficulty of using such a criterion lies in limiting the prior knowledge of  $\mathbf{u}_p^*$  and the active set of constraints (FRANCOIS, 2014). It is important to notice that, for unconstrained problems with a linear objective function in the  $\mathbf{u}$  decision variables, this criterion is impossible to be met, being a limitation of the method.

The modifier-adaptation method appears as an alternative to the other methods, being presented with the main characteristic of not being necessary to estimate model parameters. It reduces the dependence on the identification step to guarantee the convergence to the real optimum point of the process and also deals with model mismatch. For this, it is important to emphasize that the modifier adaptation strategy, when using the first-order terms, depends on the calculation of the gradients of the objective function and constraints of the process, which necessarily depend on the measurements.

On the other hand, the gradients' calculation also represents one of the difficulties of the method, mainly in terms of practical implementations

(MARCHETTI *et al.*, 2010, 2009). The strategies for calculating the gradients can be distinguished from those that use steady-state or dynamic information.

When considering steady-state information, at least  $(n_u + 1)$  operating points are required to determine all gradients, as the primary method used is finite differences. When using dynamic information, the objective is to calculate the gradients using the information obtained during the transient period between the steady-state points corresponding to the successive iterations of the RTO. For this, one of the possibilities is applying dynamic identification, such that the gradients are obtained through a dynamic model obtained during the transient operation (BAMBERGER and ISERMANN, 1978; GARCIA and MORARI, 1981; ZHANG and ROBERTS, 1990; ZHANG and FORBES, 2008). The main advantage of this approach is reducing waiting time compared to stationary disturbances since it is not necessary to wait to reach a new steady-state. However, additional disturbances may be necessary to obtain the excitation degree needed for identification (MARCHETTI *et al.*, 2010).

MANSOUR and ELLIS (2003) evaluated methods for calculating the gradients, applied to the ISOPE method, as this strategy also depends on the information of the gradients of the output variables, as seen in Equation 2.35. The simpler and intuitive way of gradients calculation is applying the finite-difference method (MARCHETTI, 2009), written as follows:

$$\frac{\partial y_{p_i}}{\partial u_j} = \frac{y_{p_i}(\mathbf{u}_k + h\mathbf{e}_j) - y_{p_i}(\mathbf{u}_k)}{h}, \quad h > 0, \quad i = 1, \dots, n_y \quad \text{and} \quad j = 1, \dots, n_u \quad (2.71)$$

where  $h$  is the amplitude of the perturbation and  $\mathbf{e}_j$  is the unit vector in the direction  $j$ .

As already mentioned, one of the disadvantages of estimating the gradients using the finite-difference method is the need to perform  $n_u$  perturbations at each iteration and wait for the process to reach a new steady-state after each of the performed disturbances.

Another possible approach is through the use of past measurements obtained during the RTO iterations, as proposed, for example, in the strategies called dual ISOPE (BRDYŚ and TATJEWSKI, 1994). This methodology reduces the total number of perturbations to be applied for calculating the gradients and does not require a fixed spatial arrangement, as occurs in the finite-difference method. In this approach, a constraint in the search space is added to obtain the new operational point, taking into account past information.

FRANCOIS and BONVIN (2013) proposed a strategy to obtain gradients of the objective function and constraints from transient process information. In this strategy, the gradients are obtained from variational analysis of the objective

function  $\phi$ , constraints  $G$  and the process model. The authors showed that the time needed for convergence was of the order of the settling time, which means a reduced time when compared to the original MA framework. However, the authors also showed that some improvement in gradient estimation is still needed.

MARCHETTI *et al.* (2010) proposed a new formulation for the modifier adaptation called dual modifier adaptation. This methodology has as its main goal the analysis and control of the accuracy of the calculated gradients since this characteristic is one of the difficulties of the original modifier adaptation method. In the dual modifier-adaptation, a constraint related to the gradient estimation error is added to the problem in Equation 2.64, which imposes that the error should be limited to an upper bound. This procedure is carried out by analyzing the truncation error and the measurement noise as follows:

$$\frac{\sigma_{max}}{2} \|S^{-1}diag(SS^T)\| + \frac{\sigma_{noise}}{l_{min}} \leq \varepsilon_{UB} \quad (2.72)$$

where the first term in the left hand side of the equation represents the truncation error,  $\sigma_{max}$  is the upper limit on the spectral radius of the Hessian of the process mapping, and  $S$  is the matrix of differences of input variables (previously defined in Equation 2.55). The second term in the left hand side is the error associated to measurement noise,  $l_{min}$  is the shortest distance between all possible pairs of complement affine subspaces<sup>1</sup> that can be generated from  $S$  and  $\sigma_{noise}$  is the noise level. The term in the right hand side of the equation,  $\varepsilon_{UB}$  is the desired upper bound of the gradient error norm.

Equation 2.72 represents a constraint to be added to the optimization problem, satisfying the quality of the gradients. However, MARCHETTI *et al.* (2010) highlights that this constraint is non-convex, being necessary to add a new constraint that can guarantee feasible convex regions in the optimization problem. Indeed, MARCHETTI *et al.* (2010) propose that the optimization problem should be solved on each side of the hyperplane generated by the most recent operating points,  $(\mathbf{n}_k)^T \mathbf{u} = \mathbf{b}_k$ , where  $\mathbf{n}_k$  is the vector normal to the hyperplane generated by the  $n_u$  last. Therefore, the constraint to be added corresponding to the half

---

<sup>1</sup>In a vector space of dimension  $n_u$ , a point in this vector space is also an affine subspace of dimension 0, a line is an affine subspace of dimension 1, and a plane is an affine subspace of dimension 2. An affine subspace of dimension  $n_u - 1$  is said an hyperplane, defined as  $\mathbf{n}^T \mathbf{u} = b$ , where  $\mathbf{n}$  is the normal vector and  $b$  is a scalar. Given a set of  $(n_u + 1)$  points in a subspace of dimension  $n_u$ ,  $\mathcal{S} := \{\mathbf{u}_1, \dots, \mathbf{u}_{n_u+1}\}$ , a proper subset  $\mathcal{S}^A \subseteq \mathcal{S}$  of  $n_u^A \in 1, \dots, n_u$  points generates an affine subspace of dimension  $n_u^A - 1$ . The complement subset  $\mathcal{S}^C := \mathcal{S} \setminus \mathcal{S}^A$  of  $(n_u + 1 - n_u^A)$  points generates the complement affine subspace of dimension  $(n_u - n_u^A)$ . See MARCHETTI *et al.* (2010) for its compute.

subspace  $(\mathbf{n}_k)^T \mathbf{u} \geq \mathbf{b}_k$  is written as follows:

$$(\mathbf{n}_k)^T \mathbf{u} \geq b_k + \rho_k \|\mathbf{n}_k\| \quad (2.73)$$

where  $\rho_k$  is the minimum distance of a point from the hyperplane.

Analogously, the constraint to be added corresponding to the half subspace  $(\mathbf{n}_k)^T \mathbf{u} \leq \mathbf{b}_k$  is written as follows:

$$(\mathbf{n}_k)^T \mathbf{u} \leq b_k + \rho_k \|\mathbf{n}_k\| \quad (2.74)$$

According to MARCHETTI *et al.* (2010), the next operating point  $\mathbf{u}^{k+1}$  is chosen in the set  $\{\mathbf{u}_{k+1}^{pos}, \mathbf{u}_{k+1}^{neg}\}$  as the value that minimize the modified objective function, where  $\mathbf{u}_{k+1}^{pos}$  is the solution of the optimization problem solved in the half subspace  $(\mathbf{n}_k)^T \mathbf{u} \geq \mathbf{b}_k$ , and  $\mathbf{u}_{k+1}^{neg}$  is the solution of the optimization problem solved in the half subspace  $(\mathbf{n}_k)^T \mathbf{u} \leq \mathbf{b}_k$ , respectively.

LÓPEZ (2012) proposed an RTO strategy called Nested Optimization. This methodology is based on the Modifiers-Adaptation strategy, and a new way of updating the modifiers has been proposed. The proposed methodology adds an external optimization layer to the optimization problem presented in Equation 2.64. In the external layer, the modifiers are used as decision variables provided to the internal optimization layer. In the inner layer, the optimization problem in Equation 2.64 is solved in order to obtain the decision variables  $\mathbf{u}$ . After the process reaches a new steady-state, the cost function value is feedback to the external layer, which repeats the process until the values of the modifiers converge. It is important to notice that this methodology is based on the hypothesis that the optimum point of the modifiers also corresponds to the optimum of the setpoints.

WENZEL *et al.* (2015) proposed a modifier adaptation technique based on the usage of quadratic approximation models for process mapping, such that the gradients at the current point are calculated analytically. A trust-region method is applied through covariance analyses of the previously obtained regression set to determine the next setpoint.

GAO *et al.* (2016) proposed a new methodology based on the original work of GAO and ENGELL (2005), combining elements introduced in the adaptation method using quadratic approximations proposed in WENZEL *et al.* (2015), mainly concerning the calculation of the gradients from previous process measurements.

SINGHAL *et al.* (2016) proposed an RTO strategy based on approximate problems arising from the original problem. The resulting optimization problems were quadratic programming (QP) or quadratic objective function with quadratic

constraints. The quadratic programming problem is posed as follows:

$$\begin{aligned}
\mathbf{u}_{k+1}^* &= \arg \min_{\Delta \mathbf{u}} \quad \nabla^T \phi_{ec,k} \Delta \mathbf{u} + \frac{1}{2} \Delta \mathbf{u}^T \mathbf{Q} \Delta \mathbf{u} \\
\text{s.t.} \quad & \mathbf{g}_j(\mathbf{u}_k) + \sum_{i=1}^{n_u} \lambda_{i,j} |\Delta \mathbf{u}_i| \leq 0, \\
& \nabla^T \mathbf{g}_{j,k} \Delta \mathbf{u} \leq \delta_j \forall j \in \mathcal{A}_\epsilon, \\
& \mathbf{u}_{min} - \mathbf{u}_k \leq \Delta \mathbf{u} \leq \mathbf{u}_{max} - \mathbf{u}_k, \\
& \mathbf{u}_{k+1} = \mathbf{u}_k + \Delta \mathbf{u}
\end{aligned} \tag{2.75}$$

where  $\nabla \phi_{ec,k}$  is the gradient of objective function  $\phi_{ec}$  at  $\mathbf{u}_k$ ,  $\nabla \mathbf{g}_{j,k}$  is the gradient of constraint  $\mathbf{g}_j$  at  $\mathbf{u}_k$ ,  $\mathbf{Q}$  is positive definite matrix defined as the Hessian upper bounding matrix,  $\lambda_{i,j}$  are Lipschitz constants for  $j$ -th constraint and each  $i$ -th decision variable, and  $\mathcal{A}_\epsilon$  represents the set of active constraints of the problem, defined as:

$$\mathcal{A}_\epsilon = \{j \in \{1, \dots, n_g\} : -\epsilon_j \leq \mathbf{g}_j(\mathbf{u}_k) \leq 0\} \tag{2.76}$$

where  $\epsilon_j$  is an arbitrary positive scalar.

The upper bounding matrix is obtained through the following mathematical lemma:

**Lemma 2.2.1** *Upper bounding matrix*

Let  $f : \mathbb{R}^{n_u} \rightarrow \mathbb{R}$  be twice continuously differentiable over the compact set  $\mathcal{U} \subset \mathbb{R}^{n_u}$  such that:

$$-M_{ij} < \frac{\partial^2 f}{\partial u_i \partial u_j} < M_{ij}, \quad M_{ij} > 0, \quad \forall \mathbf{u} \in \mathcal{U}, \quad i, j = 1, \dots, n_u \tag{2.77}$$

Let  $\Delta \mathbf{u}_{k+1} = \mathbf{u}_{k+1} - \mathbf{u}_k$ . Then, the change in function  $f$  between  $\mathbf{u}_k$  and  $\mathbf{u}_{k+1}$  can be bounded as:

$$f(\mathbf{u}_{k+1}) \leq f(\mathbf{u}_k) + \nabla^T f(\mathbf{u}_k) \Delta \mathbf{u}_{k+1} + \frac{1}{2} \Delta \mathbf{u}_{k+1}^T \mathbf{Q} \Delta \mathbf{u}_{k+1} \tag{2.78}$$

where  $\mathbf{Q}$  is a diagonal matrix with diagonal elements given by:

$$\mathbf{Q}_{ii} = \sum_{j=1}^{n_u} M_{ij}, \quad i = 1, \dots, n_u \tag{2.79}$$

Another approach proposed by SINGHAL *et al.* (2016) which, according to the authors, promotes faster convergence, is the problem written as a quadratic

objective function with quadratic constraints. In this case, the problem is posed as follows:

$$\begin{aligned}
\mathbf{u}_{k+1}^* &= \arg \min_{\Delta \mathbf{u}_{k+1}} \quad \nabla^T \phi_{ec,k} + \frac{1}{2} \Delta \mathbf{u}_{k+1}^T \mathbf{Q} \Delta \mathbf{u}_{k+1} \\
\text{s.t.} \quad & \mathbf{g}_j(\mathbf{u}_k) + \nabla^T \mathbf{g}_{j,k} \Delta \mathbf{u}_{k+1} + \frac{1}{2} \Delta \mathbf{u}_{k+1}^T \mathbf{Q}_j \Delta \mathbf{u}_{k+1} \leq 0, \\
& \mathbf{u}_{min} - \mathbf{u}_k \leq \Delta \mathbf{u}_{k+1} \leq \mathbf{u}_{max} - \mathbf{u}_k, \\
& \mathbf{u}_{k+1} = \mathbf{u}_k + \Delta \mathbf{u}_{k+1}
\end{aligned} \tag{2.80}$$

where  $\mathbf{Q}_j$  is the upper bounding matrix of the constraint  $\mathbf{g}_j$ .

SINGHAL *et al.* (2016) found that the proposed method guarantees the feasibility of the optimization strategy in real time, in addition to increasing the speed of convergence when compared to the optimization strategy based on a QP problem. Additionally, the authors proposed a strategy for updating the upper bounding matrix of hessian and constraints, based on a structure of the trust-region method, allowing for even faster convergence.

FERREIRA *et al.* (2018) developed a strategy combining the modifier adaptation with Gaussian Processes models<sup>2</sup>. In this approach, the Gaussian Process models are applied to recursively estimates the plant-model mismatch using the process measurements. The main goal of the proposed strategy is to eliminate the gradient estimation step, which was a drawback of the original strategy proposed by MARCHETTI (2009). The main idea of the strategy is to replace the zeroth- and first-order adaptation terms with a term that represents the plant-model mismatch, being estimated by a Gaussian Process. The problem is described as follows:

$$\begin{aligned}
\mathbf{u}^* &= \arg \min_{\mathbf{u}} \quad \Phi_{mod}(\mathbf{u}, \boldsymbol{\alpha}) = \Phi(\mathbf{u}, \boldsymbol{\alpha}) + GP_k^{(\Phi_p - \Phi)}(\mathbf{u}) \\
\text{s.t.} \quad & \mathbf{G}_{mod_j}(\mathbf{u}, \boldsymbol{\alpha}) = \mathbf{G}_j(\mathbf{u}, \boldsymbol{\alpha}) + GP_k^{(\mathbf{G}_{p,j} - \mathbf{G}_j)}(\mathbf{u}) \leq 0, \\
& j = 1, \dots, n_g, \\
& \mathbf{u}_{min} \leq \mathbf{u} \leq \mathbf{u}_{max}
\end{aligned} \tag{2.81}$$

where  $GP_k^{(\Phi_p - \Phi)}(\mathbf{u}) \in \mathbb{R}$  is a GP estimated at the  $k$ -th iteration in order to estimate the objective function plant-model mismatch  $(\Phi_p - \Phi)$ . Analogously,  $GP_k^{(\mathbf{G}_{p,j} - \mathbf{G}_j)}(\mathbf{u}) \in \mathbb{R}^{n_g}$  is the Gaussian Process model estimated at the  $k$ -th iteration in order to estimate the mismatch between the plant and model of the  $j$ -th constraint  $(\mathbf{G}_{p,j} - \mathbf{G}_j)$ ,  $\forall j = 1, \dots, n_g$ .

In the problem represented by Equation 2.81, it is implicit the dependence of

---

<sup>2</sup>An introduction to Gaussian Processes (GP) models is presented in Section 3.1

the Gaussian Process on its parameters (also called hyperparameters). Indeed, this kind of model presents a set of parameters that need to be estimated. In the strategy proposed by FERREIRA *et al.* (2018), the GP models are updated at each RTO iteration, such that the data set for identification are also updated at each iteration, keeping a limited number of historical records, for instance, the last  $N$  measurements.

DEL RIO CHANONA *et al.* (2019) proposed a modifier-adaptation scheme combining GP and trust-region methods, based on the previous work of FERREIRA *et al.* (2018). A first proposed strategy applies a trust region method based on limiting the the decision variables search region. The trust region radius is updated based on the accuracy of the Gaussian Process applied to estimate plant-model mismatches of the objective function and constraints. The following optimization problem represents this approach:

$$\begin{aligned}
\mathbf{u}_{k+1}^* &= \arg \min_{\Delta \mathbf{u}} \quad \Phi_{mod}(\mathbf{u}_k + \Delta \mathbf{u}, \boldsymbol{\alpha}) = \Phi(\mathbf{u}_k + \Delta \mathbf{u}, \boldsymbol{\alpha}) + \\
&\quad GP_k^{(\Phi_p - \Phi)}(\mathbf{u}_k + \Delta \mathbf{u}) \\
\text{s.t.} \quad &\mathbf{G}_{mod_j}(\mathbf{u}_k + \Delta \mathbf{u}, \boldsymbol{\alpha}) = \mathbf{G}_j(\mathbf{u}_k + \Delta \mathbf{u}, \boldsymbol{\alpha}) + \\
&\quad GP_k^{(\mathbf{G}_{p,j} - \mathbf{G}_j)}(\mathbf{u}_k + \Delta \mathbf{u}), j = 1, \dots, n_g, \\
&\mathbf{u}_{min} - \mathbf{u}_k \leq \Delta \mathbf{u} \leq \mathbf{u}_{max} - \mathbf{u}_k, \\
&\mathbf{u}_{k+1} = \mathbf{u}_k + \Delta \mathbf{u}, \\
&\Delta \mathbf{u}_i \leq \|\Delta_k\|, i = 1, \dots, n_u
\end{aligned} \tag{2.82}$$

where  $\Delta \mathbf{u} \in \mathbb{R}^{n_u}$  is the decision variable of the problem and represents the increment in the previous control action  $\mathbf{u}_k$ ,  $\boldsymbol{\alpha} \in \mathbb{R}^{n_p}$  are the process model parameters and  $\|\Delta_k\| \geq 0$  is the radius of the trust-region.

The trust-region radius update criteria is based on:

- The ratio of actual cost reduction to predicted cost reduction from iteration  $k$  to iteration  $k + 1$ :

$$\rho_{k+1} = \frac{\Phi_p(\mathbf{u}_k) - \Phi_p(\mathbf{u}_{k+1})}{\Phi_{mod}(\mathbf{u}_k, \boldsymbol{\alpha}) - \Phi_{mod}(\mathbf{u}_{k+1}, \boldsymbol{\alpha})} \tag{2.83}$$

- The violation of any inequality constraint:

$$\mathbf{G}_{p,j}(\mathbf{u}_{k+1}) > 0 \quad \forall j = 1, \dots, n_g \tag{2.84}$$

The trust-region radius<sup>3</sup> is reduced if the ratio of cost reduction is below a

---

<sup>3</sup>Trust-region updating rules are presented in Section 3.2.

predefined tuning parameter value or a plant constraint is violated after implementing the last calculated action  $\mathbf{u}_{k+1}$ . Else, the trust-region radius is increased if there is no violation of constraints and the ratio of cost reduction is above a predefined tuning parameter. Otherwise, the trust-region radius remain unchanged.

A second approach proposed by DEL RIO CHANONA *et al.* (2019) uses the variance estimate from the Gaussian Processes to define multiple trust-regions directly on the cost and constraint predictions. The optimization problem is written as follows:

$$\begin{aligned}
\mathbf{u}^* = \arg \min_{\mathbf{u}} \quad & \Phi_{mod}(\mathbf{u}, \boldsymbol{\alpha}) = \Phi(\mathbf{u}, \boldsymbol{\alpha}) + GP_k^{(\Phi_p - \Phi)}(\mathbf{u}) \\
\text{s.t.} \quad & \mathbf{G}_{modj}(\mathbf{u}, \boldsymbol{\alpha}) = \mathbf{G}_j(\mathbf{u}, \boldsymbol{\alpha}) + GP_k^{(G_{j,p} - G_j)}(\mathbf{u}), \\
& \sigma(GP_k^{(\Phi_p - \Phi)})(\mathbf{u}) \leq \|\Delta_k\|^{(\Phi_p - \Phi)}, \\
& \sigma(GP_k^{(G_{j,p} - G_j)})(\mathbf{u}) \leq \|\Delta_k\|^{(G_{j,p} - G_j)}, \forall j = 1, \dots, n_g
\end{aligned} \tag{2.85}$$

where  $\sigma(GP_k^{(\Phi_p - \Phi)})$  is the standard deviation associated with the Gaussian Process of the objective function  $GP_k^{(\Phi_p - \Phi)}$ ,  $\sigma(GP_k^{(G_{j,p} - G_j)})$  is the standard deviation associated with the Gaussian Process of the  $j$ -th constraint  $GP_k^{(G_{j,p} - G_j)}$ , and  $\|\Delta_k\|^{(\Phi_p - \Phi)}$  and  $\|\Delta_k\|^{(G_{j,p} - G_j)} \forall j = 1, \dots, n_g$  are the trust-region radii for the Gaussian Process predictions of the plant-model mismatches of objective function and constraints.

The constraints represented by equations

$$\sigma(GP_k^{(\Phi_p - \Phi)})(\mathbf{u}) \leq \|\Delta_k\|^{(\Phi_p - \Phi)} \tag{2.86}$$

$$\sigma(GP_k^{(G_{j,p} - G_j)})(\mathbf{u}) \leq \|\Delta_k\|^{(G_{j,p} - G_j)}, \forall j = 1, \dots, n_g \tag{2.87}$$

mean that the decision variable  $\mathbf{u}$  should remain in a region (trust region) where the model has higher accuracy (less uncertainty, represented by the standard deviation of the Gaussian Process). The trust region radius  $\|\Delta_k\|^{(\Phi_p - \Phi)}$  of the cost prediction is updated following the same criteria given by Equation 2.83. For the constraints prediction trust-region radii,  $\|\Delta_k\|^{(G_{j,p} - G_j)}$ , it is updated based on the constraint violation.

DEL RIO CHANONA *et al.* (2021) brought concepts of Bayesian Optimization into RTO based on modifier adaptation with Gaussian Process by considering the concept of acquisition functions<sup>4</sup>. The main advantage of the proposed strategy is considering a metric to obtaining the next point which deals with the exploration and exploitation trade-off.

---

<sup>4</sup>An introduction to acquisition functions is presented in section 3.3

## 2.2.4 Optimization by Regulation

The formulation of the RTO problem through regulation consists of transforming the economic optimization problem into a control problem, thus avoiding the solution of the economic optimization problem itself (CHACHUAT *et al.*, 2009). One of the motivations of this formulation is justified by the low frequency of execution of the RTO layer. As this layer employs a steady-state model of the process, optimization is only carried out if the plant conditions can be considered at steady-state. Thus, the time between executions of the RTO must be enough for the process to reach a new steady-state after the application of the last action. This situation becomes even more complicated when disturbances occur, which postpones the optimization since the stationarity condition of the process must be verified, being necessary to wait even longer until a new steady-state point is reached. According to ENGELL (2007), classic RTO structures may perform well in situations where disturbances are infrequent. However, for disturbances that occur at times below the sampling time of the RTO layer, this structure will not bring all possible economic benefits.

Then, the optimization structures by regulation appear to avoid the issues previously presented, which is done through a control problem that acts in the process with significantly shorter sampling times. The strategies typically employed are called self-optimizing control (SKOGESTAD, 2000a) and the NCO Tracking (FRANCOIS *et al.*, 2005).

One of the difficulties of the optimization by regulation approach is related to obtaining the variables to be controlled, which, when kept constant at their reference values by adjusting the manipulated variables, take the process to the optimum point (MORARI *et al.*, 1980; SKOGESTAD, 2000a). Also, this kind of formulation typically considers that the setactive constraints remain unchanged when disturbances occur, which may not be true (SUN *et al.*, 2016).

### 2.2.4.1 Self Optimizing Control

Self-optimizing control (SOC) is defined as a control structure capable of achieving an acceptable loss in the economic performance index with constant setpoint values for the controlled variables (SKOGESTAD, 2000a). For the authors, the loss is defined as the difference between the current value of the economic objective function and its value at the true process optimum, that is:

$$Loss = \phi_{ec}(\mathbf{u}_k, \mathbf{y}_k) - \phi_{ec}(\mathbf{u}_p^*, \mathbf{y}_p^*) \quad (2.88)$$

where *Loss* is the economic loss.

The formulation of self-optimizing control is not new. This strategy is based on the original works of MORARI *et al.* (1980) and FINDEISEN *et al.* (1980), which described the idea of using a control structure to keep the operation at an optimum point, taking into account the regions of active constraints and a procedure for selecting controlled variables (SKOGESTAD, 2000a).

Simply, the method of self-optimizing control consists in defining which variables would be selected to be controlled ( $c$ ) such that, when kept at its setpoints (constants), lead to an acceptable loss. In the works of SKOGESTAD (2000a,b), seven steps are described for control variable selection, as described below:

1. Analysis of the degrees of freedom: determination of the number of decision variables for the optimization problem;
2. Formulation of the optimization problem: definition of the objective function and the constraints of the optimization problem;
3. Identification of disturbances and uncertainties that impact economic performance: definition of errors associated with the model predicted values, typical disturbances that occur during operation and implementation errors for controlled variables (associated with measurement errors);
4. Offline optimization: solving the optimization problem at the nominal operating point, considered as the operating points with known disturbances ( $d^*$ ) and, if possible, also solving the problem for other disturbances values ( $d$ ), in agreement to the previous step;
5. Identify candidates for controlled variables: from the previous step, it is verified which constraints were active for the values of disturbances ( $d$ ) tested. In the case of active constraints, these are applied directly, reducing the degrees of freedom. Some desired characteristics of the controlled variables should also be considered in this step, as follows:
  - the controlled variables should be weakly dependent on disturbances;
  - the controlled variables should be easy to measure and control (in a practical way);
  - the controlled variables should be affected by the manipulated variables.
6. Evaluation of loss: the economic loss, defined in Equation 2.88 should be calculated for the possible set of controlled variables with fixed setpoints.

7. Further analysis and selection: based on the results obtained in the previous steps, the controlled variables are selected, typically the ones with lower acceptable loss.

The procedure described above uses a steady-state model of the process to obtain controlled variables, from which offline optimization is carried out, including the disturbances and uncertainties to be considered, which must be foreseen in the formulation of the problem in question. Additionally, the presented approach can be classified as a method of exhaustive search since the optimization problem needs to be solved a considerable number of times.

The advantage of the above procedure is the convergence to the optimal set of controlled variables since all the possibilities are analyzed. However, for the same reason, the computational evaluation of all these possibilities when the problem under analysis has many candidate variables becomes unfeasible. Therefore, for complex industrial units in which a large number of control variables and degrees of freedom are present, the procedure may require a high computational time and cost (SCHULTZ, 2015).

In general, the choice of controlled variables, according to JÄSCHKE and SKOGESTAD (2011), is described as:

$$\mathbf{c} = \mathbf{H}_{SO}\mathbf{y}_p \quad (2.89)$$

where  $\mathbf{H}_{SO} \in \mathbb{R}^{n_u \times n_y}$  is called the selection matrix. ALSTAD and SKOGESTAD (2007) proposed a methodology based on the null-space concept for determining the controlled variables set  $\mathbf{c}$ , which was called the null-space method. Indeed, its name is related to the fact that the matrix  $\mathbf{H}_{SO}$  belongs to the null-space of the sensitivity of output variables with respect to the disturbances, calculated at the optimum point of the plant. Mathematically:

$$\mathbf{H}_{SO}\mathbf{F} = 0 \quad (2.90)$$

where  $\mathbf{F}$  is the sensitivity matrix of the output variables with respect to the disturbances, calculated at the optimum point of the plant, given by:

$$\mathbf{F} = \nabla_{\mathbf{d}}\mathbf{y}^* \quad (2.91)$$

Assuming that the mapping of the optimal output variables as a function of the disturbances exists in the neighborhood of the nominal value of the disturbances, it is possible to write the following equation based on Taylor Series:

$$\mathbf{y}^*(\mathbf{d}) \approx \mathbf{y}^*(\mathbf{d}^*) + \mathbf{F}(\mathbf{d} - \mathbf{d}^*) \quad (2.92)$$

Alternatively, in terms of the controlled variables, multiplying both sides, on the left, by  $H_{SO}$ :

$$\mathbf{c}^*(\mathbf{d}) \approx \mathbf{c}^*(\mathbf{d}^*) + \mathbf{H}_{SO}\mathbf{F}(\mathbf{d} - \mathbf{d}^*) \quad (2.93)$$

However, if  $H_{SO}$  belongs to the null-space of  $F$ , then, necessarily:

$$\mathbf{c}^*(\mathbf{d}) \approx \mathbf{c}^*(\mathbf{d}^*) \quad (2.94)$$

That is, for any disturbance  $\mathbf{d}$ , the value of the controlled variables will be equal to the value at the optimum point so that it is not necessary to change the values of its setpoints.

A disadvantage of the methodology proposed by ALSTAD and SKOGESTAD (2007) is the assumption that the measured variables do not present measurement noise. In fact, in the situation where noisy measurements are present, the methodology developed does not result in the best possible solution (JÄSCHKE and SKOGESTAD, 2011). In subsequent work, ALSTAD *et al.* (2009) extended the methodology developed, taking into account the measurement noise.

In practice, the hypothesis of perfect measurements is not valid, and it is necessary to include the measurement errors for the determination of  $H_{SO}$ , which is contemplated in the extended null-space method. However, the methodology is only valid when the number of measurements is greater than the sum of the number of inputs and process disturbances. Additionally, the relationship between the rejection of disturbances and measurement noise is not compromised, being a disadvantage of the method (JÄSCHKE *et al.*, 2017).

In order to obtain a combination matrix  $H_{SO}$  that guarantees the compromise between the rejection of disturbances and noise, some methodologies, called minimum loss methods, were developed (ALSTAD *et al.*, 2009; HELDT, 2010; KARIWALA, 2007; KARIWALA *et al.*, 2008), which led to the same results (JÄSCHKE *et al.*, 2017), providing an expression for the array  $H_{SO}$ :

$$\mathbf{H}_{SO} = \mathbf{G}_y(\mathbf{y}_p\mathbf{y}_p^T)^{-1} \quad (2.95)$$

where  $G_y$  is the transfer function matrix of the process.

GRACIANO *et al.* (2015) proposed a complete RTO framework applying SOC concepts to select the controlled variables of the supervisory control layer. This layer was in charge of tracking the self-optimizing variables setpoints and keep the active constraints within a zone. The authors shown that the RTO with SOC concepts presented a higher profit than the classic RTO in closed loop.

### 2.2.4.2 Necessary Conditions of Optimality Tracking

The strategy of NCO tracking was initially proposed for batch processes, aiming to lead the process dynamically to its optimum condition (FRANCOIS *et al.*, 2005; SRINIVASAN *et al.*, 2003a,b). Subsequent works extended the concept of NCO tracking for continuous processes (JÄSCHKE and SKOGESTAD, 2011; SRINIVASAN and BONVIN, 2007; SRINIVASAN *et al.*, 2008).

In the NCO tracking approach, the optimization problem is rewritten as a feedback control loop, where the controlled variable is the gradient of the economic objective function. In order to satisfy the first-order optimality condition, the gradient of the objective function should be null at the optimum. Thus, the setpoint of the controlled variable in the NCO tracking is null (JÄSCHKE and SKOGESTAD, 2011). Figure 2.2 illustrates the how the NCO tracking strategy works.

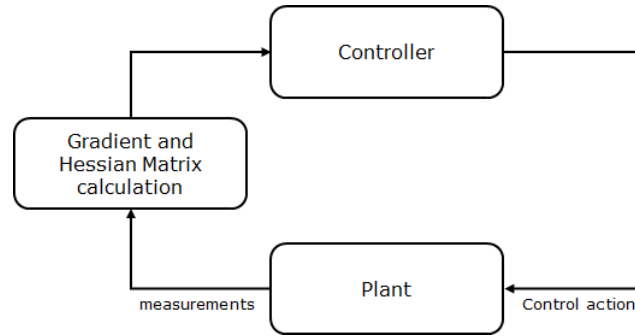


Figure 2.2: NCO tracking structure. Adapted from JÄSCHKE and SKOGESTAD (2011).

The NCO tracking strategy is primarily motivated by the fact that the majority of chemical process plants are equipped with instrumentation and regulatory control systems, thus enabling a large set of available data and measurements. Thus, this approach proposes the use of measurements to perform optimization in real time, being independent of models for successive iterations of the method. However, the strategy is not entirely independent of models, as discussed below.

The formulation of the NCO tracking strategy is based on the problem posed accordingly to Equation 2.96.

$$\begin{aligned}
 \mathbf{u}^* &= \arg \min_{\mathbf{u}} \quad \Phi_p = \phi_{ec}(\mathbf{u}, \mathbf{d}) \\
 \text{s.t.} \quad & \mathbf{G}_p = \mathbf{g}(\mathbf{u}, \mathbf{d}) \leq \mathbf{0}
 \end{aligned} \tag{2.96}$$

where  $\mathbf{u} \in \mathbb{R}^{n_u}$  are the decision variables,  $\phi_{ec} : \mathbb{R}^{n_u} \times \mathbb{R}^{n_d} \rightarrow \mathbb{R}$  is the economic objective function and  $\mathbf{g} : \mathbb{R}^{n_u} \times \mathbb{R}^{n_d} \rightarrow \mathbb{R}^{n_g}$  are the constraints, which also includes equality constraints, and  $\mathbf{d} \in \mathbb{R}^{n_d}$  is the disturbance vector.

A point worth mentioning about the NCO tracking strategy is about the disturbances ( $\mathbf{d}$ ), which, although they may vary over time, the formulation of the strategy is based on the assumption of pseudo steady-state. In this case, the disturbances do not influence the set of active constraints, which may not be true. Indeed, processes in which the set of active constraints are weakly dependent on the disturbances represent an good possibility of applying this technique.

To determine the set of active constraints at the optimum point, considering a set of nominal disturbances, the formal optimization problem is solved, using a model of the process for that. Thus, although the NCO tracking is said to be model-independent, this statement is not valid.

After determining the set of active constraints at the optimum point, the active constraints are directly applied to the plant. Thus, it is only necessary to determine the value of the inactive  $\mathbf{u}$  variables so that this problem becomes an unconstrained optimization problem. Therefore, the problem in Equation 2.96 is now rewritten according to Equation 2.97, formally eliminating the process variables from the model's equality constraints.

$$\mathbf{u}_{inac}^* = \arg \min_{\mathbf{u}_{inac}} \Phi_p = \phi_{ec}(\mathbf{u}_{inac}, \mathbf{d}) \quad (2.97)$$

where the subscript *inac* is related to the decision variables which are inactive.

Following the formulation proposed by JÄSCHKE and SKOGESTAD (2011), for the sake of notation, a change of variables is introduced, considering the nominal optimal point as a reference.

$$\mathbf{u}'_{inac} = \mathbf{u}_{inac} - \mathbf{u}_{inac}^* \quad (2.98)$$

$$\mathbf{d}' = \mathbf{d} - \mathbf{d}^* \quad (2.99)$$

where  $\mathbf{u}_{inac}^*$  and  $\mathbf{d}^*$  are the inactive decision variables and disturbances at the nominal operating point.

Therefore, the problem in Equation 2.97 is rewritten accordingly to the Equation 2.100.

$$\mathbf{u}'_{inac}{}^* = \arg \min_{\mathbf{u}'_{inac}} \Phi_p = \phi_{ec}(\mathbf{u}'_{inac}, \mathbf{d}') \quad (2.100)$$

Omitting the explicit functional dependence in  $\mathbf{d}'$ , the first-order necessary condition of optimality is imposed:

$$\nabla_{\mathbf{u}'_{inac}} \phi_{ec} = \mathbf{0} \quad (2.101)$$

Applying one step of Newton's method to solve the equivalent problem in Equation 2.101, it is possible to write the following expression:

$$\mathbf{u}'_{inac,k+1} = \mathbf{u}'_{inac,k} - \left[ \nabla^2_{\mathbf{u}} \phi \right]_k^{-1} \left[ \nabla_{\mathbf{u}} \phi \right]_k \quad (2.102)$$

Defining:

$$\mathbf{u}'_{inac,k+1} = \mathbf{u}'_{inac,k} + \Delta \mathbf{u}'_{inac,k} \quad (2.103)$$

where  $\mathbf{u}'_{inac,k}$  are the inactive decision variables updated at iteration  $k$ .

Therefore:

$$\Delta \mathbf{u}'_{inac,k} = - \left[ \nabla^2_{\mathbf{u}} \phi \right]_k^{-1} \left[ \nabla_{\mathbf{u}} \phi \right]_k \quad (2.104)$$

Equation 2.104 is a Newton's method update step, which is exact for a quadratic approximation of the problem in Equation 2.100, also satisfying the NCO represented by Equation 2.101 in one iteration.

In real applications, the update of the control action is not applied in full to avoid instability of the process and sudden control actions. For this, a tuning parameter is inserted in the control action, written as follows (JÄSCHKE and SKOGESTAD, 2011):

$$\mathbf{u}'_{inac,k+1} = \mathbf{u}'_{inac,k} + \beta \Delta \mathbf{u}'_{inac,k} \quad (2.105)$$

where  $\beta \in [0, 1]$  is a tuning parameter of the method.

From Equation 2.104, it is possible to notice that, for the implementation of the control actions, it is necessary to obtain the gradient vector and the Hessian matrix of the economic performance index with respect to the unconstrained decision variables (which is equivalent to the gradient vector and Hessian matrix in reduced space). However, the calculation of these variables represents a challenge, similar to what occurs for the Modifier-Adaptation method.

In terms of applications of the NCO tracking strategy in literature, SRINIVASAN *et al.* (2003a) applied the strategy to a batch bioreactor and compared it to other approaches, such as nominal, robust, and explicit optimization, showing performance advantages when applying the NCO tracking. FRANCOIS *et al.* (2005) applied the methodology to a batch polymerization reactor. SRINIVASAN and BONVIN (2007) applied the method to a semi-batch reactor, and a two-layer optimization strategy was proposed. In the inner layer, an NCO tracking strategy was used. In the outer layer, a process model was updated and used to perform the process optimization to monitor the set of active constraints. If this set

changes, this information is passed to the inner layer, which is updated. SRINIVASAN *et al.* (2008) applied the approach to an isothermal CSTR system, also aiming to include the information about the set of active constraints to the problem. The constrained problem was rewritten as an unconstrained problem by adding penalties in the objective function. In this way, any of the constraints can be active, and, therefore, it is not necessary to update the active constraints set.

BONVIN and SRINIVASAN (2013) highlight that a strong point of the NCO tracking approach is the possibility of combining offline and online tasks. For instance, the numerical optimization based on the plant model to determine the set of active constraints can be carried out offline, while updating the manipulated variables based on the measurements can be online. This last step can be done independently of models, similar to what was proposed in the work of SRINIVASAN and BONVIN (2007).

SUN *et al.* (2016) highlight that a practical restriction for the use of the NCO tracking approach lies in the assumption that the set of active constraints remains unchanged. In order to address this issue, the authors proposed the use of a multiparametric solution. That is, sensitivity analyzes are proposed to characterize the effect of the optimal solution with respect to small variations in the parameter values (disturbances). Another possibility is the use of parametric programming, in which the characterization of the solution is analyzed for a wide range of parameter values. This technique was applied to linear dynamic systems.

## 2.2.5 Hybrid RTO

The Hybrid RTO (H-RTO) (VALLURU *et al.*, 2015) arises aiming to eliminate the disadvantage of classic RTO strategies in waiting for the steady-state condition to estimate parameters and optimize the process. In the H-RTO strategy, the parameter estimation step is carried out online and integrated into the optimization cycle, thus avoiding waiting for the steady-state condition (DELOU *et al.*, 2021; KRISHNAMOORTHY *et al.*, 2018; MATIAS and LE ROUX, 2018, 2020; SANTOS *et al.*, 2021; VALLURU *et al.*, 2015).

Essentially, this strategy is based on a dynamic process model which has its parameters updated through a dynamic observer, such as Extended Kalman Filter (EKF) (SIMON, 2006). Thus, the transient measurements can be applied to update the model parameters and state estimation, not depending on steady-state data. Then, a steady-state model version can be obtained and applied to the steady-state optimization problem from the updated dynamic model.

In terms of structure, the main difference of the H-RTO is applying a dynamic state and parameter estimation step instead of a steady-state identification step

considered in classic RTO approach. Of course, in this case, an implicitly assumption is that a dynamic model is available.

In RTO strategies, when a dynamic model is applied for optimization purposes, it gives rise to the Dynamic RTO (D-RTO), which provides an optimal input trajectory. In this last approach, the optimization problem, the state estimation and parameter estimation steps are based on the dynamic model. Accordingly to KRISHNAMOORTHY *et al.* (2018), although the usage of dynamic model eliminates the steady-state detection, solving a nonlinear dynamic optimization problem still may be challenging for large-scale systems. Thus, steady-state RTO is still prevalent for industrial applications.

However, in the H-RTO, the optimization problem is still based on a steady-state model, which is an intermediate (or hybrid) approach between RTO and D-RTO. KRISHNAMOORTHY *et al.* (2018) and MATIAS and LE ROUX (2018) evidenced that the H-RTO strategy presents enhanced economic performance when compared to classic RTO, with a lower computational cost than D-RTO. Figure 2.3 compares the structures of classic RTO, D-RTO and H-RTO strategies.

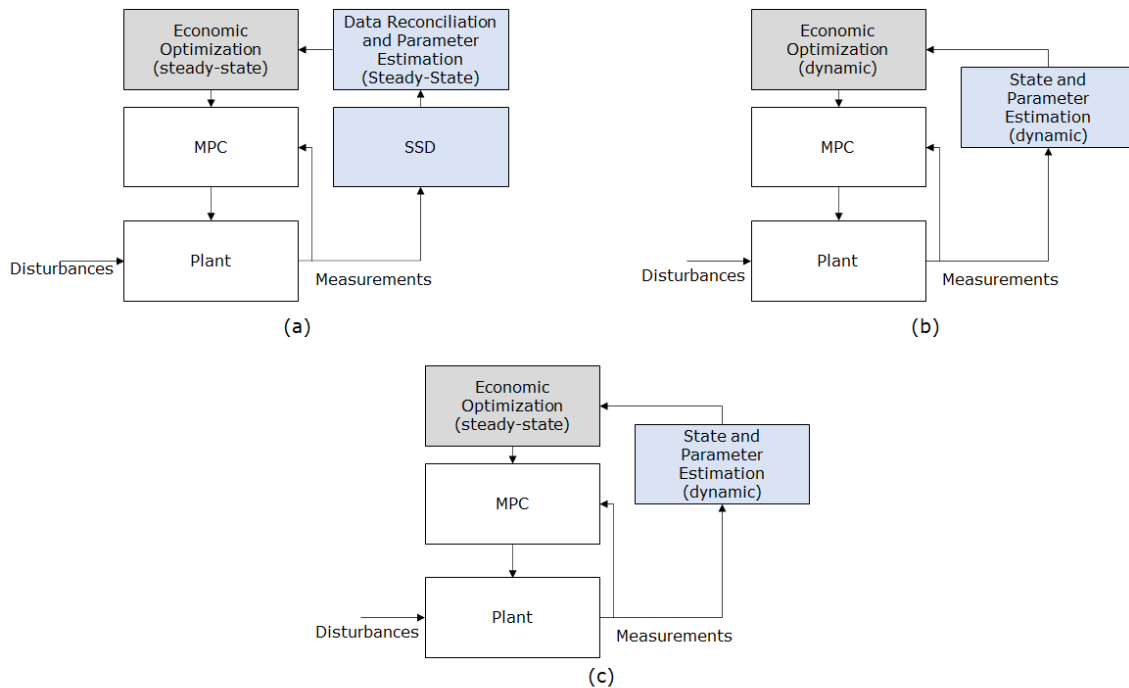


Figure 2.3: Comparison of (a) Classic RTO, (b) D-RTO and (c) H-RTO structures. Adapted from KRISHNAMOORTHY *et al.* (2018).

The works of MATIAS and LE ROUX (2018) and KRISHNAMOORTHY *et al.* (2018) were published almost concurrently and presented a very similar methodology, which in practice were equivalent to the first work of VALLURU *et al.* (2015). MATIAS and LE ROUX (2018) named the strategy as Real-time Optimization with Persistent Parameter Adaptation (ROPA) and KRISHNAMOORTHY

*et al.* (2018) named the strategy H-RTO. Here, the name H-RTO is applied since it is a hybrid approach between RTO and D-RTO.

In the work of MATIAS and LE ROUX (2018), the authors applied the H-RTO approach to the Willian-Otto Reactor and compared it to the RTO strategy. The authors showed that H-RTO outperformed the RTO strategy in terms of economic profit since a continuous adjustment of the optimal setpoints occurs, avoiding the steady-state detection step and inherently delay on the RTO cycle. They also highlighted that H-RTO could destabilize the plant depending on the tuning parameters of the methodology, such as the execution frequency, optimal decision filtering, and EKF tuning parameters. The authors claim that the tuning phase of the methodology should not be neglected. Here, it is essential to highlight that this activity is commonly accomplished through trial and error.

In the work of KRISHNAMOORTHY *et al.* (2018), the authors applied the H-RTO approach to an oil and gas production network and compared it to RTO, and D-RTO approaches. The authors claimed that H-RTO presents a similar performance to D-RTO, based on the case study of their work while enabling lower computational time. The authors discussed applying dynamic optimization instead of static optimization since, in H-RTO, a dynamic model is at hand, showing a lack of clear understanding of when static is sufficient or in what conditions dynamic optimization is justified. Of course, processes that are inherently dynamic or involve transient operations, such as batch processes, cyclic operations, and start-up and shut-down conditions, may benefit from dynamic optimization. The authors also claim that in dynamic optimization problems, the size of the problem may impact computational time, which may impose limitations on how often the optimal setpoints can be updated, leading to performance degradation or closed-loop instabilities.

VALLURU and PATWARDHAN (2019) applied the methodology originally proposed in VALLURU *et al.* (2015) to three case studies, namely the Williams-Otto Reactor, a CSTR with input multiplicity, and an ideal reactive distillation column. The authors highlighted that the proposed approach is restricted to a single unit, and a research direction is expanding the methodology to a process plant consisting of multiple unit operations.

SANTOS *et al.* (2021) proposed an H-RTO framework such that the objective function of economic optimization is one of the controlled variables in an adaptive linear MPC approach. The controller objective was tracking a setpoint for the economic objective function, which comes from the H-RTO, which applied an Unscented Kalman Filter for state and disturbance estimation. The authors also proposed the usage of soft constraints in the MPC, such that the output variables were kept within a desirable zone. The proposed approach was applied to the

Williams-Otto reactor benchmark.

CURVELO *et al.* (2021) evaluated the H-RTO performance in a wide range of examples with different transient behaviors. The authors showed that H-RTO presented similar results to D-RTO regarding economic objectives. However, care should be taken for systems with long delays, which may destabilize the system depending on the mismatch between the model and plant dead time. They claim that a dead-time compensation methodology could be applied to avoid this scenario, but no other results were shown.

MATIAS and LE ROUX (2020) proposed a strategy, namely Asynchronous ROPA (AsROPA), aiming to plant-wide optimization. Indeed, when dealing with H-RTO with multiple unit operations, the problem shifts to obtaining a dynamic model of the entire plant, which can be challenging and time-consuming. In that sense, the authors proposed to decompose the plant-wide model into submodels and, depending on their characteristics, their parameters are updated using either online or steady-state estimators. The authors proposed a systematic approach based on the analysis of plant historical data. However, this step is crucial and not straightforward.

As presented, the H-RTO depends on the plant's dynamic model. However, in practical RTO implementations, it is common to obtain a rigorous model in the stationary layer (RTO) firstly and, for the MPC controller, to obtain an approximation from empirical models, typically linear. Following this methodology, implementing the H-RTO strategy would not be possible since the parameters of the dynamic layer to be estimated do not match the parameters of the stationary layer. To overcome it, DELOU *et al.* (2021) proposed an H-RTO framework assuming that only a steady-state model is at hand. A dynamic model is developed by combining the steady-state model and a linear identified model using a Hammerstein model structure. In addition, DELOU *et al.* (2021) also expanded the concept of the work of GRACIANO *et al.* (2015) by mean of considering SOC variables in the MPC and applying the H-RTO concept based on the Hammerstein approximate dynamics instead of the classic RTO.

(MATIAS *et al.*, 2022) were the first authors to apply the methodology practically. The authors applied the H-RTO, RTO, and D-RTO methodologies to an experimental oil rig, confirming the economic improvement of the H-RTO compared to RTO and a similar result compared to D-RTO.

In summary, H-RTO is a promising direction since it is a simpler approach than D-RTO in terms of computational implementation (steady-state optimization problem versus dynamic optimization problem) and enables the economic optimization during transient periods, reducing the suboptimal periods that exist between steady-state optimizations in RTO. However, the challenge is still

obtaining an accurate dynamic model, especially for a plant-wise optimization scenario. Also, since H-RTO is a model-based strategy, the technique is subject to model adequacy criteria, which was not the focus of the previous works.

## 2.3 Model Predictive Control (MPC)

The Model Predictive Control (MPC) is an advanced control strategy commonly applied in the supervisory control layer of the chemical process, as presented in Figure 1.1. When applied in a hierarchical control structure designed for economic optimization, the MPC controller aims to lead the process to its optimum point and keep the controlled variables at their setpoints, determined by the RTO layer. The MPC algorithm applies a dynamic model for predicting the behavior of the controlled variables as a function of the manipulated variables. Based on that model, an optimization problem is solved to calculate the manipulated variables to be applied to the process, subject to constraints.

It is worth mentioning that this strategy is based on the optimal control theory and has been successfully applied in industrial applications since the 70's. Some important application and development works must be highlighted, such as the work of RICHLET *et al.* (1978) that presented the Model Predictive Heuristic Control algorithm later became known as Model Algorithmic Control (MAC). Also, the work of CUTLER and RAMAKER (1980) introduced the Dynamic Matrix Control algorithm. Thus, the MPC controller represents a widely accepted and used strategy by the industry (ELLIS *et al.*, 2014). Indeed, one of the main reasons for the MPC algorithm's successful applications in chemical processes is the controller's ability to deal with coupled variables in a Multiple Input Multiple Output (MIMO) system (FORBES *et al.*, 2015).

The MPC formulation is based on an optimization problem, aiming to minimize an objective function (controller cost) over a given time horizon, in general finite, considering a model to predict the process's dynamics. The following op-

timization problem gives a typical formulation of the MPC:

$$\begin{aligned}
\mathbf{u}^*(t) = \arg \min_{\mathbf{u} \in \Delta(S)} \quad & \phi_{MPC} = \int_{t_k}^{t_k+P} \left[ \|\mathbf{y} - \mathbf{y}_{SP}\|_{\mathbf{W}_y}^2 + \|\mathbf{u} - \mathbf{u}_{SP}\|_{\mathbf{W}_u}^2 + \|\Delta\mathbf{u}\|_{\mathbf{W}_{\Delta u}}^2 \right] dt \\
\text{s.t.} \quad & \dot{\mathbf{x}} = \mathbf{f}_{MPC}(\mathbf{x}, \mathbf{u}, \boldsymbol{\theta}), \\
& \mathbf{y}(t) = \mathbf{h}(\mathbf{x}(t), \mathbf{u}(t)), \\
& \mathbf{G}(\mathbf{x}(t), \mathbf{u}(t)) \leq \mathbf{0}, \\
& \mathbf{u}_{min} \leq \mathbf{u} \leq \mathbf{u}_{max}, \\
& \mathbf{y}_{min} \leq \mathbf{y} \leq \mathbf{y}_{max}, \\
& \Delta\mathbf{u}_{min} \leq \Delta\mathbf{u} \leq \Delta\mathbf{u}_{max}, \\
& \mathbf{x}(t_k) = \mathbf{x}_k
\end{aligned} \tag{2.106}$$

where  $\mathbf{W}_y \in \mathbb{R}^{n_y \times n_y}$  is the positive semi definite diagonal matrix of controlled variables weighting factors,  $\mathbf{W}_u \in \mathbb{R}^{n_u \times n_u}$  is the positive semi definite diagonal matrix of manipulated variables weighting factors and  $\mathbf{W}_{\Delta u} \in \mathbb{R}^{n_u \times n_u}$  is the positive semi definite diagonal matrix of manipulated variables movement suppression factors. The decision variables of the problem are the manipulated variables trajectory ( $\mathbf{u} \in S(\Delta)$ ). In addition,  $S(\Delta)$  represents a set of piecewise constant functions with period  $\Delta$ , and  $P$  is the time horizon. The dynamic trajectories of state variables  $\mathbf{x}(t)$  are predicted using a dynamic model represented by  $\mathbf{f}_{MPC}$ , with model parameters  $\boldsymbol{\theta} \in \mathbb{R}^{n_\theta}$ .  $\mathbf{x}_k$  is the state vector measured or estimated at the current time  $t_k$ . The equations  $\mathbf{G}$  are constraints imposed on states and manipulated variables and  $\mathbf{h}$  represents the relationship between state and output variables.

In Equation 2.106, the operator  $\|\cdot\|_M^2$  is used to denote a square of a weighted Euclidean norm of a vector, where  $\mathbf{M}$  is a positive semidefinite matrix (i.e.,  $\|\cdot\|_M^2 = \cdot^T \mathbf{M} \cdot$ ). Based on that, it is possible to notice that the objective function of the MPC controller is quadratic and is generally written considering three main terms. The first term ( $\|\mathbf{y} - \mathbf{y}_{SP}\|_{\mathbf{W}_y}^2$ ) represents deviations of the controlled variables in relation to its setpoints, represented by  $\mathbf{y}_{SP}$ . These values are typically calculated by an RTO layer above the MPC controller.

The second term,  $\|\mathbf{u} - \mathbf{u}_{SP}\|_{\mathbf{W}_u}^2$ , in an analogous way, represents the deviations of the manipulated variables from its reference values,  $\mathbf{u}_{SP}$ , which can also be calculated by the RTO layer.

The last term,  $\|\Delta\mathbf{u}\|_{\mathbf{W}_{\Delta u}}^2$ , represents the MPC control action effort, which compares the control action at the current iteration with the previous one.

The problem in Equation 2.106 is a dynamic optimization problem. The so-

lution of this problem is an optimal dynamic trajectory that leads the system to its reference values (setpoints). For practical applications, typically, the Receding Horizon strategy is commonly applied, which also rewrites the problem in Equation 2.106 in its discrete version, as presented in problem 2.107 (ABRAHAM *et al.*, 1999; MACIEJOWSKI, 2000; TATJEWSKI, 2007).

$$\begin{aligned}
\mathbf{u}^* = \arg \min_{\Delta \mathbf{u}} & \sum_{i=1}^P \left( \mathbf{y}_{k+i|k} - \mathbf{y}_{SP,k+i|k} \right)^T \mathbf{W}_y \left( \mathbf{y}_{k+i|k} - \mathbf{y}_{SP,k+i|k} \right) + \\
& \sum_{i=1}^M \left( \mathbf{u}_{k+i|k} - \mathbf{u}_{SP,k+i|k} \right)^T \mathbf{W}_u \left( \mathbf{u}_{k+i|k} - \mathbf{u}_{SP,k+i|k} \right) + \\
& \sum_{i=0}^{M-1} \Delta \mathbf{u}_{k+i|k}^T \mathbf{W}_{\Delta u} \Delta \mathbf{u}_{k+i|k} \\
\text{s.t.} & \quad \forall i = 0, \dots, P-1, \\
& \quad \Delta \mathbf{u}_{k+i|k} = \mathbf{u}_{k+i|k} - \mathbf{u}_{k|k}, \\
& \quad \mathbf{x}_{k+i+1|k} = \mathbf{f}_{MPC}(\mathbf{x}_{k+i|k}, \mathbf{u}_{k+i|k}, \boldsymbol{\theta}), \\
& \quad \mathbf{y}_{k+i+1|k} = \mathbf{h}(\mathbf{x}_{k+i+1|k}, \mathbf{u}_{k+i+1|k}) + \boldsymbol{\epsilon}_k, \\
& \quad \mathbf{G}(\mathbf{y}_{k+i|k}, \mathbf{u}_{k+i|k}) \leq \mathbf{0}, \\
& \quad \mathbf{u}_{min} - \mathbf{u}_{k+i|k} \leq \Delta \mathbf{u}_{k+i|k} \leq \mathbf{u}_{max} - \mathbf{u}_{k+i|k}, \\
& \quad \Delta \mathbf{u}_{min} \leq \Delta \mathbf{u}_{k+i|k} \leq \Delta \mathbf{u}_{max}, \\
& \quad \mathbf{y}_{min} \leq \mathbf{y}_{k+i+1|k} \leq \mathbf{y}_{max}, \\
& \quad \Delta \mathbf{u}_{k+i|k} = \mathbf{0} \quad \forall i \geq M, \\
& \quad \mathbf{x}_{k|k} = \mathbf{x}_k
\end{aligned} \tag{2.107}$$

where  $P$  and  $M$  are the prediction and control horizons, respectively.  $\Delta \mathbf{u} \in \mathbb{R}^P$  is the decision variable which represents the sequence of input increments, and then, the receding horizon principle implies that only the first increment is applied, such that  $\mathbf{u}_{k|k} = \mathbf{u}_{k-1|k} + \Delta \mathbf{u}_{k|k}$ .  $\boldsymbol{\epsilon} \in \mathbb{R}^{n_y}$  is a disturbance model, included to deal with unmeasured disturbances in addition to model uncertainties, considered as an output correction term.

It is possible to notice that the MPC formulation has tuning parameters, which are the weighting matrices  $\mathbf{W}_y$ ,  $\mathbf{W}_u$ , and  $\mathbf{W}_{\Delta u}$ , and the prediction ( $P$ ) and control horizons ( $M$ ). For the discrete-time formulation, the sampling time is another parameter that has to be well selected. Additionally, the formulation presented consider hard constraints in output variables. Several researches have studied how to introduce an extra degree of freedom, which is done by considering slack variables in the constraints, yielding soft-constraints (MAYNE *et al.*, 2000), aiming to the solution feasibility.

The solution of the problem in Equation 2.107 consists in  $M$  control actions for each manipulated variable. The dynamic model of the MPC is evaluated from an initial condition corresponding to the last plant measurement until the time instant corresponding to the prediction horizon  $P$ . As the value of  $P$  is always greater than  $M$ , the last control action  $\mathbf{u}_M$  is repeated until the prediction horizon instant, as follows:

$$\mathbf{u}^* = \left[ \mathbf{u}_1, \mathbf{u}_2, \underbrace{\mathbf{u}_M, \dots, \mathbf{u}_M}_{\substack{P-M \\ \text{elements equals to } \mathbf{u}_M}} \right] \quad (2.108)$$

The state and output variables are calculated at  $P$  intervals, as follows:

$$\mathbf{x} = [\mathbf{x}_1, \dots, \mathbf{x}_P] \quad (2.109)$$

$$\mathbf{y} = [\mathbf{y}_1, \dots, \mathbf{y}_P] \quad (2.110)$$

Although  $M$  control actions are calculated in the receding horizon strategy, only the first action is applied to the plant. After a sampling time, the problem 2.107 is solved again, applying only the first action of the new solution trajectory (MACIEJOWSKI, 2000). This strategy is applied for rejecting disturbances that may occur within a sample time. This strategy also allows a closed-loop control system (feedback control system) and compensates the errors in predicted values obtained using the MPC dynamic model.

MAYNE *et al.* (2000) define the MPC as a form of control in which the current control action is determined by solving, at each sampling instant, a finite horizon open-loop optimal control problem, using the current state of the plant as the initial condition, yielding an optimal control sequence and the first control action in this sequence is applied to the plant, although infinite horizons strategies also exist (ODLOAK, 2004).

Until now, any assumption has been mentioned about the MPC model. Typically, a linear dynamic model is used, resulting in a Quadratic Programming problem (QP problem). Furthermore, if there are no constraints, it is possible to obtain an analytical solution for the control actions. When the model used is nonlinear, the controller is now called NMPC. In this case, the resolution of the system is carried out by nonlinear programming algorithms, such as Sequential Quadratic Programming (SQP).

Also, the MPC model should always be as simple as possible, aiming at the slightest computational effort. In literature, several models forms have been explored, such as step response, transfer functions, or state-space forms. The use of models based on finite impulse response (FIR), autoregressive moving average

with exogenous inputs model (ARMAX), and Autoregressive with exogenous input model has also been applied (BARAMOV and HAVLENA, 2005; HEIRUNG *et al.*, 2015; LIU *et al.*, 2012; XIE *et al.*, 2012). However, as the chemical processes are typically nonlinear, the linear models are generally identified near a nominal point of operation, or there is a linearization step of nonlinear models around one or more points of operation.

Many factors can lead to an accuracy loss, such as a change of an operational point or other phenomena that happened in the process, like the catalyst deactivation, heat exchangers fouling, or even equipment modifications that occurred in an industrial unit. The MPC models need to be assessed and updated to ensure their predictive ability is still at an acceptable level. If the model errors start to increase, an automatic identification step for model updating would greatly aid in the proactive sustainment of MPC performance. Another strategy to deal with the modeling errors is to correct the model predictions using the plant measurements once it becomes available through a bias update scheme (FORBES *et al.*, 2015).

Applying linear models in MPC may be limited to regions around the reference point where the model was previously identified due to process' nonlinearities. There are techniques available to deal with these issues and increase the prediction accuracy and the ability to represent the process not limited to a single operational point. A possible solution is to apply different models depending on the input variables ranges, similar to the gain scheduling technique. Another possibility is to apply NMPC controllers, which would improve the accuracy of the model. However, it would increase the computational cost of executing the cycles and the complexity of maintenance (ELLIS *et al.*, 2014; FORBES *et al.*, 2015; LEE, 2011).

The formulation presented in Equations 2.106 and 2.107 are not unique. Some works includes Infinite Horizon MPC and the usage of soft-constraints, aiming to control feasibility. A comprehensive review regarding MPC formulations are presented in GARCÍA *et al.* (1989), MORARI and H. LEE (1999) and MAYNE (2014). A survey about industrial applications of MPC is presented in QIN and BADGWELL (2003).

## **2.4 Strategies for Integration of RTO and Supervisory Control Layer**

The RTO system commonly applied in the industry is based on a hierarchical control structure. The RTO layer typically uses a rigorous phenomenological

stationary model to obtain the economic optimum point of the process. The optimal solution is passed as setpoints of the controlled variables and the reference values of the manipulated variables to the supervisory control layer. This layer uses advanced control strategies, such as the MPC algorithm, which applies, traditionally, linear models identified from tests in the plant.

However, as the models applied in each layer are different, the predicted values for the optimal operating point are not compatible between the two layers, generating suboptimal or infeasible points. It means that the setpoints provided by the RTO can be inconsistent and unattainable due to the difference between the models.

Another point worth mentioning is the low frequency of execution of the RTO, which is associated with the fact that this layer requires the process to reach steady-state conditions for a new optimization cycle execution. However, transient conditions occur due to the action of disturbances in the process, hindering the execution of RTO. Also, the economic information is not considered during transient periods in the RTO approach, even in situations of transition between optimal setpoints obtained by subsequent RTO cycles.

The RTO and MPC integration approaches are focused on at least one of the drawbacks mentioned before, which are the RTO low frequency or the model mismatch between control and optimization layers. Next, some possible RTO and MPC integration approaches are discussed.

### **2.4.1 Two-stage MPC: LP-MPC and QP-MPC**

The two-stage MPC, also called LP-MPC and QP-MPC, is a possible approach to increase the frequency of RTO cycles and take economic aspects into account during transient periods. This strategy solves a stationary optimization problem formulated as linear (LP) or quadratic (QP) programming, which updates the setpoints to the MPC controller. This step is an intermediate layer between the RTO and MPC. It is based on minimizing the deviations between the MPC setpoints and the optimum point provided by the RTO layer. The model applied in this step is the same as the dynamic MPC layer, enforcing the steady-state condition. The intermediate optimization layer executes cycles at the same frequency as the MPC. This strategy's stability and convergence properties are analyzed in the work of YING *et al.* (1998).

The intermediate optimization problem written as a LP problem is posed as follows (MORSHEDI *et al.*, 1985; YING *et al.*, 1998; YOUSFI and TOURNIER,

1991):

$$\begin{aligned}
\mathbf{y}_{SP-LP}, \mathbf{u}_{SP-LP} = \arg \min_{\mathbf{y}, \mathbf{u}} \quad & \phi_{LP-MPC} := \mathbf{c}_y^T (\mathbf{y} - \mathbf{y}_{SP}) + \mathbf{c}_u^T (\mathbf{u} - \mathbf{u}_{SP}) \\
\text{s.t.} \quad & \mathbf{f}_{MPC}(\mathbf{y}, \mathbf{u}, \mathbf{d}) = \mathbf{0}, \\
& \mathbf{y}_{min} - \epsilon \leq \mathbf{y} \leq \mathbf{y}_{max} + \epsilon, \\
& \mathbf{u}_{min} \leq \mathbf{u} \leq \mathbf{u}_{max}
\end{aligned} \tag{2.111}$$

where  $\mathbf{d}$  is the estimated disturbance,  $\epsilon \in \mathbb{R}^{n_y}$  is used to enforce feasibility,  $\mathbf{c}_y \in \mathbb{R}^{n_y}$  and  $\mathbf{c}_u \in \mathbb{R}^{n_u}$  are economic weights related to the economic optimization objective function, calculated as follows:

$$\mathbf{c}_y = \left. \frac{\partial \phi_{ec}}{\partial \mathbf{y}} \right|_{\mathbf{y}_{SP}, \mathbf{u}_{SP}} \tag{2.112}$$

$$\mathbf{c}_u = \left. \frac{\partial \phi_{ec}}{\partial \mathbf{u}} \right|_{\mathbf{y}_{SP}, \mathbf{u}_{SP}} \tag{2.113}$$

The intermediate optimization problem written as a QP problem is posed as follows (MUSKE and RAWLINGS, 1993):

$$\begin{aligned}
\mathbf{y}_{SP-QP}, \mathbf{u}_{SP-QP} = \arg \min_{\mathbf{y}, \mathbf{u}} \quad & \phi_{QP-MPC} := (\mathbf{y} - \mathbf{y}_{SP})^T \mathbf{c}_y^T \mathbf{c}_y (\mathbf{y} - \mathbf{y}_{SP}) + \\
& (\mathbf{u} - \mathbf{u}_{SP})^T \mathbf{c}_u^T \mathbf{c}_u (\mathbf{u} - \mathbf{u}_{SP}) \\
\text{s.t.} \quad & \mathbf{f}_{MPC}(\mathbf{y}, \mathbf{u}, \mathbf{d}) = \mathbf{0}, \\
& \mathbf{y}_{min} - \epsilon \leq \mathbf{y} \leq \mathbf{y}_{max} + \epsilon, \\
& \mathbf{u}_{min} \leq \mathbf{u} \leq \mathbf{u}_{max}
\end{aligned} \tag{2.114}$$

The LP-MPC or QP-MPC strategies ensure that the setpoints from the RTO layer to the MPC layer are feasible, which is a positive aspect for controller stability. However, it is important to notice that the models applied in the rigorous steady-state and dynamic layers remain different. During the transient period, depending on the range of the input variables, the linear model used in the LP-MPC or QP-MPC layer may not accurately represent the process. Thus, the solutions obtained by the LP-MPC or QP-MPC and the RTO layer can still be different, thus leading to a suboptimal point (YING *et al.*, 1998). Additionally, during the transient period, the optimal point cannot be updated by the RTO layer, which means that a suboptimal period still exists.

In the LP-MPC strategy, as it is a linear programming problem, the solution would be located at a vertex of the polyhedron of constraints. Thus, if the process in question suffers frequent disturbances and presents a model prediction error,

the polyhedron defined by the constraints is also altered and, consequently, does the optimal solution of the LP-MPC problem, leading to poor performance of the controller (QIN and BADGWELL, 2003). At this point, the problem posed as QP-MPC may have an advantage since the optimal solution may not necessarily be on a vertex of the polyhedron constraints.

## 2.4.2 Economic Model Predictive Control (EMPC) and the One-layer Approach

Another strategy proposed to deal with the infrequency of the RTO layer and the lack of compatibility due to the different models employed in each layer consists of solving the economic optimization and the control problem simultaneously, incorporating economic aspects in the formulation of the MPC.

There are still differences between the terms Economic Model Predictive Control (EMPC) and one-layer approach in literature. In ELLIS *et al.* (2017, 2014), the strategy Model-Based Economic Predictive Control (EMPC) replaces the classical MPC objective function with an economic performance index. According to ELLIS *et al.* (2014), the MPC quadratic deviation term does not adequately represent an process's economic performance of the process, since it is impossible to distinguish between a profit or cost term, given that the deviations are always positive and, therefore, misinterpreted as an increase in profit. Therefore, using an economic performance index was proposed to replace the objective function of MPC (AMRIT *et al.*, 2011; ENGELL, 2007).

The strategy of inserting economic aspects in the MPC formulation had already been elaborated previously, as explained in YOUSFI and TOURNIER (1991), DE GOUVÊA and ODLOAK (1996, 1998), and ZANIN *et al.* (2000, 2002). This strategy is typically called a one-layer approach, which receives its name since the steady-state and dynamic layers are solved simultaneously.

Despite the differences in nomenclature presented above, it is possible to perceive that both strategies try to address the disadvantages of the classic RTO formulation in two layers, aiming to deal with disturbances faster than the classic two-layer approach, also considering economic aspects during the transient period, and to ensure compatibility between the RTO and MPC layers.

According to ELLIS *et al.* (2014), the one-layer approach considers an economic term related to the final states of the system (terminal cost), which is de-

scribed as follows:

$$\begin{aligned}
\mathbf{u}^*(t) = \arg \min_{\mathbf{u} \in S(\Delta), \mathbf{u}_s} \quad & \phi_{OL} = w_1 \phi_{MPC} + w_2 \phi_{ec}(\mathbf{y}(t_N), \mathbf{u}_s) \\
\text{s.t.} \quad & \dot{\mathbf{x}}(t) = \mathbf{f}_{OL}(\mathbf{x}(t), \mathbf{u}(t), \boldsymbol{\theta}), \\
& \mathbf{G}(\mathbf{y}(t), \mathbf{u}(t)) \leq \mathbf{0}, \\
& \mathbf{f}_{OL}(\mathbf{x}(t_N), \mathbf{u}_s, \boldsymbol{\theta}) = \mathbf{0}, \\
& \mathbf{y}(t) = \mathbf{h}(\mathbf{x}(t), \mathbf{u}(t)), \\
& \mathbf{u}_{min} \leq \mathbf{u}(t) \leq \mathbf{u}_{max}, \\
& \mathbf{y}_{min} \leq \mathbf{y}(t) \leq \mathbf{y}_{max}, \\
& \mathbf{x}(t_k) = \mathbf{x}_k
\end{aligned} \tag{2.115}$$

where the decision variables of the problem are the manipulated variables trajectory ( $\mathbf{u} \in S(\Delta)$ ) and the manipulated variables at the steady-state condition ( $\mathbf{u}_s$ ). Also, the MPC objective function ( $\phi_{MPC}$ ) was presented in Equation 2.106. In addition,  $w_1$  and  $w_2$  are weighting factors related to the MPC objective function and the economic objective function, respectively. It is important to notice that the subscript  $OL$  is related to the one-layer approach.

On the other hand, the EMPC objective function considers an economic performance index evaluated throughout the system's trajectory, as follows:

$$\begin{aligned}
\mathbf{u}^*(t) = \arg \min_{\mathbf{u} \in S(\Delta)} \quad & \phi_{EMPC} = w_1 \phi_{MPC} + w_2 \int_{t_k}^{t_k+P} \hat{\phi}_{ec}(\mathbf{y}(t), \mathbf{u}(t)) dt \\
\text{s.t.} \quad & \dot{\mathbf{x}}(t) = \mathbf{f}_{EMPC}(\mathbf{x}(t), \mathbf{u}(t), \boldsymbol{\theta}) \\
& \mathbf{y}(t) = \mathbf{h}(\mathbf{x}(t), \mathbf{u}(t)), \\
& \mathbf{G}(\mathbf{y}(t), \mathbf{u}(t)) \leq \mathbf{0}, \\
& \mathbf{u}_{min} \leq \mathbf{u}(t) \leq \mathbf{u}_{max}, \\
& \mathbf{y}_{min} \leq \mathbf{y}(t) \leq \mathbf{y}_{max}, \\
& \mathbf{x}(t_k) = \mathbf{x}_k
\end{aligned} \tag{2.116}$$

where the subscript  $EMPC$  refers to the Economic Model Predictive Control strategy, and  $\hat{\phi}_{ec}$  is an economic objective function evaluated throughout the system's trajectory.

The formulation of the EMPC problem and the one-layer approach can be

written as follows, without loss of generality:

$$\begin{aligned}
\mathbf{u}^*(t) = \arg \min_{\mathbf{u} \in S(\Delta), \mathbf{u}_s} \quad & \phi_{EMPC} = w_1 \phi_{MPC} + w_2 \phi_{ec}(\mathbf{y}(t_N), \mathbf{u}_s) \\
\text{s.t.} \quad & \dot{\mathbf{x}}(t) = \mathbf{f}(\mathbf{x}(t), \mathbf{u}(t), \boldsymbol{\theta}), \\
& \mathbf{G}(\mathbf{y}(t), \mathbf{u}(t)) \leq \mathbf{0}, \\
& \mathbf{f}(\mathbf{y}(t_N), \mathbf{u}_s, \boldsymbol{\theta}) = \mathbf{0}, \\
& \mathbf{u}_{min} \leq \mathbf{u}(t) \leq \mathbf{u}_{max}, \\
& \mathbf{y}_{min} \leq \mathbf{y}(t) \leq \mathbf{y}_{max}, \\
& \mathbf{x}(t_k) = \mathbf{x}_k
\end{aligned} \tag{2.117}$$

where  $f$  is used to represent the dynamic model in the one-layer or EMPC approaches.

Comparing the general formulation in Equation 2.117 to the EMPC and one-layer approach formulations (Equations 2.116 and 2.115, respectively), it is possible to notice that the main difference among them are related to a equality constraint  $\mathbf{f}(\mathbf{y}(t_N), \mathbf{u}_s) = \mathbf{0}$ , which represents a terminal constraint. This constraint imposes that the process should be in a feasible steady-state at the end of the control cycle ( $t_N$ ). In the one-layer approach, the objective function considers the economic performance index at the end of the control cycle ( $t_N$ ), which means that the steady-state is the one with the best economic performance at  $t_N$ . In the EMPC formulation, the economic performance is evaluated during the process trajectory, guaranteeing the minimization along the trajectories of the control actions imposed on the process.

Although the formulations presented in Equations 2.115 and 2.116 are conceptually distinct, referring to the classic functional costs presented in dynamic optimization problems, it is possible to represent them in the Bolza, Lagrange, and Mayer forms. The Lagrange problem represents the term of the integral objective function, while the Mayer problem represents only the terminal cost term. The Bolza problem combines these two problems: the sum of Mayer and Lagrange terms. However, the problem representation in Mayer or Lagrange forms is as general as the Bolza form, and the problems can even be rewritten and become equivalent (ALMEIDA NETO, 2011). Thus, it is not a limitation to represent the economic term as a cost in the final time instead of the integral term.

Some initial approaches included the economic term in the MPC by adding a linear term into the objective function of the MPC controller (YOUSFI and TOURNIER, 1991) or a linearized term of the economic objective function (DE GOUVÊA and ODLOAK, 1996). Despite the simple formulation, this strategy may not represent the economic problem of the real process, since this op-

timization problem may be nonlinear. In addition, according to DE GOUVÊA and ODLOAK (1998), these formulations can lead the closed-loop controller to instability.

Aiming to deal with nonlinear processes, DE GOUVÊA and ODLOAK (1998) included a nonlinear term associated with the economic objective function in the MPC objective function. Although the economic term was nonlinear, the controller is still based on a linear identified model.

ENGELL (2007) presented a formulation more adherent to EMPC strategy, applied to a simulated moving bed (SMB) separation system, which consisted of four manipulated variables. In that work, the author concluded that the strategy was promising. However, with some issues to be considered, such as its stability.

DE SOUZA *et al.* (2010) proposed to include the gradient of the economic objective function to the MPC original cost function. In this way, if a small perturbation  $\Delta \mathbf{u}$  is added to the control action  $\mathbf{u}$ , the first-order approximation of the economic objective function gradient is written as follows:

$$\zeta_{\mathbf{u}+\Delta \mathbf{u}} = \nabla_{\mathbf{u}} \phi_{ec}(\mathbf{u} + \Delta \mathbf{u}) = \nabla_{\mathbf{u}} \phi_{ec}(\mathbf{u}) + \nabla^2_{\mathbf{u}} \phi_{ec}(\mathbf{u}) \Delta \mathbf{u} \quad (2.118)$$

where  $\zeta_{\mathbf{u}+\Delta \mathbf{u}}$  represents the first-order approximation of the economic objective function gradient at  $\mathbf{u} + \Delta \mathbf{u}$  and  $\Delta \mathbf{u}$  are the manipulated variables. It should be noticed that the objective function  $\phi_{ec}$  is calculated based on a steady-state model of the process, typically non-linear and rigorous.

Knowing that the economic optimal point is the operational point that satisfies the condition of the null gradient vector, the vector  $\zeta$  can be considered as a vector of deviations from a reference point, so this vector must be lead to the null value by the control strategy. Therefore, the strategy proposed by DE SOUZA *et al.* (2010) consists of including the term  $\zeta$  as a penalty in the objective function of the MPC, written as follows:

$$\phi_{OL} = \phi_{MPC} + \zeta_{\mathbf{u}+\Delta \mathbf{u}}^T \mathbf{P} \zeta_{\mathbf{u}+\Delta \mathbf{u}} \quad (2.119)$$

where  $\mathbf{P}$  is a positive semi definite matrix (matrix of weights).

One of the advantages of the strategy proposed by DE SOUZA *et al.* (2010) is that the resulting problem when applying linear models for process prediction is a QP problem. PORFÍRIO and ODLOAK (2011) succeeded in applying the strategy proposed by DE SOUZA *et al.* (2010) in a Petrobras' xylene distillation unit.

On the other hand, as a disadvantage of the strategy, the penalty term associated with economic performance requires that the objective function be convex. Otherwise, if the problem presents saddle points, the penalty term is null since

the gradient is null. However, it is not an optimal operating point.

According to ALVAREZ and ODLOAK (2012), another disadvantage of the strategy of DE SOUZA *et al.* (2010) is the lack of stability of the one-layer approach. The additional term in the objective function, represented by Equation 2.119, is updated at each iteration, which can act as a disturbance and lead to controller instability.

In order to address the two disadvantages mentioned before, ALVAREZ and ODLOAK (2012) proposed an integration strategy between the RTO and MPC layers, adding the gradient term to the MPC objective function. However, instead of using the objective economic function to calculate the gradients, a convex function is built, which consists of the difference between the control variable and the optimal setpoints provided by the RTO. This function is written as:

$$F(\mathbf{u}) = \sum_{i=1}^{n_u} K_i (u_i - u_{SPi})^2 \quad (2.120)$$

Thus, the above function is convex, and the gradient is null when the control actions are equal to the values provided by the RTO layer. Thus, the strategy translates into a penalty for deviations from the setpoints provided by the RTO, so that the controller's aim to make them null. Also, the authors considered a zone control strategy for the output variables (GONZÁLEZ and ODLOAK, 2009), such that its setpoints are decision variables of the MPC problem. It is important to highlight that the strategy proposed by ALVAREZ and ODLOAK (2012) is interesting if the decision variables optimal values are kept constant or known *a priori*. However, in practice, the economic optimization problem might need to be solved due to disturbances.

ALAMO *et al.* (2014) studied the strategy proposed by DE SOUZA *et al.* (2010), focusing on an approximation for gradient calculation, aiming to reduce computational cost. The proposed methodology was applied to an FCC unit case study, presenting an execution time three times lower than the original strategy.

RIBEIRO and SECCHI (2019) proposed a methodology for obtaining dynamic models to be applied in NMPC and D-RTO based on Hammerstein models, such that a combination of an identified steady-state model of the process based on polynomial functions and analytical expressions corresponding to the solution of invariant linear dynamic systems were applied. The proposed methodology yields analytical expressions of the dynamic model, which have the main benefit of computational time reduction. The authors also claim the possibility of application in EMPC approach.

A comprehensive review on the subject is presented in ELLIS *et al.* (2014). The possible RTO and MPC integration formulations are presented, as well as aspects

of stability, the use of nonlinear models, and their performance. More recently, ELLIS *et al.* (2017) published a book with theoretical and practical aspects of the EMPC, including aspects of closed-loop stability, associated computational cost, and state estimation.

A fundamental assumption related to designing and applying an EMPC approach is that a dynamic model is available. Some recent research has been done regarding data-driven approaches applied to EMPC formulation. ALANQAR *et al.* (2015) proposed using a Lyapunov-based EMPC scheme formulated with multiple empirical models, where linear time-invariant state-space models were applied. WU *et al.* (2019a,b) presented the theoretical foundation and computational implementation of a Lyapunov-based MPC using recurrent neural networks (RNN). It was shown that the RNN-based MPC computation time was lower than the sampling time, which implies that it could be applied in real time. ELLIS and CHINDE (2020) used a long short-term memory networks (LSTM) model for an EMPC design applied to heating, ventilation, and air conditioning (HVAC) systems. CHANDRASEKAR *et al.* (2022) applied a state-space dynamic model to predict state trajectories combined with a partial-least-squares model to predict quality variables, which are used as constraints.

Some approaches also focused on dealing with the plant-model mismatch in EMPC. VACCARI and PANNOCCHIA (2017) proposed an offset-free EMPC by combining output modifier-adaptation and EMPC, such that affine correction terms are added to the model output variables. The proposed approach depends on the plant output variables gradient, which is considered to be known. PANNOCCHIA (2018) and VACCARI and PANNOCCHIA (2018) expanded the previous approach by considering dynamic estimate techniques to obtain the gradients. FAULWASSER and PANNOCCHIA (2019) proposed the combination of modifier-adaptation and an EMPC without terminal constraints, which avoids solving the steady-state optimization problem to obtain the terminal state. The authors showed that gradient estimation is crucial for the proposed approach. HERNÁNDEZ and ENGELL (2019) also considered an output modifier-adaptation scheme, such that the dynamic model corrected instead of the input-output map. VACCARI *et al.* (2020) applied steady-state perturbations and a Broyden's approximation to obtain the gradients. VACCARI *et al.* (2021) extended the previous work by comparing gradient estimation techniques, namely Broyden's approximation and linear regression. The authors compared the results to two benchmarking problems, concluding that linear regression is superior in handling measurement noise. OLIVEIRA-SILVA *et al.* (2021) proposed a new approach for directly estimating the MA modifiers with transient measurements instead of trying to estimate the process gradients, so-called Dynamic Modifier

Estimation (DME).

In summary, the main strategies for integrating RTO and supervisory control layers aim to minimize the model differences between each layer. Although a simple strategy, the two-stage MPC method may lead to suboptimal operation since the models in each layer remain different. Also, during the transient period of the RTO, the optimal setpoint is updated once a steady-state condition is reached. The usage of one-layer and EMPC strategies presents the advantage of adding somehow an economic aspect into the controller formulation, and it is an interesting approach since both economic optimization and control are merged in a single layer, avoiding the need for an SSD step and then presenting compatibility between RTO and supervisory control layer. A critical requirement of the strategy is that a reliable dynamic model of the process is available. Despite not being an EMPC requirement, when applying nonlinear models in its formulation, computational complexities, the requirement for online identification techniques for nonlinear processes, the necessity of the optimization problem to be solved in real time, the robustness of the solution, and the stability for nonlinear systems are important issues for the practical implementation of the nonlinear EMPC for large-scale problems (ELLIS *et al.*, 2014; WÜRTH *et al.*, 2011). Thus, modeling techniques that enable the EMPC application in real time and enable the ability to represent the process accurately are crucial for EMPC viability, especially in large-scale systems. In this sense, surrogate models are an interesting direction and will be discussed in the following sections.

## Chapter 3

# Surrogate Model-Based Optimization

In general, modeling techniques are applied to represent a given object of interest. Models start to be meaningful and important when they can adequately represent the behavior of the object of interest (MELO JR and PINTO, 2008). The use of models has innumerable advantages, highlighting here the fast responses to different scenarios without the need to perform real experiments, which, in general, is costly and time consuming.

In this sense, modeling is an essential tool for optimization purposes. However, depending on the model complexity, the computational effort, the execution time, and simulation convergence, these can be issues. These difficulties become obstacles for applications that require responses in a short period. In this context, it is also worth mentioning the real-time optimization systems based on models in steady-state, which require answers about the optimum operating point of the process in study.

In cases where the computational cost and the response time become critical variables for executing a simulation or optimization, a way to minimize this problem is through the so-called surrogate models. The basic idea of the surrogate models is to apply mathematical approximations instead of rigorous models (FORRESTER *et al.*, 2008). Furthermore, using surrogate models becomes a helpful tool in applications where computational cost, execution time, and reliability are essential, such as in the scope of process optimization and control (GOMES, 2007).

Regarding the application of surrogate models in Chemical Engineering, BURNHAM *et al.* (1996) and JAECKLE and MACGREGOR (1998) applied surrogate models to identify relationships between process variables that affect given product characteristics from historical plant data. MICHALOPOULOS *et al.* (2001) used surrogate models to represent a steady-state process on an industrial scale. HOSKINS *et al.* (1991) and TERRY and HIMMELBLAU (1993) applied mathematical approximations for noise-removal from process measure-

ments data and to fault-identification. In the work of HERNANDEZ and ARKUN (1993), BAKSHI and STEPHANOPOULOS (1994), and BANERJEE *et al.* (1997), approximations were applied to describe the dynamic behavior of processes. THOMPSON and KRAMER (1994) applied a hybrid strategy combining first principles and approximate models to represent the dynamics of processes. The work of BIEGLER *et al.* (1985), PALMER and REALFF (2002a), PALMER and REALFF (2002b), NASCIMENTO *et al.* (2000), and GOMES (2007) applied surrogate models for optimization purposes.

BIEGLER *et al.* (1985) analyzed and compared the performance of optimization problems using rigorous and approximated models. Despite being a promising strategy in terms of computational effort and time, the convergence of the optimization problem to the optimal point when applying surrogate models depends on the accuracy of prediction of the objective function and the constraints of the optimization problem. In other words, the problem based on the surrogate models must preserve characteristics related to the NCOs. In that work, the necessary conditions of the model were presented to guarantee optimality.

NASCIMENTO *et al.* (2000) applied neural network models to optimize an industrial polymerization process. The polymerization was optimized using the simulation of a phenomenological model developed by GIUDICI *et al.* (1998) as a virtual plant, increasing the polymer production up to 30%.

PALMER and REALFF (2002a) presented strategies for chemical processes optimization using surrogate models based on obtained data from rigorous models. Aspects of computational experiments were evaluated, such as the dispersion of points in the domain and the contribution to metamodel prediction bias when using the Minimum Bias Latin Hypercube Design (MBLHD).

In the work of WELCH and SACKS (1991), a general methodology for obtaining and using surrogate models is presented, taking into account multiple simulation response variables and multiobjective optimization problems. The proposed steps are presented below:

1. Postulate a model for each response variable  $y_j$  ( $\forall j = 1, \dots, n_y$ ) as a function of the input variables  $\mathbf{u}$ ;
2. Perform a design of experiments of a set of  $N$  vectors  $\mathbf{u}$  to generate an initial set of responses;
3. Use the obtained data to estimate the parameters of the proposed models. Before proceeding to the next step, it is necessary to check the models' accuracy and, if necessary, propose a new model structure and estimate its parameters; Generate response surfaces using the model predictions. This step aims to visualize the input and output variables' relationship, trends,

and possible optimal points. Even if there are some model errors, this analysis allows to determine a subspace where the new experiments should be prioritized;

4. Perform an optimization step;
5. If necessary, constrain the region of  $\mathbf{u}$ . If Step 3 indicates that the models obtained are not accurate yet, the region of  $\mathbf{u}$  can also be constrained to a promising region, based on the analysis carried out in Step 4 and the tentative optimization of Step 5. It may be necessary to return to Step 2 to collect new responses from a new set of  $\mathbf{u}$ . Otherwise, proceed to the next step;
6. Perform a real experiment to confirm the optimum point obtained in Step 5. If the predicted optimum is unsatisfactory, return to step 2 for reducing the region of  $\mathbf{u}$  and collect more data.

In step 2 of the procedure described by WELCH and SACKS (1991), it is important to notice that the number of experiments ( $N$ ) was not defined. Thus, it is important to highlight that not all approximation models can obtain predictions with the desired accuracy when the number of experiments is insufficient. Typically, polynomial and Gaussian Process models are models that can be generated with a small data set. Spline models, in general, use a larger data set, however smaller than the size required for the neural network model. Even with an adequately sized data set, it is still possible to obtain unsatisfactory approximations. This fact is related to the differences between the characteristics of the actual data set and the type of surface generated by the approximations (PALMER and REALFF, 2002b).

There are several classes of models that can be employed as surrogate models, such as polynomial basis functions, radial basis functions, neural networks, Support Vector Regression (SVR) and Gaussian Process (CARPIO *et al.*, 2018a).

Some researches compared classes of surrogate models for chemical processes optimization purposes. GOMES (2007) compared neural networks and Gaussian Process (Kriging model) to model an optimization test function and a crude oil atmospheric distillation. Regarding prediction errors, GOMES (2007) showed a similar performance when comparing Gaussian Process and neural networks. CARPIO (2019) compared polynomial, neural networks and Gaussian Process models applied to optimization test functions (Six-hump camel-back, Griewank, Bird, and Rosebrock functions) and a biorefinery plant example. CARPIO (2019) showed that the Gaussian Process presented lower prediction error when compared to the other models in all test functions considered.

Based on the aforementioned works, GP seems to be a powerful class of models to be applied as surrogate models. Also, it has been applied for RTO purposes, combining techniques of Sequential Approximation Optimization (SAO) (DEL RIO CHANONA *et al.*, 2019; FERREIRA *et al.*, 2018; GOMES, 2007; GOMES *et al.*, 2006, 2008) and Bayesian Optimization (DEL RIO CHANONA *et al.*, 2021).

### 3.1 Gaussian Process Models

**Definition 3.1.1** *Gaussian process model (RASMUSSEN, 2006).* A Gaussian process is a collection of random variables, any finite number of which have a joint Gaussian distribution.

As a Gaussian distribution is specified by means of its mean and covariance, the same applies to GP models. Let  $\mu(\mathbf{u})$  and  $k(\mathbf{u}, \mathbf{u}')$  be the mean and covariance functions of a real process  $f(\mathbf{u})$ , respectively. Here,  $\mathbf{u}$  is the independent (input) variable and  $\mathbf{u}'$  represents another different vector.

It is typical for more realistic situations to have access to the real process measurements, which means that the data may be noisy. Then  $y = f(\mathbf{u}) + \varepsilon$ , where  $\varepsilon$  is an additive independent identically distributed Gaussian noise with zero-mean and variance  $\sigma_n^2$ .

The mean and covariance are defined as follows:

$$\mu(\mathbf{u}) = E[f(\mathbf{u})] \tag{3.1}$$

$$k(\mathbf{u}, \mathbf{u}') = E[(f(\mathbf{u}) - \mu(\mathbf{u}))(f(\mathbf{u}') - \mu(\mathbf{u}'))] \tag{3.2}$$

The GP model can be stated as follows:

$$f(\mathbf{u}) \approx GP(\mu(\mathbf{u}), k(\mathbf{u}, \mathbf{u}')) \tag{3.3}$$

It is also important to define the training and test data sets, which are used to GP model training and testing, respectively. Let the training set be defined as  $\mathbf{U} \in \mathbb{R}^{n \times m}$ , such that each column represents a sample point and the lines are the coordinates of each vector  $\mathbf{u}_i$ , which means that  $\mathbf{U} = [\mathbf{u}_1, \dots, \mathbf{u}_m]$ . The independent variables (responses) are obtained and represented by  $\mathbf{Y} \in \mathbb{R}^{n_y \times m}$ , such that  $n_y$  is the number of output variables. Analogously,  $\mathbf{U}^* \in \mathbb{R}^{n \times m^*}$ , such that  $\mathbf{U}^* = [\mathbf{u}_1^*, \dots, \mathbf{u}_{m^*}^*]$ , and  $\mathbf{Y}^* \in \mathbb{R}^{n_y \times m^*}$  are the predictors and output variables test data set. Thus, the training and test sets have  $m$  and  $m^*$  experiments, respectively.

If there are  $m$  training points and  $m^*$  test points then  $\mathbf{K}(\mathbf{U}, \mathbf{U}^*) \in \mathbb{R}^{m \times m^*}$  denotes the covariance matrix evaluated at all pairs of training and test points. Analogously,  $\mathbf{K}(\mathbf{U}, \mathbf{U}) \in \mathbb{R}^{m \times m}$  represents the covariance matrix evaluated at all

pairs of training points,  $\mathbf{K}(\mathbf{U}^*, \mathbf{U}^*) \in \mathbb{R}^{m^* \times m^*}$  represents the covariance matrix evaluated at all pairs of test points, and  $\mathbf{K}(\mathbf{U}^*, \mathbf{U}) \in \mathbb{R}^{m^* \times m}$  represents the covariance matrix evaluated at all pairs of test and training points, respectively.

In practice, the mean function is expressed conveniently in terms of a linear combination of basis functions, such that its parameters  $\boldsymbol{\beta}$  are inferred from training data. Let  $\mathcal{F}$  be a regression function, typically considered as a polynomial function with parameters  $\boldsymbol{\beta} \in \mathbb{R}^{n_\beta}$  in which  $n_\beta$  is the number of parameters. Thus:

$$\mathcal{F}(\mathbf{u}) = \mathbf{h}(\mathbf{u})^T \boldsymbol{\beta} \quad (3.4)$$

where  $\mathbf{h}(\mathbf{u})$  are basis functions.

Therefore, the GP's posterior mean function (*i.e.*, after training) applied to the test set can be written as follows:

$$\mathbf{M}_f(\mathbf{U}^*) = \mathcal{F}(\mathbf{U}^*) + \mathbf{K}(\mathbf{U}^*, \mathbf{U}) \mathbf{K}_y^{-1} (\mathbf{Y} - \mathcal{F}(\mathbf{U})) \quad (3.5)$$

where  $\mathbf{M}_f \in \mathbb{R}^{m^*}$ , such that  $\mathbf{M}_f(\mathbf{U}^*) = [\mu_f(\mathbf{u}_1^*), \dots, \mu_f(\mathbf{u}_{m^*}^*)]^T$ ,  $\mu_f$  represents the GP's posterior mean function applied to the test set,  $\mathcal{F}(\mathbf{U}) = [\mathcal{F}(\mathbf{U}_1), \dots, \mathcal{F}(\mathbf{U}_m)]^T$  and  $\mathcal{F}(\mathbf{U}^*) = [\mathcal{F}(\mathbf{U}_1^*), \dots, \mathcal{F}(\mathbf{U}_{m^*}^*)]^T$  are the regression function applied to observations of the training and test sets, and  $\mathbf{K}_y = \mathbf{K}(\mathbf{U}, \mathbf{U}) + \sigma_n^2 \mathbf{I}_{m \times m}$ .

Additionally, the GP's posterior covariance function applied to the test set can be written as follows:

$$\mathbf{S}_f(\mathbf{U}^*) = \mathbf{S}_{f,zm}(\mathbf{U}^*) + \mathbf{R}^T (\mathbf{B}^{-1} + \mathcal{F}(\mathbf{U}) \mathbf{K}_y^{-1} \mathcal{F}^T(\mathbf{U}))^{-1} \mathbf{R} \quad (3.6)$$

where  $\mathbf{S}_f$  and  $\mathbf{S}_{f,zm}$  are vectors of the posterior covariance functions in the case of a non zero mean regression function and a zero mean regression function, respectively. These functions applied to the test set give  $\mathbf{S}_f(\mathbf{U}^*) = [\sigma_f^2(\mathbf{u}_1^*), \dots, \sigma_f^2(\mathbf{u}_{m^*}^*)]^T$ ,  $\mathbf{S}_{f,zm} = [\sigma_{f,zm}^2(\mathbf{u}_1^*), \dots, \sigma_{f,zm}^2(\mathbf{u}_{m^*}^*)]^T$ , such that,  $\sigma_f^2$  and  $\sigma_{f,zm}^2$  are the GP's posterior covariance functions in the case of a non zero mean regression function and a zero mean regression function, respectively.  $\mathbf{S}_{f,zm}(\mathbf{U}^*) = \mathbf{K}(\mathbf{U}^*, \mathbf{U}^*) - \mathbf{K}(\mathbf{U}^*, \mathbf{U}) \mathbf{K}_y^{-1} \mathbf{K}(\mathbf{U}, \mathbf{U}^*)$  represents the GP's posterior covariance for the specific case the zero mean function,  $\mathbf{B}$  is considered the prior covariance matrix of the regression parameters  $\boldsymbol{\beta}$  assumed to be normally distributed, *i.e.*,  $\boldsymbol{\beta} = \mathcal{N}(\mathbf{b}, \mathbf{B})$ , and  $\mathbf{R}$  is a matrix calculated by  $\mathbf{R} = \mathcal{F}(\mathbf{U}^*) - \mathcal{F}(\mathbf{U}) \mathbf{K}_y^{-1} \mathbf{K}(\mathbf{U}, \mathbf{U}^*)$ .

The posterior regression coefficients are calculated as follows:

$$\tilde{\boldsymbol{\beta}} = \left( \mathbf{B}^{-1} + \mathcal{F}(\mathbf{U}) \mathbf{K}_y^{-1} \mathcal{F}^T(\mathbf{U}) \right) \left( \mathcal{F}(\mathbf{U}) \mathbf{K}_y^{-1} \mathbf{Y} + \mathbf{B}^{-1} \mathbf{b} \right) \quad (3.7)$$

A particular case of the posterior mean and variance equations can be obtained for the situation when the mean function is considered to be zero. The posterior equations are written as follows:

$$\boldsymbol{\mu}_{f,zm}(\mathbf{U}^*) = \mathbf{K}(\mathbf{U}^*, \mathbf{U})\mathbf{K}_y^{-1}\boldsymbol{\Upsilon} \quad (3.8)$$

$$\sigma_{f,zm}^2(\mathbf{U}^*) = \mathbf{K}(\mathbf{U}^*, \mathbf{U}^*) - \mathbf{K}(\mathbf{U}^*, \mathbf{U})\mathbf{K}_y^{-1}\mathbf{K}(\mathbf{U}, \mathbf{U}^*) \quad (3.9)$$

In the situation where the prior on  $\boldsymbol{\beta}$  becomes vague, which means that  $\mathbf{B}^{-1} \rightarrow \mathbf{0}$ , the posterior equations are written as follows:

$$\boldsymbol{\mu}_f(\mathbf{U}^*) = \boldsymbol{\mu}_{f,zm}(\mathbf{U}^*) + \mathbf{R}^T\bar{\boldsymbol{\beta}} \quad (3.10)$$

$$\sigma_f^2(\mathbf{U}^*) = \sigma_{f,zm}^2(\mathbf{U}^*) + \mathbf{R}^T(\mathcal{F}(\mathbf{U})\mathbf{K}_y^{-1}\mathcal{F}^T(\mathbf{U}))^{-1}\mathbf{R} \quad (3.11)$$

where  $\bar{\boldsymbol{\beta}} = (\mathcal{F}(\mathbf{U})\mathbf{K}_y^{-1}\mathcal{F}^T(\mathbf{U}))^{-1}\mathcal{F}(\mathbf{U})\mathbf{K}_y^{-1}\boldsymbol{\Upsilon}$ .

### 3.1.1 Covariance Functions

One important topic related to the GP models is the covariance functions, as it encodes the assumptions about an unknown function  $f$ . A simpler covariance function is the constant covariance function, written as follows:

$$k_{const}(\mathbf{u}, \mathbf{u}') = \sigma_0^2 \quad (3.12)$$

The linear covariance function is written as follows:

$$k_{linear}(\mathbf{u}, \mathbf{u}') = \sum_j^{n_u} \sigma_j^2 \mathbf{u}_j \mathbf{u}'_j \quad (3.13)$$

The polynomial covariance function is written as follows:

$$k_p(\mathbf{u}, \mathbf{u}') = \sigma_s^2 (\mathbf{u} - \mathbf{u}')^T \boldsymbol{\Lambda} (\mathbf{u} - \mathbf{u}' + c)^a \quad (3.14)$$

in which  $\sigma_s^2 \in \mathbb{R}$ ,  $\boldsymbol{\Lambda} = \text{diag}(\lambda_1, \dots, \lambda_n)$ ,  $a$ , and  $c$  are the parameters of the covariance function model.

An example of a covariance function is the Squared Exponential (SE), written as follows:

$$k_{SE}(\mathbf{u}, \mathbf{u}') = \sigma_s^2 \exp\left(\frac{1}{2}(\mathbf{u} - \mathbf{u}')^T \boldsymbol{\Lambda} (\mathbf{u} - \mathbf{u}')\right) \quad (3.15)$$

in which  $\sigma_s^2 \in \mathbb{R}$  and  $\mathbf{\Lambda} = \text{diag}(\lambda_1, \dots, \lambda_n)$  are the parameters of the covariance function model.

The Matérn covariance function, also known as the modified Bessel covariance function, is written as follows:

$$k_M(\mathbf{u}, \mathbf{u}') = \frac{\sigma_s^2}{\Gamma(\nu)2^{\nu-1}} \left( 2\sqrt{\nu}(\mathbf{u} - \mathbf{u}')^T \mathbf{\Lambda}(\mathbf{u} - \mathbf{u}') \right)^\nu \left( 2\sqrt{\nu}(\mathbf{u} - \mathbf{u}')^T \mathbf{\Lambda}(\mathbf{u} - \mathbf{u}') \right) \quad (3.16)$$

## 3.2 Sequential Approximation Optimization Methods (SAO)

Sequential Approximation Optimization Methods are typically applied when the original optimization problem is computationally expensive, taking too much time to obtain a solution. It can be related to the complexity and dimension of the model behind the optimization problem, commonly written as an equality constraint.

In order to speed up the optimization step or, at least, achieve a reasonably fast one, the rigorous model is approximated by an inexpensive function, limited to a subregion, also called the trust-region. The trust-region is used to successively define a limited search domain in which a subproblem is solved, based on approximation functions (JACOBS *et al.*, 2004).

Given an optimization problem based on a rigorous model as presented in Equation 2.1, a Sequential Approximation Optimization strategy applied to this problem can be written as follows:

$$\begin{aligned} \mathbf{u}_{opt,k} &= \arg \min_{\mathbf{u}} \hat{\phi}_{ec}(\mathbf{u}) \\ \text{s.t.} \quad & \hat{\mathbf{g}}(\mathbf{u}) \leq \mathbf{0}, \\ & \mathbf{u}_{min} \leq \mathbf{u}_{LB,k} \leq \mathbf{u} \leq \mathbf{u}_{UB,k} \leq \mathbf{u}_{max}, \\ & \mathbf{u}_{LB,k} = \mathbf{u}_{c,k} - \Delta_k, \\ & \mathbf{u}_{UB,k} = \mathbf{u}_{c,k} + \Delta_k \end{aligned} \quad (3.17)$$

where  $\hat{\phi}_{ec}$  is an approximation of original objective function  $\phi_{ec}$ ,  $\hat{\mathbf{g}}$  is an approximation of the original problem constraints  $\mathbf{g}$ ,  $\mathbf{u}$  are decision variables of the problem,  $\mathbf{u}_{min}$  and  $\mathbf{u}_{max}$  are the original problem domain,  $\mathbf{u}_{LB,k}$  and  $\mathbf{u}_{UB,k}$  are the lower and upper bounds at iteration  $k$  defined by the trust-region,  $\mathbf{u}_{c,k}$  is the trust-region

center and  $\Delta_k$  is the trust-region radius at iteration  $k$ . In the problem represented by Equation 3.17, it assumed that the equality constraints related to the model equations were already substituted into the equations. Also, without loss of generality, it can represent surrogate models obtained to represent the functions  $\phi_{ec}$  and  $\mathbf{g}$  or the output variables  $\mathbf{y}$  directly. In the latter, as  $\phi_{ec} = \phi_{ec}(\mathbf{u}, \mathbf{y}(\mathbf{u}))$  and if the mapping function can be represented in the explicit form by  $\mathbf{y} = \mathbf{f}(\mathbf{u})$  then  $\hat{\phi}_{ec} = \hat{\phi}_{ec}(\mathbf{u})$ , where the dependence on the model parameters was omitted for the sake of notation.

Similar to the model adequacy criteria presented in Section 2.2.1.1, the NCO of the optimization problem based on a surrogate model should be equivalent to the original problem. According to GIUNTA and ELDRED (2000), the consistency conditions between the surrogate and original functions must hold at  $\mathbf{u}_{c,k}$ , such that:

$$\mathcal{L}(\mathbf{u}_{c,k}) = \hat{\mathcal{L}}(\mathbf{u}_{c,k}) \quad (3.18)$$

$$\nabla \mathcal{L}(\mathbf{u}_{c,k}) = \nabla \hat{\mathcal{L}}(\mathbf{u}_{c,k}) \quad (3.19)$$

where  $\mathcal{L}$  and  $\hat{\mathcal{L}}$  are the Lagrangian function of the original and surrogate model-based optimization problems, respectively.

According to GIUNTA and ELDRED (2000), the gradient of the Lagrangian function of the original problem ( $\nabla \mathcal{L}$ ) calculation may also be computationally expensive. Also, additional issues may occur if the gradient presents non-smooth trends in the objective function and constraints values. For this reason, the authors proposed a strategy of trust-region updating without gradient calculation, applying a metric of surrogate functions accuracy at the optimum point achieved at the  $k$ -th iteration, based on the previous work of RODRÍGUEZ *et al.* (1998), written as follows:

$$\rho_k = \min(\rho_{\phi_{obj,k}}, \rho_{\mathbf{g},k}) \quad (3.20)$$

$$\rho_{\phi,k} = \frac{\phi_{ec}(\mathbf{u}_{c,k}) - \phi_{ec}(\mathbf{u}_{opt,k})}{\hat{\phi}_{ec}(\mathbf{u}_{c,k}) - \hat{\phi}_{ec}(\mathbf{u}_{opt,k})} \quad (3.21)$$

$$\rho_{g_i,k} = \frac{g_i(\mathbf{u}_{c,k}) - g_i(\mathbf{u}_{opt,k})}{\hat{g}_i(\mathbf{u}_{c,k}) - \hat{g}_i(\mathbf{u}_{opt,k})} \quad i = 1, \dots, n_g \quad (3.22)$$

where  $\rho_{\phi,k}$  and  $\rho_{\mathbf{g},k}$  are measures of the actual versus predicted change in objective function and constraints at the optimum point obtained at iteration  $k$ .

The trust-region updating rules can be summarized as follows:

1.  $\rho_k < 0$ : the surrogate models are inaccurate. Thus, the optimum solution at iteration  $k$  is rejected, so that  $\mathbf{u}_{c,k+1} = \mathbf{u}_{c,k}$ . Also, shrink the trust-region by a

factor of  $\gamma_{red}$  to improve model accuracy (which is supposed to be achieved by applying a limited region).

2.  $0 \leq \rho_k < \eta_1$ : the surrogate models are marginally accurate. Thus, the optimum solution at the  $k$ -th iteration is not rejected, so that  $\mathbf{u}_{c,k+1} = \mathbf{u}_{opt,k}$ . As the surrogate models need to be improved, also shrink the trust-region by a factor of  $\gamma_{red}$ .
3.  $\eta_1 \leq \rho_k < \eta_2$ : the surrogate models are moderately accurate. Thus, the optimum solution at the  $k$ -th iteration is not rejected, so that  $\mathbf{u}_{c,k+1} = \mathbf{u}_{opt,k}$  and the trust-region radius is kept the same value of the previous iteration.
4.  $\rho_k \geq \eta_2$  and  $\|\mathbf{u}_{opt,k} - \mathbf{u}_{c,k}\| < \Delta_k$ : the surrogate models are accurate and the optimum solution at the  $k$ -th iteration lies inside the trust-region bounds. Thus, keep the last solution  $\mathbf{u}_{c,k+1} = \mathbf{u}_{opt,k}$  and maintain the previous trust-region radius.
5.  $\rho_k \geq \eta_2$  and  $\|\mathbf{u}_{opt,k} - \mathbf{u}_{c,k}\| = \Delta_k$ : the surrogate models are accurate and the optimum solution at the  $k$ -th iteration lies on the trust-region bounds. Thus, keep the last solution  $\mathbf{u}_{c,k+1} = \mathbf{u}_{opt,k}$  and increase the trust-region radius by a factor of  $\gamma_{inc}$ .

where  $\gamma_{inc}$  and  $\gamma_{red}$  are the trust-region radius increase and reduction factors, respectively, such that  $0 < \gamma_{red} < \gamma_{inc}$ . Also,  $\eta_1$  and  $\eta_2$  are threshold values for the  $\rho$  metrics, such that  $0 < \eta_1 < \eta_2 < 1$ .

GOMES (2007) applied the SAO strategy, considering the rules for updating the trust-region proposed by GIUNTA and ELDRED (2000). The author concluded that these criteria were insufficient, especially when the trust-region is too narrow, so the values of the original and surrogate functions are too close. In this situation, the value of  $\rho_k$  can present large positive or negative values, as the difference of the functions is close to zero, which may lead to unnecessary trust-region shrinking. Thus, GOMES (2007) proposed a strategy for updating the trust-region based on the previous work of GIUNTA and ELDRED (2000), adding criteria regarding the maximum error of surrogate models predictions.

### 3.3 Bayesian Optimization

The Bayesian Optimization was originated in the work of KUSHNER (1964), ZHILINSKAS (1975), and MOČKUS (1975), and was popularized in the work of JONES *et al.* (1998). This approach aims to solve an optimization problem based

on global statistical model of an unknown objective function. Typically, this strategy is applied when the objective function is expensive to evaluate (GELBART *et al.*, 2014). Regarding the statistical model applied in Bayesian Optimization, Gaussian Process is common employed (FRAZIER, 2018).

The Bayesian Optimization starts with an initial design of experiments, which will be applied to obtain a first training data set for model building. Let denote the initial set of experiments in terms of the input variables as  $\mathbf{U}^{(0)} \in \mathbb{R}^{m \times n_u}$ , where  $m$  is the number of design points and  $n_u$  the dimension of the problem (number of decision variables). The unknown function is evaluated at each  $\mathbf{u} \in \mathbf{U}^{(0)}$ , yielding measured variables  $\Theta^{(0)} \in \mathbb{R}^{m \times n_\Theta}$ , which may encompass the objective function, the constraints functions and the output variables. Thus,  $n_\Theta = n_y + n_g + 1$ .

With the input and output data set  $\{\mathbf{U}^{(0)}, \Theta^{(0)}\}$ , it is possible to fit the surrogate models. Based on it, an optimization step is carried out to obtain a candidate point. The unknown function is evaluated at this point and the training set is updated by adding the last information. Then, the surrogate model can be also updated. Therefore, each new experiment point refines the surrogate model, aiming to increase its accuracy, also increasing the probability of finding the optimal of the true problem by using surrogate models (COUCKUYT *et al.*, 2014). This process is repeated until a predetermined stop criterion is achieved (UENO *et al.*, 2016).

In the new candidate point selection step, also called inner optimization problem (GELBART *et al.*, 2014), a metric function is applied as objective function, which is called acquisition function, here denoted as  $\mathcal{AF} : \mathbb{R}^{n_u} \rightarrow \mathbb{R}$ . This function is used to map beliefs about the unknown function as a way to measure the gain for unknown values of the function that will be evaluated at a new input variable locations. Common acquisition functions applied in Bayesian Optimization are the probability of improvement, expected improvement, and lower (upper) confidence bound (WANG *et al.*, 2017). A new candidate solution  $\mathbf{u}_{cand} \in \mathbb{R}^{n_u}$  is chosen by maximizing the acquisition function, which can be described as follows:

$$\begin{aligned} \mathbf{u}_{cand} &= \arg \max_{\mathbf{u}} \mathcal{AF}(\mathbf{u}) \\ \text{s.t.} \quad & \mathbf{u}_{min} \leq \mathbf{u} \leq \mathbf{u}_{max} \end{aligned} \tag{3.23}$$

where  $\mathcal{AF} : \mathbb{R}^{n_u} \rightarrow \mathbb{R}$  is the acquisition function.

After obtaining  $\mathbf{u}_{cand}$ , the unknown function is evaluated and this data is added to the previous training data set, yielding an updated training set  $\{\mathbf{U}^{(k+1)}, \Theta^{(k+1)}\}$  which is applied to update the surrogate model and the algo-

rithm go to a new iteration while a given stop criteria is not fulfilled.

The expected improvement acquisition function is described as follows. Let  $\phi_{min}$  be the minimum value of the objective function  $\phi_{ec}$  found at iteration  $k$ , here considering the optimization problem aims to minimize a function. A next sampling point can be chosen so that it is possible to obtain a decrease in the objective function value. Applying a surrogate model to obtain predictions of the objective function, denoted by  $\hat{\phi}_{ec}$ , the improvement at a next candidate point  $\mathbf{u}_{cand}$  is defined as  $\mathcal{I} = \max(\phi_{min} - \hat{\phi}_{ec}(\mathbf{u}_{cand}), 0)$ . As the objective function in Bayesian Optimization is approximated by a Gaussian Process, the expression for  $\mathcal{I}$  is a random variable. Therefore, to obtain the expected improvement, the expected value operator is applied to the improvement  $\mathcal{I}$ :

$$\mathcal{AF}_{EI}(\mathbf{u}) = E[\mathcal{I}(\mathbf{u})] = E[\max(\phi_{min} - \hat{\phi}_{ec}(\mathbf{u}), 0)] \quad (3.24)$$

where  $\mathcal{AF}_{EI} : \mathbb{R}^{n_u} \rightarrow \mathbb{R}$  is the expected improvement acquisition function and  $E[\cdot]$  is the expected value function.

By applying the expected value definition, it is possible to obtain the following expression for the expected improvement:

$$\mathcal{AF}_{EI}(\mathbf{u}) = (\phi_{min} - \mu_f(\mathbf{u}))\mathcal{P}_{\mathcal{Z}} \left( \frac{\phi_{min} - \mu_f(\mathbf{u})}{\sigma_f(\mathbf{u})} \right) + \sigma_f(\mathbf{u})p_{\mathcal{Z}} \left( \frac{\phi_{min} - \mu_f(\mathbf{u})}{\sigma_f(\mathbf{u})} \right) \quad (3.25)$$

where  $\mu_f(\mathbf{u})$  and  $\sigma_f(\mathbf{u})$  are the posterior mean and standard-deviation values of the Gaussian process applied to approximate  $\phi_{ec}$ , and  $\mathcal{P}_{\mathcal{Z}}$  and  $p_{\mathcal{Z}}$  are the cumulative distribution function and normal probability density function of the standard normal random variable, respectively.

The probability of improvement (PI) acquisition function is an alternative function to  $\mathcal{AF}_{EI}$ . Intuitively, it represents the probability of the objective function at a new sampling point being lower than  $\phi_{min}$ . That is:

$$\mathcal{AF}_{PI}(\mathbf{u}) = Pr(\phi_{ec}(\mathbf{u}) < \phi_{min}) = \mathcal{P}_{\mathcal{Z}} \left( \frac{\phi_{min} - \mu_f(\mathbf{u})}{\sigma_f(\mathbf{u})} \right) \quad (3.26)$$

The lower confidence bound (LCB) acquisition function, also called Gaussian process lower confidence bound (GP-LCB) in minimization problems, or Gaussian process upper confidence bound (GP-UCB) in maximization problems, is defined as follows:

$$\mathcal{AF}_{GP-LCB}(\mathbf{u}) = -(\mu_f(\mathbf{u}) - \sqrt{\beta}\sigma_f(\mathbf{u})) \quad (3.27)$$

where  $\beta$  is a tuning parameter. The intuition behind  $\mathcal{AF}_{GP-LCB}$  is that at each iteration, the new sampling point is the one which maximizes  $\mathcal{AF}_{GP-LCB}$ , which means that  $\mu_f(\mathbf{u}) - \sqrt{\beta}\sigma_f(\mathbf{u})$  is minimized. This term can be interpreted as the lower confidence value of the mean.

The acquisition functions are typically applied in Bayesian optimization to decide what sampling point to try next to the trade-off between exploration and exploitation. An acquisition function can emphasize more on the modeling uncertainties rather than the predictions (represented by the Gaussian process posterior mean  $\mu_f$ ). Therefore, this acquisition function tends to present an exploratory behavior. Consequently, more points are evaluated until they reach the optimum point. The advantage of exploratory behavior is a high probability of the algorithm obtaining a global solution instead of a local solution. On the other hand, it is also possible to design acquisition functions that emphasize the prediction values instead of the uncertainties, which is called an exploitation behavior (WANG *et al.*, 2017).

Figure 3.1 presents a few iterations of the Bayesian optimization applied to a one-dimension problem. The objective function is  $\phi_{ec}(u) = -\sin(3u) - u^2 - 0.7u$ , which has a maximum at  $u^* = -0.3593$ .

The acquisition functions presented before are all designed for unconstrained Bayesian optimization problems. In order to deal with constrained optimization problems, SCHONLAU (2015) proposed an extension of the original Expected Improvement, named Expected Improvement with Constraints (EIC), which is defined as follows:

$$\mathcal{AF}_{EIC}(\mathbf{u}) = \mathcal{AF}_{EI}(\mathbf{u}) \prod_{j=1}^{n_g} Pr(g_j(\mathbf{u} \leq 0)) \quad (3.28)$$

where the term  $Pr(g_j(\mathbf{u} \leq 0))$  represents the probability of the  $j$ -th constraint to be satisfied. Also, it is interesting to notice that it is possible to separate the probabilities of satisfying the constraints from the expected improvement of the objective function due to assumed independence (GELBART, 2015). The term  $\prod_{j=1}^{n_g} Pr(g_j(\mathbf{u} \leq 0))$  is also called probability of feasibility of the problem.

HAWE and SYKULSKI (2008) proposed an acquisition function based on the probability of improvement in constrained multi-objective optimization problems. The proposed acquisition is written as a product of the original probability of improvement and a term that represents the probability of feasibility, written as follows:

$$\mathcal{AF}_{PIC}(\mathbf{u}) = \mathcal{AF}_{PI}(\mathbf{u}) \prod_{j=1}^{n_g} \mathcal{P}_{\mathcal{Z}} \left( \frac{0 - \mu_{g_j}(\mathbf{u})}{\sigma_{g_j}(\mathbf{u})} \right) \quad (3.29)$$

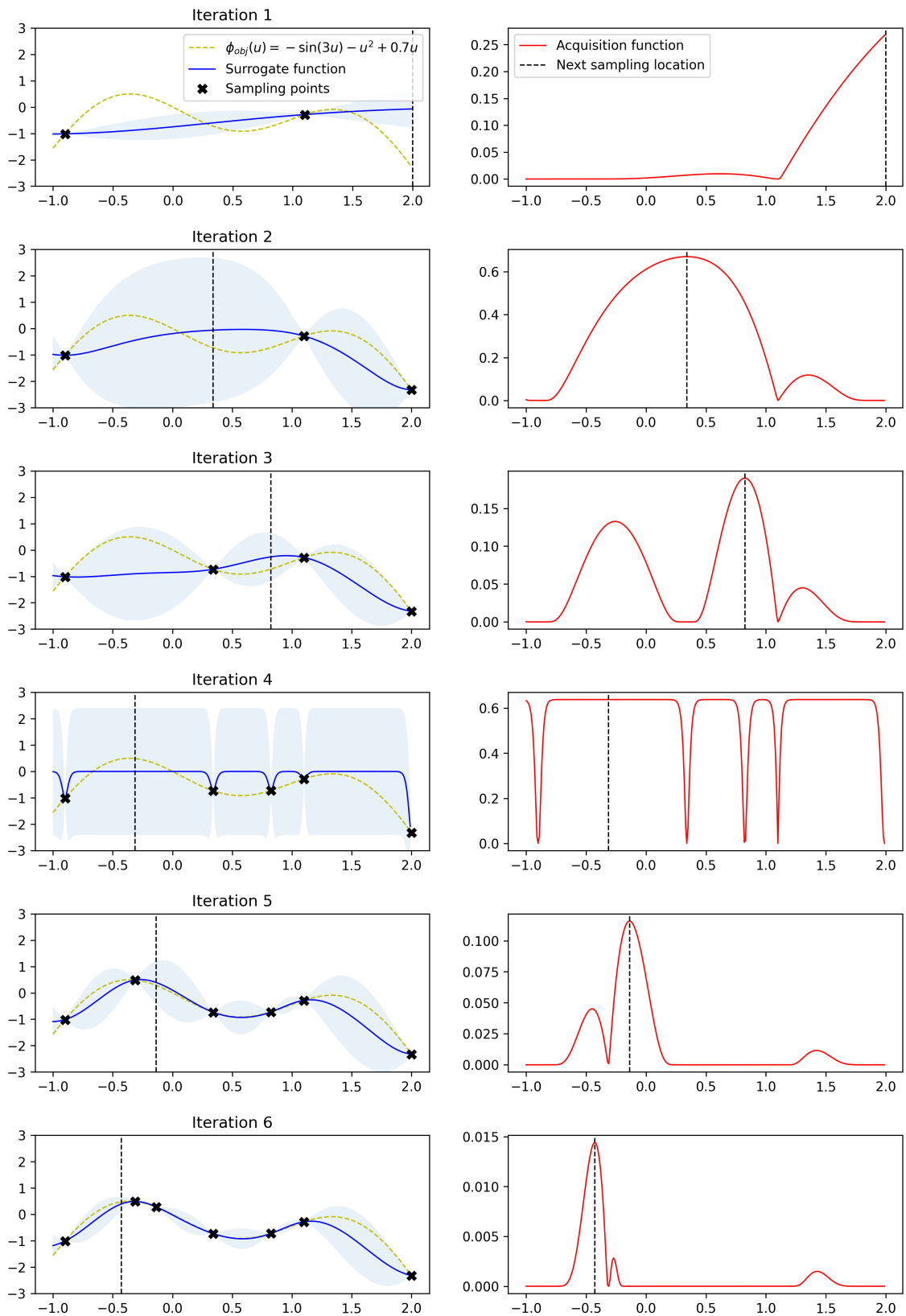


Figure 3.1: First five iterations of Bayesian Optimization applied to the function  $\phi_{ec} = -\sin(3u) - u^2 - 0.7u$  inside the domain  $-1 \leq u \leq 2$ . The function maximum occurs at  $u^* = -0.3593$  and  $\phi_{ec}(u^*) = 0.50$ .

where  $\mu_{g_j}$  and  $\sigma_{g_j}$  are the mean and standard-deviation of the Gaussian-process applied to approximate the  $j$ -th constraint, respectively.

CARPIO *et al.* (2018b) presented an surrogate model based optimization framework based on the Probability of Improvement acquisition function. In the proposed formulation, GP were applied to model the objective function and constraints, such that a constrained PI acquisition function was considered, and the probability of fulfilling each constraint was also considered as the optimization problem constraint.

### 3.4 Data Generation for Surrogate Models Building

Regarding obtaining data for surrogate model building, some precautions must be taken when obtaining the data since some choices may not be appropriate. Similar to the experimental design used in real experiments (i.e., non-computational), experiments techniques can be employed to reduce the number of experiments and create a set of statistically representative dependent and independent variables for parameter estimation. The task of running simulations for different input variables and obtaining the output or response variables is called a computational experiment (SACKS *et al.*, 1989).

According to PALMER and REALFF (2002a), a suitable data set must have different values for a given variable in each experiment. This characteristic is obtained through random sampling. On the other hand, this technique has the disadvantage of forming very close data sets, the so-called clusters. The impact of sampling with this pattern is the possibility of increasing the model's prediction error in regions where sampling was not done. An adequate sampling would be the situation of points well distributed throughout the sampling space and not grouped.

A technique that presents a better distribution of the sampled points is the Latin Hypercube Design (LHD) or Latin Hypercube Sampling (LHS), proposed by MCKAY *et al.* (1979), which is typically used when GP models are used (FORRESTER *et al.*, 2008; GOMES, 2007). This sampling technique also uses random sampling. However, its sampling strategy better represents the portions of the vector space. For this, consider the case in which it is desired to sample  $m$  points in the vector space  $D \in \mathbb{R}^n$ . The LHS strategy is described as follows:

1. Divide the interval for each dimension into  $m$  non-overlapping intervals of equal probability (for example, using a uniform probability distribution, such that the intervals must be the same size);
2. Randomly sample, from a uniform probability distribution, a point in each

interval in each dimension.

- Put together the points of each dimension randomly.

When reduced to the two-dimensional case, that is, the vector space  $D \in \mathbb{R}^2$ , this particular case is called Latin Square Sampling because the vector space represents a plane, that is, a square when normalizing the  $x$  and  $y$  axes between 0 and 1. Taking the example where  $m = 4$  and  $n = 2$ , each dimension is divided into 4 intervals, obtaining a square with  $4^2 = 16$  intervals. In this case, a simple way to perform the sampling via the LHS technique is to fill the square with permutations of positive integer numbers up to  $m$ , that is, 1, 2, 3, 4. Also, the numbers are distributed so that each number appears only once in each column and row. Subsequently, one of the numbers (1, 2, 3, 4) is selected, representing the intervals that will be sampled (FORRESTER *et al.*, 2008). This procedure is illustrated in Figure 3.2.

2	<b>1</b>	3	4
3	2	4	<b>1</b>
<b>1</b>	4	2	3
4	3	<b>1</b>	2

Figure 3.2: Latin Hypercube Sampling applied to the two-dimensional domain ( $n = 2$ ) with  $m = 4$  sampling points.

In Figure 3.2, the number 1 was considered to illustrate the intervals that would be selected for sampling. However, any other number could also be selected.

For the case of dimension  $n > 2$ , that is, building a hypercube, the procedure is done like that exemplified for the two-dimensional case. Let  $x$  be the  $m \times n$  dimension matrix, that is, the sampling of  $m$  points with  $n$  dimension. The sampling is done with random permutations of the possible non-zero integers 1, 2, 3, ...,  $m$  and later normalized in the interval  $[0, 1]$  (FORRESTER *et al.*, 2008). An example with  $m = 10$  and  $n = 3$  is shown in Figure 3.3.

One of the metrics commonly applied to verify if a sampling technique has a space-filling characteristic is the *maximin* metrics, introduced by JOHNSON *et al.* (1990). Indeed, this metric is based on the distance of the points. The following properties of the distance metrics should also verify (WU, 2017).

**Definition 3.4.1** *Distance Metrics* Let  $\psi(\mathbf{u}, \mathbf{v})$  be a distance metric such that  $(\mathbf{u}, \mathbf{v}) \in$

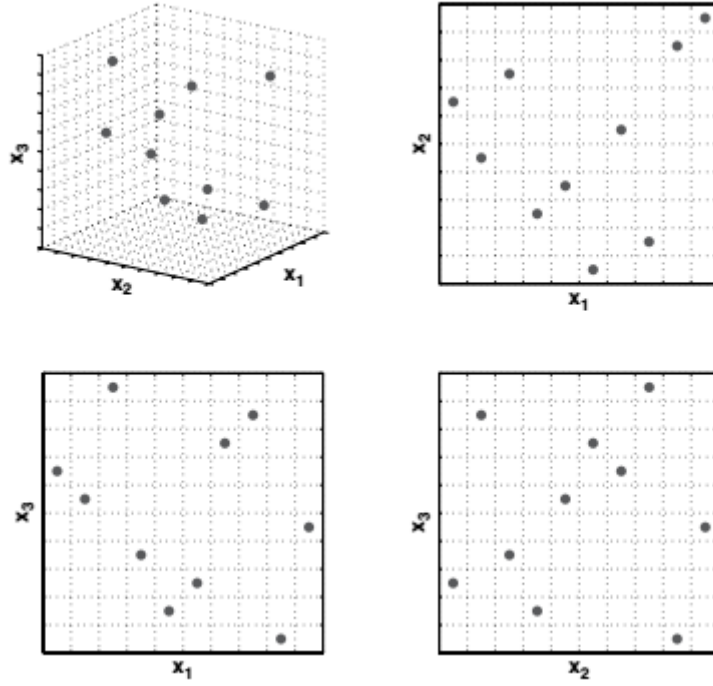


Figure 3.3: Latin Hypercube Sampling Technique applied to a three-dimension ( $n = 3$ ) with  $m = 10$  sampling points.

$\mathbb{R}^n$ . Thus, the following equations should be satisfied:

$$\psi(\mathbf{u}, \mathbf{v}) = \psi(\mathbf{v}, \mathbf{u}) \quad (3.30)$$

$$\psi(\mathbf{u}, \mathbf{v}) \geq 0 \quad (3.31)$$

$$\psi(\mathbf{u}, \mathbf{v}) = 0 \Leftrightarrow \mathbf{u} = \mathbf{v} \quad (3.32)$$

$$\psi(\mathbf{u}, \mathbf{v}) \leq \psi(\mathbf{u}, \mathbf{w}) + \psi(\mathbf{w}, \mathbf{v}) \quad (3.33)$$

For instance, the function below represents a possible distance metric to be applied:

$$\psi(\mathbf{u}, \mathbf{v}) = \left[ \sum_{j=1}^n |u_j - v_j|^k \right]^{1/k} \quad (3.34)$$

Indeed, if  $k = 1$ , the function would be the absolute-value norm, also called  $\ell_1$ -norm. When  $k = 2$ , the distance will be calculated by the Euclidian norm, also called  $\ell_2$ -norm.

Based on the definition above, it is also possible to define the minimax metrics.

**Definition 3.4.2** *minimax metrics* (WU, 2017)

Let  $D$  be a set of sampling points, so that

$$\psi(\mathbf{x}, D) = \min_{\mathbf{x}_i \in D} \psi(\mathbf{x}, \mathbf{x}_i) \quad (3.35)$$

Let  $X = [0, 1]^n$ , so that  $n$  is the problem dimension. Thus:

$$\psi_{max} = \max_{x \in X} \psi(x, D) \quad (3.36)$$

be the maximum distance in  $X$ .

The distance  $\psi_{max}$  is the fill distance, which means the largest gap among the experiment points or the radius of the largest ball that can be placed in  $X$ , which does not contain any point in  $D$ .

Therefore, it is possible to find an experiment with a set of sampling points  $D$ , which minimizes the distance  $\psi_{max}$ . That is:

$$\min_D \psi_{max} = \min_D \max_{x \in X} \psi(x, D) \quad (3.37)$$

Equation 3.37 is the criterion for generating a sampling points set by the minimax distance design.

**Definition 3.4.3** Maximin metrics (WU, 2017)

Let  $D$  be a set of sampling points. The minimum distance between any two points  $x_1, x_2$  in  $D$  is

$$r = \frac{\min_{x_1, x_2 \in D} \psi(x_1, x_2)}{2} \quad (3.38)$$

where  $r$  is the separation distance or packing radius, which is the radius of the largest ball that can be placed around every design point such that there is no overlapping between two balls.

In this way, it is possible to obtain an experiment that maximize the distance  $r$ . Thus:

$$\max_D r = \frac{\max_D \min_{x_1, x_2 \in D} \psi(x_1, x_2)}{2} \quad (3.39)$$

Equation 3.39 is the criterion for generating a sampling points set by the maximin distance design.

By applying the maximin metrics, it is possible to design an LHS design with space-filling characteristics, which is called maximin LHS, defined as follows:

**Definition 3.4.4** maximin Latin Hypercube Sampling

A sampling point set  $D$  said to be maximin LHS can be generated by solving the following optimization problem:

$$\max_D \min_{x_1, x_2 \in D} \psi(x_1, x_2) \quad (3.40)$$

where  $D$  is the maximin LHS (MmLHS).

According to JOSEPH *et al.* (2015), the MmLHS design guarantees the space-filling characteristic in all the  $n$  dimensions and uniform projection in a single dimension. However, projections properties in the other dimensions may not be good.

In order to deal with uniform projection in all dimensions, techniques called the Maximum Projection Design were proposed. When a design is projected onto a subspace, the distance between the points is calculated with respect to the factors that define the subspace. This technique uses a weighted Euclidian distance, where the weights for the factor defining the subspace are equal to one and the weights are zero for the remaining factors (JOSEPH *et al.*, 2015), written as follows:

$$\psi(\mathbf{x}_i, \mathbf{x}_j, \boldsymbol{\omega}) = \left[ \sum_{k=1}^n \omega(x_{i,k} - x_{j,k})^2 \right]^{1/2} \quad (3.41)$$

where  $\boldsymbol{\omega} \in \mathbb{R}^n$  represents the weights vector.

In this approach, the sampling points  $D$  is obtained as follows (JOSEPH *et al.*, 2015):

$$\min_D \sum_{i=1}^{n-1} \sum_{j=i+1}^n \frac{1}{\psi(\mathbf{x}_i, \mathbf{x}_j, \boldsymbol{\omega})} \quad (3.42)$$

SANTNER *et al.* (2003) present other strategies that use different criteria from those previously presented. These strategies are based on statistical criteria, such as the Maximum Entropy and several variations based on the Mean Square Error of Prediction. The authors state that, in general, the Design of Experiments based on these methods tend to be robust and require great computational effort. Other strategies are also a combination of space-filling techniques and the maximum entropy criteria named sequential strategies.

Sequential strategies are techniques that allow the selection of new sampling points as the optimization iterations progress. For example, the previously presented procedure proposed by WELCH and SACKS (1991) can be considered a sequential strategy, as it suggests obtaining new sampling points to ensure model accuracy and convergence of optimization. BERNARDO *et al.* (1992) proposed a sequential strategy for the optimization of integrated electrical circuits. The proposed method refines the region as a possible candidate for the optimum point.

# Chapter 4

## A Comparison of Strategies based on Gaussian Process for RTO purposes

### 4.1 Introduction

A central question regarding RTO strategy is the model development, since it enables the model-based optimization problem. This model is a steady-state model of the process and is typically described by a first principles, rigorous and nonlinear model (ELLIS *et al.*, 2014). Due to the inherent dynamic characteristic of process plants, such that disturbances, measurements uncertainties, and noise, it is necessary a way of updating the RTO model, based on the information available through process measurements.

The two-step approach (CHEN and JOSEPH, 1987; HAIMES and WISMER, 1972; SHI-SHANG *et al.*, 1987) is the most intuitive RTO strategy, which is based on using process measurements to update the model. To achieve it, an identification step is carried out, aiming to minimize the difference of model prediction and plant measurements. Once the model is updated, an optimization step is then executed (MARCHETTI *et al.*, 2016).

Despite of the simplicity of the concept behind the two-step approach, this strategy may have limitations from the point of view of optimality (MARCHETTI *et al.*, 2009). Indeed, this strategy will converge to the model optimum, which will only match the plant optimum if the model-adequacy criteria are verified (FORBES and MARLIN, 1996).

In order to deal with this limitation, some methodologies have been proposed (BRDYŚ *et al.*, 1986; BRDYŚ and TATJEWSKI, 1994; GAO and ENGELL, 2005; LIN *et al.*, 1988; MARCHETTI *et al.*, 2010, 2009; ROBERTS, 1979; TATJEWSKI *et al.*, 2001; ZHANG and ROBERTS, 1991), which are based on a modification of the original optimization problem, by including input-affine corrections terms

in objective and constraints. This approach requires an estimate of plant gradient (first-order correction term), which is calculated through process measurements.

However, it is exactly in the calculation of the gradients that one of the difficulties of the method also lies in terms of practical implementations. In more recent works, the gradients are obtained from fitted surfaces. For example, GAO *et al.* (2016) proposed the usage of local quadratic approximations of objective functions and constraints. FERREIRA *et al.* (2018) developed a strategy combining the modifier adaptation with Gaussian Process models (MA-GP), which can be interpreted as higher-order correction terms. DEL RIO CHANONA *et al.* (2019) extended the previous work by applying trust-region concepts to the optimization problem, taking advantage of the Gaussian process model uncertainty estimate at a given point. DEL RIO CHANONA *et al.* (2021) proposed the usage of acquisition functions as a strategy for selecting points for Gaussian Process fitting and optimization. DELOU *et al.* (2022) considered modified-adaptation based on GP models applied to the output measured variables (MAy-GP) instead of the objective and constraints functions, typically considered in previous works.

In Chemical Engineering field, GP models were employed to represent a surrogate-model of complex and costly simulations in an optimization environment. This complex models are typically represented by first-principles models, which are present in process simulators (CABALLERO and GROSSMANN, 2008; CARPIO, 2019; CARPIO *et al.*, 2018a; DAVIS and IERAPETRITOU, 2007, 2010; EASON and BIEGLER, 2016; GOMES, 2007; GOMES *et al.*, 2006, 2008; HELMDACH *et al.*, 2017; PALMER and REALFF, 2002a). For selected applications and examples, the reader is referred to MCBRIDE and SUNDMACHER (2019) and references therein.

A simple approach based on surrogate models consists of training a surrogate model and applying it to optimization purposes. A data set is generated through design and analysis of computer experiments (DACE) techniques, such as Latin Hypercube Design (LHS) (MCKAY *et al.*, 1979). Based on this initial data set, a surrogate model is trained and the model can be applied for optimization purposes (CHANG *et al.*, 2014; CHI *et al.*, 2012; FORRESTER and KEANE, 2009; GOMES *et al.*, 2008; REGIS, 2016). Some research considers solving the optimization problem limited to a sub-region, which is also called the trust region GIUNTA and ELDRED (2000). The trust region is used to successively define a limited search domain in which a sub-problem is solved, based on approximation functions (GIUNTA and ELDRED, 2000; JACOBS *et al.*, 2004). The main advantage of this technique is to keep the model accurate locally, bounded by the trust-region.

Another optimization strategy based on surrogate models is the Bayesian Op-

timization approach. It is generally applied to problems that are expensive to evaluate. The key elements of the Bayesian Optimization strategy is (i) the surrogate model of the objective function and constraints, typically described as a Gaussian Process regression, and (ii) an acquisition function (WILSON *et al.*, 2018). One important step of the Bayesian Optimization is the inner-optimization step, which yields the new experiment to be applied to the real problem. It is based on an objective function, named acquisition function, which balances the trade off between exploration and exploitation (WANG *et al.*, 2017) in the Bayesian Optimization approach. Some common acquisition functions are the probability of improvement (PI), the expected improvement (EI) and the lower confidence bound (LCB) (WILSON *et al.*, 2018).

CARPIO (2019) proposed a complete framework for optimization of rigorous simulations, considering the probability of improvement as acquisition function. Also, when solving a constrained optimization problem, the author considered the constrained probability of improvement function, which considers the probability of feasibility.

DEL RIO CHANONA *et al.* (2021) combined concepts of Bayesian Optimization and modifier adaptation based on Gaussian process originally proposed by FERREIRA *et al.* (2018) by considering acquisition functions for Real-Time Optimization purposes. In the proposed strategy, a first-principles model is applied in order to optimize the real process. However, due to plant-model mismatch, MA-GP is also considered. The real process is optimized iteratively using the acquisition functions to select the next sampling point, bounded by a trust region. The sampling points are used to update the GP model. The results showed that the proposed strategy led the plant to its optimum point.

One important assumption of the previous works aiming to RTO applications (DEL RIO CHANONA *et al.*, 2021; DEL RIO CHANONA *et al.*, 2019; FERREIRA *et al.*, 2018; GOMES, 2007; GOMES *et al.*, 2006, 2008) is that a first-principles model is available. However, this assumption may not hold and a data-driven optimization may be required.

In this work, it is proposed a framework based on Bayesian optimization to update the GP model iteratively, which is applied to describe the plant, without the need of any previous rigorous model. A comparison between Bayesian Optimization MA-GP (DEL RIO CHANONA *et al.*, 2021) and the proposed strategy is carried out. Also, a third comparison is considered, which is related to the application of GP models to describe the measured output variables or the objective and constraints functions. Lastly, three acquisition functions are applied in the strategies, namely the Probability of Improvement, the Expected Improvement and the Lower Confidence Bound. The strategies are applied to two case studies,

an Exothermic CSTR System and the Willians-Otto Reactor.

## 4.2 Gaussian Processes Model Structure

In the present work, a Gaussian Process (GP) model structure was considered as the steady-state nonlinear function. Mathematically, a GP is described as follows:

$$y_j^{GP}(\mathbf{u}) = GP(\mu_{f,j}(\mathbf{u}), \sigma_{f,j}^2(\mathbf{u})) \quad (4.1)$$

where  $y_j^{GP}$  is the GP model output of the  $j$ -th system output  $y_j$ ,  $\mathbf{u}$  is the input variables vector,  $\mu_{f,j}$  is the posterior mean function and  $\sigma_{f,j}^2$  is the posterior variance function, calculated as follow:

$$\mu_{f,j}(\mathbf{u}) = \mathbf{r}_j^T(\mathbf{u}, \mathbf{U}) \mathbf{K}_j(\mathbf{U})^{-1} \mathbf{Y}_j + \mathcal{F}_j(\mathbf{u}, \boldsymbol{\beta}_j) \quad (4.2)$$

$$\sigma_{f,j}^2(\mathbf{u}) = \sigma_{n_j}^2 - \mathbf{r}_j^T(\mathbf{u}, \mathbf{U}) \mathbf{K}_j(\mathbf{U})^{-1} \mathbf{r}_j(\mathbf{u}, \mathbf{U}) \quad (4.3)$$

where  $\mathbf{U} \in \mathbb{R}^{n_u \times N}$  and  $\mathbf{Y}_j \in \mathbb{R}^N$  are  $N$ -sized input-output data set considered for GP training,  $\mathbf{K}_j \in \mathbb{R}^{N \times N}$  is a matrix whose elements are calculated as  $K_{j,l,m} = k_j(\mathbf{u}_l, \mathbf{u}_m) + \sigma_{v_j}^2 \delta_{l,m}$ ,  $\forall (l, m) \in [1, \dots, N]$ ,  $\delta_{l,m}$  is the Kronecker's delta function,  $\sigma_{v_j}^2$  is a parameter,  $\mathcal{F}_j$  is a regression function, typically considered as a polynomial function with parameters  $\boldsymbol{\beta}_j \in \mathbb{R}^{n_{\beta_j}}$  in which  $n_{\beta_j}$  is the number of parameters,  $\mathbf{r}_j(\mathbf{u}, \mathbf{U}) = [k_j(\mathbf{u}, \mathbf{u}_1), \dots, k_j(\mathbf{u}, \mathbf{u}_N)]^T$ , where  $k_j(\cdot, \cdot)$  is a kernel function, described in the present work as the squared-exponential kernel function:

$$k_j(\mathbf{u}, \mathbf{u}_l) = \sigma_{n_j}^2 \exp\left(-\frac{1}{2}(\mathbf{u} - \mathbf{u}_l)^T \boldsymbol{\Lambda}_j (\mathbf{u} - \mathbf{u}_l)\right) \quad (4.4)$$

where  $\sigma_{n_j}^2$  is a variance, which is also a model identifiable parameter and  $\boldsymbol{\Lambda}_j = \text{diag}(\lambda_{j_1}, \dots, \lambda_{j_{n_u}})$  is a scaling matrix. Therefore, the GP's hyperparameters are defined as:

$$\boldsymbol{\Psi}_j = [\boldsymbol{\beta}_j, \sigma_{n_j}, \sigma_{v_j}, \lambda_{j_1}, \dots, \lambda_{j_{n_u}}]^T \quad (4.5)$$

The GP hyperparameters are identified through a maximum likelihood approach, such that the log-likelihood objective function is considered. A complete description of GP and its hyperparameters estimation can be found in RASMUSSEN (2006).

In GP models, the specification of the prior mean and covariance functions, here described as the  $\mathcal{F}_j$  regression function and the kernel function  $k_j$  is essential

since it encodes the assumptions about the function to be learned from. Although the squared-exponential kernel function is the default kernel function in GP models, many other covariance functions can be applied. For instance, some examples of these functions are the constant, the linear, the polynomial, the Matérn, the  $\gamma$ -exponential, and the Rational Quadratic covariance functions. Each of these functions has its characteristics and can be tested to give a better fit to a regression problem (RASMUSSEN, 2006). Additionally, the GP models are non-parametric, which is an important characteristic of this class of models. It means that the nature and number of parameters are not predefined, such that it is learned from data (DEL RIO CHANONA *et al.*, 2021). Therefore, due to non-parametric characteristics, the GP models are useful in situations with little prior knowledge about the data.

RASMUSSEN (2006) highlight that the application of GP models requires the inversion of large matrices, which are typically not sparse, since GP uses all samples in training data set to perform a prediction. Indeed, accordingly to GRAMACY (2020), the problem scales in  $\mathcal{O}(m^3)$ , while the storage of matrices that are applied in predictions are in  $\mathcal{O}(m^2)$ . Therefore, depending on the scale of the problem, the computational time of GP models might be an issue.

In addition, RASMUSSEN (2006)

### 4.3 Modifier Adaptation based on GP models and Bayesian Optimization

The first to propose the use of GP in the context of Modifier Adaptation (MA) was FERREIRA *et al.* (2018), here called MA-GP. Later, DEL RIO CHANONA *et al.* (2019) expanded the framework by introducing the trust region approach and how to include GP uncertainty directly into the optimization problem. DEL RIO CHANONA *et al.* (2021) expanded the methodology in theoretical terms, including the concept of Acquisition Functions to promote exploration characteristics to the framework. They also showed the global convergence properties of unconstrained MA-GP.

The main idea behind MA-GP is to use GP to model the mismatch between the cost and constraint functions separately, such that:

$$\Phi_p - \Phi \approx GP \left( \mu_k^{(\Phi_p - \Phi)}(\mathbf{u}), \left( \sigma_k^{(\Phi_p - \Phi)} \right)^2(\mathbf{u}) \right) \quad (4.6)$$

$$\mathbf{G}_{p_l} - \mathbf{G}_l \approx GP \left( \mu_k^{(\mathbf{G}_{p_l} - \mathbf{G}_l)}(\mathbf{u}), \left( \sigma_k^{(\mathbf{G}_{p_l} - \mathbf{G}_l)} \right)^2(\mathbf{u}) \right) \quad \forall l \in [1, \dots, n_g] \quad (4.7)$$

where  $\mu_k^{(\Phi_p - \Phi)}(\mathbf{u})$  and  $\left(\sigma_k^{(\Phi_p - \Phi)}\right)^2(\mathbf{u})$  represent the posterior mean function and the posterior variance of the GP approximation of the objective function plant-model mismatch  $\Phi_p - \Phi$ . Analogously,  $\mu_k^{(G_{p_l} - G_l)}(\mathbf{u})$  and  $\left(\sigma_k^{(G_{p_l} - G_l)}\right)^2(\mathbf{u})$  represent the posterior mean function and the posterior variance of the GP approximation of the  $l$ -th constraint plant-model mismatch  $G_{p_l} - G_l$ . Here, the subscript  $k$  represents that the posterior mean and variance functions were updated considering data obtained until iteration  $k$ .

The trust-region MA-GP problem can be described as follows:

$$\begin{aligned}
\Delta \mathbf{u}_{k+1} = \arg \min_{\Delta \mathbf{u}} \quad & \Phi_{mod} := \Phi(\mathbf{u}_k + \Delta \mathbf{u}, \mathbf{y}) + \mu_k^{(\Phi_p - \Phi)}(\mathbf{u}_k + \Delta \mathbf{u}) \\
\text{s.t.} \quad & G_l(\mathbf{u}_k + \Delta \mathbf{u}, \mathbf{y}) + \mu_k^{(G_{p_l} - G_l)}(\mathbf{u}_k + \Delta \mathbf{u}) \leq 0, \\
& l = 1, \dots, n_g, \\
& \mathbf{f}_{ss}(\mathbf{y}, \mathbf{u}_k + \Delta \mathbf{u}, \boldsymbol{\alpha}) = \mathbf{0}, \\
& \mathbf{u}_{min} - \mathbf{u}_k \leq \Delta \mathbf{u} \leq \mathbf{u}_{max} - \mathbf{u}_k, \\
& \|\Delta \mathbf{u}\| \leq \Delta_k
\end{aligned} \tag{4.8}$$

where  $\Delta_k$  is the trust-region radius in the  $k$ -th RTO iteration and the procedures for updating the trust-region are described in DEL RIO CHANONA *et al.* (2021). Additionally, if Acquisition Functions are considered in the optimization problem represented by Equation 4.8, the objective function is then replaced by a given  $\mathcal{AF}$  function, which uses GP posterior mean and posterior variance functions.

Alternatively, instead of applying the modifiers into objective function and constraints, DELOU *et al.* (2022) proposed to model the output variables ( $\mathbf{y}$ ) plant-model mismatch and then use this information in optimization, here denoted as MAy-GP, such that:

$$\mathbf{y}_{p_j} - \mathbf{y}_j \approx GP \left( \mu_k^{(y_{p_j} - y_j)}(\mathbf{u}), \left( \sigma_k^{(y_{p_j} - y_j)} \right)^2(\mathbf{u}) \right) \quad \forall j \in [1, \dots, n_y] \tag{4.9}$$

where  $\mu_k^{(y_{p_j} - y_j)}(\mathbf{u})$  and  $\left(\sigma_k^{(y_{p_j} - y_j)}\right)^2(\mathbf{u})$  represent the posterior mean function and the posterior variance of the GP approximation of the  $j$ -th output variable plant-model mismatch  $\mathbf{y}_{p_j} - \mathbf{y}_j$ .

Thus, the corrected (or modified) model prediction can be calculated as follows:

$$\mathbf{y}_{modj} = \mathbf{y}_j + \mu_k^{(y_{p_j} - y_j)} \quad \forall j \in [1, \dots, n_y] \tag{4.10}$$

Then, the alternative formulation of the trust-region MAy-GP can be described as follows:

$$\begin{aligned}
\Delta \mathbf{u}_{k+1} &= \arg \min_{\Delta \mathbf{u}} \Phi(\mathbf{u}_k + \Delta \mathbf{u}, \mathbf{y}_{mod}) \\
\text{s.t.} \quad & \mathbf{G}_l(\mathbf{u}_k + \Delta \mathbf{u}, \mathbf{y}_{mod}) \leq 0 \quad l = 1, \dots, n_g, \\
& \mathbf{f}_{ss}(\mathbf{y}, \mathbf{u}_k + \Delta \mathbf{u}, \boldsymbol{\alpha}) = \mathbf{0}, \\
& \mathbf{y}_{mod} = \mathbf{y} + \boldsymbol{\mu}_k^{(y_p - y)}(\mathbf{u}_k + \Delta \mathbf{u}), \\
& \mathbf{u}_{min} - \mathbf{u}_k \leq \Delta \mathbf{u} \leq \mathbf{u}_{max} - \mathbf{u}_k, \\
& \|\Delta \mathbf{u}\| \leq \Delta_k
\end{aligned} \tag{4.11}$$

where  $\boldsymbol{\mu}_k^{(y_p - y)} = \left[ \mu_k^{(y_{p1} - y_1)}, \dots, \mu_k^{(y_{pn_y} - y_{ny})} \right]^T$ . In DELOU *et al.* (2022), the use of Acquisition Functions was not reported and it will be also explored in the present work.

## 4.4 Proposed Methodology

The main idea behind the proposed methodology is develop a data-driven solution, where the GP model can be iteratively trained based on acquired data from plant and use it to solve the optimization problem. The main advantage of the proposed methodology is that it does not depend on any first-principles model.

In the present work, the GP models are applied to either describe the objective and constraints functions or measured output variables, such that the objective function and constraints can be calculated and applied for optimization purposes. By considering the model development in terms of the output variables, it enables flexibility since these models can be applied to any model-based techniques, such as controllers and observers.

The plant output variables are approximated by GP models as follows:

$$y_{pj} \approx GP \left( \mu_k^{(y_{pj})}, \left( \sigma_k^{(y_{pj})} \right)^2 \right) \quad \forall j \in [1, \dots, n_y] \tag{4.12}$$

where  $\mu_k^{(y_{pj})}$  and  $\left( \sigma_k^{(y_{pj})} \right)^2$  represent the posterior mean function and the posterior variance of the GP approximation of the  $j$ -th plant output variable  $y_{pj}$ .

Then, objective function and constraints can be approximated using the GP

posterior mean for its calculation.

$$\Phi_p \approx \phi_{ec} \left( \boldsymbol{\mu}_k^{(y_{p_j})}, \mathbf{u} \right) \quad (4.13)$$

$$\mathbf{G}_p \approx \mathbf{G} \left( \boldsymbol{\mu}_k^{(y_{p_j})}, \mathbf{u} \right) \quad (4.14)$$

where  $\boldsymbol{\mu}_k^{(y_p)} = \left[ \mu_k^{(y_{p_1})}, \dots, \mu_k^{(y_{p_{n_y}})} \right]^T$

In order to apply Acquisition Functions, the mean and variance of calculated objective function and constraints functions based on output variables GP models are needed. The mean value can be calculated straightforward, following Equations 4.13 and 4.14. In order to calculate the variance, the output variables variance need to be propagated. Supposing the objective function and constraints functions are linear combinations of the output variables, it follows that:

$$(\sigma^\phi)_k^2 = \mathbf{c}^\phi T \boldsymbol{\Sigma}_k^y \mathbf{c}^\phi \quad (4.15)$$

$$\left( \sigma^{G_l} \right)_k^2 = \mathbf{c}^{G_l T} \boldsymbol{\Sigma}_k^y \mathbf{c}^{G_l} \quad l \in [1, \dots, n_g] \quad (4.16)$$

where  $\mathbf{c}^\phi \in \mathbb{R}^{n_y}$  and  $\mathbf{c}^{G_l} \in \mathbb{R}^{n_y}$  are coefficients for calculating associated to each output variable in objective function and the  $l$ -th constraint function and  $\boldsymbol{\Sigma}_k^y \in \mathbb{R}^{n_y \times n_y}$ , such that  $\boldsymbol{\Sigma}_k^y = \text{diag} \left( \left( \sigma_k^{(y_{p_1})} \right)^2, \dots, \left( \sigma_k^{(y_{p_{n_y}})} \right)^2 \right)$ . If the objective function and constraints functions are not calculated based on linear combination of the output variables, Equations 4.15 and 4.16 still hold, however, the vectors  $\mathbf{c}^\phi$  and  $\mathbf{c}^{G_l}$  are replaced by a the vector of partial derivatives of each function with respect to each output variable (TELLINGHUISEN, 2001), such that:

$$\mathbf{c}^\phi = \frac{\partial \phi_{ec}}{\partial \mathbf{y}} \quad (4.17)$$

$$\mathbf{c}^{G_l} = \frac{\partial G_l}{\partial \mathbf{y}} \quad , \forall l \in [1, \dots, n_g] \quad (4.18)$$

To give clarity about the variance propagation equations presented, an simple example is present in Example 4.4.1.

**Example 4.4.1** *Error Propagation.* Consider an objective function defined by

$$\phi_{ec}(\mathbf{u}) = ay_{p_1} + by_{p_2} + cu \quad (4.19)$$

where  $a, b, c \in \mathbb{R}$  and  $\mathbf{y}_p = [y_{p_1}, y_{p_2}]$ .

Thus, it follows that:

$$\mathbf{c}^\phi = [a \ b]^T \quad (4.20)$$

The variance of the function  $\phi_{ec}$ , based on the variance of the variables  $\mathbf{y}_p$ , is calculated as follows:

$$(\sigma^\phi)^2 = \mathbf{c}^{\phi T} \boldsymbol{\Sigma}^y \mathbf{c}^\phi \quad (4.21)$$

$$= [a \ b] \begin{bmatrix} (\sigma^{(y_{p1})})^2 & 0 \\ 0 & (\sigma_k^{(y_{p2})})^2 \end{bmatrix} [a \ b]^T \quad (4.22)$$

$$= a^2 (\sigma^{(y_{p1})})^2 + b^2 (\sigma_k^{(y_{p2})})^2 \quad (4.23)$$

A simple version of expression 4.15, considering that  $\boldsymbol{\Sigma}^y$  is a diagonal matrix, can be written as follows:

$$(\sigma^\phi)^2 = \sum_{j=1}^{n_y} \left( \frac{\partial \phi_{ec}}{\partial \mathbf{y}_{p_j}} \right)^2 (\sigma_k^{(y_{p_j})})^2 \quad (4.24)$$

Equation 4.24 can be written based on the following property of variance function (TELLINGHUISEN, 2001):

$$\sigma^2(ax_1 + bx_2) = a^2\sigma^2(x_1) + b^2\sigma^2(x_2) + 2abCov(x_1, x_2) \quad (4.25)$$

where *Cov* is the covariance function.

Here, since it is considered that the variables  $\mathbf{y}_p$  are independent, it follows that the covariance term is null.

Thus, based on the output variable GP models and definitions above, the mean and variance of objective function and constraints can be calculated, such that Acquisition Functions can be applied in the optimization problem, which is written as follows:

$$\begin{aligned} \Delta \mathbf{u}_{k+1} &= \arg \max_{\Delta \mathbf{u}} \mathcal{AF}(\mathbf{u}_k + \Delta \mathbf{u}) \\ \text{s.t.} \quad & \mathbf{G}_l(\mathbf{u}_k + \Delta \mathbf{u}, \mathbf{y}_{mod}) \leq 0 \quad l = 1, \dots, n_g, \\ & \mathbf{y}_{mod} = \boldsymbol{\mu}_k^{(y_p)}(\mathbf{u}_k + \Delta \mathbf{u}), \\ & \mathbf{u}_{min} - \mathbf{u}_k \leq \Delta \mathbf{u} \leq \mathbf{u}_{max} - \mathbf{u}_k, \\ & \|\Delta \mathbf{u}\| \leq \Delta_k \end{aligned} \quad (4.26)$$

Alternatively, if it is considered that the objective function and the constraints

functions can be measured directly from the plant, as proposed in the MA-GP approach, each function can be approximated directly by a GP model, such that:

$$\Phi_p \approx GP \left( \mu_k^{(\Phi_p)}(\mathbf{u}), \left( \sigma_k^{(\Phi_p)} \right)^2(\mathbf{u}) \right) = \hat{\phi}_{ec}(\mathbf{u}) \quad (4.27)$$

$$\mathbf{G}_{pl} \approx GP \left( \mu_k^{(\mathbf{G}_{pl})}(\mathbf{u}), \left( \sigma_k^{(\mathbf{G}_{pl})} \right)^2(\mathbf{u}) \right) = \hat{\mathbf{g}}(\mathbf{u}) \quad \forall l \in [1, \dots, n_g] \quad (4.28)$$

Thus, the optimization problem formulation is straightforward and described as follows:

$$\begin{aligned} \Delta \mathbf{u}_{k+1} &= \arg \max_{\Delta \mathbf{u}} \mathcal{AF}(\mathbf{u}_k + \Delta \mathbf{u}) \\ \text{s.t.} \quad & \mu_k^{(\mathbf{G}_{pl})}(\mathbf{u}_k + \Delta \mathbf{u}) \leq 0 \quad l = 1, \dots, n_g, \\ & \mathbf{u}_{min} - \mathbf{u}_k \leq \Delta \mathbf{u} \leq \mathbf{u}_{max} - \mathbf{u}_k, \\ & \|\Delta \mathbf{u}\| \leq \Delta_k \end{aligned} \quad (4.29)$$

where it was considered that the objective function model was already substituted in the Acquisition Function expression.

Additionally, an extension of the work of DELOU *et al.* (2022) is considered, applying acquisition functions to solve the optimization problem based on the MAy-GP strategy, which is described as follows:

$$\begin{aligned} \Delta \mathbf{u}_{k+1} &= \arg \max_{\Delta \mathbf{u}} \mathcal{AF}(\mathbf{u}_k + \Delta \mathbf{u}) \\ \text{s.t.} \quad & \mathbf{G}_l(\mathbf{u}_k + \Delta \mathbf{u}, \mathbf{y}_{mod}) \leq 0 \quad l = 1, \dots, n_g, \\ & \mathbf{f}_{ss}(\mathbf{y}, \mathbf{u} + \Delta \mathbf{u}, \boldsymbol{\alpha}) = \mathbf{0}, \\ & \mathbf{y}_{mod} = \mathbf{y}(\mathbf{u}_k + \Delta \mathbf{u}, \boldsymbol{\alpha}) + \mu_k^{(y_p - y)}(\mathbf{u}_k + \Delta \mathbf{u}), \\ & \mathbf{u}_{min} - \mathbf{u}_k \leq \Delta \mathbf{u} \leq \mathbf{u}_{max} - \mathbf{u}_k, \\ & \|\Delta \mathbf{u}\| \leq \Delta_k \end{aligned} \quad (4.30)$$

Last but not least, in this work, the Probability of Improvement for constrained problems was used as Acquisition Function and compared to Expected Improvement and Lower-Confidence Bound. The main advantage of this strategy is that the probability of feasibility acts like a penalty in the objective function, aiming to keep the problem feasibility.

Figure 4.1 presents a summary of the modeling strategies applied in the present work and the comparisons that was considered regarding the methods described before.

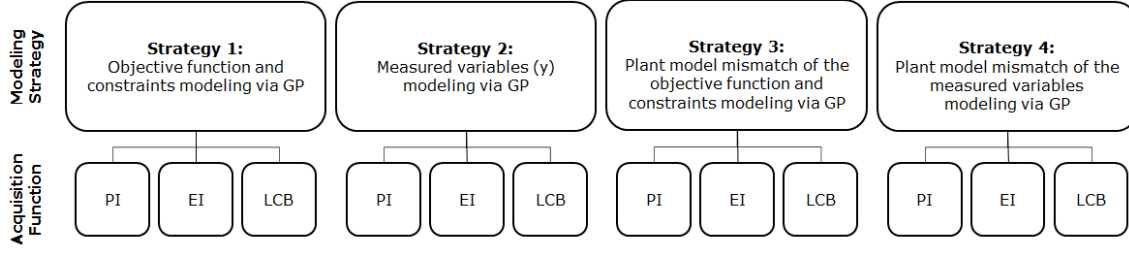


Figure 4.1: Summary of Modeling strategies and comparison to be studied in this work.

In Figure 4.1, Strategy 1 considers that the optimization problem objective function and constraints functions are identified by GP models, as described in Equations 4.27 and 4.28. The equivalent optimization problem is described by Equation 4.29. Strategy 2 considers that the measured variables ( $\mathbf{y}$ ) are identified by GP models, as described in Equation 4.12. Thus, the optimization problem is written as described by Equation 4.26. The Strategy 3 considers that the plant-model mismatch of the objective function and constraints function are modeled by a GP model. This strategy is similar to the MA-GP. Finally, the Strategy 4 is the MAY-GP approach and considers that the plant-model mismatch of the measured variables are modeled by a GP model, as described in Equation 4.10. The equivalent optimization problem is described by Equation 4.30. Different acquisition functions were also compared in each strategy, such that the constrained Probability of Improvement (PI), the constrained Expected Improvement (EI) and the constrained Lower Confidence Bound (LCB) were considered.

The acquisition functions may present multiple local minima, which require global optimization algorithms to find the global optimum point. CARPIO (2019) considered a combination of a stochastic optimization algorithm to find an initial guess of the optimal solution and a deterministic to refine it. DEL RIO CHANONA *et al.* (2021) applied a multi-start heuristic in order to avoid local minima solutions. Here, a multi-start heuristic was also considered, such that 20 initial guess points were randomly sampled within the trust region.

The trust region was updated at each iteration, following the criteria also considered in the work of DEL RIO CHANONA *et al.* (2021), originally proposed by RODRÍGUEZ *et al.* (1998). A metric based on the ratio of actual cost reduction to predicted cost reduction is considered.

In the case where the GP models are applied to approximate the objective function  $\phi_{ec}$ , the metrics are calculated as follows:

$$\rho_{k+1} = \frac{\phi_{ec}(\mathbf{y}_{p_k}, \mathbf{u}_k) - \phi_{ec}(\mathbf{y}_{p_{k+1}}, \mathbf{u}_k + \Delta \mathbf{u}_{k+1})}{\hat{\phi}_{ec}(\mathbf{u}_k) - \hat{\phi}_{ec}(\mathbf{u}_k + \Delta \mathbf{u}_{k+1})} \quad (4.31)$$

However, if the GP models are applied to approximate the measured output variables ( $\mathbf{y}$ ), the metrics is calculated as follows:

$$\rho_{k+1} = \frac{\phi_{ec}(\mathbf{y}_{p_k}, \mathbf{u}_k) - \phi_{ec}(\mathbf{y}_{p_{k+1}}, \mathbf{u}_k + \Delta \mathbf{u}_{k+1})}{\phi_{ec}(\mathbf{y}_{mod_k}, \mathbf{u}_k) - \phi_{ec}(\mathbf{y}_{mod_{k+1}}, \mathbf{u}_k + \Delta \mathbf{u}_{k+1})} \quad (4.32)$$

The trust region is updated by the following criteria:

If  $\rho_{k+1} > \eta_2$  or  $\|\Delta \mathbf{u}_{k+1}\| = \Delta_k$  :

$$\Delta_{k+1} = \gamma_{inc} \Delta_k$$

$$\mathbf{u}_{k+1} = \mathbf{u}_k + \Delta \mathbf{u}_{k+1}$$

Else If  $\rho_{k+1} < \eta_1$  :

$$\Delta_{k+1} = \gamma_{red} \Delta_k \quad (4.33)$$

$$\mathbf{u}_{k+1} = \mathbf{u}_k$$

Else :

$$\Delta_{k+1} = \Delta_k$$

$$\mathbf{u}_{k+1} = \mathbf{u}_k + \Delta \mathbf{u}_{k+1}$$

where  $\gamma_{inc}$  and  $\gamma_{red}$  are the trust-region radius increase and reduction factors, respectively, such that  $0 < \gamma_{red} < \gamma_{inc}$ . Also,  $\eta_1$  and  $\eta_2$  are threshold values for the  $\rho$  metrics, such that  $0 < \eta_1 < \eta_2 < 1$ . In this work,  $\gamma_{inc} = 1.2$ ,  $\gamma_{red} = 0.8$ ,  $\eta_1 = 0.2$  and  $\eta_2 = 0.7$ .

The RTO strategies described above are applied to case studies which are presented in Section 4.5. A number of RTO iterations ( $n_{iter}$ ) is considered in each case study as well a number of noise realizations ( $n_r$ ). Thus, it is possible to compare the distribution of the noise realization of each iteration in terms of the objective function value and the input variable values.

The following metric based on the work of QUELHAS *et al.* (2013) is applied to compared the performance of the strategies:

$$\Delta \Phi_{sol,k}(\%) = \frac{100}{\phi_{ec}^*} (\Phi_{sol,k} - \text{diag}(\phi_{ec}^* \mathbf{I}_{n_r})) \quad (4.34)$$

where  $\Phi_{sol,k} \in \mathbb{R}^{n_r}$  is the vector of the  $k$ -th iteration objective function value obtained in each noise realization,  $\phi_{ec}^* \in \mathbb{R}$  is the objective function value at the plant optimum, and  $\Delta \Phi_{sol,k} \in \mathbb{R}^{n_r}$  is the relative deviation of the the  $k$ -th RTO iteration objective function value obtained in each noise realization from the objective function value at the plant optimum.

An overall metric is obtained as the average of the values obtained in each

noise realization, which is written as follows:

$$\Delta\bar{\Phi}_{sol,k}(\%) = \frac{1}{n_r} \sum_{j=1}^{n_r} \Delta\Phi_{sol,k} \quad (4.35)$$

where  $\Delta\bar{\Phi}_{sol,k} \in \mathbb{R}$  represents the average of the deviations values from the plant optimum obtained in the noise realizations at the  $k$ -th RTO iteration.

Analogously, the relative distance of the decision variables from the optimum point achieved in the last RTO iteration in each noise realization was evaluate, which is described as follows:

$$\Delta\mathbf{u}_j(\%) = 100 \left\| \left[ \frac{\mathbf{u}_{i,j}^* - \mathbf{u}_{i,opt}^*}{\mathbf{u}_{i,opt}^*}, \dots, \frac{\mathbf{u}_{n_u,j}^* - \mathbf{u}_{n_u,opt}^*}{\mathbf{u}_{n_u,opt}^*} \right] \right\| \quad (4.36)$$

where  $\Delta\mathbf{u} \in \mathbb{R}^{n_r}$  is the relative distance of the decision variables form the optimum point  $\mathbf{u}_{opt}^* \in \mathbb{R}^{n_u}$  achieved in the last iteration,  $\mathbf{u}_j^*$  is the vector of decision variables achieved in the last RTO iteration obtained in the  $j$ -th noise realization.

Additionally, the surrogate model prediction error was evaluated considering the model obtained in the last iteration model (last update). It was evaluated at the average of the input variables obtained at each RTO iterations in each noise realization, *i.e.*,  $\mathbf{u}_{sol} = [mean(\mathbf{u}_1), mean(\mathbf{u}_2), \dots, mean(\mathbf{u}_{n_{iter}})]$ , where  $\mathbf{u}_k$ ,  $k = 1, \dots, n_{iter}$  is the  $k$ -th iteration solution considering the  $n_r$  noise realizations. Thus, in the case where the GP models are applied to approximate the objective function  $\phi_{ec}$ , the Root Mean Squared Error (RMSE) was calculated as follows:

$$RMSE(\mathbf{u}_{sol}) = \sqrt{\frac{\sum_{k=1}^{n_{iter}} (\hat{\phi}_{ec}(\mathbf{u}_{sol,k}) - \phi_{ec}(\mathbf{y}_p(\mathbf{u}_{sol,k}), \mathbf{u}_{sol,k}))^2}{n_{iter}}} \quad (4.37)$$

If the GP models are applied to approximate the measured output variables ( $\mathbf{y}$ ), the metrics is calculated as follows:

$$RMSE(\mathbf{u}_{sol}) = \sqrt{\frac{\sum_{k=1}^{n_{iter}} (\phi_{ec}(\mathbf{y}_{mod}(\mathbf{u}_{sol,k}), \mathbf{u}_{sol,k})) - \phi_{ec}(\mathbf{y}_p(\mathbf{u}_{sol,k}), \mathbf{u}_{sol,k}))^2}{n_{iter}}} \quad (4.38)$$

## 4.5 Case Studies

This section present the different case studies considered in order to apply the methodology described in Section 4.4.

### 4.5.1 Case Study: Exothermic CSTR Reactor

The first example considers a continuous stirred tank reactor (CSTR) equipped with an external jacket. In this reactor, a reversible exothermic reaction  $A \leftrightarrow B$  takes place (ECONOMOU *et al.*, 1986). The dynamic model is achieved to describe the process:

$$\frac{dC_A}{dt} = \frac{1}{\tau}(C_{A,in} - C_A) - k_A \exp \frac{-E_A}{RT} C_A + k_B \exp \frac{-E_B}{RT} C_B \quad (4.39)$$

$$\frac{dC_B}{dt} = -\frac{1}{\tau} C_B + k_A \exp \frac{-E_A}{RT} C_A - k_B \exp \frac{-E_B}{RT} C_B \quad (4.40)$$

$$\frac{dT}{dt} = \frac{-\Delta H}{\rho C_p} \left( -k_A \exp \frac{-E_A}{RT} C_A + k_B \exp \frac{-E_B}{RT} C_B \right) + \frac{1}{\tau}(T_{in} - T) + \frac{Q}{\rho C_p V} \quad (4.41)$$

where  $C_A$ ,  $C_B$  and  $T$  are the state variables and represent  $A$  species concentration,  $B$  species concentration and reactor temperature, respectively. The feed temperature and  $A$  concentration are represented by  $T_{in}$  and  $C_{A,in}$ , respectively.  $k_A$  and  $k_B$  are the pre-exponential factor for the forward and reverse reactions, respectively, and  $E_A$  and  $E_B$  are the corresponding activation energies.  $\tau$  is the residence time in the reactor,  $\Delta H$  is the heat of reaction,  $C_p$  is the specific heat capacity of the mixture,  $\rho$  is the mixture specific weight,  $V$  is the reactor volume,  $R$  is the gas constant.  $Q$  is the input variable, which represents the heat rate provided to the reactor by a jacket. The parameters values of the CSTR reactor is presented in Table 4.1.

Table 4.1: Exothermic CSTR model parameters.

Exothermic CSTR model parameters	
$T_{in} = 400 \text{ K}$	$\tau = 60 \text{ s}$
$k_A = 5000 \text{ s}^{-1}$	$k_B = 10^6 \text{ s}^{-1}$
$E_A = 10^4 \text{ cal/mol}$	$E_B = 1.5 \times 10^4 \text{ cal/mol}$
$R = 1.987 \text{ cal/(mol K)}$	$\Delta H = -5000 \text{ cal/mol}$
$\rho = 1 \text{ kg/L}$	$C_p = 1000 \text{ cal/(kg K)}$
$C_{A,in} = 1 \text{ mol/L}$	$V = 100 \text{ L}$

The economic optimization problem attempts to find the balance between the reactant conversion and heat cost. The optimization problem is described as fol-

lows (ZHANG *et al.*, 2019):

$$\begin{aligned}
Q^* = \arg \min_Q \quad & \phi_{ec} = \frac{C_A}{C_{A,in}} + 7 \times 10^{-7} Q \\
\text{s.t.} \quad & \mathbf{f}_{ss}(C_A, C_B, T, Q) = \mathbf{0}, \\
& 0 \leq C_A \leq 1 \text{ (mol/L)}, \\
& 0 \leq C_B \leq 1 \text{ (mol/L)}, \\
& 400 \leq T \leq 500 \text{ (K)}, \\
& 0 \leq Q \leq 10^5 \text{ (cal/s)}
\end{aligned} \tag{4.42}$$

In order to apply modifier-adaptation strategies (MA-GP and MAy-GP), a model with structural plant-model mismatch is considered, such that the model parameters were modified as follows:

$$k_{Amodel} = 0.9k_A \tag{4.43}$$

$$k_{Bmodel} = 0.5k_B \tag{4.44}$$

In the Exothermic CSTR case study, it was considered that an initial GP model was available, which was trained considering three points inside the optimization domain. These points correspond to the steady-state condition for the values of heat input listed in Table 4.2.

Table 4.2: CSTR Exothermic Reactor initial training points

Point	$Q$ (cal/s)
1	$8.5 \times 10^4$
2	$9.0 \times 10^4$
3	$9.5 \times 10^4$

## 4.5.2 Case Study: The Willians-Otto Reactor

Willians-Otto Reactor (WILLIAMS and OTTO, 1960) was chosen as the case study due to its nonlinear behavior and relevance in real-time optimization problems, previously studied in FORBES *et al.* (1994); FORBES and MARLIN (1996); MARCHETTI *et al.* (2010); MARCHETTI (2009); MARCHETTI *et al.* (2009).

It is important to say that the system studied in the present work is a simplification of the original benchmarking presented by WILLIAMS and OTTO (1960), considering only the reactor section, presented in Figure 4.2.

The reactor is a continuous stirred tank (CSTR) with a thermal jacket in order to control the reaction temperature  $T_R$ . The reactor has two input streams, related

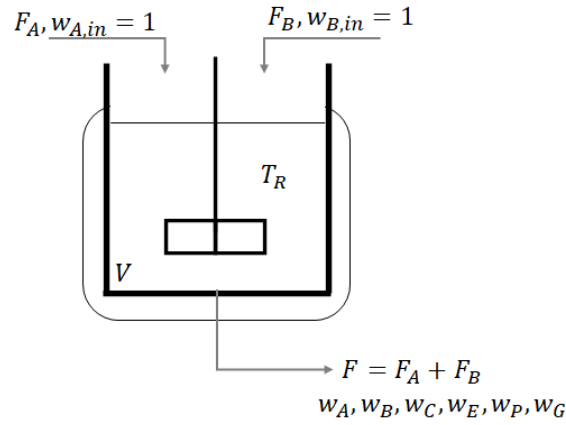


Figure 4.2: Willians-Otto Reactor.

to  $A$  and  $B$  species, and one output stream, which contains unreacted  $A$  and  $B$  species, an intermediary species  $C$ , products  $P$  and  $E$  and a byproduct  $G$ . It is assumed that the reactor has no overall accumulation, which implies that the total mass flow of output and input streams are equal. The mass balance and the reaction equations are described below.

Reaction System Equations:



Mass Balance Equations:

$$W \frac{dw_A}{dt} = F_A - (F_A + F_B)w_A - W r_1 \quad (4.48)$$

$$W \frac{dw_B}{dt} = F_B - (F_A + F_B)w_B - \frac{M_B}{M_A} W r_1 - W r_2 \quad (4.49)$$

$$W \frac{dw_C}{dt} = -(F_A + F_B)w_C + \frac{M_C}{M_A} W r_1 - \frac{M_C}{M_B} W r_2 - W r_3 \quad (4.50)$$

$$W \frac{dw_E}{dt} = -(F_A + F_B)w_E + \frac{M_E}{M_B} W r_2 \quad (4.51)$$

$$W \frac{dw_P}{dt} = -(F_A + F_B)w_P + \frac{M_P}{M_B} W r_2 - \frac{M_P}{M_C} W r_3 \quad (4.52)$$

$$W \frac{dw_G}{dt} = -(F_A + F_B)w_G + \frac{M_G}{M_C} W r_3 \quad (4.53)$$

where  $w_i$  ( $i = A, B, C, E, P, G$ ) is the mass fraction of the  $i$ -th species,  $F_A$  and  $F_B$  are the mass flowrate of  $A$  and  $B$ , respectively,  $M_i$  is the molar mass of the  $i$ -th species,  $W$  is the mass inside the reactor and  $r_j$  ( $j = 1, 2, 3$ ) is the reaction rate of  $j$ -th reaction, expressed in mass basis.

The specific reaction rate is given as follows:

$$k_j = k_{j,0} \exp \left[ \frac{-E_{a,j}}{R(T_R + 273.15)} \right] \quad (4.54)$$

The parameters related to the Willians-Otto equations are presented in Table 4.3.

Table 4.3: Willians-Otto Reactor Parameters (MARCHETTI, 2009).

Parameter	Description	Parameter Value	Unit
$k_{1,0}$	Specific Reaction Rate of Reaction 1	$1.6599 \times 10^6$	$s^{-1}$
$k_{2,0}$	Specific Reaction Rate of Reaction 2	$7.2117 \times 10^8$	$s^{-1}$
$k_{3,0}$	Specific Reaction Rate of Reaction 3	$2.6745 \times 10^{12}$	$s^{-1}$
$E_{a,1}/R$	Energy Activation of Reaction 1	6666.7	K
$E_{a,2}/R$	Energy Activation of Reaction 2	8333.3	K
$E_{a,3}/R$	Energy Activation of Reaction 3	11111	K
$M_A$	Molar Mass of Species A	100	—
$M_B$	Molar Mass of Species B	100	—
$M_C$	Molar Mass of Species C	200	—
$M_E$	Molar Mass of Species E	200	—
$M_P$	Molar Mass of Species P	300	—
$M_G$	Molar Mass of Species G	100	—
$W$	Total weight inside reactor	2105	kg

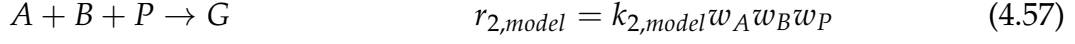
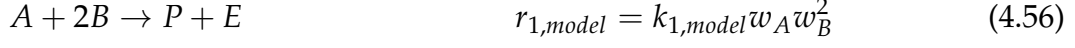
Regarding the economic optimization problem, a constrained economic optimization problem of the Willians-Otto reactor is considered, based on the work of DEL RIO CHANONA *et al.* (2021), which is described as follows:

$$\begin{aligned}
 F_B^*, T_R^* = \arg \min_{F_B, T_R} \quad & \phi_{ec} = -(1043.38 w_P F + 20.92 w_E F + \\
 & - 79.23 F_A - 118.34 F_B) \\
 \text{s.t.} \quad & f(\mathbf{w}, F_B, T_R) = \mathbf{0}, \\
 & w_A - 0.12 \leq 0, \\
 & w_G - 0.08 \leq 0, \\
 & 4 \leq F_B \leq 7 \text{ (kg/s)}, \\
 & 70 \leq T_R \leq 100 \text{ (}^\circ\text{C)}
 \end{aligned} \quad (4.55)$$

where  $\phi_{ec}$  is the profit (in  $\$/s$ ),  $f(\mathbf{w}, F_B, T_R)$  is the steady-state equation system, and  $F$  is the reactor outlet flow rate, considered as  $F = F_A + F_B$  (global mass balance). The constants in the objective function are the products selling prices and the reagent costs in  $\$/kg$ .

In order to apply modifier-adaptation strategies (MA-GP and MAy-GP), a

model with structural plant-model mismatch is considered, such that the model reaction system does not include the intermediate component C nor its composition is measured. The two reactions of the model are:



The model equations are written as follow:

$$W \frac{dw_A}{dt} = F_A - (F_A + F_B)w_A - Wr_{1,model} - r_{2,model} \quad (4.58)$$

$$W \frac{dw_B}{dt} = F_B - (F_A + F_B)w_B - \frac{M_B}{M_A}Wr_{1,model} - Wr_{2,model} \quad (4.59)$$

$$W \frac{dw_E}{dt} = -(F_A + F_B)w_E + \frac{M_E}{M_B}Wr_{2,model} \quad (4.60)$$

$$W \frac{dw_P}{dt} = -(F_A + F_B)w_P + \frac{M_P}{M_B}Wr_{1,model} - \frac{M_P}{M_B}Wr_{2,model} \quad (4.61)$$

$$W \frac{dw_G}{dt} = -(F_A + F_B)w_G + \frac{M_P}{M_B}Wr_{2,model} \quad (4.62)$$

$$(4.63)$$

where  $w_i$  ( $i = A, B, E, P, G$ ) is the mass fraction of the  $i$ -th species,  $F_A$  and  $F_B$  are the mass flowrate of  $A$  and  $B$ , respectively,  $M_i$  is the molar mass of the  $i$ -th species,  $W$  is the mass inside the reactor and  $r_j$  ( $j = 1, 2$ ) is the reaction rate of  $j$ -th reaction, expressed in mass basis.

In the Williams-Otto Reactor case study, it was considered that an initial GP model was available, which was trained considering five points inside the optimization domain. These points correspond to the steady-state condition for the values of input variables presented in Table 4.4. It is also important to mention that these points are the same considered in the works of DEL RIO CHANONA *et al.* (2021) and DELOU *et al.* (2022), aiming to enable comparison of the strategies.

Table 4.4: Williams-Otto Reactor initial points.

Point	$F_B$ (kg/s)	$T_R$ (°C)
1	5.7	74
2	6.35	74.9
3	6.6	75
4	6.75	79
5	6.9	83

### 4.5.3 Optimization Solver

The optimization problems were solved considering the function "fmincon" from MATLAB ©, considering the interior-point method, with termination tolerance on decision variables of  $10^{-10}$  and termination tolerance on the objective function value of  $10^{-6}$ . The tolerance in terms of the constraints was also considered to be  $10^{-6}$ .

## 4.6 Results and Discussion

In this section, the results of the optimization strategies based on the proposed methodology applied to each case study are presented.

### 4.6.1 Exothermic CSTR

In the Exothermic CSTR case study, it was considered 20 RTO iterations with 20 noise realizations in each iteration. Figure 4.3 presents the objective function ( $\phi_{ec}$ ) value achieved at the last RTO iteration for 20 noise realizations in each RTO strategy. The results are shown for the constrained function PI (Probability of Improvement), EI (Expected Improvement), and LCB (Lower Confidence Bound).

From Figure 4.3, it is possible to notice that the optimum value (green triangle) is within the objective function value distributions in all strategies and all acquisition functions. In practice, it means that these strategies are able to drive the plant to its optimum point. Additionally, the objective function values distribution achieved a narrow distribution in all strategies evaluated.

Regarding average performance, the relative deviation from the plant optimum in terms of the objective function was calculated using Equation 4.34. It was calculated for each strategy and each acquisition function, considering the 20 noise realizations at the last RTO iteration. The distribution of the relative average deviation from the plant optimum in terms of the objective function is presented in Figure 4.4.

From Figure 4.4, it is possible to notice that the relative deviation from the optimum presents the order of magnitude of  $10^{-3}\%$ . Strategy 1 presents the highest relative average deviation among the strategies for all acquisition functions tested. On average, it is possible to notice that the lowest relative average deviation was obtained using Strategy 4 and the LCB acquisition function. Indeed, the relative average deviations obtained when using LCB were lower than the other acquisition functions.

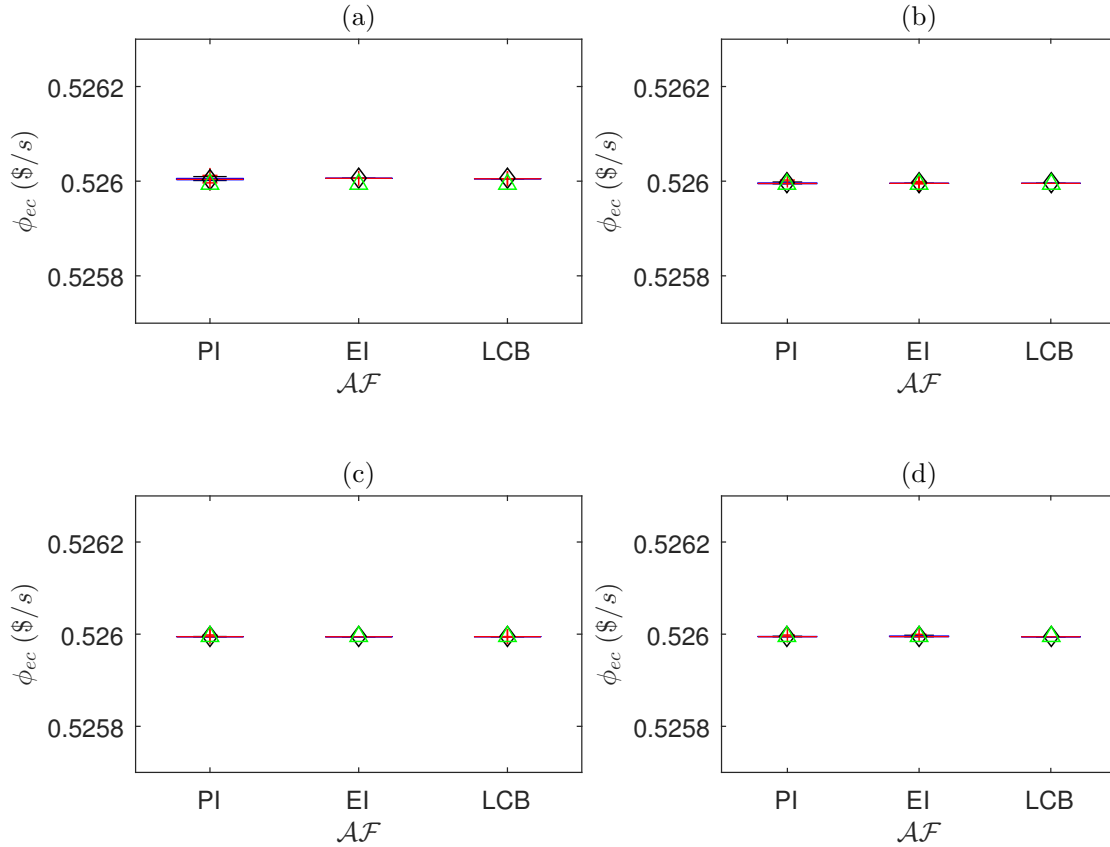


Figure 4.3: Economic objective function at RTO last iteration for 20 noise realization and for each acquisition function (PI, EI and LCB) using: (a) Strategy 1 (objective function and constraints modeling via GP), (b) Strategy 2 (measured variables ( $\mathbf{y}$ ) modeling via GP), (c) Strategy 3 (MA-GP), and (d) Strategy 4 (MAY-GP). Black diamonds represent the average of 20 realizations. Green triangle represents the plant optimum.

The relative distance from the optimum in terms of the decision variable was also evaluated considering the last iteration and the noise realizations. Figure 4.5 presents the relative deviation in terms of the optimization problem decision variables.

From Figure 4.5, it is possible to notice that the deviation from the optimum point is, on average limited to 1.2%, which is the average deviation value obtained in Strategy 1 using the PI acquisition function. Indeed, the deviation values obtained in Strategy 1 are higher than those obtained in other strategies. Since the optimization problem is unconstrained, a higher deviation in terms of deviation variables from the optimum point may be related to the surrogate model accuracy. In order to evaluate the model accuracy, the RMSE was calculated following Equation 4.38. The average results in the noise realizations are presented in Table 4.5.

From Table 4.5, it is possible to notice that the higher RMSE is obtained in

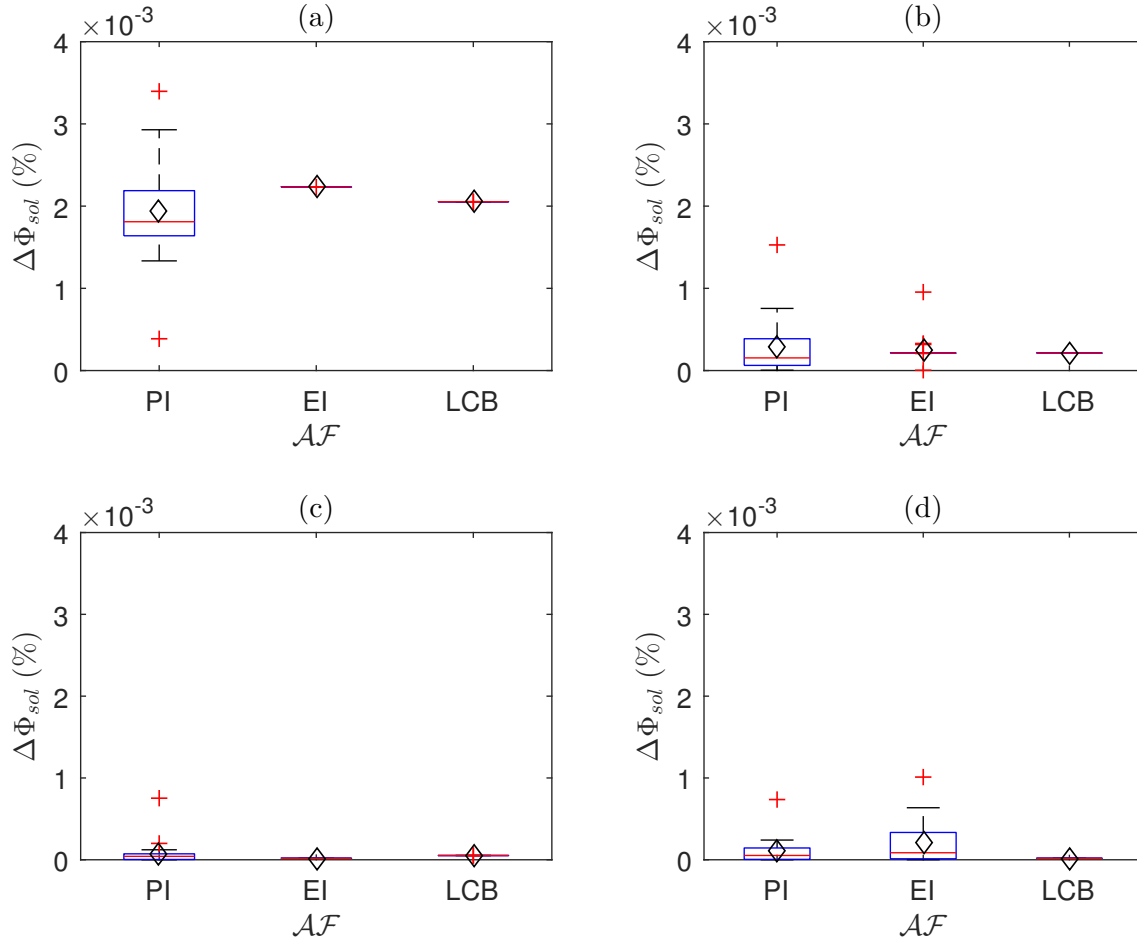


Figure 4.4: Relative average deviation from the plant optimum of the economic objective function values at RTO last iteration for 20 noise realization and for each acquisition function (PI, EI and LCB) using: (a) Strategy 1 (objective function and constraints modeling via GP), (b) Strategy 2 (measured variables ( $\mathbf{y}$ ) modeling via GP), (c) Strategy 3 (MA-GP), and (d) Strategy 4 (MAy-GP). Black diamonds represent the average of 20 realizations.

Table 4.5: RMSE of the objective function predictions in the strategies evaluated.

Strategy/ Acquisition Function	PI	EI	LCB
$RMSE(\times 10^6)$ - Strategy 1	8.31	8.54	8.42
$RMSE(\times 10^6)$ - Strategy 2	0.58	0.44	0.58
$RMSE(\times 10^6)$ - Strategy 3	2.01	2.06	2.06
$RMSE(\times 10^6)$ - Strategy 4	2.01	2.06	2.01

Strategy 1, which agrees with the higher deviations obtained in decision variables and objective function obtained before. In Strategy 1, it is also verified that the RMSE values are independent of the acquisition functions applied. Also, Strategy 2 presented the lowest RMSE value compared to other strategies. However, the deviation from the optimum point in decision variables was comparable to

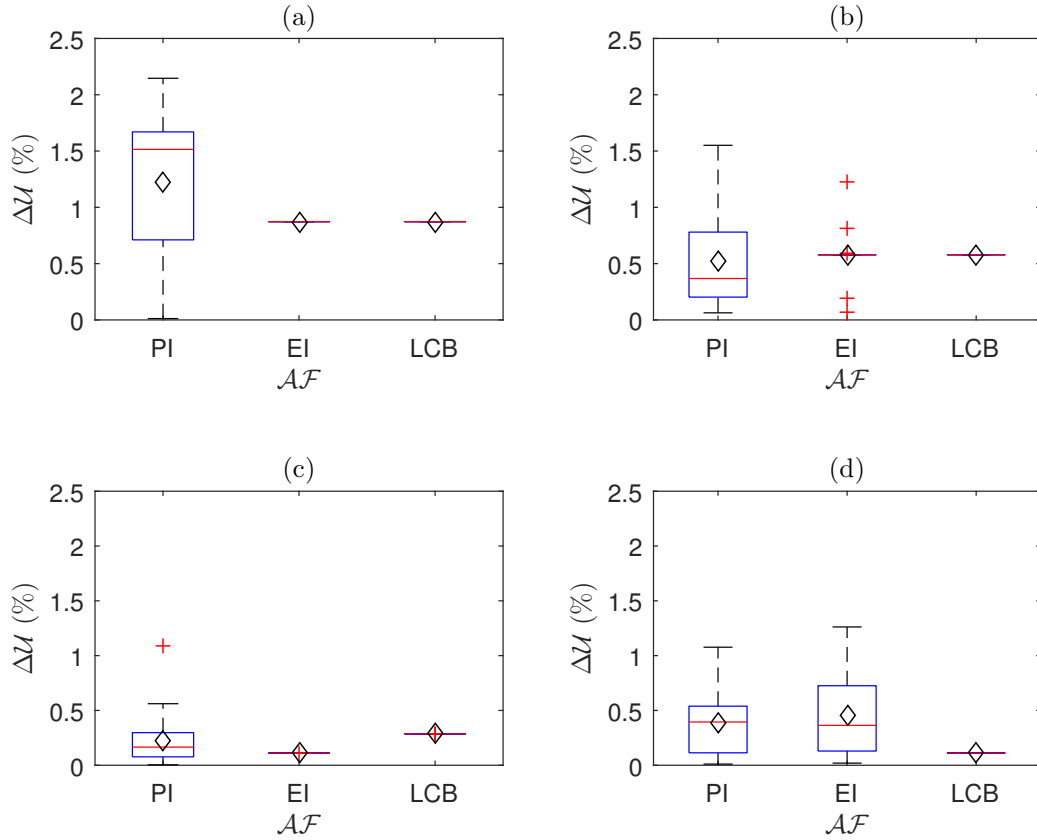


Figure 4.5: Relative average deviation from the plant optimum of the decision variables at RTO last iteration for 20 noise realization and for each acquisition function (PI, EI and LCB) using: (a) Strategy 1 (objective function and constraints modeling via GP), (b) Strategy 2 (measured variables ( $\mathbf{y}$ ) modeling via GP), (c) Strategy 3 (MA-GP), and (d) Strategy 4 (MA $\mathbf{y}$ -GP). Black diamonds represent the average of 20 realizations.

Strategies 3 and 4.

Figures 4.6, 4.7, 4.8 and 4.9 present the objective function and the input variable values at each RTO iteration for 20 noise realizations obtained in Strategies 1, 2, 3 and 4, respectively.

In Figures 4.6, 4.7, 4.8 and 4.9, it is possible to notice a similar behavior of the RTO iterations in the three acquisition functions. In all strategies, it is noticed that the last iteration (green triangles) values are uniform and also close to the optimum point (pink star). This result agrees with the deviations from the optimum point verified in Figures 4.4 and 4.5. It is also possible to notice that in all strategies, the PI acquisition function presented an exploration behavior compared to the other acquisition functions, which can be seen in the trajectories.

Regarding computational time, Figure 4.5 presents the average iteration time of each strategy.

From Figure 4.10, it is possible to notice that strategies 1 and 2 present a lower

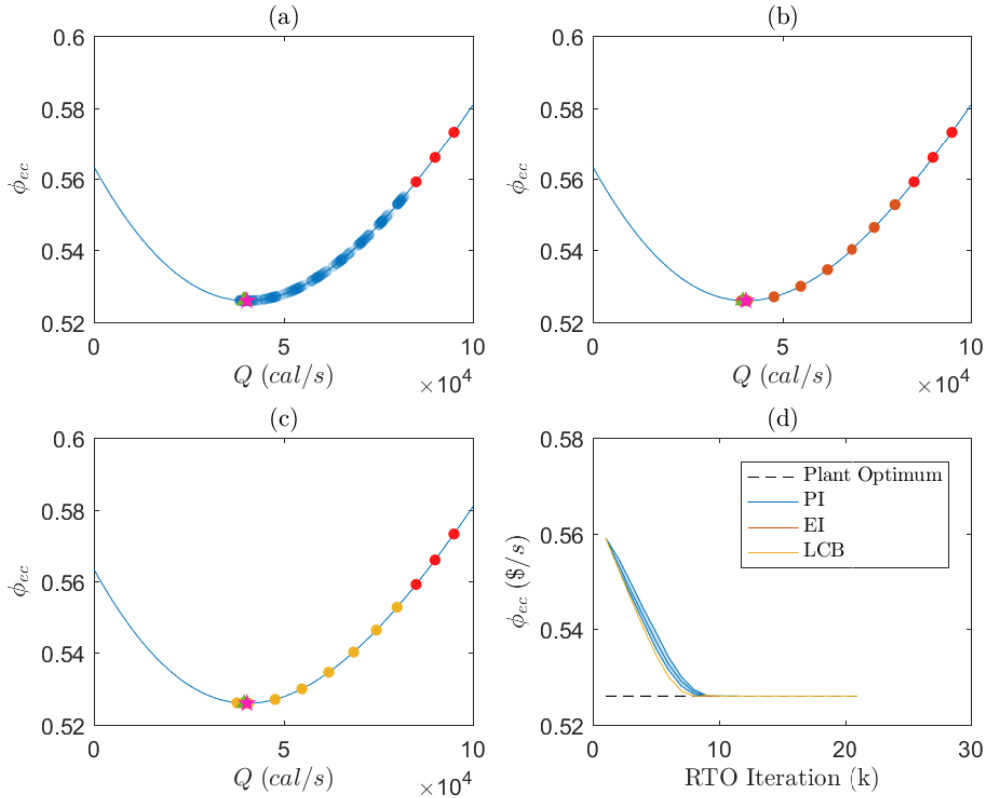


Figure 4.6: RTO iterations using Strategy 1 (objective function and constraints modeling via GP) and comparing different acquisition functions: (a) *PI*, (b) *EI* and (c) *LCB*. (d) The cost evolution for acquisition functions *PI*, *EI*, *LCB* during the 20 iterations. Red dots represent the initial GP training points. Green triangles represent the last iterate of each RTO run. The blue continuous line represents the objective function and input variable relationship and the pink star represents plant optimum.

average computational time than strategies 3 and 4. Indeed, strategies 3 and 4 apply a rigorous model in the optimization step, while in strategies 1 and 2, only identified Gaussian Process models are applied. It is also possible to notice that the average iteration time obtained when applying the Probability of Improvement acquisition function is higher than the average iteration time for the other acquisition function tested for all strategies considered. This last result is in agreement with the exploratory behavior showed in Figures 4.6 to 4.9.

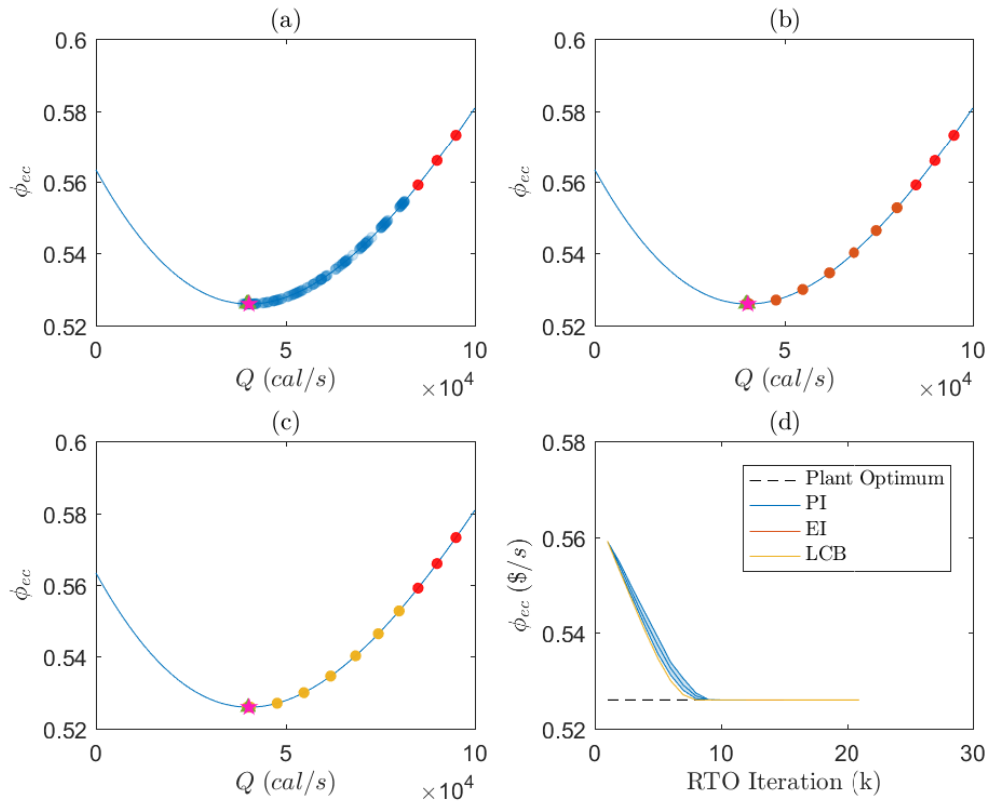


Figure 4.7: RTO iterations using the GP models for Strategy 2 (measured variables  $(\mathbf{y})$  modeling via GP and comparing different acquisition functions: (a) *PI*, (b) *EI* and (c) *LCB*. (d) The cost evolution for acquisition functions *PI*, *EI*, *LCB* during the 20 iterations. Red dots represent the initial GP training points. Green triangles represent the last iterate of each RTO run. The blue continuous line represents the objective function and input variable relationship and the pink star represents plant optimum.

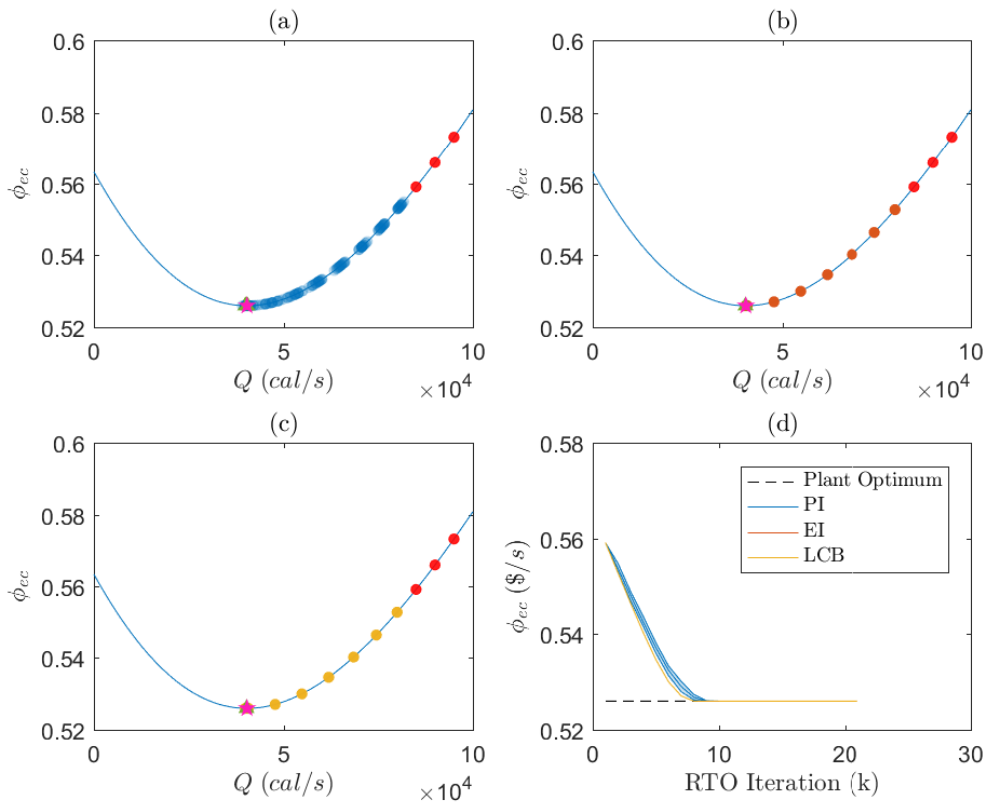


Figure 4.8: RTO iterations using the GP models for Strategy 3 (MA-GP) and comparing different acquisition functions: (a) *PI*, (b) *EI* and (c) *LCB*. (d) The cost evolution for acquisition functions *PI*, *EI*, *LCB* during the 20 iterations. Red dots represent the initial GP training points. Green triangles represent the last iterate of each RTO run. The blue continuous line represents the objective function and input variable relationship and the pink star represents plant optimum.

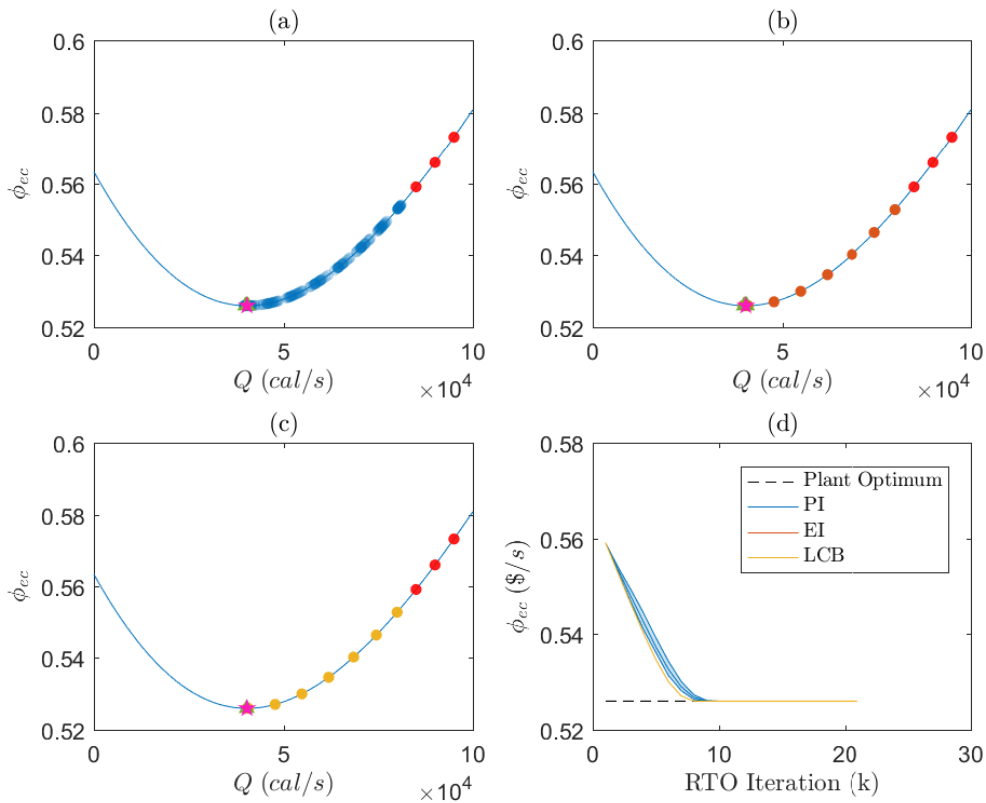


Figure 4.9: RTO iterations using Strategy 4 (MAy-GP) and comparing different acquisition functions: (a) *PI*, (b) *EI* and (c) *LCB*. (d) The cost evolution for acquisition functions *PI*, *EI*, *LCB* during the 20 iterations. Red dots represent the initial GP training points. Green triangles represent the last iterate of each RTO run. The blue continuous line represents the objective function and input variable relationship and the pink star represents plant optimum.

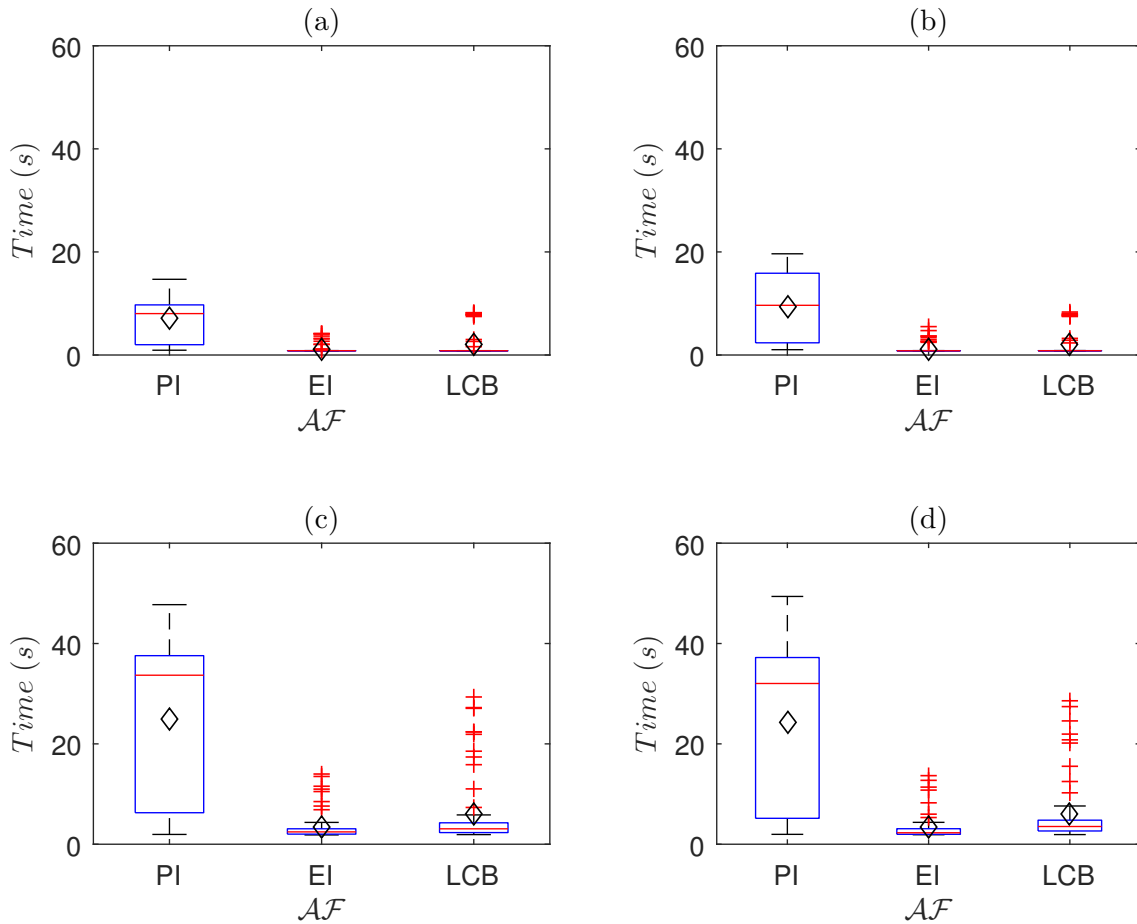


Figure 4.10: Average Iteration Time for each acquisition function (PI, EI and LCB) using: (a) Strategy 1 (objective function and constraints modeling via GP), (b) Strategy 2 (measured variables ( $\mathbf{y}$ ) modeling via GP), (c) Strategy 3 (MA-GP), and (d) Strategy 4 (MAy-GP). Black diamonds represent the average of the 20 RTO iterations considering 20 realizations.

The average iteration time of each strategy is also presented in Table 4.6.

Table 4.6: Average iteration time obtained in each strategy.

Strategy/ Acquisition Function	PI	EI	LCB
Strategy 1	7.15	1.20	1.96
Strategy 2	9.45	1.23	1.97
Strategy 3	24.88	3.54	6.08
Strategy 4	24.20	3.27	6.04
Ratio between strategies 1 and 3	0.29	0.34	0.32
Ratio between strategies 2 and 4	0.39	0.37	0.33

From Table 4.6, it is possible to notice that the ratio between the average iteration time of strategies 1 and 3 is 0.29, 0.34 and 0.32, when considering acquisition functions *PI*, *EI*, and *LCB*, respectively. When comparing strategies 2 and 4, the ratio between the average iteration time of strategies 2 and 4 is 0.39, 0.37 and 0.33, when considering acquisition functions *PI*, *EI*, and *LCB*, respectively. As mentioned before, the reduction in the average iteration time of strategies 1 and 2 is related to not considering a first-principles model, since only GP models are applied.

In this first case study, the strategies were able to drive the plant to a neighborhood of the plant optimum. The relative deviation from the plant optimum in terms of the objective function is in order of magnitude of  $10^{-3}\%$ , which means that the strategies presented a small deviation from the plant optimum. This result was also verified regarding the relative deviation from the plant optimum of the decision variable. Among the strategies, Strategy 1 presented the highest deviation from the plant optimum, which agrees with the higher RMSE of the objective function predictions. Regarding the acquisition functions tested, the results were comparable in each strategy. The *PI* acquisition function presented an exploration behavior compared to *EI* and *LCB* acquisition functions. It was also showed that the strategies 1 and 2 presented a reduction in the average iteration time when compared to strategies 3 and 4, respectively, since strategies 1 and 2 do not apply a first-principles model for optimization purposes.

#### 4.6.2 Williams-Otto Reactor

In the Williams-Otto Reactor case study, it was also considered 20 RTO iterations with 20 noise realizations in each iteration. Figure 4.11 presents the objective function ( $\phi_{ec}$ ) value achieved at the last RTO iteration for 20 noise realization in each RTO strategy for each acquisition function.

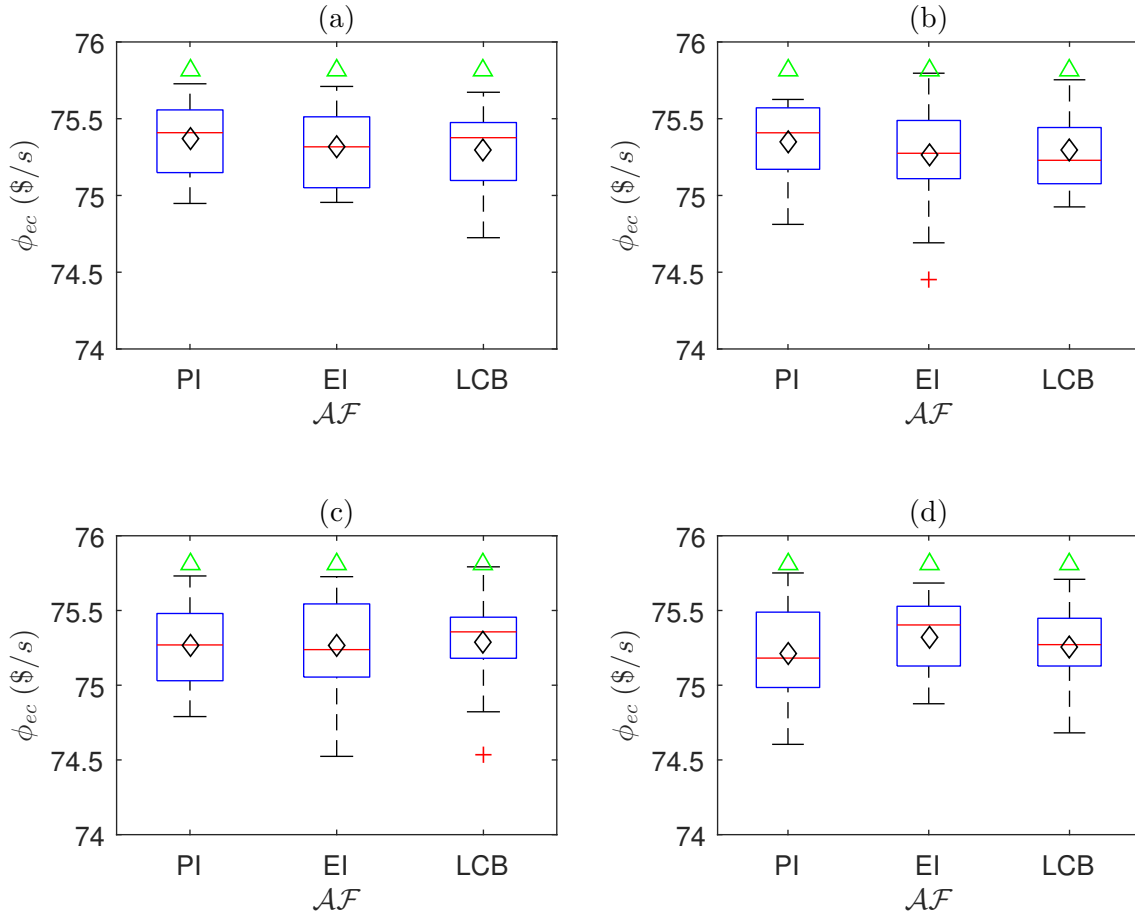


Figure 4.11: Economic objective function at RTO last iteration for 20 noise realization and for each acquisition function (PI, EI, LCB) using: (a) Strategy 1 (objective function and constraints modeling via GP), (b) Strategy 2 (measured variables ( $\mathbf{y}$ ) modeling via GP), (c) Strategy 3 (MA-GP), and (d) Strategy 4 (MAy-GP). Black diamonds represent the average of 20 realizations. Green triangle represents the plant optimum.

From Figure 4.11, it is possible to notice that all strategies could drive the plant close to its optimum point, as the upper-whisker of the boxplots of the objective function values are close to the optimum value (green triangle). This result was also verified by DEL RIO CHANONA *et al.* (2021), which related it to the low cost sensitivity along one of the active constraints compared to the noise level. Here, it is also important to highlight that an interior-point method was considered to solve the optimization problem. Thus, since the plant's optimum point is at the intersection of the constraints (active constraints), the interior-point method would not achieve the constraints, as it is a barrier method.

Regarding average performance, the relative deviation from the plant optimum in terms of the objective function was calculated using Equation 4.34. It was calculated for each strategy and each acquisition function, considering the 20 noise realizations at the last RTO iteration. The distribution of the relative

average deviation from the plant optimum in terms of the objective function is presented in Figure 4.12.

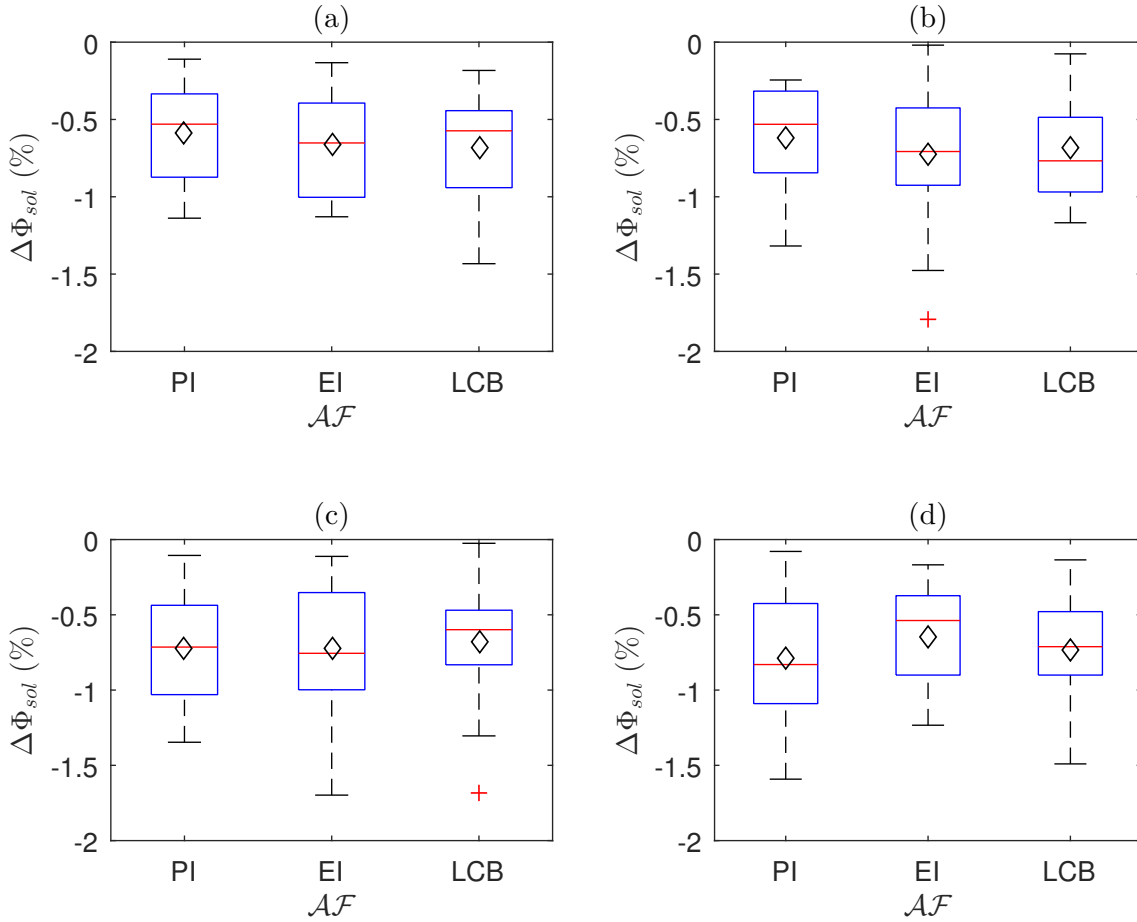


Figure 4.12: Relative average deviation from the plant optimum of the economic objective function values at RTO last iteration for 20 noise realization and for each acquisition function (PI, EI and LCB) using: (a) Strategy 1 (objective function and constraints modeling via GP), (b) Strategy 2 (measured variables ( $\mathbf{y}$ ) modeling via GP), (c) Strategy 3 (MA-GP), and (d) Strategy 4 (MAy-GP). Black diamonds represent the average of 20 realizations.

From Figure 4.12, it is possible to notice that the relative deviation from the optimum is limited to  $-1.5\%$ , represented by the lower-whisker in the boxplot charts. Regarding average performance, the order of magnitude of the deviations obtained in all strategies is similar. Regarding the acquisition functions tested, it is possible to notice that the distribution of the relative deviation is dependent on the acquisition function, which may be related to the exploration-exploitation characteristic of each acquisition function.

The relative distance from the optimum in terms of the decision variable was also evaluated, considering the last iteration and the noise realizations. Figure 4.13 presents the relative deviation in terms of the optimization problem decision variables.

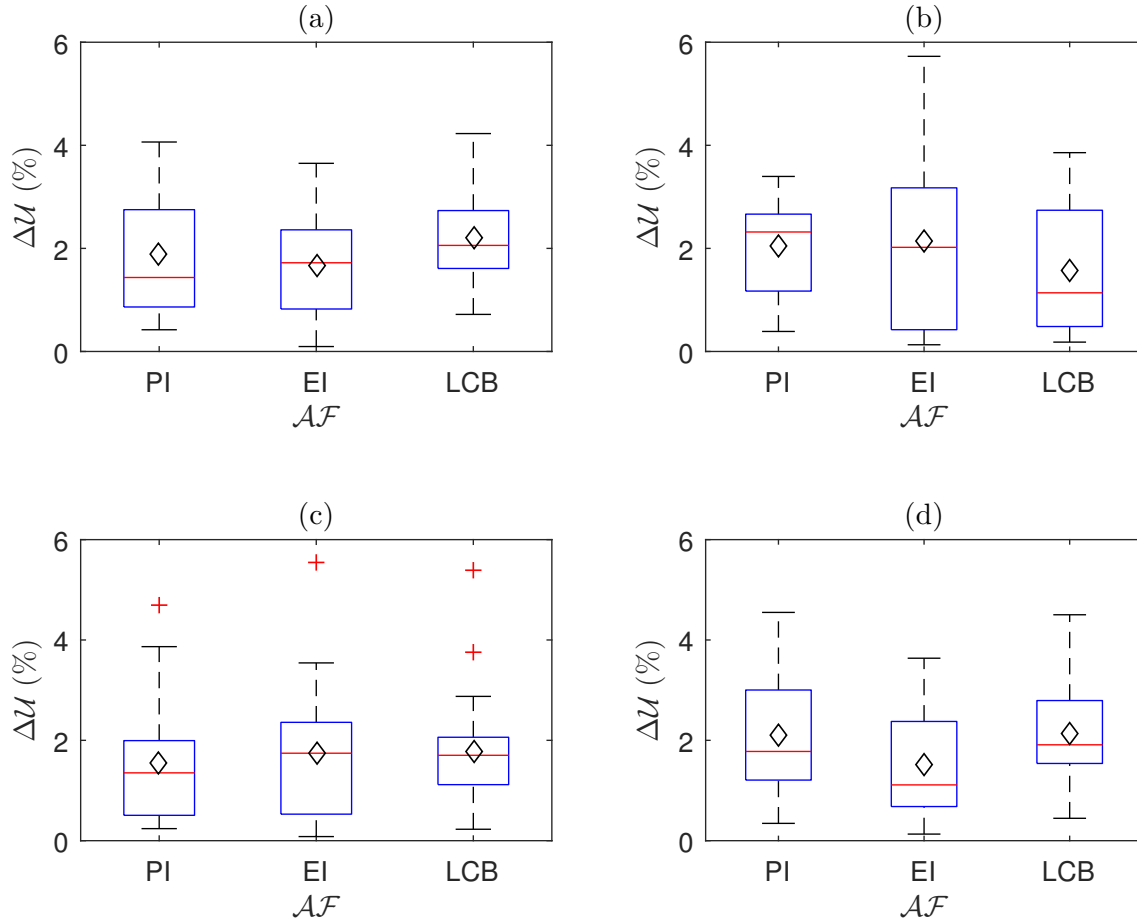


Figure 4.13: Relative average deviation from the plant optimum of the decision variables at RTO last iteration for 20 noise realization and for each acquisition function (PI, EI and LCB) using: (a) Strategy 1 (objective function and constraints modeling via GP), (b) Strategy 2 (measured variables ( $y$ ) modeling via GP), (c) Strategy 3 (MA-GP), and (d) Strategy 4 (MA $y$ -GP). Black diamonds represent the average of 20 realizations.

From Figure 4.13, it is possible to notice that the deviation from the optimum point is, on average limited to 2%, achieving a maximum deviation of 6% obtained during the noise realization in Strategy 2 using EI acquisition function. Regarding the model accuracy, the RMSE was calculated following Equation 4.38. Table 4.7 presents the average results in the noise realizations.

Table 4.7: RMSE of the objective function predictions in the strategies evaluated.

Strategy/ Acquisition Function	PI	EI	LCB
$RMSE(\times 10^3)$ - Strategy 1	3.60	4.70	2.90
$RMSE(\times 10^3)$ - Strategy 2	4.10	3.80	4.10
$RMSE(\times 10^3)$ - Strategy 3	0.90	1.30	0.70
$RMSE(\times 10^3)$ - Strategy 4	1.30	1.20	1.30

From Table 4.7, it is possible to notice that the RMSE values present the same order of magnitude. It is interesting to notice that the RMSE values obtained in Strategies 3 and 4 are comparable and lower than those obtained in Strategies 1 and 2. This result may be related to the fact that Strategies 3 and 4 apply a first-principle model with a correction of plant-model mismatch based on GP models, while Strategies 1 and 2 are based only on GP models. Thus, it suggests that the first-principle model may contribute to higher accuracy, although the RMSE values are in the same order of magnitude.

Figures 4.14, 4.15, 4.16 and 4.17 present the objective function and the input variable values at each RTO iteration for 20 noise realizations obtained in Strategies 1, 2, 3 and 4, respectively.

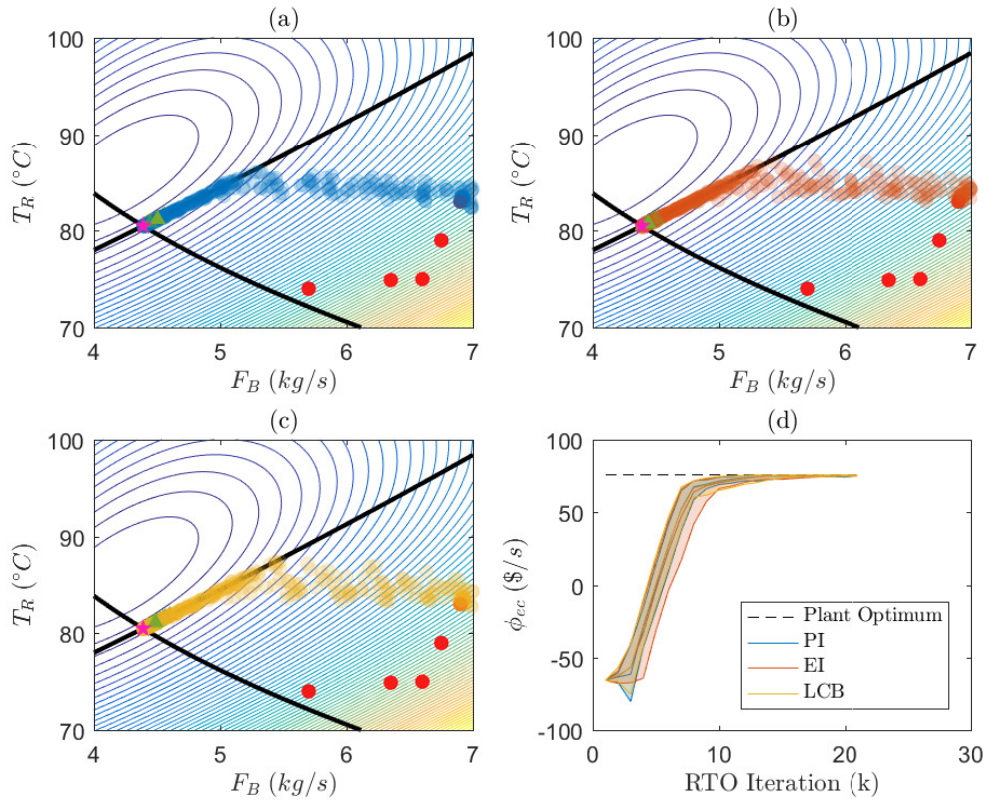


Figure 4.14: RTO iterations using Strategy 1 (objective function and constraints modeling via GP) and comparing different acquisition functions: (a) *PI*, (b) *EI* and (c) *LCB*. (d) The cost evolution for acquisition functions *PI*, *EI*, *LCB* during the 20 iterations. Red dots represent the initial GP training points. Green triangles represent the last iterate of each RTO run. Black continuous lines represent the constraint limits and the pink star represents the plant optimum.

In Figures 4.6, 4.7, 4.8 and 4.9, it is possible to notice that the behavior of the RTO iterations in all strategies is similar and shown the ability to drive the plant to a neighborhood of the plant optimum. Also, the results obtained in this work are compatible with the results obtained in DEL RIO CHANONA *et al.* (2021). In

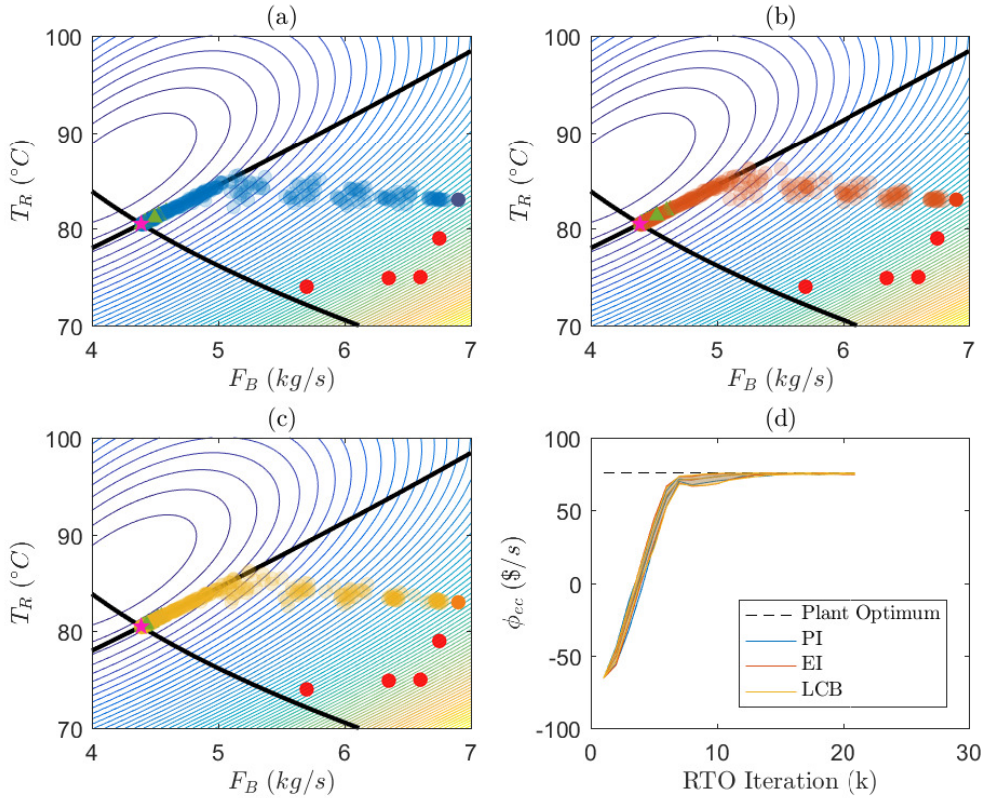


Figure 4.15: RTO iterations using Strategy 2 (measured variables ( $\mathbf{y}$ ) modeling via GP) and comparing different acquisition functions: (a) *PI*, (b) *EI* and (c) *LCB*. (d) The cost evolution for acquisition functions *PI*, *EI*, *LCB* during the 20 iterations. Red dots represent the initial GP training points. Green triangles represent the last iterate of each RTO run. Black continuous lines represent the constraint limits and the pink star represents plant optimum.

this previous work, the last RTO iteration point (green triangle) is spread following an active constraint. Thus, the results obtained in the present work showed a more uniform distribution than those obtained in the previous work. Regarding the acquisition functions applied in each RTO strategy, the performance is comparable, and all the acquisition functions led to a neighborhood of the plant optimum after the 10-th iteration. It is also interesting to notice that Strategy 1 presented an initial oscillation compared to others, as shown in Figure 4.6, which is observable to all acquisition functions applied. This fact may be related to the GP inaccuracy at the initial point, which led to exploratory behavior.

Regarding computational time, Figure 4.13 presents the average iteration time of each strategy.

From Figure 4.18, it is possible to notice that strategies 1 and 2 present a lower average computational time than strategies 3 and 4. Indeed, strategies 3 and 4 apply a rigorous model in the optimization step, while in strategies 1 and 2, only identified Gaussian Process models are applied. It is also possible to notice that

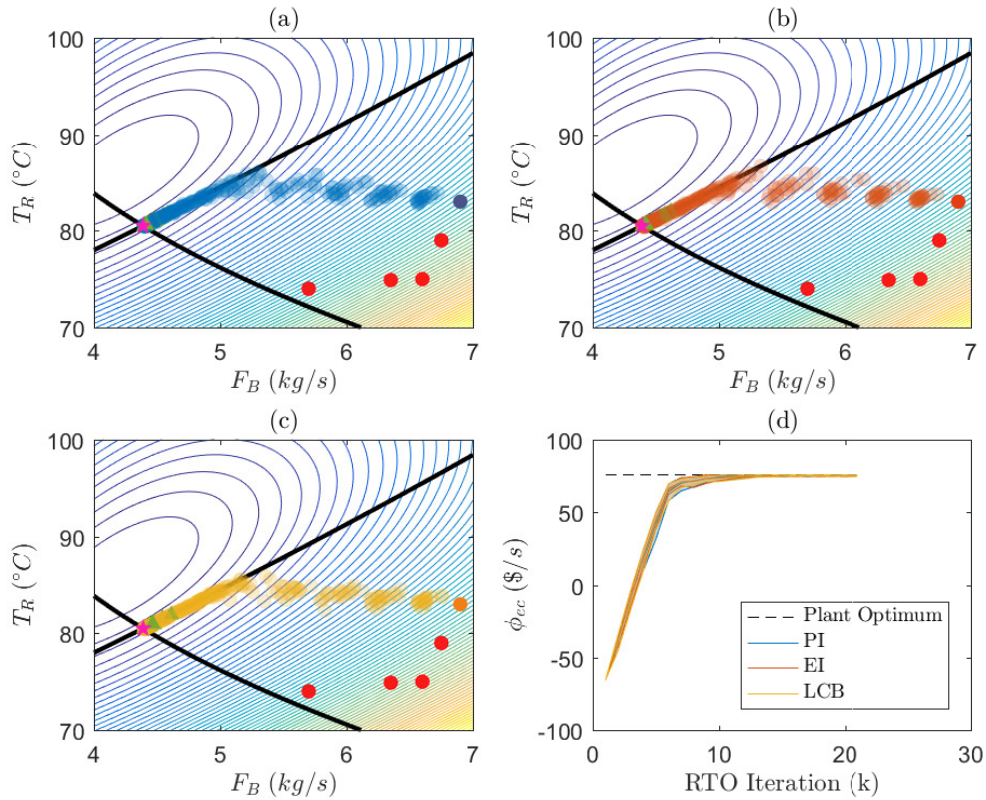


Figure 4.16: RTO iterations using Strategy 3 (MA-GP) and comparing different acquisition functions: (a) *PI*, (b) *EI* and (c) *LCB*. (d) The cost evolution for acquisition functions *PI*, *EI*, *LCB* during the 20 iterations. Red dots represent the initial GP training points. Green triangles represent the last iterate of each RTO run. Black continuous lines represent the constraint limits and the pink star represents plant optimum.

the distribution of iteration time is similar in each strategy, being independent of the acquisition function applied. This result is in agreement to the comparisons regarding the relative average deviation from plant optimum of the economic objective function and decision variables, since the results are comparable in each strategy, not depending on the acquisition function applied.

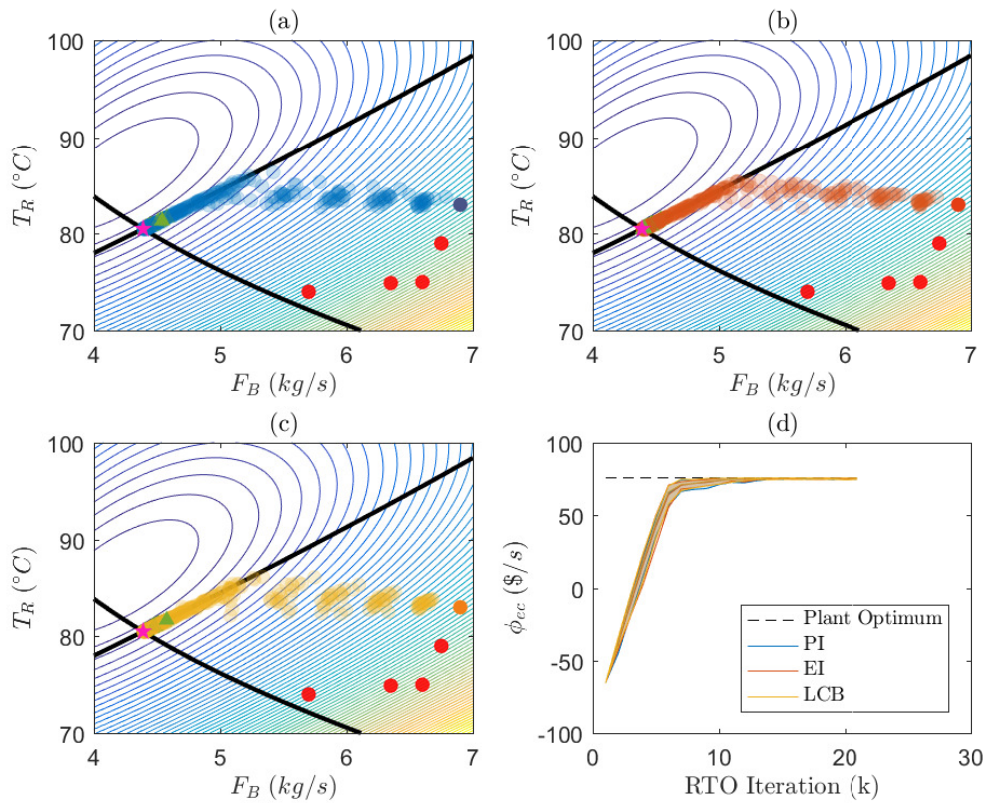


Figure 4.17: RTO iterations using Strategy 4 (MAy-GP) and comparing different acquisition functions: (a) *PI*, (b) *EI* and (c) *LCB*. (d) The cost evolution for acquisition functions *PI*, *EI*, *LCB* during the 20 iterations. Red dots represent the initial GP training points. Green triangles represent the last iterate of each RTO run. Black continuous lines represent the constraint limits and the pink star represents plant optimum.

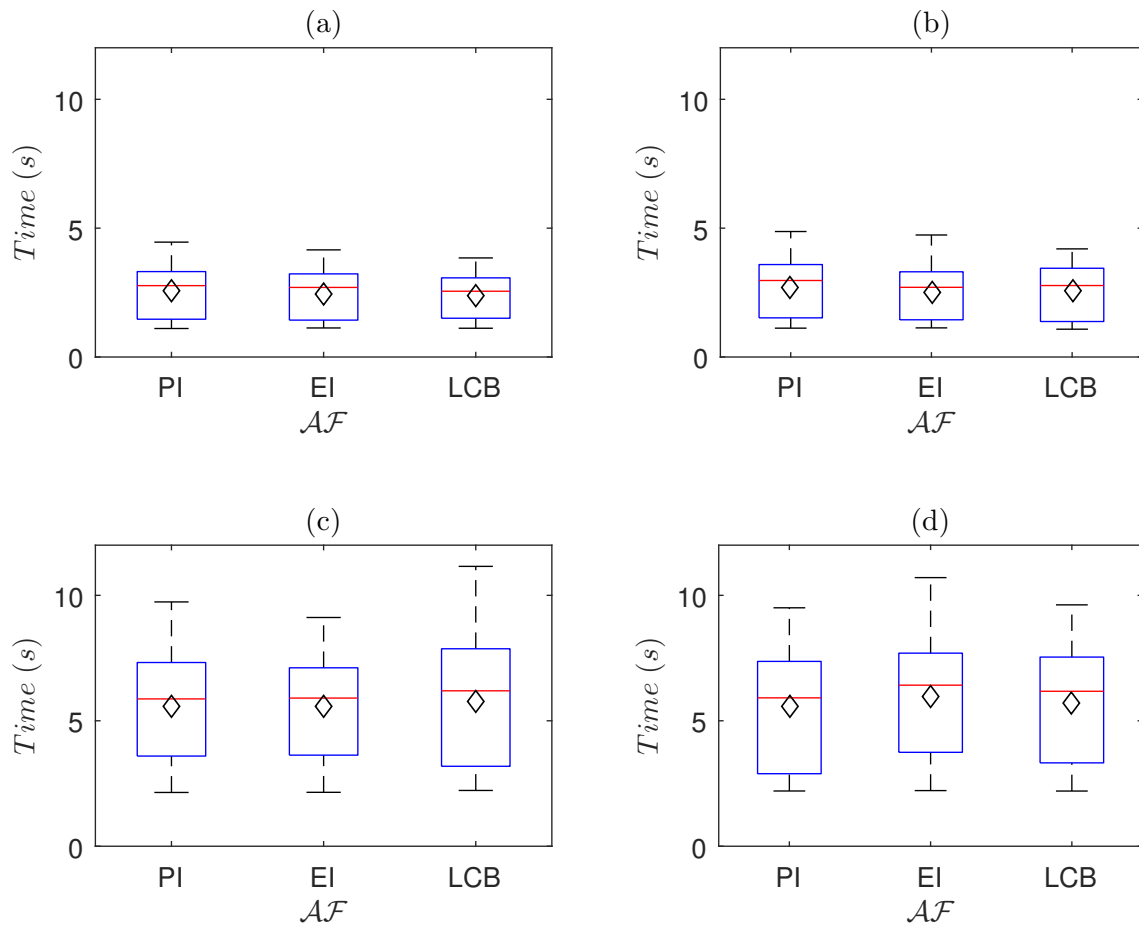


Figure 4.18: Average Iteration Time for each acquisition function (PI, EI and LCB) using: (a) Strategy 1 (objective function and constraints modeling via GP), (b) Strategy 2 (measured variables ( $\mathbf{y}$ ) modeling via GP), (c) Strategy 3 (MA-GP), and (d) Strategy 4 (MAy-GP). Black diamonds represent the average of the 20 RTO iterations considering 20 realizations.

The average iteration time of each strategy is also presented in Table 4.8.

Table 4.8: Average iteration time obtained in each strategy.

Strategy/ Acquisition Function	PI	EI	LCB
Strategy 1	2.56	2.45	2.37
Strategy 2	2.72	2.51	2.55
Strategy 3	5.60	5.59	5.77
Strategy 4	5.59	5.94	5.74
Ratio between strategies 1 and 3	0.46	0.44	0.41
Ratio between strategies 2 and 4	0.49	0.42	0.44

From Table 4.8, it is possible to notice that the ratio between the average iteration time of strategies 1 and 3 is 0.46, and 0.44 and 0.41, when considering acquisition functions *PI*, *EI*, and *LCB*, respectively. When comparing strategies 2 and 4, the ratio between the average iteration time of strategies 2 and 4 is 0.49, 0.42, and 0.44, when considering acquisition functions *PI*, *EI*, and *LCB*, respectively. As mentioned before, the reduction in the average iteration time of strategies 1 and 2 is related to not considering a first-principles model since only GP models are applied.

In this case study, all strategies could drive the plant to a neighborhood of the optimum. It was noticed that the optimum solution obtained in all strategies presented a deviation from the plant optimum, which may be related to the characteristic of the optimization method applied (interior point) since it is a barrier method and the optimum point is at active constraints. It was also noticed that all strategies presented similar behavior regarding the deviation from the plant optimum. Regarding model accuracy, the RMSE obtained in Strategies 3 and 4 were lower than the error observed in Strategies 1 and 2, which may be related to the contribution of the first-principle model to the overall accuracy since Strategies 1 and 2 are only based on an identified model. Additionally, using only identified models enabled a reduction in the average iteration time of strategies 1 and 2.

## 4.7 Partial Conclusions

In this chapter, several strategies of RTO based on the Gaussian Process and acquisition functions were compared. A framework based on the direct modeling of the output variables is proposed and compared to the approach present in literature based on modeling the plant-model mismatch, known as GP based modifier adaptation approaches. The main advantage of the proposed strategy is that it can be applied in the absence of any steady-state model of the plant, which

enables a data-driven RTO approach. The proposed methodology was applied to the exothermic CSTR reactor and the Williams-Otto reactor benchmark problem. The results obtained in both case studies, considering the proposed methodology and the modifier adaptation, were able to drive the plant to a neighborhood of the optimum point. Regarding the relative average deviation obtained in each strategy, the values obtained showed that the absolute data-driven strategy presented a similar performance when compared to the plant-model mismatch approach. Regarding the evaluated constrained acquisition functions, namely the Probability of Improvement, the Expected Improvement, and the Lower Confidence Bound, the results showed no clear advantage in selecting one acquisition function over the others. The relative average deviation value obtained in the Williams-Otto reactor was higher than the values obtained in the Exothermic CSTR, which was related to the characteristic of the optimization method applied since it was considered a barrier method and the plant optimum point is at an intersection of constraints (active constraints). Regarding average iteration time, in the two case studies, it was verified that using only identified models enabled a reduction in the average iteration time, achieving at least half of the average iteration time obtained when considering the usage of the rigorous model. Finally, similar results were obtained when considering the approximations for output variables instead of the objective function and constraints. This approach is interesting since it enables the utilization of the model for other purposes, such as control. Thus, the next steps of the research are related to obtaining dynamic models considering a steady-state model based on GP, aiming to process control purposes.

# Chapter 5

## Tracking Necessary Condition of Optimality by a Data-driven solution combining Steady-State and Transient data

A version of this chapter was published in the Journal of Process Control, Volume 118, October 2022, pages 37-54 (DEMUNER *et al.*, 2022).

### 5.1 Introduction

In chemical process plants, real-time optimization and control structures are typically designed as a multilayer hierarchical control structure, where each level has a specific function and working frequency (KRISHNAMOORTHY *et al.*, 2018).

The RTO layer aims at maximizing some performance index oriented to operational profit while satisfying constraints related to process physical ranges, product specifications, and environmental limits (ENGELL, 2007). The optimization problem solution is sent to a lower layer named supervisory control, where advanced control algorithms are applied, such as the model-based predictive control strategy (MPC).

In the RTO layer, a steady-state process model is usually applied, typically described by a first-principles, rigorous, and nonlinear model (ELLIS *et al.*, 2014). Due to disturbances, measurement uncertainties, and noise, updating the RTO model or structure is necessary, based on the information available through process measurements.

An important drawback of the RTO strategies is the dependence on a steady-

state model, which implies that a steady-state detection step should be considered before a new optimization step (ENGELL, 2007). Therefore, in the presence of disturbances, the plant operates suboptimally until it reaches a new steady-state, allowing its detection and the computation of the new optimal operating point (GRACIANO *et al.*, 2015).

To overcome the need of the steady-state detection step, some researches have explored the usage of dynamic models in the optimization step, then resulting in the dynamic RTO (D-RTO) (ELLIS *et al.*, 2014). According to GRACIANO *et al.* (2015), D-RTO requires accurate dynamic models, which could be a limitation. Also, according to KRISHNAMOORTHY *et al.* (2018), there are still open numerical issues associated with D-RTO to be addressed before industrial implementations.

Alternatively, an intermediate approach between RTO and D-RTO, represented here by Hybrid Real-Time Optimization (H-RTO), has been proposed (VALLURU *et al.*, 2015). This approach uses a dynamic model in the identification step, which is based on simultaneous parameter and state estimation. Since the parameters are updated dynamically, the steady-state version of the model is also updated iteratively. Then, it can be applied in the optimization step, removing the need for the steady-state estimation. This strategy was later studied by KRISHNAMOORTHY *et al.* (2018) and MATIAS and LE ROUX (2018), which showed that H-RTO presents better economic performance than the classical RTO approach. MATIAS and LE ROUX (2020) expanded the methodology for plant-wide optimization considering a strategy for local models identification. SANTOS *et al.* (2021) considered an H-RTO formulation where the economic objective function is a controlled variable in a linear MPC.

In the H-RTO strategies, one assumption is that a dynamic first-principles model is available, which could be a limitation. In DELOU *et al.* (2021), an H-RTO framework is proposed assuming that only a steady-state model is at hand. A dynamic model is developed by combining the steady-state model and a linear identified model using a Hammerstein model structure. Also, the MPC controlled variables are obtained through the self-optimizing variables, based on the work of GRACIANO *et al.* (2015).

Another issue related to the classical RTO approach relies on the different models applied in each layer of the hierarchical control structure. While, typically, the models of the RTO layer are rigorous and based on first-principles, the models used in the MPC control layer are usually linear and obtained from identification strategies around an operating point. Thus, it is not expected that the steady-state point of each model matches, which may generate unachievable operating points from the RTO layer to the control layer (ELLIS *et al.*, 2014).

Some strategies have been proposed to mitigate such divergences, such as using an intermediate optimization layer between the RTO and supervisory control, known as LP-MPC or QP-MPC. This strategy aims to adjust the RTO setpoints, using a steady-state version of the MPC linear model to satisfy the controller constraints. By doing so, one guarantees that all setpoints sent to the MPC are achievable (MORSHEDI *et al.*, 1985; ROTAVA and ZANIN, 2005; YING *et al.*, 1998; YOUSFI and TOURNIER, 1991). However, it is important to notice that the models applied in the rigorous stationary and dynamic layers remain different. Thus, during the transient period, a suboptimal trajectory may be followed (YING *et al.*, 1998).

Another strategy consists of simultaneously solving the economic optimization and the control problems, incorporating economic aspects in the formulation of the MPC: the one-layer optimization, later called Economic Model Predictive Control (EMPC). YOUSFI and TOURNIER (1991) and DE GOUVÊA and ODLOAK (1996) reported including a linear economic term in the Dynamic Matrix Controller (DMC). DE GOUVÊA and ODLOAK (1996) included a linearized version of the actual economic objective function in the MPC objective function. Despite the simple formulation, such strategies may not represent the economic problem of the real process since this optimization problem may be nonlinear. Aiming to deal with this issue, DE GOUVÊA and ODLOAK (1998) included in the MPC objective function a nonlinear term associated with the economic objective function. Although the economic term was nonlinear, the controller is still based on a linear identified model. DE SOUZA *et al.* (2010) proposed the inclusion of the gradient of the economic objective function in the MPC objective function. The gradient is calculated by a first-order approximation at a reference point considered as the previous operating point, which means that the first and second derivatives of the rigorous steady-state model are needed. Those values are held constant during the current control cycle. ALVAREZ and ODLOAK (2012) also proposed the inclusion of the gradient of a modified economic objective function, which is replaced by a weighted sum of the squared differences of the control action from the RTO optimal solution, aiming to deal with non-convexities. ALAMO *et al.* (2014) studied the strategy previously proposed by DE SOUZA *et al.* (2010), focusing on an approximation for gradient calculation, aiming to reduce computational cost. In an FCC unit case study, described in detail in LAUTENSCHLAGER MORO and ODLOAK (1995), the execution time compared to the original strategy was three times lower.

The aforementioned works somehow add an economic term to the controller's objective function. However, the controller formulation is still based on a linear dynamic model, while the steady-state terms are based on a rigorous model. An-

other integration approach was presented by ENGELL (2007), applying a Non-linear Model Predictive Control (NMPC) to a simulated moving bed (SMB) separation system. The NMPC objective function was replaced by an economic objective function. The author also highlighted important issues of the proposed strategy, such as its stability and the importance of the state estimation step to avoid plant-model mismatch. Indeed, the plant-model mismatch may limit the EMPC convergence towards the plant optimum point. In this sense, some works proposed using the Modifier-Adaptation technique (MARCHETTI *et al.*, 2009) in the EMPC formulation to deal with this issue and then meeting the first-order necessary conditions of optimality (NCO) of the plant (FAULWASSER and PANNOCCHIA, 2019; OLIVEIRA-SILVA *et al.*, 2021; VACCARI and PANNOCCHIA, 2017; VACCARI *et al.*, 2021).

Additionally, computational complexities, the requirement for online identification techniques for nonlinear processes, the robustness of the solution, and the stability for nonlinear systems are important issues for the practical implementation of the nonlinear EMPC for large-scale problems (ELLIS *et al.*, 2014).

Some recent researches have incorporated identified nonlinear models into the formulation of NMPC and EMPC. WU *et al.* (2019a,b) presented the theoretical foundation and computational implementation of a Lyapunov-based MPC using recurrent neural networks (RNN). It was shown that the RNN-based MPC computation time was lower than the sampling time, which implies that it could be applied in real time. ELLIS and CHINDE (2020) used a long short-term memory networks (LSTM) model for an EMPC design applied to heating, ventilation, and air conditioning (HVAC) systems. Some works developed the Koopman-based model identification technique to represent nonlinear systems by finite-dimensional linear approximation (KORDA and MEZIĆ, 2018). As the main advantage, a linear MPC can be applied. However, a model mismatch is expected due to the approximation, such that a disturbance estimation may be applied to obtain offset-free control (NARASINGAM *et al.*, 2022; SON *et al.*, 2020).

Another class of models that has been widely applied in nonlinear modeling and control is the Hammerstein and Wiener models. These models were applied for modeling and control of nonlinear processes such as neutralization (FRUZZETTI *et al.*, 1997), fluid catalytic cracking process (HARNISCHMACHER and MARQUARDT, 2007b), gas-lift based oil production (MIYOSHI *et al.*, 2018), processes with the presence of valve stiction (BACCI DI CAPACI *et al.*, 2018, 2019; FÜRST *et al.*, 2020), and a nonlinear electric oven (QUACHIO and GARCIA, 2019). This structure combining static and dynamic blocks is useful in terms of RTO and NMPC, mainly if the static term represents the steady-state behavior of an output variable. If so, the steady-state model could also be applied in the

RTO layer (DELOU *et al.*, 2021; RIBEIRO and SECCHI, 2019) or even in an EMPC framework.

The static block of a Hammerstein model structure is typically represented by a polynomial basis function, mainly related to its simplicity and the existence of well-known algorithms for its identification, such as the Narendra-Gallman algorithm (NGA) (NARENDRA and GALLMAN, 1966). However, any other function could be applied, for instance, Neural Networks (WANG and CHEN, 2008), Support Vector Machines (TÖTTERMAN and TOIVONEN, 2009), and first-principles model (DELOU *et al.*, 2021). If a process steady-state model is unavailable, it could also be identified through an input/output relationship based on measured data. For this, a characteristic that might be required is that the models can be constructed with a limited amount of data (CARPIO *et al.*, 2018a). In this sense, Gaussian Processes are often well fitted from relatively small data sets compared to other meta-modeling forms (FORRESTER and KEANE, 2009; PALMER and REALFF, 2002a).

In this work, a new framework for RTO and NMPC integration is proposed, based on a one-layer approach. This strategy is centered on a Hammerstein model structure, such that its static nonlinear function is represented by an identified process steady-state model. Indeed, an important assumption here is that none of the steady-state and dynamic models are available, such that those models are identified using plant data. This assumption differs from the related previous works where a dynamic phenomenological model (KRISHNAMOORTHY *et al.*, 2018; MATIAS and LE ROUX, 2018, 2020; SANTOS *et al.*, 2021) or a steady-state model (DELOU *et al.*, 2021) were available. The steady-state model structure considered here is based on a Gaussian Process, due to its characteristic of being able to represent complex nonlinear models with accuracy and through the use of a few parameters (CARPIO *et al.*, 2018a; DEL RIO CHANONA *et al.*, 2019; FERREIRA *et al.*, 2018; FORRESTER *et al.*, 2008; PALMER and REALFF, 2002b). A great advantage of the proposed strategy based on the Hammerstein model is that the identification of steady-state and dynamic functions can be done independently, considering that steady-state mapping can be identified based on previous knowledge of the plant behavior.

The proposed one-layer framework presents full compatibility between the steady-state and dynamic models, as the control and optimization problems are solved simultaneously. To achieve it, the NMPC objective function is replaced by the objective function gradient of the economic optimization problem. Thus, the NMPC objective is to keep the gradient norm close to zero, satisfying the first-order optimality condition of the steady-state optimization problem. The proposed approach differs from ALVAREZ and ODLOAK (2012); DE SOUZA

*et al.* (2010) as only a nonlinear model is considered for both optimization and control. Additionally, in order to deal with disturbances, an adaptative characteristic of the controller is also considered. Based on a H-RTO strategy, a dynamic parameter estimation based on Extended Kalman Filter is applied to estimate disturbances and update the model.

Lastly, a Hammerstein model structure is also proposed, based on the interaction of the system's state variables, which can deal with input variables coupling and directionality.

This chapter is organized as follows. Section 5.2 presents concepts regarding Hammerstein and Gaussian Process models structures. Section 5.3 presents the proposed approach to obtain the nonlinear model, the one-layer proposed framework and the model identification technique. In Section 5.4, the Willians-Otto reactor is presented as the present work case study. In Section 5.5, the results of the proposed approach applied to the Willians-Otto Reactor benchmark are presented and compared to H-RTO and Classical RTO approaches. Finally, Section 5.6 presents the conclusions of this chapter.

## 5.2 Model Structures

In this work, a modeling approach is proposed based on a dynamic model represented by a Hammerstein model structure. The nonlinear static element of the Hammerstein model is based on a steady-state model of the process, which is based on an identified Gaussian Process. These model structures are presented below.

### 5.2.1 Gaussian Processes Model Structure

Here, the Gaussian Process are described in the same way as presented in Section 4.2. Therefore, the equations are not presented, for the sake of simplicity.

### 5.2.2 Hammerstein Model Structure

Hammerstein models have been used in nonlinear system identification since the 60's when NARENDRA and GALLMAN (1966) proposed the Narendra-Gallman algorithm (NGA) for model identification and updating, allowing its application. Mathematically, it can be described by the Hammerstein integral operator written for time-invariant systems as follows:

$$H[u(t)] = \int_{\Omega} L(\tau)NL(u(t - \tau))d\tau \quad (5.1)$$

where  $\Omega$  is the input variables domain,  $L(t)$  is the impulse response of a linear system, which has as input the nonlinear static function  $NL(\cdot)$ .

NARENDRA and GALLMAN (1966) introduced the block-diagram notation for Hammerstein Model, as presented in Figure 5.1.

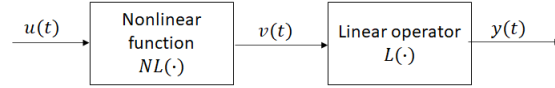


Figure 5.1: Schematic representation of the Hammerstein model. The input  $u(t)$  is transformed by the nonlinear function  $NL(\cdot)$ , which has as output the variable  $v(t)$ . This variable is applied as input for the linear dynamic operator  $L(\cdot)$ , yielding the output variable  $y(t)$ .

In Figure 5.1, the model structure consists of a nonlinear static element (function  $NL$ ) followed by a linear dynamic element (function  $L$ ). If the sequence of blocks is reversed, the structure represents a Wiener model, as presented in Figure 5.2.

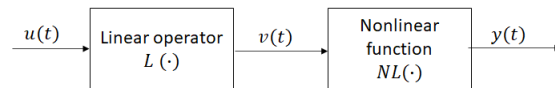


Figure 5.2: Schematic representation of the Wiener model. The input  $u(t)$  is transformed by a linear operator  $L(\cdot)$ , yielding an intermediate response  $v(t)$ . This variable is then transformed by a nonlinear transformation  $NL_1(\cdot)$ , yielding the model output response  $y(t)$ .

The class of models called Hammerstein-Wiener represents the combination of Hammerstein and Wiener models. Thus, there is a nonlinear transformation preceding the linear block and another nonlinear transformation after the linear block. This structure is represented in Figure 5.3

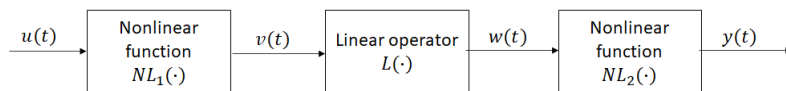


Figure 5.3: Schematic representation of the Hammerstein-Wiener model. The input  $u(t)$  is transformed by a nonlinear function  $NL_1(\cdot)$ , yielding as output the variable  $v(t)$ . This signal is then transformed by a linear operator  $L(\cdot)$ , yielding a new intermediate response  $w(t)$ . This signal is finally transformed by a nonlinear function  $NL_2(\cdot)$ , which yield the model output  $y(t)$ .

The Hammerstein models can also represent a Multiple-Input-Single-Output (MISO) system, which is straightforward by taking into account multiple inputs. Of course, MIMO representation is also possible by combining  $n_y$  MISO models, where  $n_y$  is the number of output variables (or system responses).

Several structures have been proposed in the literature for the MISO case of Hammerstein models (HARNISCHMACHER and MARQUARDT, 2007a).

BILLINGS (1980) proposed a intuitive extension of the MISO case by considering a single nonlinear transformation applied to a vector of input variables  $\mathbf{u}$ , as shown in Figure 5.4.

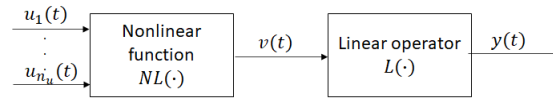


Figure 5.4: Schematic representation of the MISO Hammerstein model structure proposed by BILLINGS (1980).

In the structure presented in Figure 5.4, the nonlinear function  $NL : \mathbb{R}^{n_u} \rightarrow \mathbb{R}$  is a nonlinear transformation of the vector  $\mathbf{u}^T = [u_1, \dots, u_{n_u}]$ , yielding an intermediate response,  $v(t)$ , which will be transformed by a linear operator, yielding the output response  $y(t)$ .

Accordingly to HARNISCHMACHER and MARQUARDT (2007a), the structure with only one nonlinear transformation is not able to represent the input directionality of the input vectors. For example, systems that present distinct static gains depending on the signal of the input variable.

KORTMANN and UNBEHAUEN (1987) proposed a structure based in multiple nonlinear operators, as presented in Figure 5.5.

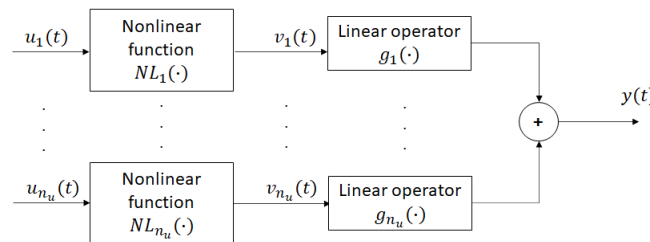


Figure 5.5: Schematic representation of the Hammerstein model proposed by KORTMANN and UNBEHAUEN (1987).

In the structure proposed by KORTMANN and UNBEHAUEN (1987), the  $i$ -th nonlinear function  $NL_i(u_i) : \mathbb{R} \rightarrow \mathbb{R}$  is applied to the  $i$ -th position of the input variable vector  $\mathbf{u}$ , yielding an intermediate output variable  $v_i(t)$ . Thus, the output variable is obtained by the equation  $y(t) = \sum v_i(t)$ .

Although the structure proposed by KORTMANN and UNBEHAUEN (1987) is able to deal with input directionality, according to HARNISCHMACHER and MARQUARDT (2007a), this structure fails to take into account nonlinear couplings between the input variables, an essential characteristic for process control. On the other hand, this structure of representation has advantages from the point of view of parameter estimation, being possible to use the parameter estimation techniques for the SISO case.

ESKINAT *et al.* (1991) proposed a structure for the MISO case in order to consider the nonlinear couplings between the input variables, as presented in Figure 5.6.

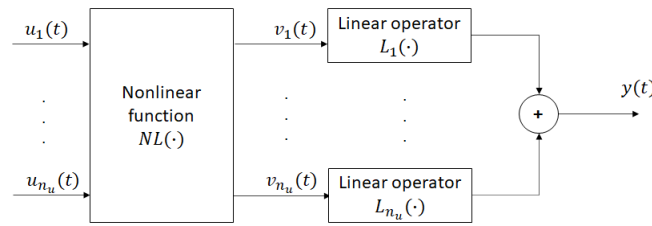


Figure 5.6: Schematic representation of Hammerstein model proposed by ESKINAT *et al.* (1991).

HARNISCHMACHER and MARQUARDT (2007a) developed a new structure for Hammerstein models, which is able to model the dynamic and nonlinear characteristics of the system independently, in addition to having developed a strategy for identifying parameters for this structure. According to the authors, the proposed structure can deal with the nonlinear coupling among the input variables with a smaller number of parameters when compared to other existing formulations. The proposed structure was applied to an FCC unit with an accuracy 50% superior to other studied structures.

In this chapter, the classic MISO Hammerstein proposed by BILLINGS (1980) and an extension of the structure proposed by ESKINAT *et al.* (1991) will be considered and compared.

## 5.3 Proposed Methodology

### 5.3.1 RTO and MPC integration framework

The proposed framework is based on the assumption that none of the steady-state and dynamic models are available, such that both models need to be identified from plant data.

The steady-state model structure considered here is based on a Gaussian Process. The dynamic model is represented by a Hammerstein model structure, such that the previously identified steady-state model is also applied as its nonlinear static element.

The dynamic model is applied to an NMPC algorithm. The model structure is discussed in detail in Section 5.3.1.1. A great advantage of the proposed strategy based on the Hammerstein model is that the identification of steady-state and dynamic functions can be done independently, considering that the steady-state mapping can be identified based on previous knowledge of the plant behav-

ior. This characteristic of independent identification can be achieved because the steady-state and dynamic functions in the Hammerstein structure are in series. The steady-state model is considered a GP model and can be identified using selected steady-state data obtained from plant historical data. After obtaining this mapping, the dynamic model can be identified through a new data set considering dynamic data from the plant. Even though the parameters are different in each model, it is not a limitation, as two parameter estimation problems can be solved independently.

As discussed before, the proposed framework is a data-driven approach. Although it is an interesting feature, the models are susceptible to lose accuracy when working at an operating point outside the training data bounds. However, it is not a limitation, and some strategies can be considered to deal with plant-model mismatch. Especially when dealing with GP models, DEL RIO CHANONA *et al.* (2019) showed that trust-regions strategies can be applied to keep the model accurate. Moreover, GP models present an interesting characteristic which is the model uncertainty estimation. Therefore, one possibility is tracking the posterior variance value and using it in the trust-region approach. Another possible approach is updating the GP model iteratively such that the model learns from the process during optimization and control cycles. In the EMPC formulation, a possible strategy is using the modifier adaptation, as presented in VACCARI and PANNOCCHIA (2017), FAULWASSER and PANNOCCHIA (2019), OLIVEIRA-SILVA *et al.* (2021), and VACCARI *et al.* (2021). These described strategies are not considered in this work but can be added to the proposed framework without loss of generality.

Another important assumption is that relevant disturbances that impact the plant are measured, at least, for steady-state model identification purposes. It means that for a given period, the disturbances were measured, and their influence was considered for steady-state model identification. During the plant operation, the disturbances do not need to be measured since the proposed framework considers a dynamic parameter estimation step by means of an Extended Kalman Filter (EKF) (SIMON, 2006), such that the unmeasured disturbances can be estimated, here denoted as  $\hat{d}$ . Additionally, in this framework, the EKF is based on the linearization of the Hammerstein model. It is important to highlight that other model parameters, such as the ones of the dynamic model, could also be adapted using the EKF strategy.

The proposed framework also aims to guarantee the compatibility of the steady-state and dynamic models. This characteristic is achieved by solving the steady-state problem simultaneously in the NMPC layer, following the one-layer strategy, which implies that a steady-state optimization step is unnecessary.

In this work, the gradient of the objective function is calculated using the steady-state model and the NMPC aims to keep the gradient norm close to zero, satisfying the first-order NCO of the steady-state optimization problem. The proposed framework is described in Figure 5.7a.

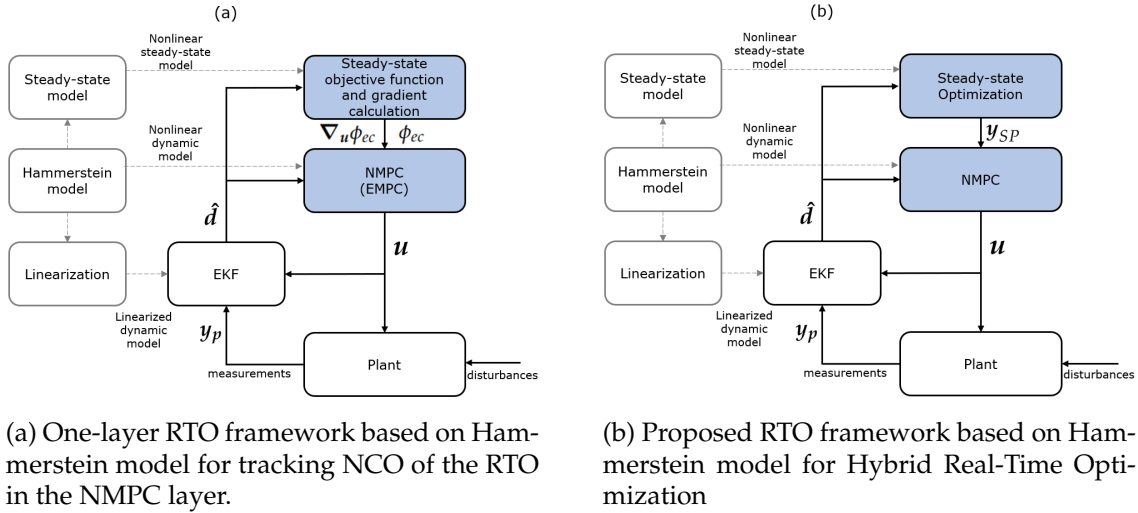


Figure 5.7: Comparative of the proposed frameworks.

The first-order NCO, also known as the first-order Karush-Kuhn-Tucker (KKT) condition, implies that if  $u^* \in \mathbb{R}^{n_u}$  is a local optimum of an optimization problem, then the first partial derivatives of the Lagrangian function with respect to  $u^*$  and to the Lagrange multipliers of the optimization problem must be zero, besides satisfying all complementary conditions (BIEGLER, 2010).

Another possible approach within this framework is to replace the NMPC objective function by the economic objective function. It is important to mention that, as the objective function is based on an input-output model, less computational effort than for a rigorous model is expected.

In addition, the elements considered in the presented framework also enable the development of a hybrid RTO (H-RTO) strategy without significant changes. The major change is adding an optimization layer to solve the steady-state optimization problem. The optimal setpoints are then sent to the NMPC. In this framework, the steady-state model is also identified as described before. Again, this strategy also allows compatibility between steady-state and dynamic layers, since the steady-state model is also present in the dynamic model, due to the Hammerstein structure. This framework is presented in Figure 5.7b. The main differences between the proposed frameworks are highlighted in Figures 5.7a and 5.7b.

An additional contribution of the present work is the development of an H-RTO strategy considering the same structure presented in Figure 5.7b and adding

a terminal cost based on the economic objective function to the NMPC objective function. It is also important to highlight that the proposed methodology is based on identified models, such that any first-principles model can be considered.

### 5.3.1.1 Dynamic and Steady-State Models Relationship

As discussed before, Hammerstein models have a typical structure of a nonlinear static function followed by a linear dynamic function. In this work, this characteristic is explored, combining a nonlinear steady-state model of the process based on a Gaussian Process and a linear dynamic model of the process. Thus, the mismatch is avoided if this nonlinear steady-state model is applied in both RTO and control layers.

In the present work, two Hammerstein structures were compared. The first structure, here denominated as Structure 1, is based on a typical Hammerstein model, as presented in Figure 5.1. This system can be represented as follows:

$$x_{j,k} = L_j(v_{j,k}, \boldsymbol{\alpha}_{dyn_j}) \quad (5.2)$$

$$y_{i,k} = x_{j,k} \quad (5.3)$$

where  $k$  is the discrete time instant,  $y_i$  represents the model prediction for the  $i$ -th output variable ( $i = 1, \dots, n_y$ ) and  $x_j$  is an intermediate variable which in this structure is equal to the model output, such that  $j = i$ . Additionally,  $v_j \in \mathbb{R}$  is the nonlinear function output,  $L_j : \mathbb{R} \times \mathbb{R}^{n_{\alpha,dyn}} \rightarrow \mathbb{R}$  is the dynamic linear operator, and  $\boldsymbol{\alpha}_{dyn_j} \in \mathbb{R}^{n_{\alpha,dyn}}$  its parameters.

Without loss of generality, the nonlinear operator that represents the process steady-state model is given by:

$$v_{j,k} = NL_j(\mathbf{u}_k, \mathbf{d}, \boldsymbol{\alpha}_j) \quad (5.4)$$

where  $\mathbf{u} \in \mathbb{R}^{n_u}$  are the manipulated variables,  $\mathbf{d} \in \mathbb{R}^{n_d}$  are process disturbances,  $NL_j : \mathbb{R}^{n_u} \times \mathbb{R}^{n_d} \times \mathbb{R}^{n_\alpha} \rightarrow \mathbb{R}$  is the nonlinear operator and  $\boldsymbol{\alpha}_j$  its parameters. Here, it is worthwhile to mention that the input variables were divided into the manipulated variables ( $\mathbf{u}$ ) and disturbances ( $\mathbf{d}$ ) for control aspects.

Another structure based on the works of ESKINAT *et al.* (1991) and HARNISCHMACHER and MARQUARDT (2007a) was considered, aiming to deal with the inherent multivariate characteristics and also the input directionality limitation. This structure will be referred to as Structure 2. In this one, the model variable output  $y_i$  ( $i = 1, \dots, n_y$ ) is a linear combination of MISO Hammerstein models (parallel structure), as presented in Figure 5.8.

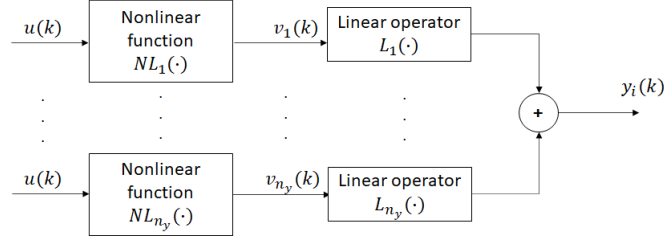


Figure 5.8: Proposed structure of Hammerstein nonlinear model (Structure 2).

Mathematically, Structure 2 can be described as follows:

$$x_{j,k}^{(i)} = L_j(v_{j,k}, \boldsymbol{\alpha}_{dyn_j}^{(i)}), \quad j = 1, \dots, n_y \quad (5.5)$$

$$y_{i,k} = \mathbf{c}^T \mathbf{x}_k^{(i)} \quad (5.6)$$

where  $y_i$  represents the MISO model prediction for the  $i$ -th output variable and  $x_j^{(i)}$  is an intermediate variable which represents each MISO Hammerstein model output, such that  $j = 1, \dots, n_y$ ,  $v_j$  is represented by Equation 5.4. It is worth mentioning that it was included a dependence of the dynamic model parameters on the  $i$ -th variable, since these are identified for each output variable  $y_i$ . In the present work, the vector  $\mathbf{c} \in \mathbb{R}^{n_y}$  has its elements equal to one. Thus,

$$y_{i,k} = \sum_{j=1}^{n_y} x_{j,k}^{(i)}(\mathbf{a}_j^{(i)}) \quad (5.7)$$

where a dependence to model parameters was added to the variable  $x_j^{(i)}$ , such that  $\mathbf{a}_j^{(i)} \in \mathbb{R}^{n_\alpha + n_{\alpha, dyn}}$  encompasses both nonlinear and linear models' parameters associated to each  $i$ -th output variable and  $j$ -th intermediate variable.

It is important to highlight that, for Structures 1 and 2, there is no limitation regarding the nonlinear operator structure. It means that, for instance, a first-principles model could be applied or also identified models based on input-output data measured from the plant.

In the present work, a steady-state model was identified based on input-output data from the plant. This approach is also related to an important premise that a reliable first-principle model is not available, also aiming to develop a data-driven solution. A GP model was considered for the input-output model relationship, which is often well fitted from relatively small data sets compared to other meta-modeling forms (FORRESTER and KEANE, 2009; PALMER and REALFF, 2002a).

Therefore, the relationship given by Equation 5.4 can be rewritten as follows:

$$v_{j,k} = NL_j(\mathbf{u}_k, \mathbf{d}_k, \boldsymbol{\alpha}_j) \quad (5.8)$$

$$= y_{j,k}^{ss} \quad (5.9)$$

$$= GP(\mu_{f,j}(\mathbf{u}_k, \mathbf{d}_k), \sigma_{f,j}(\mathbf{u}_k, \mathbf{d}_k)) \quad (5.10)$$

where  $y_j^{ss}$  is the  $j$ -th output variable steady-state value,  $GP$  represents the Gaussian process with posterior mean and variance functions  $\mu_{f,j}$  and  $\sigma_{f,j}$ , respectively. The steady-state model parameters  $\boldsymbol{\alpha}_j$  are equivalent to GP hyperparameters, as presented in Equation 4.5.

Regarding the dynamic operator, the dynamic linear structure was considered as discrete transfer functions, described as follow:

$$L_j^{(i)}(z) = \frac{b_{1j}^{(i)}z^{-1} + b_{2j}^{(i)}z^{-2} + \dots + b_{n_zj}^{(i)}z^{-n_z}}{1 + a_{1j}^{(i)}z^{-1} + a_{2j}^{(i)}z^{-2} + \dots + a_{n_pj}^{(i)}z^{-n_p}} \quad (5.11)$$

where  $n_p$  is the number of poles and  $n_z$  is the number of zeros of the transfer functions. Therefore, the dynamic model parameters vector is described as follows:

$$\boldsymbol{\alpha}_{dynj}^{(i)} = [b_{1j}^{(i)}, \dots, b_{n_zj}^{(i)}, a_{1j}^{(i)}, \dots, a_{n_pj}^{(i)}]^T \quad (5.12)$$

For now on, for the sake of notation simplicity, when representing the non-linear dynamic model (Hammerstein model), the following description will be considered in further developments:

$$\mathbf{y}_k = \mathbf{f}_{dyn}(\mathbf{y}_{k-1}, \mathbf{u}_{k-1}, \mathbf{d}_{k-1}, \bar{\mathbf{a}}) \quad (5.13)$$

where  $\mathbf{f}_{dyn} \in \mathbb{R}^{n_y}$  is a vector of Hammerstein model functions that represents the system output variables and  $\bar{\mathbf{a}} \in \mathbb{R}^{n_y(n_\alpha + n_{\alpha,dyn})}$  is an extended vector of parameters that encompasses all Hammerstein models parameters. Therefore,  $\bar{\mathbf{a}} = [\bar{\mathbf{a}}_{ss}^T \bar{\mathbf{a}}_{dyn}^T]^T$ , where  $\bar{\mathbf{a}}_{ss} \in \mathbb{R}^{n_y(n_\alpha)}$  is an extended vector of parameters that encompasses all GP hyperparameters for all output variable and  $\bar{\mathbf{a}}_{dyn} \in \mathbb{R}^{n_y(n_{\alpha,dyn})}$  is an extended vector of all linear dynamic models parameters.

Analogously, the steady-state model will be described as follows:

$$\mathbf{y}_k^{ss} = \mathbf{f}_{ss}(\mathbf{u}_k, \mathbf{d}_k, \bar{\mathbf{a}}_{ss}) \quad (5.14)$$

where  $\mathbf{f}_{ss} \in \mathbb{R}^{n_y}$  is a vector of steady-state model functions that represents the system output variables, here represented as the GP described in Equation 5.10.

### 5.3.1.2 Dynamic Parameter and State Estimation

In this work, the dynamic parameter estimation step is considered for estimating unmeasured disturbances, while the GP hyperparameters and dynamic model parameters were not updated.

An Extended Kalman Filter (EKF) (SIMON, 2006) is considered for this purpose, which will be based on the linearized version of the Hammerstein model. An augmented state variable is created  $\hat{\mathbf{z}}_k^- = [\hat{\mathbf{y}}_k^- \hat{\mathbf{d}}_k^-]^T$ , such that the disturbances are considered as additional states. Thus, the *a priori* prediction equations are:

$$\hat{\mathbf{z}}_k^- = \begin{bmatrix} f_{dyn}(\mathbf{y}_{k-1}^+, \mathbf{u}_{k-1}, \hat{\mathbf{d}}_{k-1}^+, \bar{\mathbf{a}}) \\ \hat{\mathbf{d}}_{k-1}^+ \end{bmatrix} + \begin{bmatrix} \boldsymbol{\omega}_{y,k} \\ \boldsymbol{\omega}_{d,k} \end{bmatrix} \quad (5.15)$$

$$\mathbf{P}_k^- = \mathbf{F}_k \mathbf{P}_{k-1}^+ \mathbf{F}_k^T + \mathbf{Q} \quad (5.16)$$

where  $\boldsymbol{\omega}_{y,k}$  and  $\boldsymbol{\omega}_{d,k}$  are artificial zero-mean noise, such that  $\boldsymbol{\omega}_{d,k} \sim \mathcal{N}(\mathbf{0}, \mathbf{Q}_y)$  and  $\boldsymbol{\omega}_{d,k} \sim \mathcal{N}(\mathbf{0}, \mathbf{Q}_d)$ , where  $\mathcal{N}$  represents the normal distribution, with zero mean and covariance parameters  $\mathbf{Q}_y$  and  $\mathbf{Q}_d$ . In terms of notation, the hat operator denotes that a variable is an estimated value. Additionally, superscripts  $-$  and  $+$  represent *a priori* and *a posteriori* estimations, respectively.  $\mathbf{P}$  is the augmented state covariance matrix,  $\mathbf{Q} = \text{diag}(\mathbf{Q}_y, \mathbf{Q}_d)$  is the augmented noise covariance matrix and  $\mathbf{F}$  is the augmented state transition matrix, defined as follows:

$$\mathbf{F}_k = \left. \frac{\partial f_{dyn}}{\partial \hat{\mathbf{z}}} \right|_{\hat{\mathbf{z}}_k^-} \quad (5.17)$$

$$= \left. \begin{bmatrix} \frac{\partial f_{dyn}}{\partial \mathbf{y}} & \frac{\partial f_{dyn}}{\partial \mathbf{d}} \\ \mathbf{0}_{n_d \times n_y} & \mathbf{I}_{n_d \times n_d} \end{bmatrix} \right|_{\hat{\mathbf{z}}_k^-} \quad (5.18)$$

The *a posteriori* correction equations are defined as follow:

$$\mathbf{K}_k = \mathbf{P}_k^- \mathbf{C}^T (\mathbf{C} \mathbf{P}_k^- \mathbf{C}^T + \mathbf{R})^{-1} \quad (5.19)$$

$$\hat{\mathbf{z}}_k^+ = \hat{\mathbf{z}}_k^- + \mathbf{K}_k (\mathbf{y}_k - \hat{\mathbf{y}}_{p_k}^-) \quad (5.20)$$

$$\mathbf{P}_k^+ = (\mathbf{I} - \mathbf{K}_k \mathbf{C} \mathbf{P}_k^-) \quad (5.21)$$

$$\mathbf{y}_k^+ = \mathbf{C} \hat{\mathbf{z}}_k^+ \quad (5.22)$$

where  $\mathbf{K}$  is the Kalman Filter gain matrix,  $\mathbf{R}$  is the measured variables covariance matrix and  $\mathbf{C} = [\mathbf{I}_{n_y \times n_y} \mathbf{0}_{n_y \times n_d}]$ .

### 5.3.1.3 Steady-State Optimization Strategy

The steady-state economic optimization is based on Equation 2.3, described as follows:

$$\begin{aligned} \mathbf{u}^* &= \arg \min_{\mathbf{u}} \phi_{ec}(\mathbf{y}_{ss}, \mathbf{u}) \\ \text{s.t.} \quad & \mathbf{y}_{ss} = \mathbf{f}_{ss}(\mathbf{u}, \mathbf{d}_k^+, \bar{\mathbf{a}}_{ss}), \\ & \mathbf{g}(\mathbf{y}_{ss}, \mathbf{u}) \leq \mathbf{0} \end{aligned} \quad (5.23)$$

It is important to emphasize that in the optimization problem represented by Equation 5.23, the steady-state model is based on an identified GP model, as described in Section 5.3.1.1. Additionally, in the one-layer approach framework, the optimization problem is not solved but the gradient norm is considered as the NMPC objective function.

The gradient vector of the objective function is calculated as follows:

$$\nabla_{\mathbf{u}} \phi_{ec} = \left( \frac{\partial \mathbf{y}_{ss}}{\partial \mathbf{u}} \right)^T \frac{\partial \phi_{ec}}{\partial \mathbf{y}_{ss}} + \frac{\partial \phi_{ec}}{\partial \mathbf{u}} \quad (5.24)$$

In Equation 5.24, it is assumed that the steady-state model gives only the output variables. However, another possible approach, not considered in this work, is considering the objective function as another output variable. In that case, the gradient calculation would be straightforward, as the objective function would be a function of the decision variable only. However, this approach may be limited for scenarios of constant market changes, such as raw material costs and product prices.

It is also important to mention that for a constrained problem like the one presented in Equation 5.23, the first-order NCO imply that the gradient of the Lagrangian function with respect to decision variables must be zero. The null condition of the objective function gradient itself is a first-order NCO for an unconstrained optimization problem. Thus, for a constrained optimization problem, additional constraints should also be added to the NMPC optimization problem in order to keep the solution feasibility.

Moreover, if one intends to implement an H-RTO framework, the optimization problem represented by Equation 5.23 should be solved and its solution will provide setpoints for the NMPC controller, as presented in Figure 5.7b.

### 5.3.1.4 Nonlinear Model Predictive Control

The Nonlinear Model Predictive Control works in a receding horizon strategy and it is described in the discretized formulation by Equation 5.25 (ABRAHAM

et al., 1999; MACIEJOWSKI, 2000; TATJEWSKI, 2007).

$$\begin{aligned}
\Delta \mathbf{u}^* &= \arg \min_{\Delta \mathbf{u}} \phi_c(\mathbf{y}, \mathbf{u}) \\
\text{s.t.} \quad & \forall i = 0, \dots, P-1, \\
& \Delta \mathbf{u}_{k+i|k} = \mathbf{u}_{k+i+1|k} - \mathbf{u}_{k+i|k}, \\
& \mathbf{y}_{k+i+1|k} = \mathbf{f}_{dyn}(\mathbf{y}_{k+i|k}, \mathbf{u}_{k+i|k}, \mathbf{d}_k^+, \bar{\mathbf{a}}) + \boldsymbol{\epsilon}_k, \\
& \mathbf{G}_{NMPC}(\mathbf{y}_{k+i|k}, \mathbf{u}_{k+i|k}) \leq \mathbf{0}, \\
& \mathbf{u}_{min} - \mathbf{u}_{k+i|k} \leq \Delta \mathbf{u}_{k+i|k} \leq \mathbf{u}_{max} - \mathbf{u}_{k+i|k}, \\
& \Delta \mathbf{u}_{min} \leq \Delta \mathbf{u}_{k+i|k} \leq \Delta \mathbf{u}_{max}, \\
& \mathbf{y}_{min} \leq \mathbf{y}_{k+i+1|k} \leq \mathbf{y}_{max}, \\
& \Delta \mathbf{u}_{k+i|k} = \mathbf{0} \quad \forall i \geq M, \\
& \mathbf{y}_{k|k} = \mathbf{y}_k^+
\end{aligned} \tag{5.25}$$

where  $\phi_c$  is the controller objective function,  $P$  and  $M$  are the prediction and control horizons, respectively.  $\Delta \mathbf{u} \in \mathbb{R}^P$  is the decision variable which represents the sequence of input increments, and then, the receding horizon principle implies that only the first increment is applied, such that  $\mathbf{u}_{k+1|k} = \mathbf{u}_{k|k} + \Delta \mathbf{u}_{k|k}$ . The NMPC algorithm is also based on a nonlinear dynamic model  $\mathbf{f}_{dyn}$  as defined in Equation 5.13. Additionally,  $\mathbf{y} \in \mathbb{R}^{n_y}$  is the vector of output variables,  $\boldsymbol{\epsilon} \in \mathbb{R}^{n_y}$  is a disturbance model, included to deal with unmeasured disturbances in addition to model uncertainties, considered as an output correction term,  $\mathbf{G}_{NMPC} : \mathbb{R}^{n_y} \times \mathbb{R}^{n_u} \rightarrow \mathbb{R}^{n_{sc}}$  is a vector of inequality constraints of the controller optimization problem.

The classical NMPC objective function is described as follows:

$$\begin{aligned}
\phi_{NMPC} &= \sum_{i=1}^P \left( \mathbf{y}_{k+i|k} - \mathbf{y}_{SP,k+i|k} \right)^T \mathbf{W}_y \left( \mathbf{y}_{k+i|k} - \mathbf{y}_{SP,k+i|k} \right) + \\
& \quad \sum_{i=0}^{M-1} \left( \mathbf{u}_{k+i|k} - \mathbf{u}_{SP,k+i|k} \right)^T \mathbf{W}_u \left( \mathbf{u}_{k+i|k} - \mathbf{u}_{SP,k+i|k} \right) + \\
& \quad \sum_{i=0}^{M-1} \Delta \mathbf{u}_{k+i|k}^T \mathbf{W}_{\Delta u} \Delta \mathbf{u}_{k+i|k}
\end{aligned} \tag{5.26}$$

where  $\mathbf{W}_y \in \mathbb{R}^{n_y \times n_y}$  is the positive semi-definite diagonal matrix of controlled variables weighting factors,  $\mathbf{W}_u \in \mathbb{R}^{n_u \times n_u}$  is the positive semi-definite diagonal matrix of manipulated variables weighting factors and  $\mathbf{W}_{\Delta u} \in \mathbb{R}^{n_u \times n_u}$  is the positive semi-definite diagonal matrix of manipulated variables movement suppression factors.

Additionally, if an economic term is considered on the NMPC formulation aiming to develop an one-layer strategy, the controller's objective function may become, without loss of generality:

$$\phi_c = W_{\phi_{NMPC}}\phi_{NMPC} + W_{\phi_{ec}}\phi_{ec} + W_{\nabla\phi_{ec}}\|\nabla_u\phi_{ec}\|^2 + W_{\phi_{ec}^{(P)}}\phi_{ec}^{(P)} \quad (5.27)$$

where  $W_{\phi_{NMPC}} \in \mathbb{R}$ ,  $W_{\phi_{ec}} \in \mathbb{R}$ ,  $W_{\nabla\phi_{ec}} \in \mathbb{R}$ , and  $W_{\phi_{ec}^{(P)}} \in \mathbb{R}$  are weighting factors related to the classical NMPC objective function, the objective function of the economic optimization problem, the norm of the gradient of this economic objective function, and the final value of this objective function, at the end of prediction horizon (P). In the latter case, it means that  $\phi_{ec}^{(P)} = \phi_{ec}(\mathbf{y}_{k+P|k}, \mathbf{u}_{k+P|k})$ .

Regarding the EMPC problem represented by Equation 5.25 with objective function generically represented by Equation 5.27, the stability of this controller can not be guaranteed, especially when no terminal constraint is added (ELLIS *et al.*, 2014). FAULWASSER *et al.* (2018) showed that for EMPC controllers without terminal constraints, the closed-loop system converges asymptotically into any arbitrarily small neighborhood of the optimal steady-state, by increasing the prediction horizon. It is important to highlight that this stabilizing strategy may lead to an increase in computational cost. Thus, there are other possible stabilizing strategies in literature that could be applied, such as adding a terminal constraint to the controller formulation which is not covered in this work. An overview of the EMPC stability topic is presented in the work of RAWLINGS *et al.* (2012).

In this work, the stability proof of the proposed frameworks is not addressed. In order to have a stable closed-loop solution, a sufficient long prediction horizon is considered.

### 5.3.2 Classic RTO Framework - RTO + QP-MPC

In this section, a framework based on a Classic RTO approach with an intermediate QP-MPC and a Linear MPC is presented. The framework is described by Figure 5.9. This framework represents the RTO framework in Section 5.5.3.

The steady-state optimization layer only updates its outputs when the plant data is considered to be at steady-state condition, which is verified by a steady-state detection step (SSD). If the system is at steady-state, the model parameters are updated. The optimum outputs are then sent to an intermediate optimization layer (QP-MPC).

The QP-MPC aims to adjust the RTO setpoints, using a steady-state version of the MPC linear model in order to satisfy the controller constraints. The execution of this intermediate layer occurs at the same frequency of the MPC (YING *et al.*, 1998).

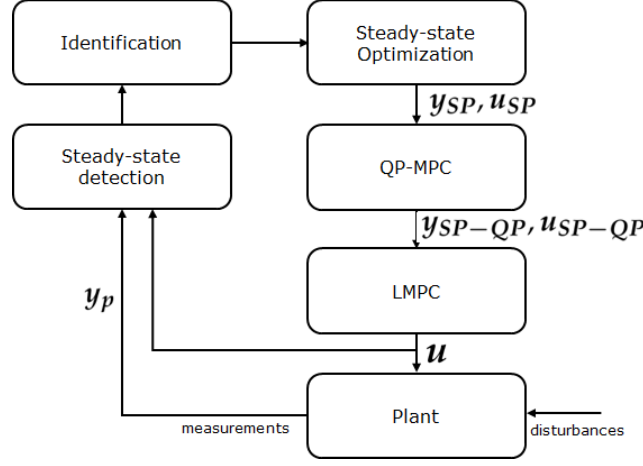


Figure 5.9: Classic RTO framework in two layers considering an intermediate QP-MPC.

The QP-MPC optimization problem is described as follows YING *et al.* (1998):

$$\begin{aligned}
 \mathbf{y}_{SP-QP}, \mathbf{u}_{SP-QP} = \arg \min_{\mathbf{y}, \mathbf{u}} \quad & \phi_{QP-MPC} = (\mathbf{y} - \mathbf{y}_{SP})^T \mathbf{c}_y^T \mathbf{c}_y (\mathbf{y} - \mathbf{y}_{SP}) + \\
 & (\mathbf{u} - \mathbf{u}_{SP})^T \mathbf{c}_u^T \mathbf{c}_u (\mathbf{u} - \mathbf{u}_{SP}) \\
 \text{s.t.} \quad & \mathbf{y} = \mathbf{y}_{ref} + \mathbf{K}_{LMPC}(\mathbf{u} - \mathbf{u}_{ref}), \\
 & \mathbf{u}_{min} \leq \mathbf{u} \leq \mathbf{u}_{max}, \\
 & \mathbf{y}_{min} \leq \mathbf{y} \leq \mathbf{y}_{max}
 \end{aligned} \tag{5.28}$$

where  $\mathbf{K}_{LMPC} \in \mathbb{R}^{n_y \times n_u}$  is the LMPC model static gain,  $\mathbf{u}_{ref}$  and  $\mathbf{y}_{ref}$  are the input and output reference values in which the linear model was identified,  $\mathbf{c}_y \in \mathbb{R}^{n_y}$  and  $\mathbf{c}_u \in \mathbb{R}^{n_u}$  are economic weights related to the economic optimization objective function, calculated as follows:

$$\mathbf{c}_y = \left. \frac{\partial \phi_{ec}}{\partial \mathbf{y}} \right|_{\mathbf{y}_{SP}, \mathbf{u}_{SP}} \tag{5.29}$$

$$\mathbf{c}_u = \left. \frac{\partial \phi_{ec}}{\partial \mathbf{u}} \right|_{\mathbf{y}_{SP}, \mathbf{u}_{SP}} \tag{5.30}$$

A linear MPC (LMPC) is considered in the present work in order to compare the performance of the proposed EMPC framework to a classic RTO in two-layers approach.

The LMPC is based on a Quadratic Dynamic Matrix Control (QDMC), which considers manipulated and controlled variables constraints, based on a Quadratic Programming (QP) Optimization Problem (GARCIA and MORSHEDI, 1986). The controlled variables predictions are described as a step response model as fol-

lows:

$$\mathbf{y} = \mathbf{S}\Delta\mathbf{u} + \mathbf{y}_k + \mathbf{F} \quad (5.31)$$

Expanding the expression gives:

$$\begin{bmatrix} \mathbf{y}_{k+1} \\ \mathbf{y}_{k+2} \\ \mathbf{y}_{k+3} \\ \vdots \\ \mathbf{y}_{k+P-1} \\ \mathbf{y}_{k+P} \end{bmatrix} = \begin{bmatrix} \mathbf{S}_1 & \mathbf{0}_{n_y \times n_u} & \mathbf{0}_{n_y \times n_u} & \cdots & & \mathbf{0}_{n_y \times n_u} \\ \mathbf{S}_2 & \mathbf{S}_1 & \mathbf{0}_{n_y \times n_u} & \cdots & & \mathbf{0}_{n_y \times n_u} \\ \mathbf{S}_3 & \mathbf{S}_2 & \mathbf{S}_1 & \cdots & & \mathbf{0}_{n_y \times n_u} \\ \vdots & \vdots & \vdots & \vdots & \vdots & \vdots \\ \mathbf{S}_{P-1} & \mathbf{S}_{P-2} & \mathbf{S}_{P-3} & \cdots & \mathbf{S}_{P-M+1} & \mathbf{S}_{P-M} \\ \mathbf{S}_P & \mathbf{S}_{P-1} & \mathbf{S}_{P-2} & \cdots & \mathbf{S}_{P-M+2} & \mathbf{S}_{P-M+1} \end{bmatrix} \begin{bmatrix} \Delta\mathbf{u}_k \\ \Delta\mathbf{u}_{k+1} \\ \Delta\mathbf{u}_{k+2} \\ \vdots \\ \Delta\mathbf{u}_{k+M-2} \\ \Delta\mathbf{u}_{k+M-1} \end{bmatrix} + \begin{bmatrix} \mathbf{y}_k \\ \mathbf{y}_k \\ \mathbf{y}_k \\ \vdots \\ \mathbf{y}_k \\ \mathbf{y}_k \end{bmatrix} + \begin{bmatrix} \mathbf{F}_1 \\ \mathbf{F}_2 \\ \mathbf{F}_3 \\ \vdots \\ \mathbf{F}_{P-1} \\ \mathbf{F}_P \end{bmatrix} \quad (5.32)$$

where  $P$  is the prediction horizon,  $M$  is the control horizon,  $\mathbf{0}_{n_y \times n_u} \in \mathbb{R}^{n_y \times n_u}$  is a matrix of zeros,  $\mathbf{S}_k \in \mathbb{R}^{n_y \times n_u}$  is known as the dynamic matrix, which defines the response of each control variable related to each input variable. The dynamic matrix is defined as follows:

$$\mathbf{S}_k = \sum_{j=1}^k \mathbf{H}_j \quad (5.33)$$

where:

$$\mathbf{H}_j = \begin{bmatrix} h_{1,1,j} & h_{1,2,j} & \cdots & h_{1,nu,j} \\ h_{2,1,j} & h_{2,2,j} & \cdots & h_{2,nu,j} \\ \vdots & \vdots & \cdots & \vdots \\ h_{ny,1,j} & h_{ny,2,j} & \cdots & h_{ny,nu,j} \end{bmatrix} \quad (5.34)$$

where each  $h_{i,k,j}$  represents the impulse response of the variable  $i$  ( $i = 1, \dots, n_y$ ) related to the input variable  $k$  ( $k = 1, \dots, n_u$ ) in the time instant  $j$ .

Additionally,  $\mathbf{F}_i \in \mathbb{R}^{n_y}$  is calculated by the equation below:

$$\mathbf{F}_i = \sum_{n=1}^i \boldsymbol{\phi}_n \quad (5.35)$$

where  $\boldsymbol{\phi}_n$  represents the response of the output to past control actions related to the instant  $n$  and is defined by the following equation:

$$\boldsymbol{\phi}_n = \sum_{l=n+1}^N \mathbf{H}_l \Delta\mathbf{u}(k+n-j) \quad (5.36)$$

where  $N \geq P$  is the plant stabilization period.

The QP is described as follows:

$$\begin{aligned} \Delta \mathbf{u}^* = \arg \min_{\Delta \mathbf{u}} \quad & \phi_{LMPC} := \Delta \mathbf{u}^T \mathbf{Q} \Delta \mathbf{u} + 2\mathbf{C}_f \Delta \mathbf{u} \\ \text{s.t.} \quad & \Delta \mathbf{u}_{min} \leq \Delta \mathbf{u} \leq \Delta \mathbf{u}_{max}, \\ & \mathbf{u}_{min} \leq \mathbf{u} \leq \mathbf{u}_{max}, \\ & \mathbf{y}_{min} \leq \mathbf{y} \leq \mathbf{y}_{max} \end{aligned} \quad (5.37)$$

where  $\Delta \mathbf{u} \in \mathbb{R}^{n_u M}$  is the increment in the manipulated variables,  $\phi_{LMPC}$  is the objective function of the LMPC,  $\Delta \mathbf{u}_{min} \in \mathbb{R}^{n_u M}$  and  $\Delta \mathbf{u}_{max} \in \mathbb{R}^{n_u M}$  are the minimum and maximum bounds of control actions increments,  $\mathbf{u}_{min} \in \mathbb{R}^{n_u M}$  and  $\mathbf{u}_{max} \in \mathbb{R}^{n_u M}$  are the minimum and maximum bounds of the manipulated variables,  $\mathbf{y}_{min} \in \mathbb{R}^{n_y P}$  and  $\mathbf{y}_{max} \in \mathbb{R}^{n_y P}$  are the minimum and maximum bounds of the controlled variables, and  $\mathbf{Q} \in \mathbb{R}^{n_u M \times n_u M}$  and array  $\mathbf{C}_f \in \mathbb{R}^{n_u M}$  are described as follow:

$$\mathbf{Q} = \mathbf{S}^T \mathbf{W}^T \mathbf{W} \mathbf{S} + \mathbf{R} \quad (5.38)$$

$$\mathbf{C}_f^T = \mathbf{e}^T \mathbf{W}^T \mathbf{W} \mathbf{S} \quad (5.39)$$

where  $\mathbf{W} \in \mathbb{R}^{P n_y \times P n_y}$  is the matrix related to control variables weight in objective function,  $\mathbf{R} \in \mathbb{R}^{n_u M \times n_u M}$  is the matrix of manipulated variables suppression and  $\mathbf{e} \in \mathbb{R}^{n_y P}$  is the deviation of open-loop response due to past control actions of the controlled variables from setpoint ( $\mathbf{y}_{OL} - \mathbf{y}_{SP}$ ), where  $\mathbf{y}_{OL} = \mathbf{y}_k + \mathbf{F}$ , the last two terms of Equation 5.31.

## 5.4 Case Study: The Willians-Otto Reactor

### 5.4.1 Model Equations

The Willians-Otto Reactor equations were described in Chapter 4, in Section 4.5.2. The same equations for the plant are considered here.

### 5.4.2 Economical Optimization Problem

The economic optimization of the Willians-Otto reactor as presented in FORBES and MARLIN (1996); MARCHETTI *et al.* (2009) consists of obtaining the optimal values of  $B$  feed rate and reactor temperature, which maximize profit. The profit is based on the revenue associated with  $E$  and  $P$  selling and operational costs related to raw materials (reagents  $A$  and  $B$ ). In the nominal case, at

disturbance absence, the  $A$  flow rate is fixed at  $1.8275 \text{ kg/s}$ . The plant optimization problem is described as follows:

$$\begin{aligned}
 F_B^*, T_R^* = \arg \min_{F_B, T_R} \quad & \phi_{ec} = -(1143.38 w_P F + 25.92 w_E F - 76.23 F_A - 114.34 F_B) \\
 \text{s.t.} \quad & \boldsymbol{w} = \boldsymbol{f}(F_B, T_R, \boldsymbol{\theta}), \\
 & 3 \leq F_B \leq 6 \text{ (kg/s)}, \\
 & 70 \leq T_R \leq 100 \text{ (}^\circ\text{C)}
 \end{aligned}
 \tag{5.40}$$

where  $\phi_{ec}$  is the profit (in  $\$/s$ ),  $\boldsymbol{f}(F_B, T_R, \boldsymbol{\theta})$  is the steady-state equation system represented by Equations 4.48 to 4.53,  $\boldsymbol{w}$  is the mass fraction species vector,  $F$  is the reactor outlet flow rate, evaluated by  $F = F_A + F_B$  (global mass balance) and  $\boldsymbol{\theta}$  is the parameters vector of the system. The values in the objective function are the products selling prices and the reagent costs in  $\$/\text{kg}$ .

For RTO problem purposes, the  $A$  species flow rate is considered a disturbance to the process. Also, the plant equations vector  $\boldsymbol{f}$  is replaced by the model equations vector  $\boldsymbol{f}_{ss}$ , as described in the optimization problem represented by Equation 5.23.

As presented in FORBES and MARLIN (1996); MARCHETTI *et al.* (2009) and also confirmed in the present work, the optimal problem solution for the nominal case is presented in Table 5.1. .

Table 5.1: Economic optimal problem solution.

Variable	Unit	Steady-State Value
$F_B$	kg/s	4.787
$T_R$	$^\circ\text{C}$	89.703
$w_A$	-	0.0875
$w_B$	-	0.3896
$w_C$	-	0.0153
$w_E$	-	0.2906
$w_P$	-	0.1095
$w_G$	-	0.1075

### 5.4.3 Controlled and Manipulated Variables

In the RTO strategies evaluated in which the classical MPC objective function is considered (RTO or H-RTO strategies) the controller designed for Willians-Otto Reactor considers species  $E$  and  $P$  mass fractions as controlled variables and the

species  $B$  mass flow rate ( $F_B$ ) and reactor temperature ( $T_R$ ) as manipulated variables. The species  $A$  mass flow rate is considered an unmeasured disturbance of the system. This choice is justified as the Willians-Otto economical problem presented in Equation 5.40 has  $E$  and  $P$  as main products of the unit and considered as revenue.

With this variables selection, a dynamic model for species  $E$  and  $P$  should be identified for application in the controller. It is also important to highlight that in EMPC strategy, the same dynamic model for  $w_E$  and  $w_P$  will be applied.

## 5.4.4 Model Identification

### 5.4.4.1 GP Model Identification

For GP model identification, it was applied the DACE package (LOPHAVEN *et al.*, 2000), available in MATLAB ©v.7.6. Each GP model was obtained in order to predict the steady-state value of each reactor outlet mass fraction. For identification, a computational experiment using the Latin Hypercube Design (LHS) strategy was employed (MCKAY *et al.*, 1979), with 30 points inside the following domain:

$$3 \leq F_B \leq 6 \text{ (kg/s)} \quad (5.41)$$

$$70 \leq T_R \leq 100 \text{ (C)} \quad (5.42)$$

$$0.5 \leq F_A \leq 3 \text{ (kg/s)} \quad (5.43)$$

Steady-state data was obtained by solving the nonlinear system of equations represented in Equations 4.48 to 4.53, where the left-hand side of the equations were considered as null due to steady-state condition.

It is also important to highlight that only  $w_E$  and  $w_P$  will be used in the RTO strategy. However, the GP model identification for other species will also be carried out to evaluate the GP performance.

### 5.4.4.2 Dynamic Linear Model Identification for the Hammerstein Model Structures

Once GP models were identified following the strategy described in Section 5.4.4.1, the dynamic linear models could be identified.

For linear model identification, a 5% step disturbance in each input variable was applied, being the reference a steady-state operating point described in Table 5.1, which represents the optimum economic operational point of the process. In that case, the disturbance value is  $F_A = 1.8275 \text{ kg/s}$ .

The identification problem for the Hammerstein models for both structures 1 and 2 is formulated as a least-squares fitting problem, as follows:

$$\begin{aligned} \bar{\mathbf{a}}_{dyn}^* &= \arg \min_{\bar{\mathbf{a}}_{dyn}} \sum_{k=1}^N [\mathbf{y}_k - \mathbf{y}_{p_k}]^2 \\ \text{s.t.} \quad & \mathbf{y}_k = f_{dyn}(\mathbf{y}_{k-1}, \mathbf{u}_{k-1}, \mathbf{d}_{k-1}, \bar{\mathbf{a}}) \end{aligned} \quad (5.44)$$

where  $N$  is the number of discrete time points,  $\mathbf{y}_{p_k}$  is the measured output variables vector at time instant  $k$ .

For structures 1 and 2, regarding the identification of the linear dynamic models, different transfer functions were tested to verify which one gives the best fit. In the present work, orders below three were considered and a maximum of 2 zeros. The Mean Squared Error (MSE) was used as a metric for selecting the transfer function order and zeros combination, which is calculated as follows:

$$MSE = \frac{1}{N} \sum_{k=1}^N [\mathbf{y}_k - \mathbf{y}_{p_k}]^2 \quad (5.45)$$

The parameter estimation problem represented by Equation 5.44 was solved by using the Nelder-Mead (NELDER and MEAD, 1965) algorithm available in the MATLAB® function *fminsearch*.

#### 5.4.4.3 Dynamic Linear Model Identification for the LMPC

For the internal model of the LMPC, discrete transfer functions of each output variable were identified based on a SISO model identification strategy, which means that a step disturbance in each input variable was done separately, while the other input variables remained constant. The reference point for model identification was considered as the economic optimal problem solution presented in Table 5.1.

The exact estimation procedure and model orders used in the previous section were applied here. From the estimated transfer function matrix, it is possible to obtain the step response model, as represented by Equation 5.31.

#### 5.4.5 Dynamic and Steady-State Characterization

For better understanding of the Willians-Otto reactor system, the equation system were linearized in order to obtain static gain and poles in a given reference point.

For system linearization, the system was transformed in a state-space formu-

lation as follows:

Original System:

$$\frac{dx}{dt} = f(x, u, d) \quad (5.46)$$

$$y = h(x, u, d) \quad (5.47)$$

Linearized System:

$$\frac{dx'}{dt} = Ax' + Bu' + B_d d' \quad (5.48)$$

$$y' = Cx' + Du' + D_d d' \quad (5.49)$$

where  $x \in \mathbb{R}^{n_x}$  is the vector of state variables,  $u \in \mathbb{R}^{n_u}$  is the vector of input variables,  $d \in \mathbb{R}^{n_d}$  is the vector of disturbances,  $y \in \mathbb{R}^{n_y}$  represents the output variables,  $f : \mathbb{R}^{n_x \times n_u \times n_d} \rightarrow \mathbb{R}^{n_x}$  is the vector of nonlinear functions of differential-equations,  $h : \mathbb{R}^{n_x \times n_u \times n_d} \rightarrow \mathbb{R}^{n_y}$  is the vector of nonlinear functions that relates input and output variables of the original system. For the linearized system, the superscript ' represents the original variable in terms of deviation variables,  $A \in \mathbb{R}^{n_x \times n_x}$ ,  $B \in \mathbb{R}^{n_x \times n_u}$ ,  $B_d \in \mathbb{R}^{n_x \times n_d}$ ,  $C \in \mathbb{R}^{n_y \times n_x}$ ,  $D \in \mathbb{R}^{n_y \times n_u}$  and  $D_d \in \mathbb{R}^{n_y \times n_d}$  are matrices of the system, defined as follows:

$$A = \frac{\partial f}{\partial x} \quad B = \frac{\partial f}{\partial u} \quad B_d = \frac{\partial f}{\partial d} \quad C = \frac{\partial h}{\partial x} \quad D = \frac{\partial h}{\partial u} \quad D_d = \frac{\partial h}{\partial d} \quad (5.50)$$

where the above matrix are all calculated at a reference point.

The steady-state gain of each output in relation to each input variable can be obtained as follows:

$$y'_{ss} = K_u u'_{ss} + K_d d'_{ss} \quad (5.51)$$

where the subscript  $ss$  represents the steady-state value of the variable,  $K_u \in \mathbb{R}^{n_y \times n_u}$  is the steady-state gain matrix of the output variables in relation to the input variables and  $K_d \in \mathbb{R}^{n_y \times n_d}$  is the steady-state gain matrix of the output variables in relation to the disturbance variables.

The gains presented in Equation 5.51 are calculated as follows:

$$K_u = \frac{\partial y'_{ss}}{\partial u'_{ss}} = -CA^{-1}B + D \quad (5.52)$$

$$K_d = \frac{\partial y'_{ss}}{\partial d'_{ss}} = -CA^{-1}B_d + D_d \quad (5.53)$$

Additionally, the poles of the dynamic system are defined as the eigenvalues

of the matrix  $A$ , obtained by solving the characteristic equation of the system:

$$|A - I\lambda| = 0 \quad (5.54)$$

The time constants of the dynamic system at a given reference point can be calculated as follows:

$$\tau_j = -\frac{1}{\lambda_j} \quad (j = 1, \dots, n_x) \quad (5.55)$$

The invariant zeros of the system defined by Equation 5.49 regarding its inputs ( $u'$ ) can be defined as the complex values of  $s$  for which the rank of the Rosembrock system matrix

$$\begin{bmatrix} A - sI & B \\ C & D \end{bmatrix} \quad (5.56)$$

drops from its normal value (normal rank). Additionally, if the complex values of  $s$  for which the transfer function of the system regarding its inputs ( $u'$ )

$$G_u(s) = C [sI - A]^{-1} B + D \quad (5.57)$$

drops from its normal value, this zeros are called transmission zeros (EMAMI-NAEINI and DOOREN, 1982).

## 5.5 Results and Discussion

This section presents the results and discussions of the proposed methodology applied to the Willians-Otto reactor. First, the Willians-Otto characterization results are presented. Subsequently, the results regarding nonlinear model identification based on Hammerstein structures are presented. Finally, the results of the proposed frameworks applied to the Willians-Otto reactor are presented.

### 5.5.1 Willians-Otto Reactor Characterization

#### 5.5.1.1 Steady-State Gain Behavior

For a better understanding of the system, the steady-state gain matrix was calculated following Equations 5.52 and 5.53 at several steady-state points inside

the domain described below:

$$\begin{aligned}
 3 &\leq F_B \leq 6 \text{ (kg/s)} \\
 70 &\leq T_R \leq 100 \text{ (}^\circ\text{C)} \\
 F_A &= 1.875 \text{ (kg/s)}
 \end{aligned}
 \tag{5.58}$$

In Figures 5.10 to 5.15, the steady-state gain for species  $A$ ,  $B$ ,  $C$ ,  $E$ ,  $P$  and  $G$  mass fractions in relation to each input variable is presented, respectively.

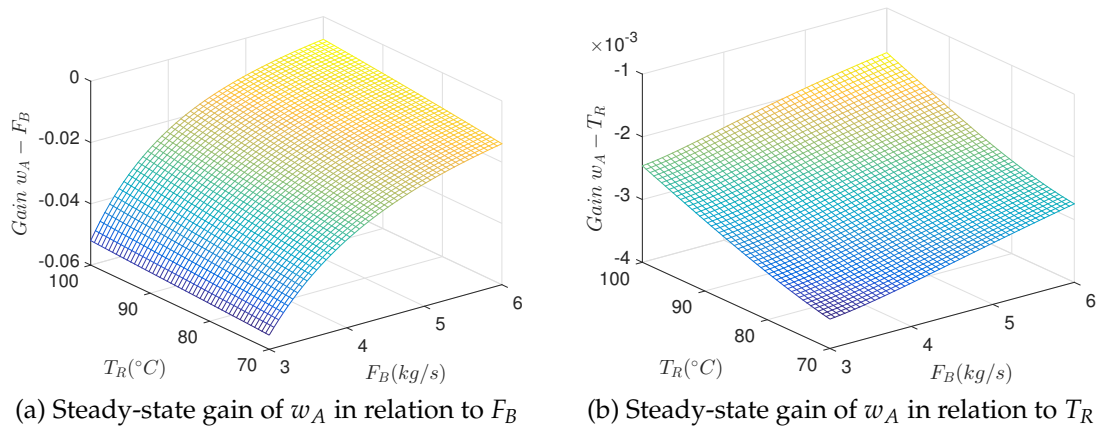


Figure 5.10: Steady-state gain of  $w_A$ .

For the output variable  $w_A$ , the steady-state gain surface presented in Figure 5.10 shows that for both input variables, the steady-state gains are negative, which means that an increase in B inlet flow ( $F_B$ ) or an increase in reactor temperature ( $T_R$ ) decrease  $w_A$  mass fraction. Indeed, both actions increase the reaction rate of  $A$  species, which implies in its concentration reduction.

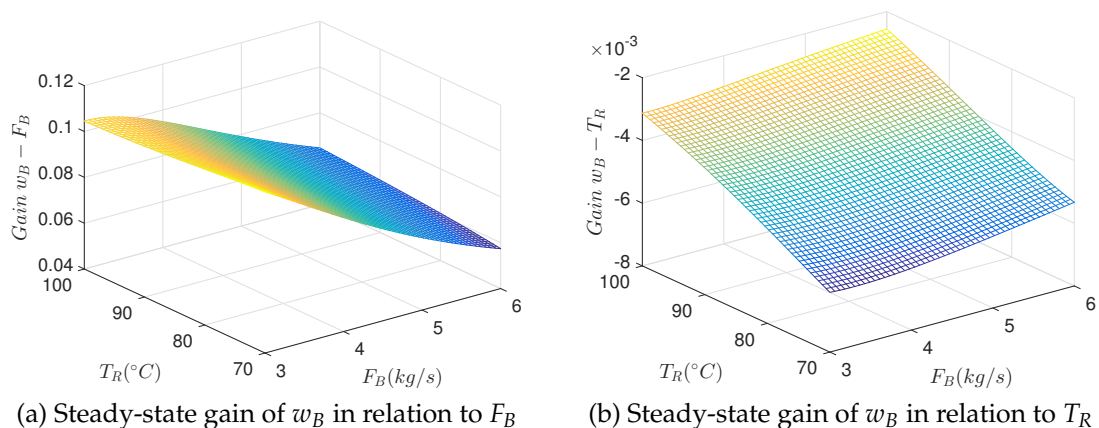


Figure 5.11: Steady-state gain of  $w_B$ .

For the output variable  $w_B$ , the steady-state gain surfaces in Figure 5.11 show that the steady-state gain is positive in relation to  $F_B$  and negative in relation to

$T_R$ . This effect of  $F_B$  can be direct explained, as it increases the  $w_B$  concentration inside the reactor. On the other side, an increase in reactor temperature decreases  $w_B$ , due to an increase in the reaction rate of  $B$  consumption.

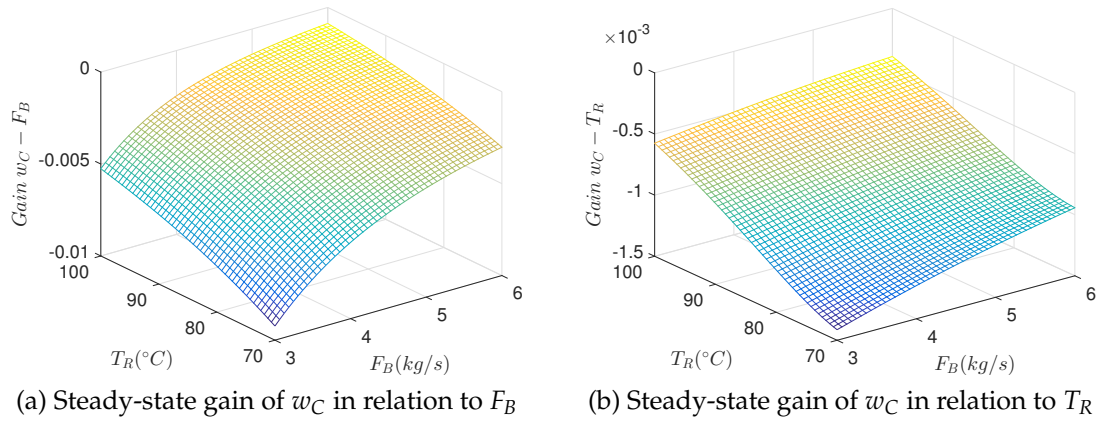


Figure 5.12: Steady-state gain of  $w_C$ .

For  $w_C$ , both steady-state gain surfaces in Figure 5.12 are negative, which means that an increase in each input variables decreases the steady-state concentration of  $w_C$ . Both effects could be explained by the increase in the reaction rate that consumes species  $C$ .

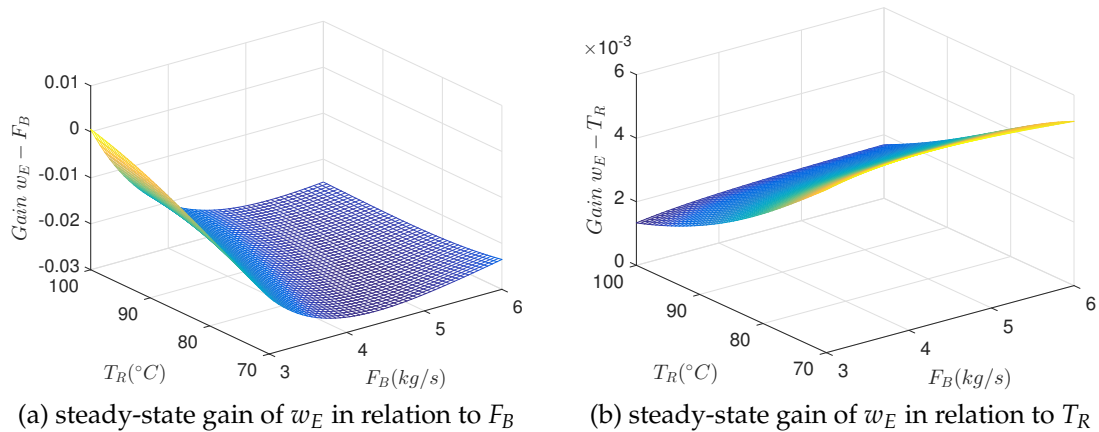


Figure 5.13: Steady-Gain of  $w_E$ .

For  $w_E$ , the steady-state gain surface in Figure 5.13 shows that the gain in relation to  $F_B$  is negative over the entire domain. For the steady-state gain related to  $T_R$ , the gain is positive over the entire domain. The effect of  $F_B$  can be explained by the overall mass balance equation, which implies in dilution of  $w_E$  species and the reduction of the residence time when increasing  $F_B$ , although it would be expected to increase the formation reaction rate of  $E$  due to increasing of concentration of the reactant  $B$ . The effect of  $T_R$  is related to the increase of species  $E$  formation, as it is a second reaction product.

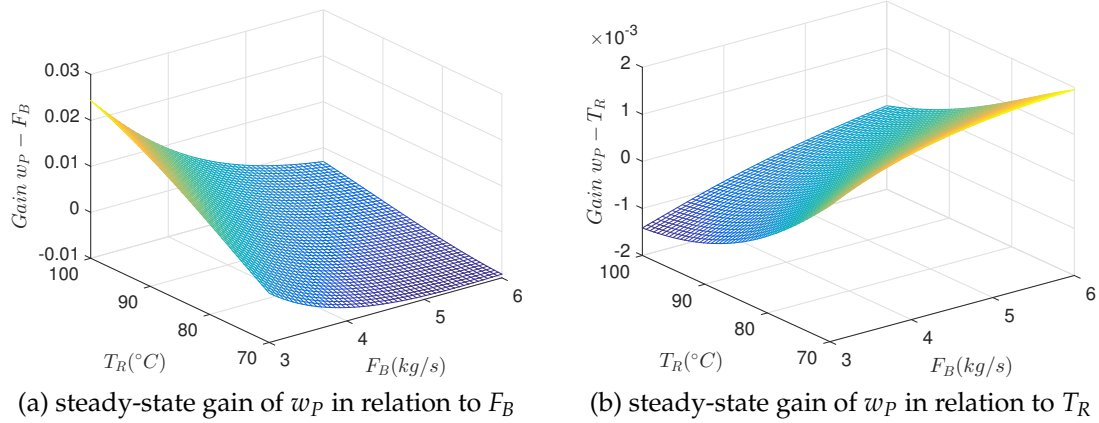


Figure 5.14: Steady-state gain of  $w_P$ .

For  $w_P$ , the steady-state gain surface in Figure 5.14 shows that both gains present signal change inside the domain.

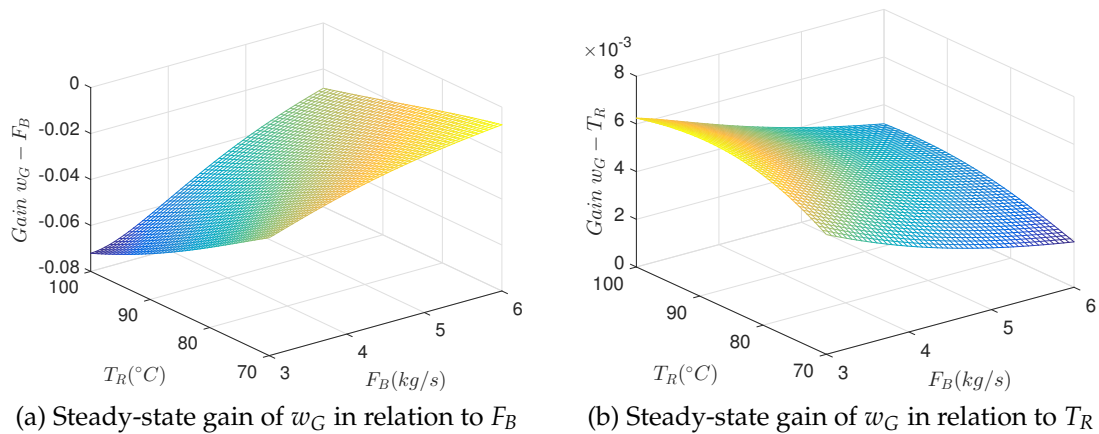


Figure 5.15: Steady-state gain of  $w_G$ .

For  $G$  species, Figure 5.15 shows that the steady-state gain associated to  $F_B$  is negative over the entire domain and the steady-state gain associated with  $T_R$  is positive over the entire domain. The explanation is the same to the  $w_E$  species: increasing  $F_B$  would dilute the  $G$  species concentration and an increase in  $T_R$  also increases  $G$  formation reaction rate.

In order to better present the gain regions for species  $E$  and  $P$ , a contour plot of its gains are presented in Figure 5.16.

The positive regions of  $w_P$  gains are represented by the gray region in Figure 5.16. For the steady-state gain related to  $F_B$ , it is possible to notice that the region comprises the entire domain of temperature ( $70 \leq T_R \leq 100$  °C). However, it is limited by  $B$  feed flow rate values, defining a curve that splits the positive and negative gain domains. Similarly, for  $w_P$  gain related to  $T_R$ , the region of positive gain is also well defined by a nonlinear curve that splits the domain.

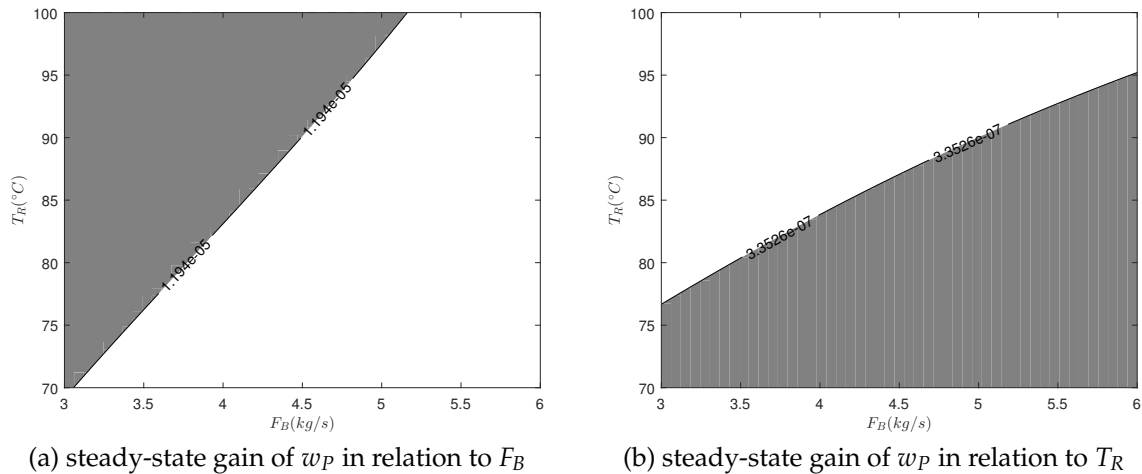


Figure 5.16: Steady-state Gain of  $w_p$  - filled region represents the positive gain region.

It is important to mention that the economic problem optimum is located in the region where the steady-state gains of  $w_p$  related to  $F_B$  and  $T_R$  are both negative.

### 5.5.1.2 Poles, Zeros and Time Constant Behavior

The poles of the dynamic system were calculated in each steady-state point to see if the system's dynamics depend on the operating point. To show this effect of the poles, the dominant time constant concept was applied, representing the system's slowest dynamics. The dominant time constant can be obtained by selecting the largest pole of the system at each operating point and calculate its opposite reciprocal.

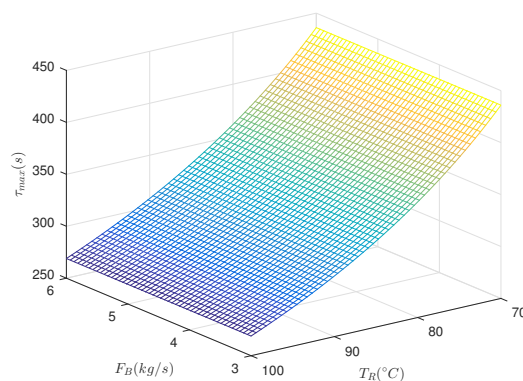


Figure 5.17: Dominant time constant of the system.

Figure 5.17 shows that the dominant time constant of the system increases when the reaction temperature decreases. It is important to say that Hammerstein models have a characteristic that the dynamic linear model is time-invariant

so that the transfer function parameters do not change, being this a possible limitation to predict actual values with accuracy.

Additionally, the dominant time constant range is 250-450s approximately. Considering a system represented by a first-order linear transfer function, it means that the settling time would be in the range of 1250-2250s, calculated using the relation  $5\tau_{max}$ , where  $\tau_{max}$  is the dominant time constant. At the plant economic optimal point, the time constant is 350s, and the settling time is 1750s (about 30 min).

Regarding the transmission zeros of the system, the zeros were calculated in each steady-state point, but no zeros were found in the studied domain.

## 5.5.2 Nonlinear Model Identification

### 5.5.2.1 Static Function: GP Model Identification

For each reactor outlet mass fraction, a GP model was obtained, representing the steady-state value of each variable as a function of the input and disturbance variables. The GP model works as a surrogate model of the Willians-Otto system of equations in steady-state. For evaluating the prediction ability of the model, the MSE was calculated considering a squared mesh of 900 points inside the domain  $[F_{Bmin}, F_{Bmax}] \times [T_{Rmin}, T_{Rmax}]$ , and the results for each output variable are presented in Table 5.2.

Table 5.2: Mean Squared Error (MSE) of GP model for each reactor outlet mass fraction at steady state.

Error	$w_A$	$w_B$	$w_C$	$w_E$	$w_P$	$w_G$
$MSE(\times 10^3)$ (basis case)	0.0739	0.3301	0.0028	0.0542	0.0107	0.0644
$MSE(\times 10^3)$ (+10% in $F_A$ )	0.0750	0.3351	0.0028	0.0550	0.0108	0.0654
$MSE(\times 10^3)$ (-10% in $F_A$ )	0.0667	0.2978	0.0024	0.0489	0.0096	0.0581

From Table 5.2, it is possible to notice that the MSE is lower than  $10^{-4}$ , which means an error below 1% for each variable. This result indicates that the GP model predictions agree with the plant data, being a potential candidate to be applied as a surrogate model to the original system.

The surface plots of  $E$  and  $P$  species mass fraction as a function of the inlet variables ( $F_B$  e  $T_R$ ) are presented in Figures 5.21 and 5.22, considering the nominal disturbance value (base case) and disturbances of +10% and -10% in  $F_A$ . The results of species  $A$ ,  $B$ ,  $C$  and  $G$  are presented in Figures 5.18 to 5.23.

In Figure 5.21, it is noticed that the input variables  $T_R$  and  $F_B$  have a smooth effect on the mass fraction of species  $E$ , and the inlet mass flow disturbances in

species  $A$  have a low influence on this output variable at the steady-state. A distinct behavior is verified for species  $P$  in Figure 5.22, which presents a maximum inside the domain. This evidence can be justified by  $P$  being formed in reaction 2 and consumed in reaction 3. Therefore, depending on the operating point, the reaction rates change. This evidence is in agreement with changes in the signal of the static gain inside the domain, as shown in Figure 5.14. Additionally, it is also noticed that the  $P$  mass fraction is significantly affected by the disturbance in species  $A$  inlet mass flow rate and its maximum point.

For species  $A$ ,  $B$ ,  $C$  and  $G$ , in Figures 5.18 to 5.23 is possible to notice that there is no extremal point inside the domain of their mass fractions. It can be noticed that the  $w_A$  mass fraction decreases when increasing  $F_B$  and  $T_R$ , which can be explained by an increase in the first reaction rate. An increase in the  $w_B$  mass fraction is noticed when increasing  $F_B$  due to its hold-up. A decrease in  $w_B$  is expected when increasing  $T_R$ , as the first and second reaction rates also increase. The  $w_C$  mass fraction is negatively affected by  $F_B$  and  $T_R$ , which can be justified by the fact that reaction rates 2 and 3 are expected to be greater than reaction rate 1 due to the kinetics parameters values. Species  $G$  mass fraction decreases when increasing  $F_B$ , mainly related to the effects on species  $C$  and  $P$ , the reactants of reaction 3 in which species  $G$  is formed. Also, increasing  $T_R$  increases  $w_G$  mass fraction due to an increase in reaction rate 3. Additionally, it is also noticed that the  $w_A$  mass fraction varies accordingly to the  $A$  species inlet mass flow rate, as expected. On the other hand, the mass fraction of  $B$  is not strongly affected by  $F_A$ . A slight decrease in species  $B$  mass fraction is expected when increasing  $F_A$  due to increasing  $w_A$  and, consequently, the first reaction rate. For species  $G$ , it is also verified that  $F_A$  has minor effects on its outlet mass fraction.

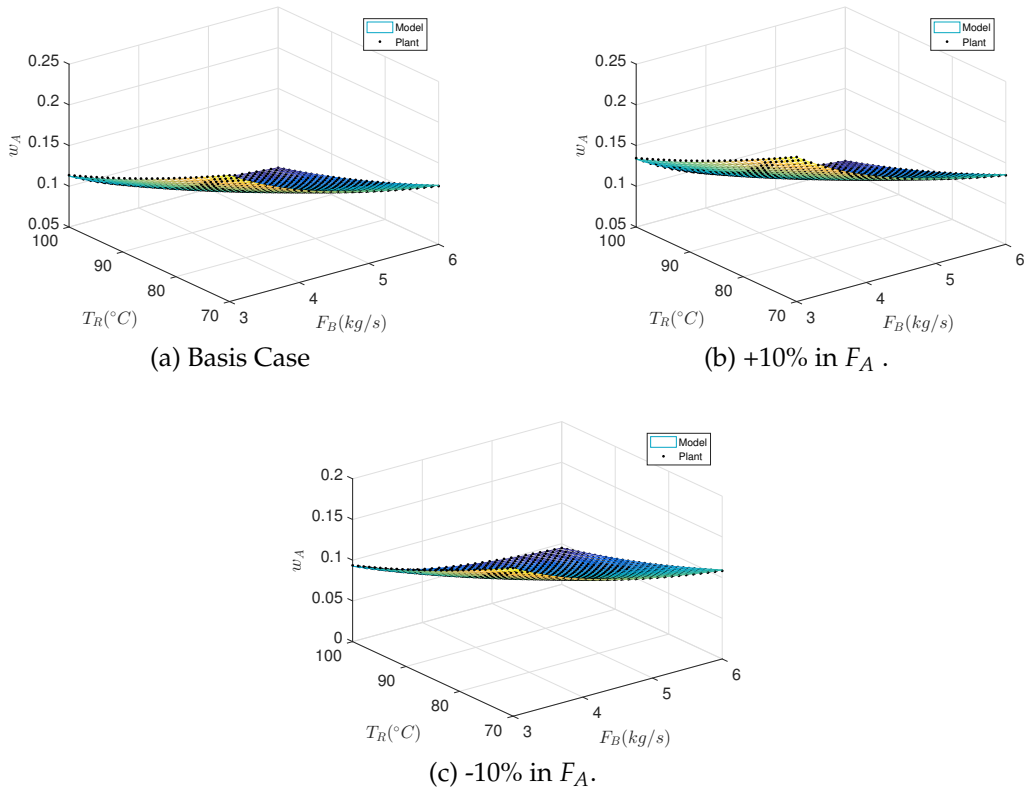


Figure 5.18:  $w_A$  predicted and actual values in three scenarios of measured disturbance ( $F_A$ ): (a) Basis case, (b) +10% and (c)-10%.

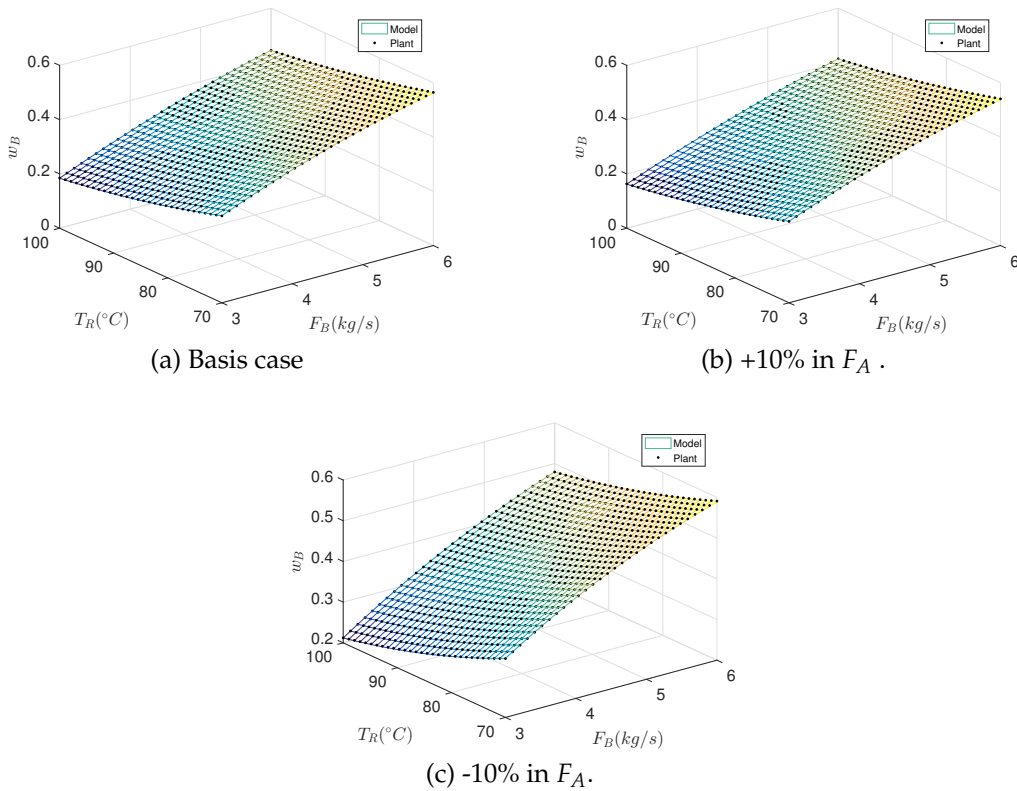


Figure 5.19:  $w_B$  predicted and actual values in three scenarios of measured disturbance ( $F_A$ ): (a) Basis case, (b) +10% and (c)-10%.

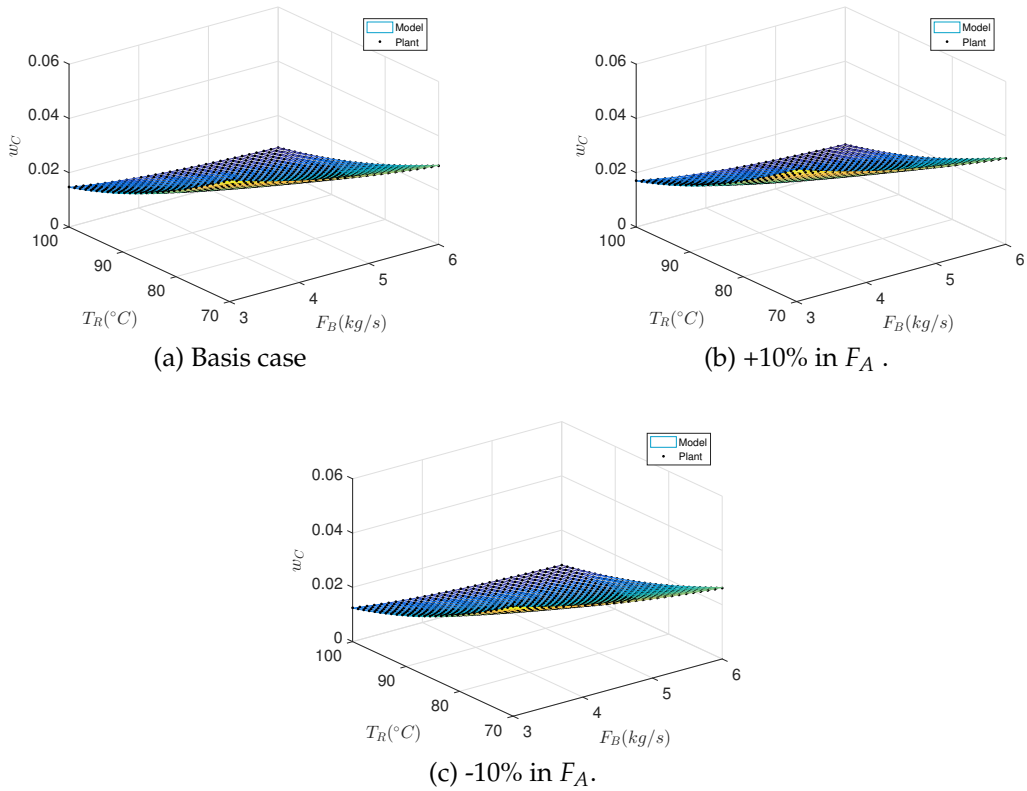


Figure 5.20:  $w_C$  predicted and actual values in three scenarios of measured disturbance ( $F_A$ ): (a) Basis case, (b) +10% and (c)-10%.

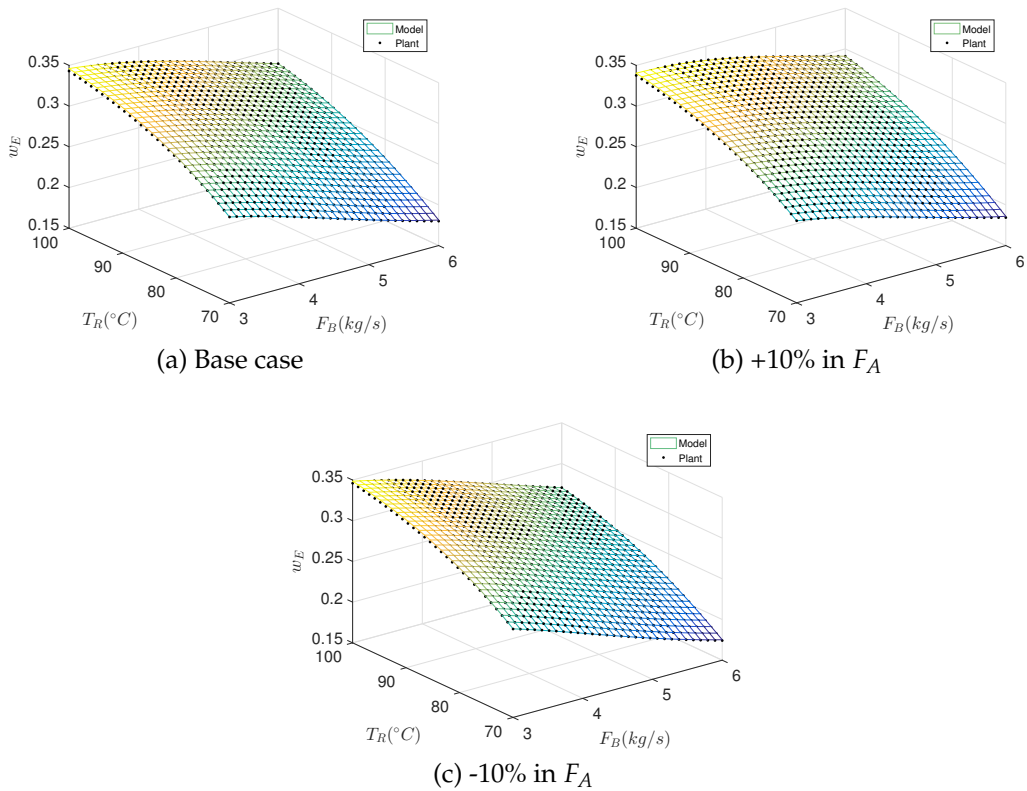


Figure 5.21:  $w_E$  predicted and actual values in three scenarios of measured disturbance ( $F_A$ ): (a) Base case, (b) +10% and (c)-10%.

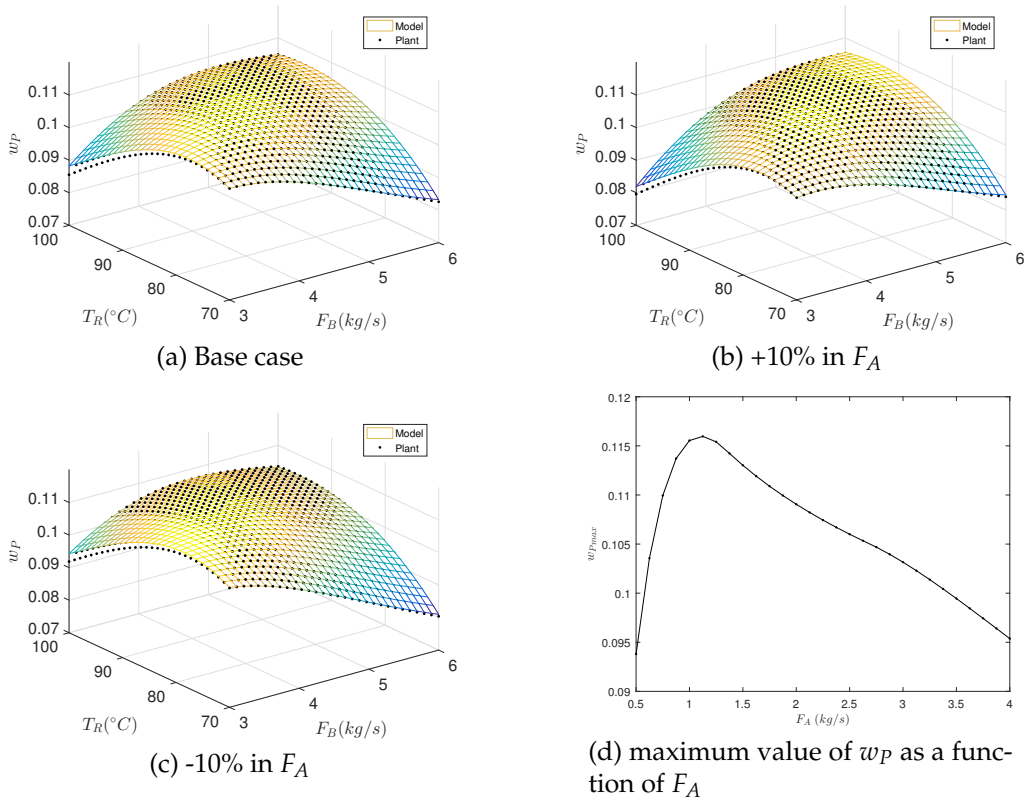


Figure 5.22:  $w_p$  predicted and actual values in three scenarios of measured disturbance ( $F_A$ ): (a) Base case, (b) +10%, (c)-10% and (d) the maximum value of  $w_p$  as a function of  $F_A$ .

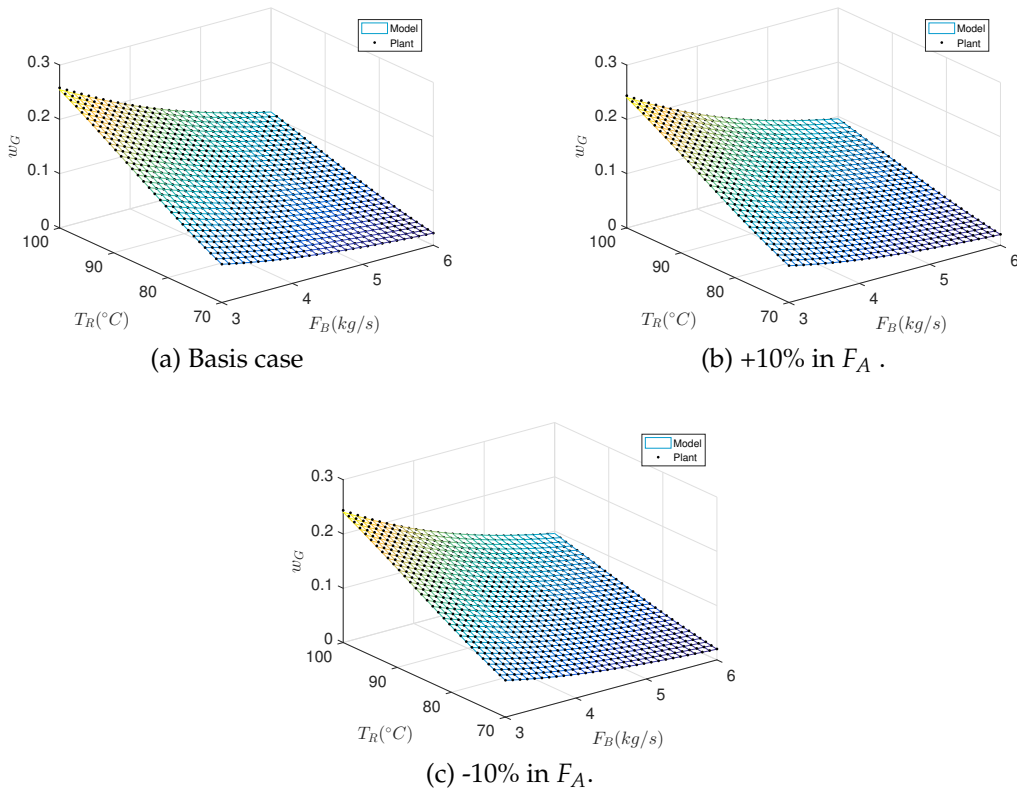


Figure 5.23:  $w_G$  predicted and actual values in three scenarios of measured disturbance ( $F_A$ ): (a) Basis case, (b) +10% and (c)-10%.

### 5.5.2.2 Hammerstein Structure 1 - Dynamic Block Identification

In Table 5.3, the Mean Squared Errors for each reactor mass fraction nonlinear model and for each configuration of the transfer function in terms of zeros and poles are presented. Analyzing Table 5.3, it is possible to note that by increasing the number of poles and zeros, especially for transfer function orders higher than 4, the MSE is also higher due to the oscillatory behavior of the fitted model. For species  $E$  and  $P$ , higher-order models did not significantly reduce the error, such that a transfer function of third order and one zero was considered.

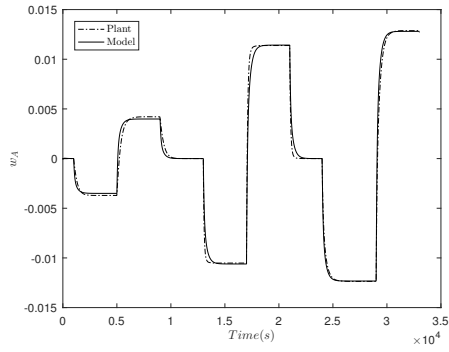
Table 5.3: Mean Squared Error (MSE) of linear model for each reactor outlet mass fraction in relation to a perturbation in  $F_B$ ,  $T_R$  and disturbance  $F_A$ .

Poles	Zeros	$w_A$	$w_B$	$w_C$	$w_E$	$w_P$	$w_G$
1	0	4.18E-07	4.54E-06	2.25E-08	1.54E-06	6.08E-07	1.88E-06
2	0	4.17E-07	4.54E-06	2.24E-08	1.54E-06	6.05E-07	1.88E-06
2	1	3.70E-07	4.52E-06	2.09E-08	1.54E-06	5.96E-07	1.88E-06
3	0	4.16E-07	4.54E-06	3.15E-07	1.54E-06	5.92E-07	1.88E-06
3	1	3.70E-07	4.52E-06	2.09E-08	1.54E-06	5.96E-07	1.87E-06
3	2	3.70E-07	4.52E-06	4.48E-08	1.54E-06	5.96E-07	1.87E-06
4	0	4.15E-07	4.54E-06	2.23E-08	2.75E-06	5.99E-07	3.15E-06
4	1	3.70E-07	1.24E-02	2.09E-08	7.65E-06	5.96E-07	1.35E-03
4	2	3.70E-07	4.50E-06	2.07E-08	1.54E-06	5.96E-07	1.87E-06
4	3	2.69E-05	2.36E-05	1.50E-05	1.54E-06	5.96E-07	1.93E-05
5	0	4.15E-07	5.97E-04	2.23E-08	1.54E-06	5.93E-07	1.88E-06
5	1	3.70E-07	2.79E-05	1.26E-07	1.54E-06	5.96E-07	1.87E-06
5	2	5.55E-07	4.52E-06	2.45E-08	1.54E-06	5.96E-07	1.87E-06
5	3	3.70E-07	3.09E-04	3.76E-06	1.54E-06	5.96E-07	1.96E-05
5	4	2.81E-06	4.44E-05	9.38E-08	3.09E-06	5.96E-07	1.87E-06

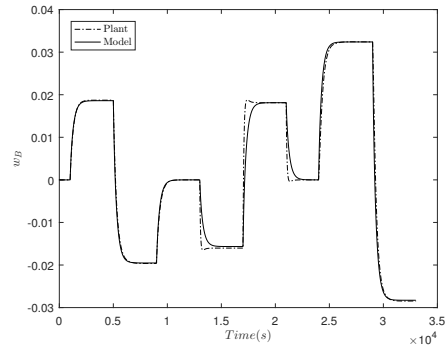
In Figures 5.24a to 5.24f, the observed dynamic response and the Hammerstein model prediction for mass fraction at reactor outlet is presented.

In Figure 5.24d, it is possible to notice that the proposed model prediction results are in agreement with the observed dynamic response for species  $E$ . However, it is observed that the plant dynamic response presents overshoot and inverse response which the proposed model does not predict.

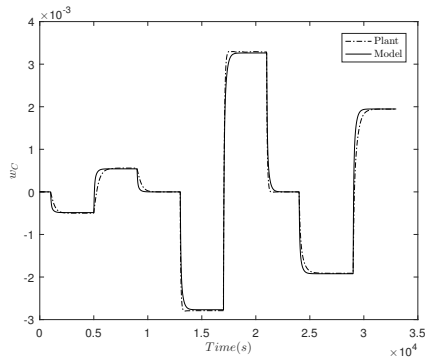
In the same way, for  $P$  species, in Figure 5.24e, it is also verified that the observed response presents inverse response and overshoots that are not predicted by the Hammerstein Model Structure 1. The steady-state values are well predicted due to the accuracy of the GP model of the Hammerstein structure (as presented in Figure 5.22). However, it can be seen that a simple linear model in the dynamic structure of the Hammerstein model has a low predictive ability of the complex dynamic behavior. For species  $A$ ,  $B$ ,  $C$  and  $G$ , it can be noticed that



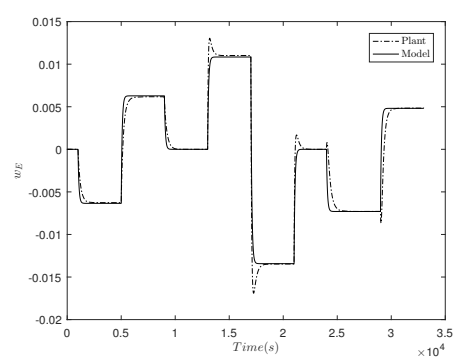
(a) Nonlinear model prediction in deviation variable of  $w_A$  using Hammerstein Model - Structure 1



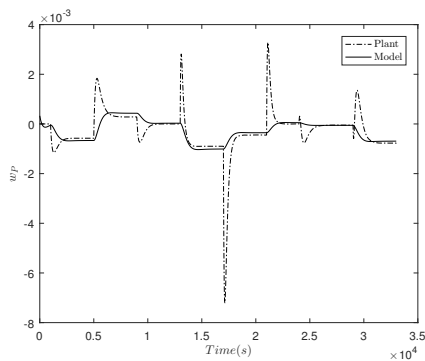
(b) Nonlinear model prediction in deviation variable of  $w_B$  using Hammerstein Model - Structure 1



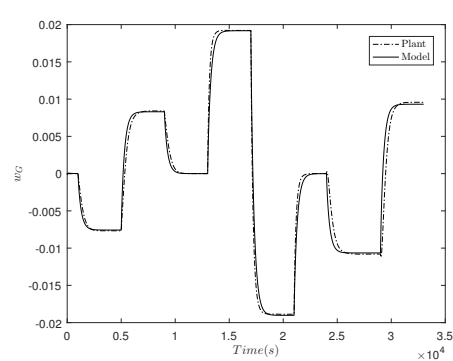
(c) Nonlinear model prediction in deviation variable of  $w_C$  using Hammerstein Model - Structure 1



(d) Nonlinear model prediction in deviation variable of  $w_E$  using Hammerstein Model - Structure 1



(e) Nonlinear model prediction in deviation variable of  $w_P$  using Hammerstein Model - Structure 1



(f) Nonlinear model prediction in deviation variable of  $w_G$  using Hammerstein Model - Structure 1

Figure 5.24: Nonlinear model prediction in deviation variables  $w_A$ ,  $w_B$ ,  $w_C$ ,  $w_E$ ,  $w_P$  and  $w_G$  using Hammerstein Model - Structure 1 with the training data set.

a linear model can represent the dynamic behavior.

### 5.5.2.3 Hammerstein Structure 2 - Dynamic Block Identification

In order to overcome the downside related to  $w_P$  dynamic behavior prediction of the MISO Structure 1 observed in Section 5.5.2.2, the proposed Hammerstein Model presented in Equation 5.7 was identified.

In the same way as the identification strategy applied for linear model identification, the maximum order of 3 for the transfer function was considered, and the maximum of two zeros was allowed. A transfer function of order 3 and one zero yield the best accuracy in the same training data set considered for Structure 1, and the resulting mean squared errors for  $w_E$  and  $w_P$  were  $MSE = 3.111 \times 10^{-8}$  and  $MSE = 5.448 \times 10^{-8}$ , respectively. For species  $E$ , the MSE decreased almost 50 times, while for species  $B$ , the MSE decreased almost 11 times compared with the results of Structure 1. Figure 5.25 presents the observed dynamics and the proposed model response for species  $E$  and  $P$ .

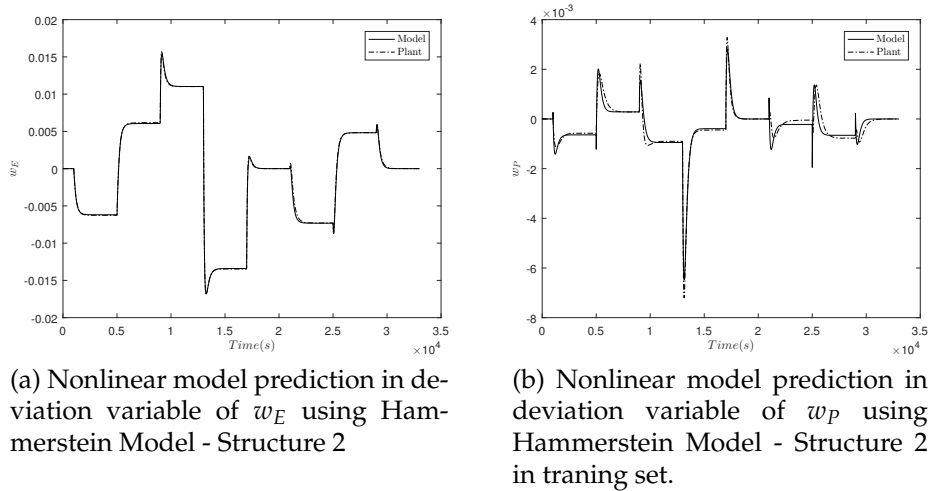
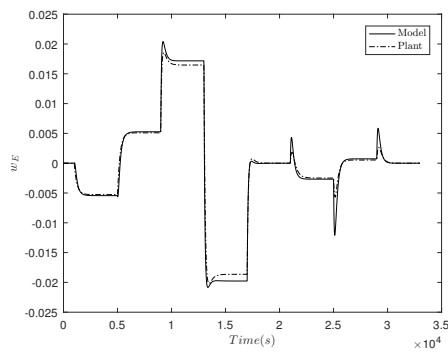


Figure 5.25: Nonlinear model prediction in deviation variable of  $w_E$  and  $w_P$  using Hammerstein Model - Structure 2 with the training data set.

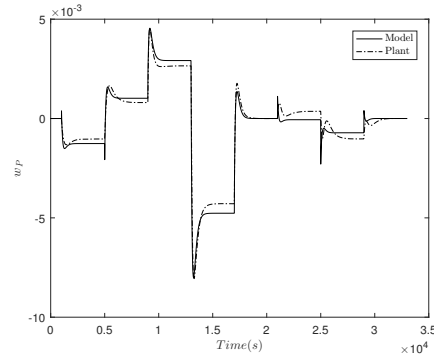
Analyzing Figure 5.25b, it is possible to notice that the model predictions are in agreement with the dynamic behavior, including inverse response and overshoot predictive ability, which shows that Hammerstein model Structure 2 should be considered instead of Structure 1 for dynamic prediction.

In order to validate the proposed model and evaluate its predictive ability in an operating point different from the reference point used for parameter estimation, perturbation in input variables were applied around the reference point  $[F_B(kg/s), T_R(^{\circ}C)] = [4, 75]$ . Figure 5.26 presents the results of the validation data set.

Analyzing Figure 5.26, it is possible to notice that the model prediction has a good agreement to the dynamic behavior using the validation data set, which



(a) Nonlinear model prediction in deviation variable of  $w_E$  using Hammerstein Model - Structure 2



(b) Nonlinear model prediction in deviation variable of  $w_P$  using Hammerstein Model - Structure 2.

Figure 5.26: Nonlinear model prediction in deviation variable of  $w_E$  and  $w_P$  using Hammerstein Model - Structure 2 with the validation data set.

represents that the model has extrapolation capability and is not overfitted. It is important to notice that the model has a slight bias compared to its final (steady-state) value after each perturbation. However, due to its overall good agreement to its dynamic and steady-state behaviors compared to the first structure, the proposed model was considered for control application.

### 5.5.3 RTO Strategies Applied to Willians-Otto Reactor

In order to compare the proposed methodology to previous works in literature, the following RTO strategies will be considered:

- EMPC1: Economic Model Predictive Control where the NMPC objective function is equal to the norm of the objective function gradient of the economic optimization problem, such that  $W_{\phi_{NMPC}} = 0$ ,  $W_{\phi_{ec}} = 0$ ,  $W_{\nabla\phi_{ec}} = 1$  and  $W_{\phi_{ec}^{(P)}} = 0$ .
- EMPC2: Economic Model Predictive Control where the NMPC objective function is equal to the economic problem objective function itself, such that  $W_{\phi_{NMPC}} = 0$ ,  $W_{\phi_{ec}} = 1$ ,  $W_{\nabla\phi_{ec}} = 0$  and  $W_{\phi_{ec}^{(P)}} = 0$ .
- H-RTO1: Hybrid Real-Time Optimization similar to the approach of MATIAS and LE ROUX (2018), such that  $W_{\phi_{NMPC}} = 1$ ,  $W_{\phi_{ec}} = 0$ ,  $W_{\nabla\phi_{ec}} = 0$  and  $W_{\phi_{ec}^{(P)}} = 0$ .
- H-RTO2: A proposed modified Hybrid Real-Time Optimization where a terminal cost using the economic objective function is added to the classical NMPC objective function, such that  $W_{\phi_{NMPC}} = 1$ ,  $W_{\phi_{ec}} = 0$ ,  $W_{\nabla\phi_{ec}} = 0$  and  $W_{\phi_{ec}^{(P)}} = 1$ .

- Perfect Model: The plant model is used in both steady-state optimization and NMPC. It means that the first-principles equations that represent the plant are applied, such that the modeling error can be considered negligible. Also, the disturbances are assumed to be known. In this case,  $W_{\phi_{NMPC}} = 1$ ,  $W_{\phi_{ec}} = 0$ ,  $W_{\nabla\phi_{ec}} = 0$  and  $W_{\phi_{ec}^{(P)}} = 0$ . The main difference between the Perfect Model and H-RTO1 structures is that the disturbances are assumed to be measured in the Perfect Model structure. In H-RTO1, the disturbances are estimated through an EKF. Also, in H-RTO1, the models applied in NMPC and RTO layers are identified models.
- RTO: A classical two-layer RTO framework with a two stage linear MPC (QP-LMPC) based on the strategy proposed in YING *et al.* (1998), where the complete framework is described in Section 5.3.2. It is worthwhile to mention that the steady-state model identified by the Gaussian Process is applied in the optimization problem defined by Equation 5.23 and an identified linear model is applied in a two-stage linear MPC.

For a fairly comparison, the controller tuning main parameters are the same for all controllers, which were obtained by trial and error. The sampling time of the controllers is  $5min$ , the prediction horizon is  $P = 100$  sampling instants, the control horizon is  $M = 1$  sampling instant, the weight matrices are  $W_y = I_{ny}$ ,  $W_u = 0$ ,  $W_{\Delta u} = 5 \times 10^{-5} I_{nu}$ . It is important to highlight that the controllers do not track the manipulated variables reference values, since  $W_u = 0$ . It is important to mention that the prediction horizon was considered to be long enough for stability purposes. The prediction horizon is ten times greater than the system's settling time. The EKF tuning was considered as  $P_0^+ = diag(10, 10, 10)$ ,  $Q = diag(10^{-3}, 10^{-3}, 10^{-1})$  and  $R = diag(10^{-4}, 10^{-4})$ . The tuning parameters for the controller and EKF were obtained by trial and error.

The simulation scenario comprises step disturbances of 30% in magnitude in unmeasured disturbances at each 60 sampling instants ( $300min$ ). The disturbances and the optimal values for  $w_E$ ,  $w_P$ ,  $F_B$  and  $T_R$  are described in Table 5.4.

Table 5.4: Disturbance values of  $F_A$  and steady-state optimal solution for the economical problem.

	$w_E$	$w_P$	$F_A$ (kg/s)	$F_B$ (kg/s)	$T_R$ (°C)
$d_1$ ( $0 \leq t < 300min$ )	0.2906	0.1095	1.8275	4.7874	89.7039
$d_2$ ( $300 \leq t < 600min$ )	0.2978	0.1139	1.2792	3.4774	85.6849
$d_3 = d_1$ ( $600 \leq t < 900min$ )	0.2906	0.1095	1.8275	4.7874	89.7039
$d_4$ ( $900 \leq t \leq 1200min$ )	0.2854	0.1062	2.3757	6.0000	92.4673

Figure 5.27 presents the closed-loop trajectories of the plant controlled variables for all the strategies considered.

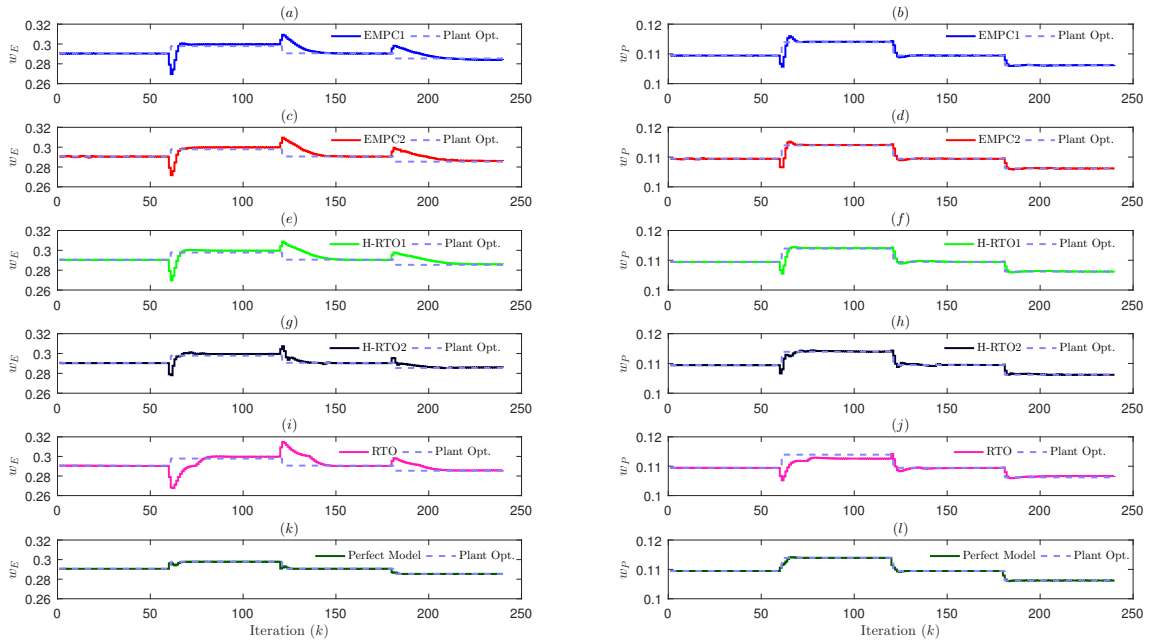


Figure 5.27: Closed-loop dynamic trajectories of controlled variables in using different RTO strategies: (a), (c), (e), (g), (i), (k)  $w_E$  and (b), (d), (f), (h), (j), (l)  $w_P$ .

Analyzing Figure 5.27, it is possible to notice that the dynamic trajectory for EMPC1 and EMPC2 presented similar behavior and both strategies led the plant to its optimum setpoints values, although the controller does not use this information in the objective function. Moreover, the controlled variables trajectory in EMPC1 tends to achieve the optimal values faster than in EMPC2. This evidence might be explained by the fact that minimizing the gradient norm is a more direct way of finding the economic objective function optimum rather than minimizing the objective function itself. When comparing H-RTO1 and H-RTO2 strategies, it is possible to notice that H-RTO2 led the controlled variables to their optimal values faster than H-RTO1. This evidence could be explained by the terminal cost present in the NMPC objective function, which enforces the controller to minimize this last term. The RTO strategy is the one that presents the slowest response in leading the plant to their optimum values. This could be explained by the fact that the optimum setpoints determined by the RTO layer are only updated when a new steady-state is reached. During the transient period, the controller tends to reject the disturbance and keep the controlled variables at their previous optimum values. Also, the RTO strategy showed an offset during the occurrence of the first disturbance for variable  $w_P$ . Additionally, the RTO strategy where a perfect model is considered and disturbance in  $F_A$  is known is the one that faster led the plant to its optimal values. From a practical perspective, this strategy may

be unrealistic. When comparing all other strategies, the H-RTO2 strategy was the one that faster led the plant to an optimum point, especially for the disturbance  $d_3$  and  $d_4$ .

Figure 5.28 presents the closed-loop trajectories of the plant manipulated variables for all the considered strategies.

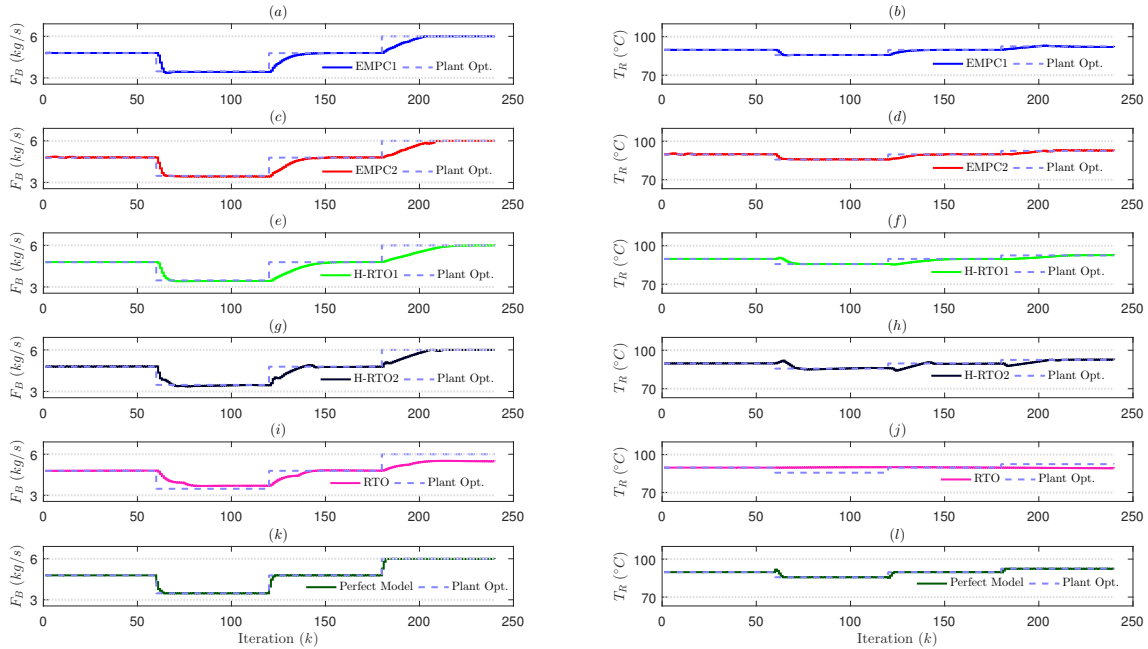


Figure 5.28: Closed-loop dynamic trajectories of manipulated variables: (a), (c), (e), (g), (i), (k)  $F_B$  and (b), (d), (f), (h), (j), (l)  $T_R$ .

In terms of the manipulated variables profile, analyzing Figure 5.28, it is possible to notice that EMPC1 strategy reaches the optimal values of the manipulated variables faster than EMPC2. As discussed for the controlled variables profile, using the economic optimization problem objective function gradient as the controller's objective function imposes faster convergence towards the optimal values of the decision variables. H-RTO2 strategy drove the manipulated variables to optimal values faster than H-RTO1. The RTO strategy does not achieve the optimal values of the manipulated variables and, consequently, does not track the controlled variables' optimal setpoints, except for the nominal points. Also, during the transient period, the RTO strategy imposes two different profiles for the manipulated variables during the transient period. One for disturbance rejection, while the controlled variables setpoints are not updated and another that starts when a new steady-state is reached, such that the disturbance is updated and the RTO updates the setpoints.

Figure 5.29 presents the closed-loop trajectories of the disturbance estimation for all the considered strategies.

In terms of disturbance estimation, analyzing Figure 5.29, all strategies con-

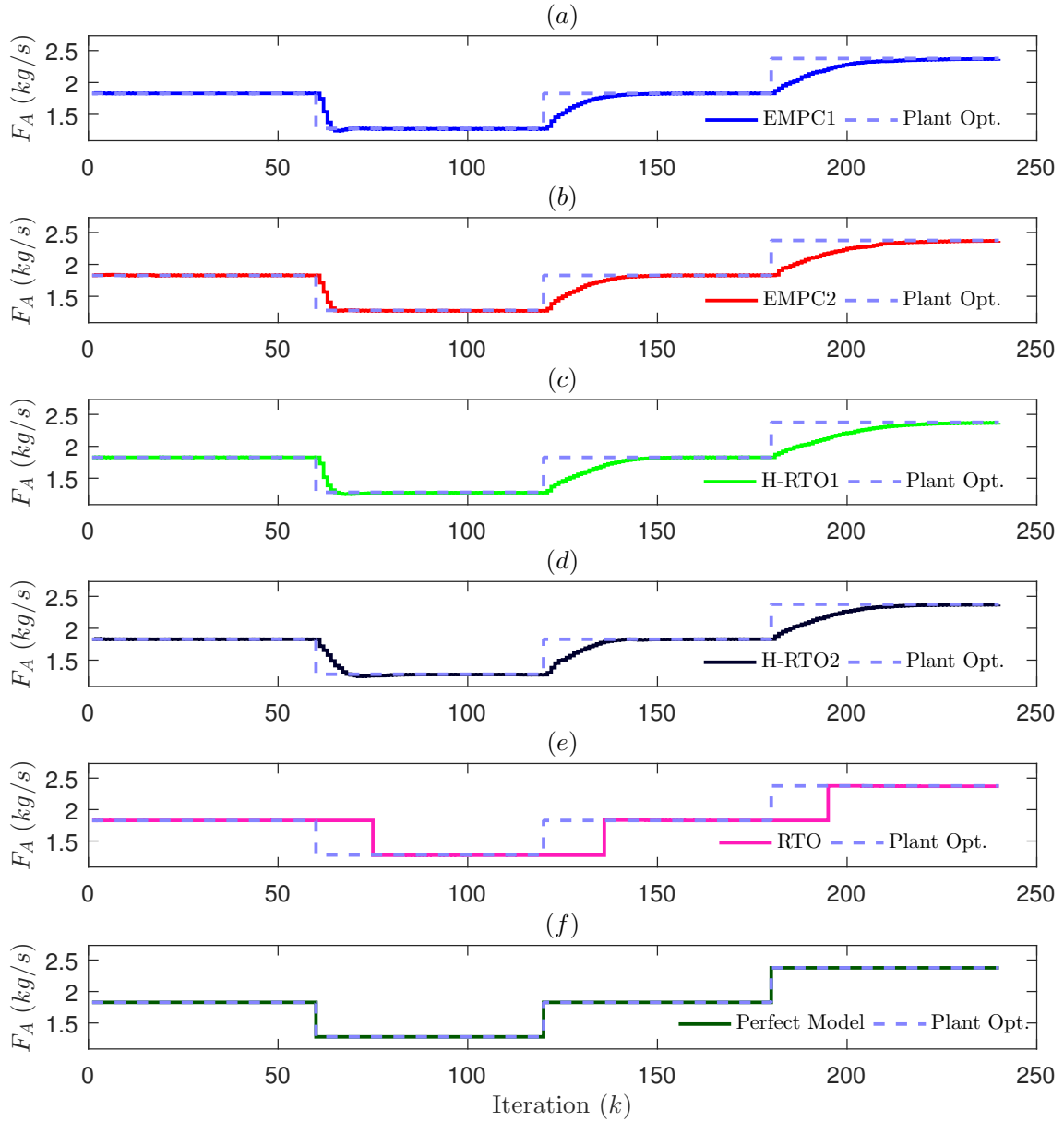


Figure 5.29: Closed-loop dynamic trajectories of disturbance estimation.

verged to the plant value. It is possible to notice that EMPC1 presented a faster convergence than the other strategies. Additionally, although the RTO strategy updates the disturbance later due to the necessity of steady-state detection, the steady-state estimation also led the estimated disturbance to the plant value.

As proposed by DELOU *et al.* (2021), in order to compare the economic performance of each strategy, the Accumulated Loss Function is calculated, defined as follows:

$$AccLoss_k = \sum_{l=0}^k \left( \left| \phi_{ec}(\mathbf{y}_l, \mathbf{u}_l, \hat{\mathbf{d}}_{l-1}^+) - \phi_{ec,l}^* \right| \right) \Delta t \quad (5.59)$$

where  $\phi_{ec}^*$  represents the plant optimum at instant  $l$  and  $\Delta t$  is the sampling time.

The accumulated Loss Function can be interpreted as a discrete version of the difference between the integral of the economic objective function and the integral of the plant optimum value. In practice, it means the loss of the RTO strategy along the horizon when compared to the plant true optimum.

Figure 5.30 presents the optimization problem objective function and the accumulation loss during the simulation. Regarding the economic objective function, except for the RTO strategy, the optimal value was achieved. For the RTO strategy, as the manipulated variables do not match their optimal values, the objective function also does not match. EMPC1 and H-RTO2 are the strategies that faster achieve the optimum value, which is justified by the controlled and manipulated variables profile.

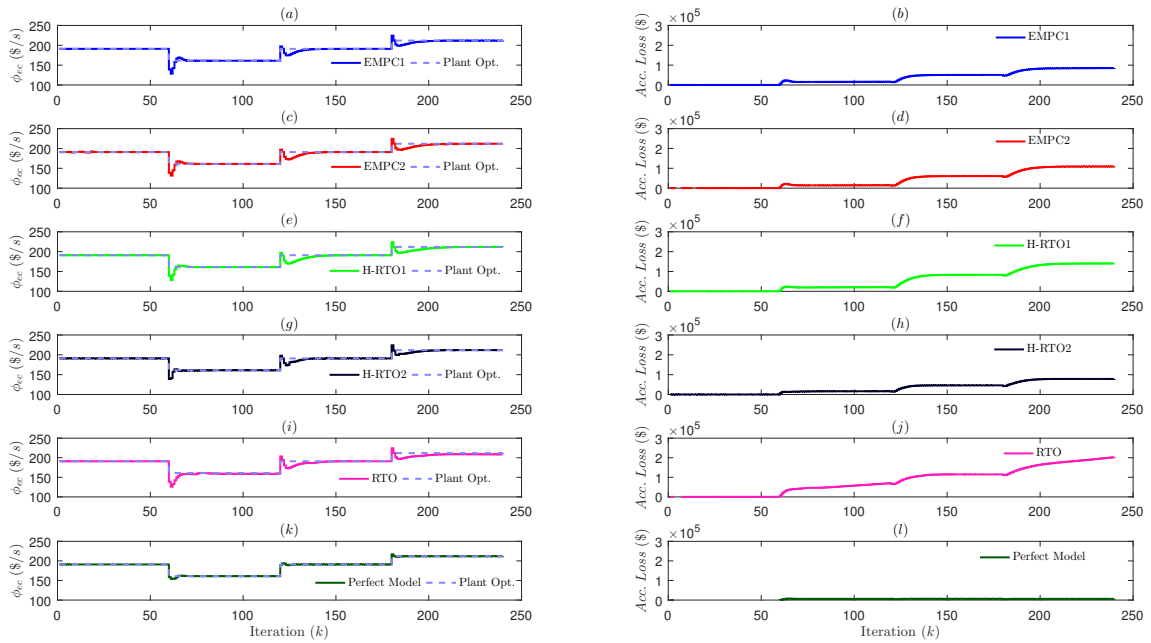


Figure 5.30: Closed-loop dynamic trajectory of economic objective function and the accumulated loss function: (a), (c), (e), (g), (i), (k) Objective function  $\phi_{ecc}$  and (b), (d), (f), (h), (j), (l) Accumulated Loss Function (\$).

Regarding the accumulated loss function in Figure 5.30, as expected, the RTO strategy is the one with higher loss, since the manipulated variables do not match their optimal values. H-RTO1 presented better performance than RTO but worse than H-RTO2, EMPC1 and EMPC2 strategies. Between EMPC1 and EMPC2, the first one presented lower loss. EMPC1 presented a performance comparable to H-RTO2. It is worthwhile to mention that the two proposed strategies (EMPC1 and H-RTO2) performed better than the others. The accumulated loss function values at the end of the simulation horizon is presented in Table 5.5.

Table 5.6 presents the computational cost of each proposed strategy based on its average iteration time in s. For its evaluation, the algorithms ran in an Intel Core® i7-9750H @2.60Hz with 32GB DDR4 RAM memory.

Table 5.5: Accumulated loss function at the end of simulation.

Strategy	Accumulated Loss Function (\$)
EMPC1	$8.52 \times 10^4$
EMPC2	$10.92 \times 10^4$
H-RTO1	$14.04 \times 10^4$
H-RTO2	$7.84 \times 10^4$
RTO	$20.32 \times 10^4$
Perfect Model	$0.6245 \times 10^4$

Table 5.6: Computational cost of each RTO strategy.

Step/ Strategy	Average iteration time (s)					
	EMPC1	EMPC2	HRTO1	HRTO2	RTO	Perfect Model
Optimization	-	-	4.06E-01	3.69E-01	3.63E-01	6.79E-01
EKF	5.20E-04	3.90E-04	8.40E-04	3.20E-04	-	-
Controller	4.03E-01	3.77E-01	4.62E-01	9.23E-02	5.71E-02	7.13E+01
Plant Integration	1.17E-02	1.46E-02	1.49E-02	1.37E-02	1.21E-02	1.03E-02
Total time (s)	4.15E-01	3.92E-01	8.84E-01	4.76E-01	4.33E-01	7.20E+01
Ratio in relation to perfect model (%)	5.76E-01	5.45E-01	1.23E+00	6.61E-01	6.01E-01	1.00E+02

From Table 5.6, it is possible to notice that the strategies that apply the GP model in the optimization step (H-RTO1, H-RTO2 and RTO) are almost two times faster than the strategy where the perfect model is used. Here, it is important to mention that in RTO strategy, the time consumed by the optimization step includes the steady-state disturbance estimation. The total average iteration time in EMPC1 and EMPC2 strategies is lower than in H-RTO1, H-RTO2 and RTO strategies. It is mainly related to the fact that the economic optimization problem is not solved in EMPC1 and EMPC2 strategies, since there is not a steady-state optimization layer in these frameworks. Additionally, the strategies based on the Hammerstein model demand on average 0.7% of the perfect model case total time. This last evidence shows the advantage of using identified nonlinear models for EMPC and H-RTO strategies, enabling its utilization in real-time applications.

As mentioned before, a key benefit of the proposed strategy is not being dependent on first-principles models. The data-driven modeling approach based on a Hammerstein model allows compatibility between optimization and control layers, even if considering a two-layer approach such as H-RTO. In future research, the developed strategy could be combined with a modifier adaptation strategy, using a GP to represent the plant-model mismatch without loss of generality. Moreover, in this work, the model predicted variables are also the plant output variables ( $\mathbf{y}$ ), being useful for control purposes. Then, a Modifier-Adaptation could be developed by considering adaptation terms in the output

variables. Moreover, GP models have an interesting feature which is an estimate of uncertainty. Thus, additional constraints could be added to the optimization and control layers regarding model accuracy, which can be helpful when the plant is operating at a point that is outside the training data.

#### 5.5.4 Comparison of the Proposed Strategies in the Presence of Noise

The results presented in Section 5.5.3 were achieved without considering measurement noise. In the present section, the proposed strategies, namely, EMPC1, EMPC2, H-RTO1, and H-RTO2, are compared to verify their robustness to noise. Here, it is important to highlight that the RTO strategy is not considered in the comparison since it was shown that EMPC and H-RTO strategies presented a better economic benefit.

In the presence of noise, EKF plays a fundamental role in filtering the measurements and disturbance estimation. Thus, the EKF tuning was considered as  $\mathbf{P}_0^+ = \text{diag}(100, 100, 100)$ ,  $\mathbf{Q} = \text{diag}(10^{-3}, 10^{-3}, 10^{-1})$  and  $\mathbf{R} = \text{diag}(10^{-4}, 10^{-4})$ . The tuning parameters for the controller and EKF were obtained by trial and error.

The measurement noise was considered as a zero-mean normal distributed noise, which was artificially added to the measurements in the following manner:

$$\mathbf{y}_p^{noise} = [\mathbf{I}_{n_y} + \text{diag}(\boldsymbol{w}_y^{noise})]\mathbf{y}_p \quad (5.60)$$

where  $\mathbf{y}_p^{noise} \in \mathbb{R}^{n_y}$  is the plant output variable measurement with noise,  $\boldsymbol{w}_y \in \mathbb{R}^{n_y}$ , such that  $\boldsymbol{w}_y^{noise} \sim \mathcal{N}(\mathbf{0}, \boldsymbol{\Sigma}_y^{noise})$ , and  $\boldsymbol{\Sigma}_y^{noise}$  is the measurement noise covariance matrix. The covariance matrix is calculated as  $\boldsymbol{\Sigma}_y^{noise} = n_{noise}\mathbf{I}_{n_y}$ , considering that  $n_{noise}$  is the noise amplitude.

Two noise amplitudes were compared:  $n_{noise} = 0.01$  (0.1%) and  $n_{noise} = 0.05$  (5%). Figures 5.31, 5.32, and 5.33 present the results of the output variables, manipulated variables, and estimated disturbance, respectively, considering 1% noise amplitude.

In Figure 5.37, the noisy measurements of  $w_E$  and  $w_P$  were filtered and smoothed by EKF, which was achieved by the tuning considered in the scenario of measurements. It is possible to notice that the filtered quantities smooth the results such that overshoots are not captured. The main risk is constraint violation since the controller considers the filtered quantities in the strategy. Here, the optimization and control problems did not consider constraints in output variables.

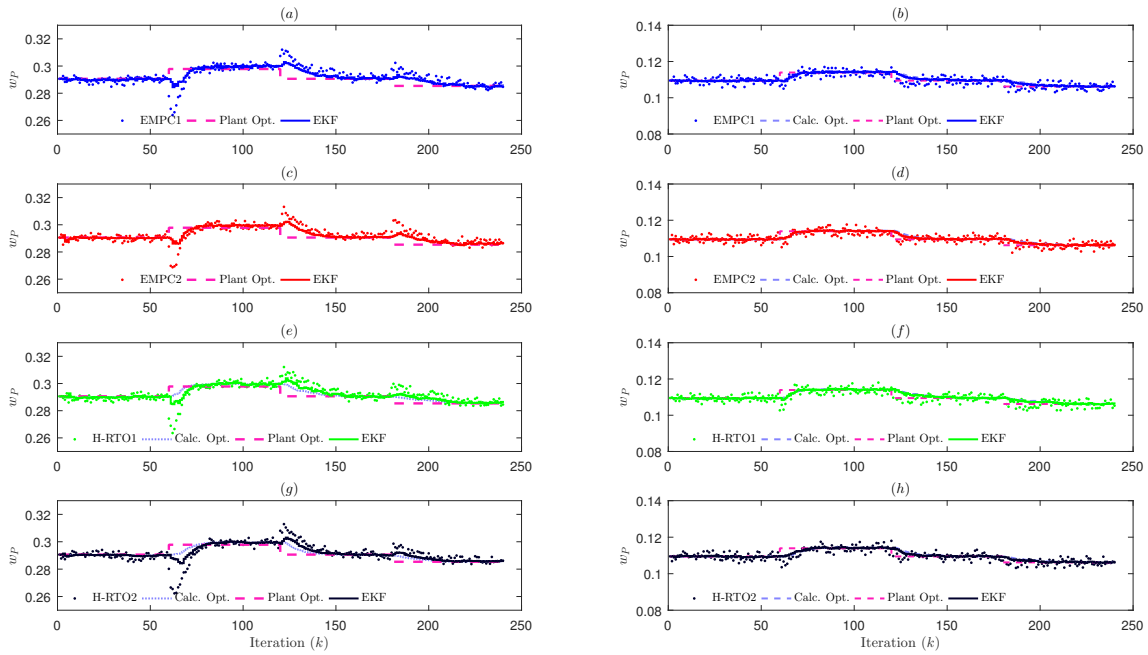


Figure 5.31: Closed-loop dynamic trajectory of economic output variables in the presence of 1% measurement noise: (a), (c), (e), (g)  $w_E$  and (b), (d), (f), (h)  $w_P$ . Dots represent the measurements with noise, solid lines represent the estimated output variables by EKF, dotted lines represent the calculated optimal setpoints of output variables and dashed lines represent the plant optimum value.

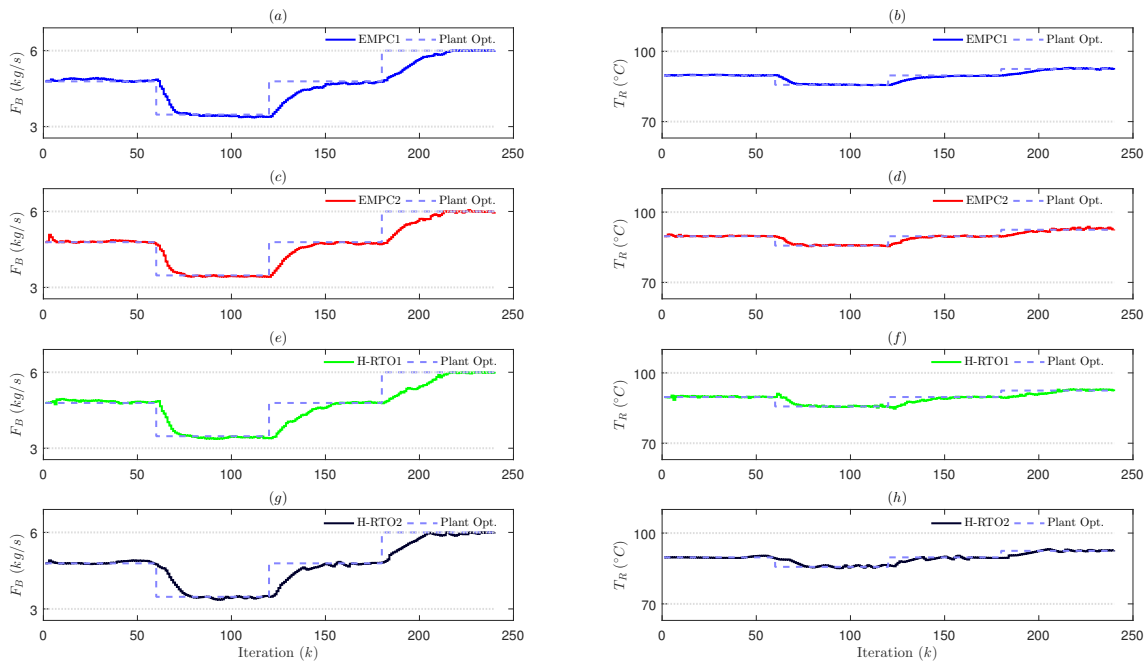


Figure 5.32: Closed-loop dynamic trajectories of manipulated variables in the presence of 1% measurement noise: (a), (c), (e), (g)  $F_B$  and (b), (d), (f), (h)  $T_R$ . Solid lines represent the optimal output variables determined by the RTO strategies and dashed lines represent the plant optimum value.

Thus, this effect was not seen. It is interesting to notice that, even considering noisy measurements, the strategies led the plant toward the optimum points.

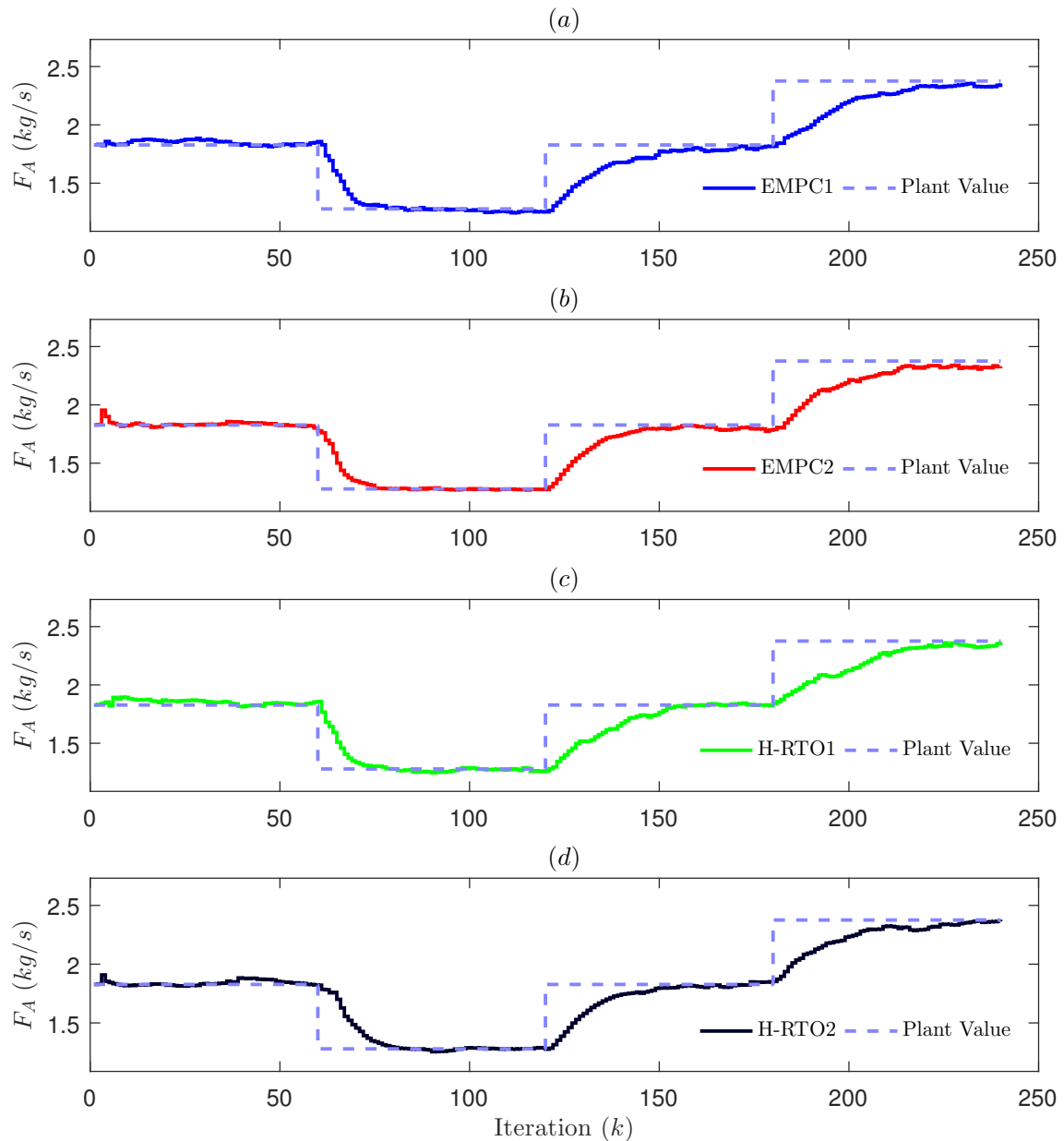


Figure 5.33: Closed-loop dynamic trajectories of disturbance estimation in the presence of 1% measurement noise. Solid lines represent disturbance estimated by EKF and dashed lines represent the disturbance plant value.

In Figure 5.32, it is possible to notice that the noise is propagated to the manipulated variables. However, it can also be noticed that the strategies were able to lead the plant toward its optimum values.

In Figure 5.33, it is possible to notice that the estimated disturbance obtained by EKF converged to the plant value. When comparing the results obtained in the noisy measurements scenario to the scenario of measurements without noise (Figure 5.29), it is noticed a slower convergence of the disturbance parameter, which is also related to the noise filtering ability observed in the output variables (Figure 5.31).

Figures 5.34, 5.35, and 5.36 present the results of the output variables, manipulated variables, and estimated disturbance, respectively, considering 5% noise amplitude.

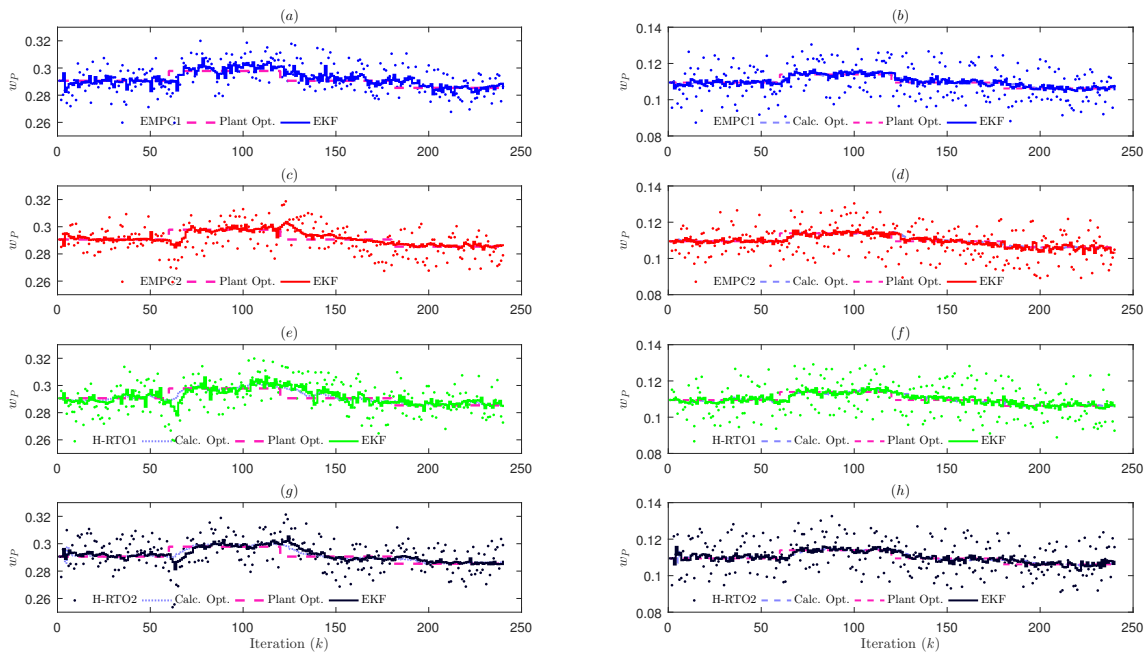


Figure 5.34: Closed-loop dynamic trajectory of output variables in the presence of 5% measurement noise: (a), (c), (e), (g)  $w_E$  and (b), (d), (f), (h)  $w_P$ . Dots represent the measurements with noise, solid lines represent the estimated output variables by EKF, dotted lines represent the calculated optimal setpoints of output variables and dashed lines represent the plant optimum value.

In Figure 5.34, it is possible to notice that the filter could smooth the noisy measurements. It is also possible to notice that the filtered values present some noise behavior related to the propagation of noise to the manipulated variables. In Figure 5.35, this effect is prominent in  $F_B$ . It is possible to notice that the strategies led the manipulated variables toward the plant's optimum value. However, the manipulated variables presented variability. In Figure 5.36, it is also noticed that the estimated disturbance presents noisy behavior, oscillating around the plant value. It is interesting to notice that in EMPC2 and H-RTO1 strategies (5.36(c) and 5.36(d), respectively), in the iteration interval of  $150 \leq k \leq 180$ , the estimated disturbance presents an integrating behavior, which is interrupted by a new disturbance that occurs at iteration  $k = 180$ . Indeed, this effect is also transferred to the controller, as can be seen by the manipulated variables profile, especially for  $F_B$  (Figures 5.35(c) and 5.35(e)), since a similar behavior is noticed.

Regarding economic information, Figures 5.37 5.38 and presents the economic objective function and the Accumulated Loss Function obtained in each strategy in the presence of 1% and 5% measurement noise amplitude.

From Figure 5.37, it can be noticed that objective function values present an

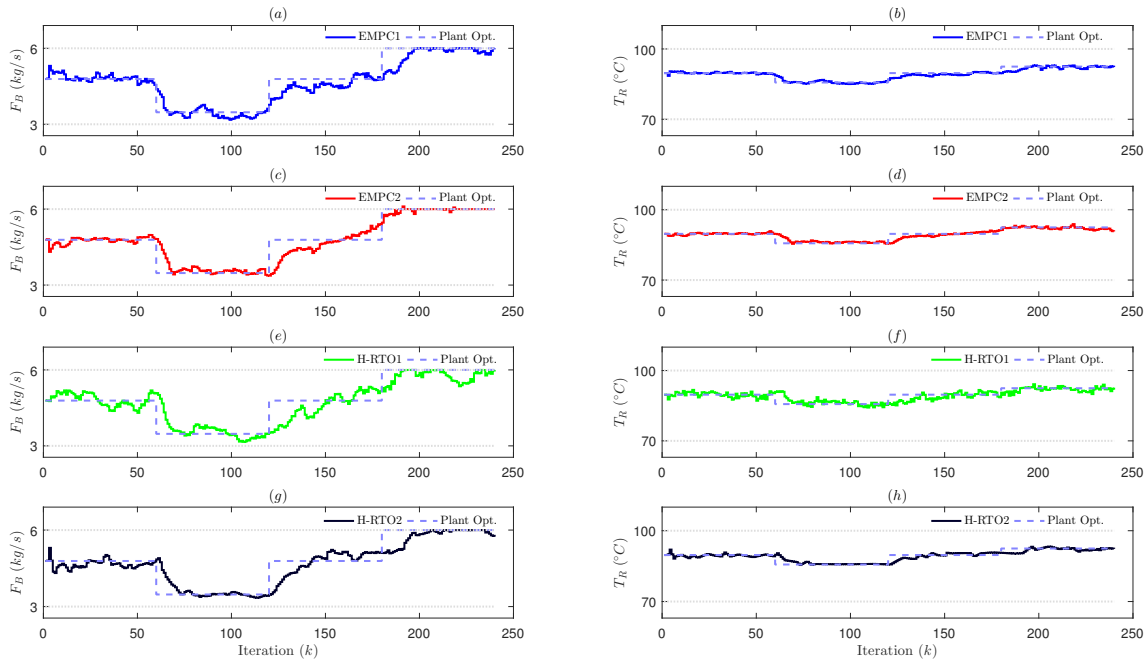


Figure 5.35: Closed-loop dynamic trajectories of manipulated variables in the presence of 5% measurement noise: (a), (c), (e), (g)  $F_B$  and (b), (d), (f), (h)  $T_R$ . Solid lines represent the optimal output variables determined by the RTO strategies and dashed lines represent the plant optimum value.

amplitude higher than 1%, which is justified by the weights associated with each measured value in the objective function and amplify the noise effect. The solid lines represent the calculated objective function value using the filtered output variables values. This effect is even more prominent in the scenario of 5% presented in Figure 5.38. In this case, it is possible to notice that the measured objective function, due to noisy measurements, presents an amplitude of almost 50%. Here, it is important to highlight that strategies that consider the objective function as a controlled variable directly, necessary need a data pretreatment step since the noise measurements can be amplified when dealing with the objective function information itself. The accumulated loss is also calculated considering the objective function filtered values. It can also be noticed that the proposed strategies led the plant toward the optimum value, such that the objective function obtained with noisy measurements oscillates around the plant's optimum value. As expected, the accumulated loss function increases when the disturbances occur since there is a gap between the plant's actual value and the true optimum value. The oscillatory behavior imposed by noisy measurements also contributes to the increase in the accumulated loss function.

Table 5.7 presents the accumulated loss function values at the end of the simulation horizon considering noise amplitudes of 1% and 5%, respectively.

From Table 5.7, it is possible to notice that EMPC2 presented the lowest ac-

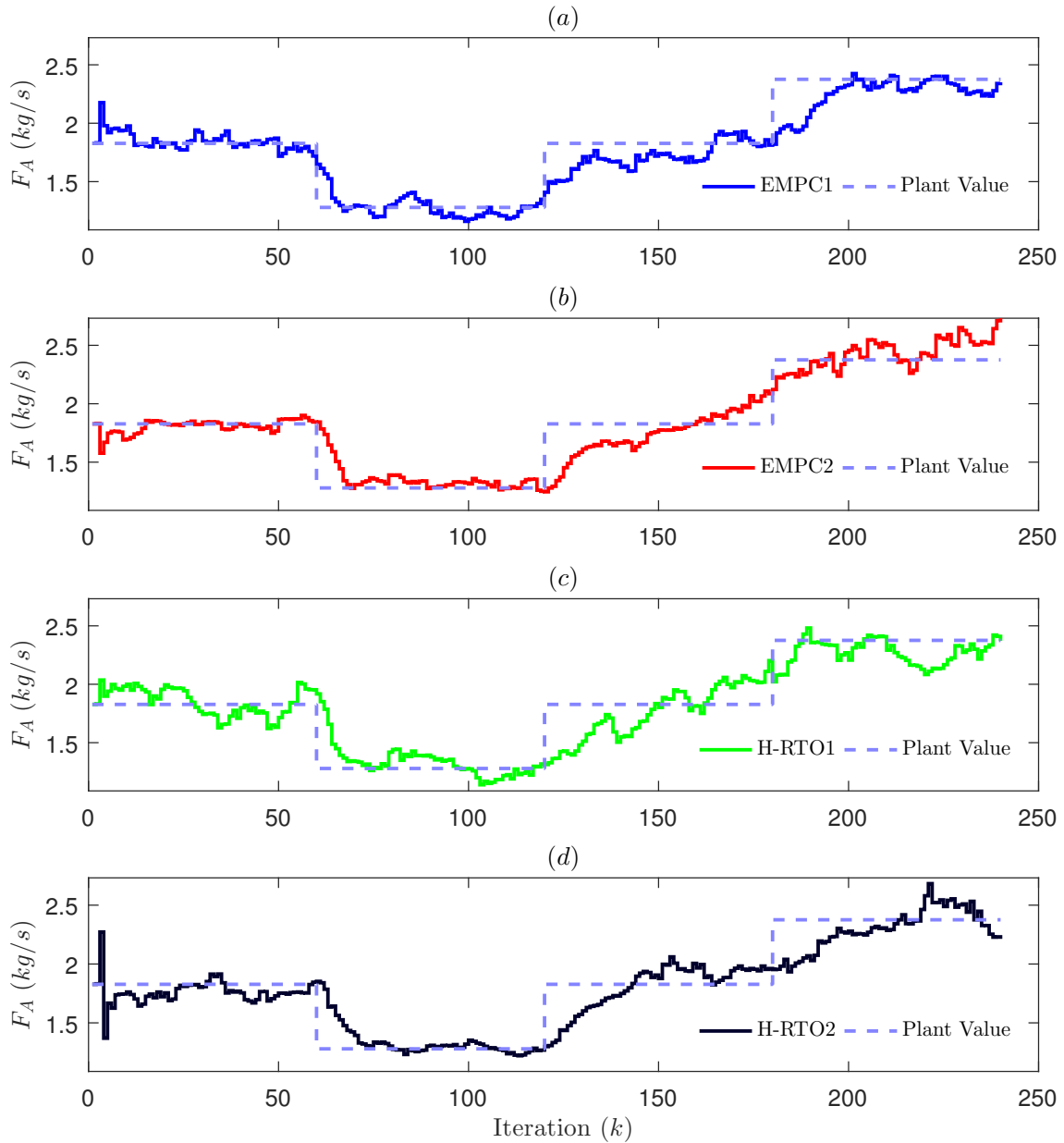


Figure 5.36: Closed-loop dynamic trajectories of disturbance estimation in the presence of 5% measurement noise. Solid lines represent the disturbance estimated by EKF and dashed lines represent the plant value.

cumulated loss function value in the two cases of noise amplitude, followed by H-RTO2. Compared to the scenario of measurements without noise, EMPC1 and H-RTO2 were the strategies that presented the lower accumulated loss function values. In the scenario of noisy measurements, H-RTO2 kept presenting lower values, while EMPC2 outperformed EMPC1. Here, it is important to highlight that EMPC1 depends on the gradient of the economic objective function, which is obtained through the dynamic model. However, it also depends on the estimated disturbance  $F_A$ , such that noise may also impact. However, it is important to highlight that a specific tuning could also improve the accumulated loss function

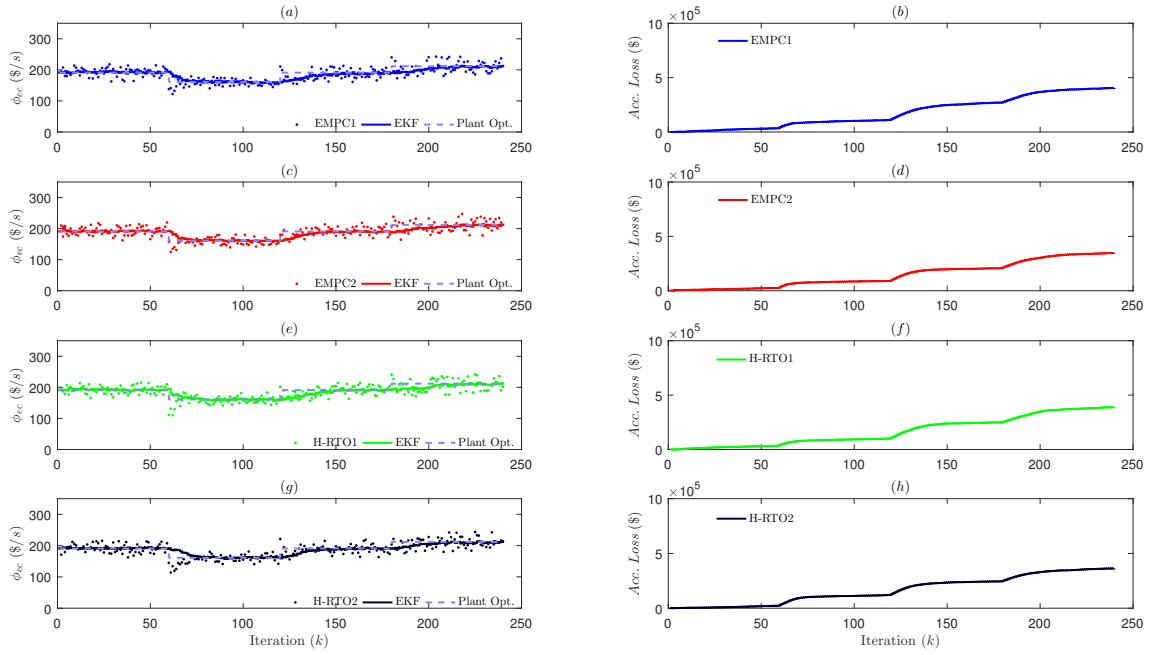


Figure 5.37: Closed-loop dynamic trajectory of economic objective function and the accumulated loss function in the presence of 1% measurement noise: (a), (c), (e), (g) Objective function  $\phi_{eco}$  (\$/s) and (b), (d), (f), (h) Accumulated Loss Function (\$). Dots represent the measured values, solid lines represent the calculated value using estimated quantity by EKF, and dashed lines represents the plant optimum value.

Table 5.7: Accumulated loss function at the end of simulation considering noisy measurements.

Strategy	Accumulated Loss Function (\$)	Accumulated Loss Function (\$)
	filtered values $n_{noise} = 0.01$ (1%)	filtered values $n_{noise} = 0.05$ (5%)
EMPC1	$4.051 \times 10^5$	$6.686 \times 10^5$
EMPC2	$3.465 \times 10^5$	$5.723 \times 10^5$
H-RTO1	$3.892 \times 10^5$	$7.261 \times 10^5$
H-RTO2	$3.627 \times 10^5$	$6.006 \times 10^5$

for each strategy. Here, the tuning was kept the same for the sake of comparison. Indeed, the EKF tuning plays a major role in strategies that uses transient data for state and parameter estimation, as also highlighted by (MATIAS and LE ROUX, 2018), and it is also an important step for the proposed strategies proposed in this chapter.

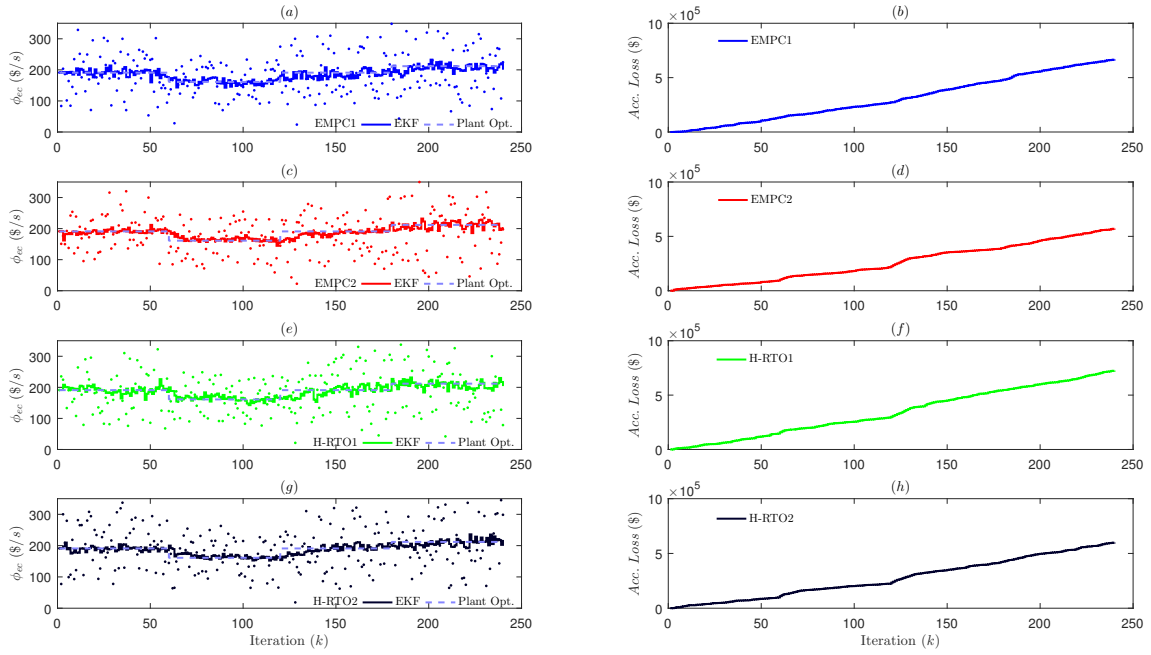


Figure 5.38: Closed-loop dynamic trajectory of economic objective function and the accumulated loss function in the presence of 5% measurement noise: (a), (c), (e), (g) Objective function  $\phi_{eco}$  and (b), (d), (f), (h) Accumulated Loss Function (\$). Dots represent the measured values, solid lines represent the calculated value using estimated quantity by EKF, and dashed lines represents the plant optimum value.

## 5.6 Partial Conclusions

This chapter presented several RTO frameworks based on an EMPC structure which considers a Hammerstein model of the plant. This modeling approach can be applied in the absence of first-principles models. In this strategy, the steady-state nonlinear mapping and the linear dynamic model identification are independent, considering that the steady-state model can be identified based on previous knowledge of the plant behavior. The modeling approach considered the interactions among the state variables and the input directionality, a limitation of some Hammerstein model structures. The proposed strategies were applied to the Willians-Otto Reactor benchmark. In terms of the prediction ability of the models, the proposed modeling approach shows an error ten times lower than the classic Hammerstein structure approach. In terms of the proposed RTO strategy, in the scenario of measurements without noise, the EMPC presented superior results than the recently proposed two-layers and H-RTO approaches in closed-loop. Also, using the economic objective function gradient as NMPC objective function (EMPC1) outperformed the one that considers the economic objective function itself (EMPC2). A modified H-RTO approach (H-RTO2) considering a terminal economic cost in the controller's objective function presented results

comparable to the EMPC1 strategy. Regarding computational cost, the EMPC strategies presented a lower average iteration time than H-RTO and conventional RTO strategies. Finally, the strategies that apply the Hammerstein model in RTO formulation demand only 0.7% of a framework where a first-principle model is considered for optimization and control. The EMPC and H-RTO strategies were also compared in the scenario of noisy measurements with amplitude of 1% and 5%. Considering the presence of noisy measurements, the proposed strategies were able to lead the plant toward the optimum point. It was shown that the EKF was able to filter the noisy measurements. However, some noise was propagated to the manipulated variables due to the noisy estimated disturbance value. Comparing the accumulated loss function values obtained for each strategy, EMPC2 presented the lowest one, followed by H-RTO2. The effect of noisy disturbance estimation may affect the gradient values used in EMPC1, which EMPC2 and H-RTO2 outperformed. Indeed, EKF tuning is an essential for strategies that apply transient data for state and parameter estimation.

# Chapter 6

## Conclusion

A central question regarding RTO strategies is the process model, since the RTO layer is typically based on the resolution of a model-based optimization problem (ELLIS *et al.*, 2014) and, therefore, the convergence to the plant's optimum also depends on it. Some strategies known as Modifier Adaptation approaches were developed in the literature to guarantee the convergence to the optimum, even if the model does not meet the local adequacy criteria proposed by FORBES and MARLIN (1996). Some recent developments in the MA approach are based on Gaussian Process (MA-GP and MAy-GP), which can be interpreted as higher order correction terms to the rigorous model (FERREIRA *et al.*, 2018). Most RTO strategies assume that a reliable process model is at hand, which may not be valid. Thus, strategies for obtaining a process model based on a data-driven approach are also necessary.

In this way, in Chapter 4, the RTO using the MA-GP approach, considered a rigorous model with GP correction terms, was compared to a pure data-driven model using a GP as an estimator. The proposed methodology was applied to the exothermic CSTR reactor and the Williams-Otto reactor benchmark problems. The results obtained in both case studies, considering the proposed methodology and the MA-GP approach, were able to drive the plant to a neighborhood of the optimum point. Regarding the relative average deviation obtained in each strategy, the values obtained showed that the data-driven strategy presented similar performance compared to the plant-model mismatch approach. The main advantage of the proposed strategy is that it can be applied in the absence of any steady-state model of the plant, which enables a data-driven RTO approach. In addition, it was also compared the GP to model the output variables instead of modeling the objective function and constraints, as established in MA-GP. The results also showed similar results using the direct output variables modeling, which is an advantage since the model can be directly applied for control purposes and is not limited to a specific optimization problem.

The results described in Chapter 4 were obtained, disregarding the process dynamics. However, in practical applications, it may need to be considered. Indeed, as the plant model used in RTO is a steady-state model, the delay in the optimization and sampling steps until the plant reaches a new steady state may be an issue. Also, another critical point in the practical implementations of RTO strategies is the integration between the optimization and supervisory control layers, especially regarding the differences between the models used in each layer, resulting in unachievable points arising from the RTO layer for the control layer.

In this sense, this thesis proposes an integrated approach of the optimization and supervisory control layers based on a data-driven modeling strategy, which can be applied in the absence of first-principles models and enables using EMPC and H-RTO approach.

In Chapter 5, a modeling approach based on a Hammerstein model structure was proposed, such that the steady-state plant model was applied as the Hammerstein model nonlinear function. The steady-state model was based on a Gaussian Process, which can be interpreted as a process mapping and identified using selected steady-state data obtained from plant historical data. A significant advantage of the proposed strategy based on the Hammerstein model is that identifying steady-state and dynamic functions can be done independently, as the steady-state and dynamic functions in the Hammerstein structure are in series. Additionally, the modeling approach considered the interactions among the state variables and the input directionality, a limitation of some Hammerstein model structures. This characteristic was achieved by considering parallel Hammerstein structures.

This modeling approach was applied to the Willians-Otto Reactor benchmark. In terms of the prediction ability of the models, the proposed modeling approach shows an error ten times lower than the classic Hammerstein structure approach. Additionally, it was also able to predict complex dynamic behavior, especially for E and P species, which are the most important from the economic perspective.

The proposed modeling approach was also applied in several RTO frameworks based on EMPC and H-RTO structures, which were compared to the classical RTO approach with a steady-state detection step. In terms of economic accumulated loss, the EMPC and H-RTO strategies presented lower losses than the classic RTO with SSD since, in this last approach, the plant operates under a sub-optimal condition until reaching a new steady state. The EMPC presented superior results than the H-RTO approaches in closed-loop. Also, using the economic objective function gradient as NMPC objective function (EMPC1) outperformed the one that considers the economic objective function itself (EMPC2). A modi-

fied H-RTO approach (H-RTO2) considering a terminal economic cost in the controller's objective function presented results comparable to the EMPC1 strategy.

Regarding computational cost, the EMPC strategies presented a lower average iteration time than H-RTO and conventional RTO strategies. As an advantage of using the identified modeling approach, the strategies that apply the Hammerstein model in RTO formulation demand only 0.7% of a framework where a first-principle model is considered for optimization and control.

Regarding the robustness of the proposed strategies to noisy measurements, the EMPC and H-RTO strategies were compared considering noise amplitudes of 1% and 5%. It was shown that the four strategies (EMPC1, EMPC2, H-RTO1, and H-RTO2) were able to lead the plant toward the plant optimum. Comparing the accumulated loss function, EMPC2 outperformed the strategies in the two cases of noise amplitude, followed by H-RTO2. It was also shown that noise is propagated into the controller through the disturbance estimation, which presents noise. Thus, it was also highlighted that EKF tuning plays a significant role in the proposed strategies since it considers the use of transient data.

## 6.1 Future Research

Based on the contributions of this work, the following topics are suggested as future research:

- Apply the proposed RTO framework to other case studies to evaluate the computational cost reduction in large-scale problems.
- Apply the proposed modeling approach based on Hammerstein models in D-RTO problems.
- Combine the MAy-GP strategy and the proposed modeling strategy based on the Hammerstein model to improve the plant-model mismatch correction.
- Evaluate the usage of dynamic GP models based on a data-driven approach, and add a trust-region constraint to the EMPC optimization problem based on the GP uncertainty.

# References

- ABRAHAM, R., MARSDEN, J. E., RATIU, T., 1999, *Model Predictive Control*. New York, Springer.
- ALAMO, T., FERRAMOSCA, A., GONZÁLEZ, A. H., LIMON, D., ODLOAK, D., 2014, "A gradient-based strategy for the one-layer RTO + MPC controller", *Journal of Process Control*, v. 24, n. 4, pp. 435–447.
- ALANQAR, A., ELLIS, M., CHRISTOFIDES, P. D., 2015, "Economic model predictive control of nonlinear process systems using multiple empirical models". In: *2015 American Control Conference (ACC)*, pp. 4953–4958.
- ALMEIDA NETO, E., 2011, *Otimização Dinâmica em Tempo Real: Arquitetura de Software, Diagnóstico e Análise de Inviabilidades*. Tese de D.Sc., Universidade Federal do Rio Grande do Sul, Porto Alegre, RS, Brasil.
- ALSTAD, V., SKOGESTAD, S., 2007, "Null space method for selecting optimal measurement combinations as controlled variables", *Industrial and Engineering Chemistry Research*, v. 46, n. 3, pp. 846–853.
- ALSTAD, V., SKOGESTAD, S., HORI, E. S., 2009, "Optimal measurement combinations as controlled variables", *Journal of Process Control*, v. 19, n. 1, pp. 138–148.
- ALVAREZ, L. A., ODLOAK, D., 2012, "Integration of RTO with MPC through the gradient of a convex function", *IFAC Proceedings Volumes*, v. 45, n. 15, pp. 268 – 273. doi: <<https://doi.org/10.3182/20120710-4-SG-2026.00019>>. Availability: <<http://www.sciencedirect.com/science/article/pii/S1474667016304542>>. 8th IFAC Symposium on Advanced Control of Chemical Processes.
- AMRIT, R., RAWLINGS, J. B., ANGELI, D., 2011, "Economic optimization using model predictive control with a terminal cost", *Annual Reviews in Control*, v. 35, n. 2, pp. 178–186.

- ARKUN, Y., STEPHANOPOULOS, G., 1980, "Studies in the synthesis of control structures for chemical processes: Part IV. Design of steady-state optimizing control structures for chemical process units", *AIChE Journal*, v. 26, n. 6, pp. 975–991.
- BACCI DI CAPACI, R., VACCARI, M., PANNOCCHIA, G., 2018, "Model predictive control design for multivariable processes in the presence of valve stiction", *Journal of Process Control*, v. 71, pp. 25–34. doi: <<https://doi.org/10.1016/j.jprocont.2018.09.006>>. Availability: <<https://www.sciencedirect.com/science/article/pii/S0959152418303093>>.
- BACCI DI CAPACI, R., VACCARI, M., SCALI, C., PANNOCCHIA, G., 2019, "Enhancing MPC formulations by identification and estimation of valve stiction", *Journal of Process Control*, v. 81, pp. 31–39. doi: <<https://doi.org/10.1016/j.jprocont.2019.05.020>>. Availability: <<https://www.sciencedirect.com/science/article/pii/S0959152419300551>>.
- BAILEY, J. K., HRYMAK, A. N., TREIBER, S. S., HAWKINS, R. B., 1993, "Non-linear optimization of a hydrocracker fractionation plant", *Computers and Chemical Engineering*, v. 17, n. 2, pp. 123–138.
- BAKSHI, B. R., STEPHANOPOULOS, G., 1994, "Representation of process trends-IV. Induction of real-time patterns from operating data for diagnosis and supervisory control", *Computers and Chemical Engineering*, v. 18, n. 4, pp. 303–332.
- BAMBERGER, W., ISERMANN, R., 1978, "Adaptive on-line steady-state optimization of slow dynamic processes", *Automatica*, v. 14, n. 3, pp. 223–230.
- BANERJEE, A., ARKUN, Y., OGUNNAIKE, B., PEARSON, R., 1997, "Estimation of Nonlinear Systems Using Linear Multiple", *AIChE Journal*, v. 43, n. 5, pp. 1204–1226.
- BARAMOV, L., HAVLENA, V., 2005, "Enhancing ARX-Model Based MPC by Kalman Filter and Smoother", *IFAC Proceedings Volumes*, v. 38, n. 1, pp. 694 – 699.
- BERNARDO, M. C., BUCK, R., LIU, L., NAZARET, W., SACKS, J., WELCH, W. J., 1992, "Integrated circuit design optimization using a sequential strategy", *IEEE Transactions on Computer-Aided Design*, v. 11, n. 3,

pp. 361–372. Availability: <<http://ieeexplore.ieee.org/lpdocs/epic03/wrapper.htm?arnumber=124423>>.

BIEGLER, L. T., GROSSMANN, I. E., WESTERBERG, A. W., 1985, “A Note on Approximation Techniques Used for Process Optimization”, *Computers & Chemical Engineering*, v. 9, n. 2, pp. 201–206.

BIEGLER, L. T., 2010, *Nonlinear programming*. Mos-Siam Series on Optimization. Philadelphia, SIAM. ISBN: 0898717027; 9780898717020.

BILLINGS, S. A., 1980, “Identification of nonlinear systems—A survey”, *IEE Proceedings D - Control Theory and Applications*, v. 127, n. 6, pp. 272–285.

BINETTE, J.-C., SRINIVASAN, B., 2016, “On the Use of Nonlinear Model Predictive Control without Parameter Adaptation for Batch Processes”, *Processes*, v. 4, n. 3. doi: <10.3390/pr4030027>. Availability: <<https://www.mdpi.com/2227-9717/4/3/27>>.

BONVIN, D., SRINIVASAN, B., 2013, “On the role of the necessary conditions of optimality in structuring dynamic real-time optimization schemes”, *Computers and Chemical Engineering*, v. 51, pp. 172–180.

BRDYŚ, M., CHEN, S., ROBERTS, P. D., 1986, “An extension to the modified two-step algorithm for steady-state system optimization and parameter estimation”, *International Journal of Systems Science*, v. 17, n. 8, pp. 1229–1243.

BRDYŚ, M., TATJEWSKI, P., 1994, “An Algorithm for Steady-State Optimizing Dual Control of Uncertain Plants”, *IFAC Proceedings Volumes*, v. 27, n. 11, pp. 215–220.

BURNHAM, A. J., VIVEROS, R., MACGREGOR, J. F., 1996, “Frameworks for latent variable multivariate regression”, *Journal of Chemometrics*, v. 10, n. 1, pp. 31–45.

CABALLERO, J. A., GROSSMANN, I. E., 2008, “An algorithm for the use of surrogate models in modular flowsheet optimization”, *AIChE Journal*, v. 54, n. 10, pp. 2633–2650. doi: <<https://doi.org/10.1002/aic.11579>>. Availability: <<https://aiche.onlinelibrary.wiley.com/doi/abs/10.1002/aic.11579>>.

CARPIO, R. R., 2019, *Otimização do Processo de Produção de Etanol de Segunda Geração em um Sistema Integrado à Primeira Geração*. Tese de D.Sc., COPPE/UFRJ, Rio de Janeiro, RJ, Brasil.

- CARPIO, R. R., FURLAN, F. F., GIORDANO, R. C., SECCHI, A. R., 2018a, "A Kriging-based approach for conjugating specific dynamic models into whole plant stationary simulations", *Computers & Chemical Engineering*, v. 119, pp. 190 – 194. doi: <<https://doi.org/10.1016/j.compchemeng.2018.09.009>>. Availability: <<http://www.sciencedirect.com/science/article/pii/S0098135418305465>>.
- CARPIO, R. R., GIORDANO, R. C., SECCHI, A. R., 2018b, "Enhanced surrogate assisted framework for constrained global optimization of expensive black-box functions", *Computers & Chemical Engineering*, v. 118, pp. 91–102. doi: <<https://doi.org/10.1016/j.compchemeng.2018.06.027>>. Availability: <<https://www.sciencedirect.com/science/article/pii/S0098135418303181>>.
- CHACHUAT, B., SRINIVASAN, B., BONVIN, D., 2009, "Adaptation strategies for real-time optimization", *Computers and Chemical Engineering*, v. 33, n. 10, pp. 1557–1567.
- CHANDRASEKAR, A., GARG, A., ABDULHUSSAIN, H. A., GRITSICHINE, V., THOMPSON, M. R., MHASKAR, P., 2022, "Design and application of data driven economic model predictive control for a rotational molding process", *Computers and Chemical Engineering*, v. 161, pp. 107713. doi: <<https://doi.org/10.1016/j.compchemeng.2022.107713>>. Availability: <<https://www.sciencedirect.com/science/article/pii/S0098135422000564>>.
- CHANG, J.-S., LIU, W.-L., TANG, J.-K., LIN, W.-C., CHIOU, Y.-J., 2014, "Expected improvement in efficient experimental design supported by a global optimizer", *Journal of the Taiwan Institute of Chemical Engineers*, v. 45, n. 4, pp. 1369–1388. doi: <<https://doi.org/10.1016/j.jtice.2014.02.005>>. Availability: <<https://www.sciencedirect.com/science/article/pii/S1876107014000406>>.
- CHEN, C. Y., JOSEPH, B., 1987, "On-line optimization using a two-phase approach: an application study", *Industrial & Engineering Chemistry Research*, v. 26, n. 9, pp. 1924–1930.
- CHI, G., HU, S., YANG, Y., CHEN, T., 2012, "Response surface methodology with prediction uncertainty: A multi-objective optimisation approach", *Chemical Engineering Research and Design*, v. 90, n. 9, pp. 1235–1244. doi: <<https://doi.org/10.1016/j.cherd.2011>>.

12.012>. Availability: <<https://www.sciencedirect.com/science/article/pii/S0263876211004849>>.

COUCKUYT, I., DHAENE, T., DEMEESTER, P., 2014, “ooDACE Toolbox: A Flexible Object-Oriented Kriging Implementation”, *Journal of Machine Learning Research*, v. 15, n. 91, pp. 3183–3186. Availability: <<http://jmlr.org/papers/v15/couckuyt14a.html>>.

CURVELO, R., DE A. DELOU, P., DE SOUZA, M. B., SECCHI, A. R., 2021, “Investigation of the use of transient process data for steady-state Real-Time Optimization in presence of complex dynamics”. In: Türkay, M., Gani, R. (Eds.), *31st European Symposium on Computer Aided Process Engineering*, v. 50, *Computer Aided Chemical Engineering*, Elsevier, pp. 1299–1305. Availability: <<https://www.sciencedirect.com/science/article/pii/B978032388506550200X>>.

CUTLER, C. R., RAMAKER, B. L., 1980, “Dynamic matrix control - A computer control algorithm”, *Joint Automatic Control Conference*, v. 17, pp. 72. doi: <10.1109/JACC.1980.4232009>.

DARBY, M. L., NIKOLAOU, M., JONES, J., NICHOLSON, D., 2011, “RTO: An overview and assessment of current practice”, *Journal of Process Control*, v. 21, n. 6, pp. 874–884. Availability: <<http://dx.doi.org/10.1016/j.jprocont.2011.03.009>>.

DAVIS, E., IERAPETRITOU, M., 2007, “A kriging method for the solution of nonlinear programs with black-box functions”, *AIChE Journal*, v. 53, n. 8, pp. 2001–2012. doi: <<https://doi.org/10.1002/aic.11228>>. Availability: <<https://aiche.onlinelibrary.wiley.com/doi/abs/10.1002/aic.11228>>.

DAVIS, E., IERAPETRITOU, M., 2010, “A centroid-based sampling strategy for kriging global modeling and optimization”, *AIChE Journal*, v. 56, n. 1, pp. 220–240. doi: <<https://doi.org/10.1002/aic.11881>>. Availability: <<https://aiche.onlinelibrary.wiley.com/doi/abs/10.1002/aic.11881>>.

DE GOUVÊA, M. T., ODLOAK, D., 1996, “Control and Optimization of a Fluid Catalytic Cracking Converter”. In: *Congresso Brasileiro de Automática*, June.

DE GOUVÊA, M. T., ODLOAK, D., 1998, “One-layer real time optimization of LPG production in the FCC unit: procedure, advantages and disad-

vantages”, *Computers & Chemical Engineering*, v. 22, n. 1997, pp. S191–S198.

DE SOUZA, G., ODLOAK, D., ZANIN, A. C., 2010, “Real time optimization (RTO) with model predictive control (MPC)”, *Computers & Chemical Engineering*, v. 34.

DEL RIO CHANONA, E. A., PETSAGKOURAKIS, P., BRADFORD, E., GRACIANO, J. E. A., CHACHUAT, B., 2021, “Real-time optimization meets Bayesian optimization and derivative-free optimization: A tale of modifier adaptation”, *Computers & Chemical Engineering*, v. 147, pp. 107249. doi: <<https://doi.org/10.1016/j.compchemeng.2021.107249>>. Availability: <<https://www.sciencedirect.com/science/article/pii/S0098135421000272>>.

DEL RIO CHANONA, E., GRACIANO, J. A., BRADFORD, E., CHACHUAT, B., 2019, “Modifier-Adaptation Schemes Employing Gaussian Processes and Trust Regions for Real-Time Optimization”, *IFAC-PapersOnLine*, v. 52, n. 1, pp. 52 – 57. doi: <<https://doi.org/10.1016/j.ifacol.2019.06.036>>. Availability: <<http://www.sciencedirect.com/science/article/pii/S2405896319301211>>. 12th IFAC Symposium on Dynamics and Control of Process Systems, including Biosystems DYCOPS 2019.

DELOU, P. A., CURVELO, R., DE SOUZA, M. B., SECCHI, A. R., 2021, “Steady-state real-time optimization using transient measurements in the absence of a dynamic mechanistic model: A framework of HRT0 integrated with Adaptive Self-Optimizing IHMPC”, *Journal of Process Control*, v. 106, pp. 1–19. doi: <<https://doi.org/10.1016/j.jprocont.2021.08.013>>. Availability: <<https://www.sciencedirect.com/science/article/pii/S0959152421001384>>.

DELOU, P. A., CURVELO, R., DEMUNER, R. B., DE SOUZA, M. B., SECCHI, A., 2022, “Real-Time Optimization using Output Modifier Adaptation based on Gaussian Process and its use in a Hammerstein NMPC”. In: *2022 European Control Conference (ECC)*.

DEMUNER, R. B., DE AZEVEDO DELOU, P., SECCHI, A. R., 2022, “Tracking necessary condition of optimality by a data-driven solution combining steady-state and transient data”, *Journal of Process Control*, v. 118, pp. 37–54. doi: <<https://doi.org/10.1016/j.jprocont.2022>>.

08.001>. Availability: <<https://www.sciencedirect.com/science/article/pii/S0959152422001433>>.

EASON, J. P., BIEGLER, L. T., 2016, "A trust region filter method for glass box/black box optimization", *AIChE Journal*, v. 62, n. 9, pp. 3124–3136. doi: <<https://doi.org/10.1002/aic.15325>>. Availability: <<https://aiche.onlinelibrary.wiley.com/doi/abs/10.1002/aic.15325>>.

ECONOMOU, C. G., MORARI, M., PALSSON, B. O., 1986, "Internal Model Control: extension to nonlinear system", *Industrial & Engineering Chemistry Process Design and Development*, v. 25, n. 2, pp. 403–411. doi: <[10.1021/i200033a010](https://doi.org/10.1021/i200033a010)>. Availability: <<https://doi.org/10.1021/i200033a010>>.

ELLIS, M., LIU, J., CHRISTOFIDES, P. D., 2017, *Economic Model Predictive Control: Theory, Formulations and Chemical Process Applications*. Advances in Industrial Control. 1 ed. New York, Springer International Publishing.

ELLIS, M., DURAND, H., CHRISTOFIDES, P. D., 2014, "A tutorial review of economic model predictive control methods", *Journal of Process Control*, v. 24, n. 8, pp. 1156–1178. Availability: <<http://dx.doi.org/10.1016/j.jprocont.2014.03.010>>.

ELLIS, M. J., CHINDE, V., 2020, "An encoder–decoder LSTM-based EMPC framework applied to a building HVAC system", *Chemical Engineering Research and Design*, v. 160, pp. 508–520. doi: <<https://doi.org/10.1016/j.cherd.2020.06.008>>. Availability: <<https://www.sciencedirect.com/science/article/pii/S0263876220302690>>.

EMAMI-NAEINI, A., DOOREN, P. V., 1982, "Computation of zeros of linear multivariable systems", *Automatica*, v. 18. doi: <[10.1016/0005-1098\(82\)90070-x](https://doi.org/10.1016/0005-1098(82)90070-x)>. Availability: <[http://gen.lib.rus.ec/scimag/index.php?s=10.1016/0005-1098\(82\)90070-x](http://gen.lib.rus.ec/scimag/index.php?s=10.1016/0005-1098(82)90070-x)>.

ENGELL, S., 2007, "Feedback control for optimal process operation", *Journal of Process Control*, v. 17, n. 3, pp. 203–219.

ESKINAT, E., JOHNSON, S. H., LUYBEN, W. L., 1991, "Use of Hammerstein models in identification of nonlinear systems", *AIChE Journal*, v. 37, n. 2, pp. 255–268.

FAULWASSER, T., PANNOCCHIA, G., 2019, "Toward a Unifying Framework Blending Real-Time Optimization and Economic Model Predictive

- Control", *Industrial & Engineering Chemistry Research*, v. 58, n. 30, pp. 13583–13598. doi: <10.1021/acs.iecr.9b00782>. Availability: <<https://doi.org/10.1021/acs.iecr.9b00782>>.
- FAULWASSER, T., GRÜNE, L., MÜLLER, M. A., 2018, "Economic Nonlinear Model Predictive Control", *Foundations and Trends in Systems and Control*, v. 5, n. 1, pp. 1–98. doi: <10.1561/26000000014>. Availability: <<http://dx.doi.org/10.1561/26000000014>>.
- FERREIRA, T. D. A., SHUKLA, H. A., FAULWASSER, T., JONES, C. N., BONVIN, D., 2018, "Real-Time optimization of Uncertain Process Systems via Modifier Adaptation and Gaussian Processes". In: *2018 European Control Conference (ECC)*, pp. 465–470.
- FINDEISEN, W., BAILEY, F. N., BRDYS, M., MALINOWSKI, K., TATJEWSKI, P., WOZNIAK, A., 1980, *Control and Coordination in Hierarchical Systems*. 1 ed. New York, John Wiley & Sons.
- FORBES, J. F., MARLIN, T. E., MACGREGOR, J. F., 1994, "Model adequacy requirements for optimizing plant operations", *Computers and Chemical Engineering*, v. 18, n. 6, pp. 497–510.
- FORBES, J. F., MARLIN, T., 1996, "Design cost: a systematic approach to technology selection for model-based real-time optimization systems", *Computers & Chemical Engineering*, v. 20, n. 6-7, pp. 717–734.
- FORBES, J. F., MARLIN, T. E., 1995, "95/02144 Model accuracy for economic optimizing controllers: The bias update case", *Fuel and Energy Abstracts*, v. 36, pp. 145.
- FORBES, M. G., PATWARDHAN, R. S., HAMADAH, H., GOPALUNI, R. B., 2015, "Model Predictive Control in Industry: Challenges and Opportunities", *IFAC-PapersOnLine*, v. 48, n. 8, pp. 531 – 538. 9th IFAC Symposium on Advanced Control of Chemical Processes ADCHEM 2015.
- FORRESTER, A., SOBESTER, A., KEANE, A., 2008, *Engineering Design via Surrogate Modelling: A Practical Guide*. 1 ed. UK, John Wiley & Sons.
- FORRESTER, A. I. J., KEANE, A. J., 2009, "Recent advances in surrogate-based optimization", *Progress in Aerospace Sciences*, v. 45, pp. 50–79.
- FRANCOIS, G., SRINIVASAN, B., BONVIN, D., 2005, "Use of measurements for enforcing the necessary conditions of optimality in the presence

of constraints and uncertainty”, *Journal of Process Control*, v. 15, n. 6, pp. 701–712.

FRANCOIS, G., 2014, *Optimisation en Temps Réel: Optimiser les Performances des Procédés Chimiques malgré l’Incertitude et les Erreurs de Modélisation*. Habilitation à diriger les recherches de l’université de lorraine, Université de Lorraine, Lorraine.

FRANCOIS, G., BONVIN, D., 2013, “Use of Transient Measurements for Real - Time Optimization via Modifier Adaptation”, *Récents Progrès en Génie des Procédés*, pp. 1–8.

FRAZIER, P. I., 2018. “A Tutorial on Bayesian Optimization”. doi: <10.48550/ARXIV.1807.02811>. Availability: <<https://arxiv.org/abs/1807.02811>>.

FÜRST, Y., BRANDT, S., KRIEGEL, M., 2020, “Thermal modelling of three-way mixing valves using Bézier curves for parameter estimation applications”, *Journal of Process Control*, v. 90, pp. 56–62. doi: <<https://doi.org/10.1016/j.jprocont.2020.04.004>>. Availability: <<https://www.sciencedirect.com/science/article/pii/S0959152420302018>>.

FRUZZETTI, K., PALAZOĞLU, A., MCDONALD, K., 1997, “Nolinear model predictive control using Hammerstein models”, *Journal of Process Control*, v. 7, n. 1, pp. 31–41. doi: <[https://doi.org/10.1016/S0959-1524\(97\)80001-B](https://doi.org/10.1016/S0959-1524(97)80001-B)>. Availability: <<https://www.sciencedirect.com/science/article/pii/S095915249780001B>>.

GAO, W., ENGELL, S., 2005, “Iterative set-point optimization of batch chromatography”, *Computers & chemical engineering*, v. 29, n. 6, pp. 1401–1409.

GAO, W., WENZEL, S., ENGELL, S., 2016, “A reliable modifier-adaptation strategy for real-time optimization”, *Computers and Chemical Engineering*, v. 91, pp. 318–328. Availability: <<http://dx.doi.org/10.1016/j.compchemeng.2016.03.019>>.

GARCÍA, C. E., PRETT, D. M., MORARI, M., 1989, “Model predictive control: Theory and practice—A survey”, *Automatica*, v. 25, n. 3, pp. 335–348. doi: <[https://doi.org/10.1016/0005-1098\(89\)90002-2](https://doi.org/10.1016/0005-1098(89)90002-2)>. Availability: <<https://www.sciencedirect.com/science/article/pii/0005109889900022>>.

- GARCIA, C. E., MORARI, M., 1981, "Optimal Operation of Integrated Processing Systems. Part I: Open-loop on-line optimizing control", *AIChE Journal*, v. 27, n. 6, pp. 960–968.
- GARCIA, C. E., MORSHEDI, A. M., 1986, "Quadratic Programming Solution of Dynamic Matrix Control (QDMC)", *Chemical Engineering Communications*, v. 46, n. 1-3, pp. 73–87.
- GELBART, M. A., 2015, *Constrained Bayesian Optimization and Applications*. Tese de D.Sc., Harvard University, Cambridge, Massachusetts.
- GELBART, M. A., SNOEK, J., ADAMS, R. P., 2014. "Bayesian Optimization with Unknown Constraints". doi: <10.48550/ARXIV.1403.5607>. Availability: <<https://arxiv.org/abs/1403.5607>>.
- GIUDICI, R., NASCIMENTO, C., BEILER, I. C., SCHERBAKOFF, I., 1998, "Modeling of industrial nylon-6,6 polycondensation process in a twin-screw extruder reactor. I. phenomenological model and parameter adjusting", *Journal of Applied Polymer Science*, v. 67.
- GIUNTA, A., ELDRED, M., 2000, "Implementation of a trust region model management strategy in the DAKOTA optimization toolkit". In: *8th Symposium on Multidisciplinary Analysis and Optimization*. Availability: <<https://arc.aiaa.org/doi/abs/10.2514/6.2000-4935>>.
- GOMES, M. V. D. C., 2007, *Otimização Sequencial por Aproximações - Uma Aplicação em Tempo Real para o Refino de Petróleo*. Tese de D.Sc., Universidade Federal do Rio de Janeiro, Rio de Janeiro, RJ, Brasil.
- GOMES, M. V., DAVID, I., BOGLE, L., ODLOAK, D., BISCAIA, E. C., 2006, "An application of metamodels for process optimization". In: Marquardt, W., Pantelides, C. (Eds.), *16th European Symposium on Computer Aided Process Engineering and 9th International Symposium on Process Systems Engineering*, v. 21, *Computer Aided Chemical Engineering*, Elsevier, pp. 1449–1454. Availability: <<https://www.sciencedirect.com/science/article/pii/S1570794606802518>>.
- GOMES, M. V., BOGLE, I. D. L., BISCAIA, E. C., ODLOAK, D., 2008, "Using kriging models for real-time process optimisation". In: Braunschweig, B., Joulia, X. (Eds.), *18th European Symposium on Computer Aided Process Engineering*, v. 25, *Computer Aided Chemical Engineering*, Elsevier, pp. 361–366. Availability: <<https://www.sciencedirect.com/science/article/pii/S157079460880065X>>.

- GONZÁLEZ, A. H., ODLOAK, D., 2009, "A stable MPC with zone control", *Journal of Process Control*, v. 19, n. 1, pp. 110–122. doi: <<https://doi.org/10.1016/j.jprocont.2008.01.003>>. Availability: <<https://www.sciencedirect.com/science/article/pii/S0959152408000097>>.
- GRACIANO, J. E. A., JÄSCHKE, J., LE ROUX, G. A., BIEGLER, L. T., 2015, "Integrating self-optimizing control and real-time optimization using zone control MPC", *Journal of Process Control*, v. 34, pp. 35–48. doi: <<https://doi.org/10.1016/j.jprocont.2015.07.003>>. Availability: <<https://www.sciencedirect.com/science/article/pii/S0959152415001523>>.
- GRAMACY, R. B., 2020, *Surrogates: Gaussian Process Modeling, Design and Optimization for the Applied Sciences*. Boca Raton, Florida, Chapman Hall/CRC. <http://bobby.gramacy.com/surrogates/>.
- HAIMES, Y. Y., WISMER, D. A., 1972, "A computational approach to the combined problem of optimization and parameter identification", *Automatica*, v. 8, n. 3, pp. 337–347.
- HARNISCHMACHER, G., MARQUARDT, W., 2007a, "A multi-variate Hammerstein model for processes with input directionality", *Journal of Process Control*, v. 17, n. 6, pp. 539–550.
- HARNISCHMACHER, G., MARQUARDT, W., 2007b, "Nonlinear model predictive control of multivariable processes using block-structured models", *Control Engineering Practice*, v. 15, n. 10, pp. 1238–1256. doi: <<https://doi.org/10.1016/j.conengprac.2006.10.016>>. Availability: <<https://www.sciencedirect.com/science/article/pii/S0967066106002012>>. Special Issue - International Symposium on Advanced Control of Chemical Processes (ADCHEM).
- HAWE, G. I., SYKULSKI, J. K., 2008, "Probability of improvement methods for constrained multi-objective optimization". In: *2008 IET 7th International Conference on Computation in Electromagnetics*, pp. 50–51.
- HEIDERINEJAD, M., LIU, J., CHRISTOFIDES, P., 2012, "Economic Model Predictive Control of Nonlinear Process Systems Using Lyapunov Techniques", *AIChE Journal*, v. 58, n. 3, pp. 855–870.
- HEIRUNG, T. A. N., YDSTIE, B. E., FOSS, B., 2015, "Dual MPC for FIR Systems: Information Anticipation", *IFAC-PapersOnLine*, v. 48, n. 8, pp. 1033 – 1038.

- HELDT, S., 2010, "Dealing with structural constraints in self-optimizing control engineering", *Journal of Process Control*, v. 20, n. 9, pp. 1049–1058.
- HELMDACH, D., YASENEVA, P., HEER, P. K., SCHWEIDTMANN, A. M., LAPKIN, A. A., 2017, "A Multiobjective Optimization Including Results of Life Cycle Assessment in Developing Biorenewables-Based Processes", *ChemSusChem*, v. 10, n. 18, pp. 3632–3643. doi: <<https://doi.org/10.1002/cssc.201700927>>. Availability: <<https://chemistry-europe.onlinelibrary.wiley.com/doi/abs/10.1002/cssc.201700927>>.
- HERNANDEZ, E., ARKUN, Y., 1993, "Control of nonlinear systems using polynomial ARMA models", *AIChE Journal*, v. 39, n. 3, pp. 446–460.
- HERNÁNDEZ, R., ENGELL, S., 2019, "Economics Optimizing Control with Model Mismatch Based on Modifier Adaptation\*\*This work is part of the Collaborative Research Center "Integrated Chemical Processes in Liquid Multiphase Systems" - InPROMPT. Financial support by the Deutsche Forschungsgemeinschaft (DFG) is gratefully acknowledged (TR63)", *IFAC-PapersOnLine*, v. 52, n. 1, pp. 46–51. doi: <<https://doi.org/10.1016/j.ifacol.2019.06.035>>. Availability: <<https://www.sciencedirect.com/science/article/pii/S240589631930120X>>. 12th IFAC Symposium on Dynamics and Control of Process Systems, including Biosystems DYCOPS 2019.
- HOSKINS, J. C., KALIYUR, K. M., HIMMELBLAU, D. M., 1991, "Fault diagnosis in complex chemical plants using artificial neural networks", *AIChE Journal*, v. 37, n. 1, pp. 137–141.
- JACOBS, J., ETMAN, L., VAN KEULEN, F., ROODA, J., 2004, "Framework for sequential approximate optimization", *Structural and Multidisciplinary Optimization*, v. 27, n. 5, pp. 384– 400. doi: <<https://doi.org/10.1007/s00158-004-0398-8>>. Availability: <<http://www.sciencedirect.com/science/article/pii/S2405896319301211>>.
- JAECKLE, C. M., MACGREGOR, J. F., 1998, "Product design through multivariate statistical analysis of process data", *AIChE Journal*, v. 44, n. 5, pp. 1105–1118. Availability: <<http://doi.wiley.com/10.1002/aic.690440509>>.
- JÄSCHKE, J., SKOGESTAD, S., 2011, "NCO tracking and self-optimizing control in the context of real-time optimization", *Journal of Process Control*, v. 21, n. 10, pp. 1407–1416.

- JÄSCHKE, J., CAO, Y., KARIWALA, V., 2017, "Self-optimizing control – A survey", *Annual Reviews in Control*, v. 43, pp. 199–223.
- JOHNSON, M. E., MOORE, L. M., YLVISAKER, D., 1990, "Minimax and maximin distance designs", *Journal of Statistical Planning and Inference*, v. 26, n. 2, pp. 131–148.
- JOHNSTON, L. P. M., KRAMER, M. A., 1995, "Maximum likelihood data rectification: Steady-state systems", *AIChE Journal*, v. 41, n. 11, pp. 2415–2426. doi: <<https://doi.org/10.1002/aic.690411108>>. Availability: <<https://aiche.onlinelibrary.wiley.com/doi/abs/10.1002/aic.690411108>>.
- JONES, D. R., SCHONLAU, M., WELCH, W. J., 1998, "Efficient Global Optimization of Expensive Black-Box Functions", *Journal of Global Optimization*, v. 13, n. 4 (Dec), pp. 455–492. doi: <10.1023/A:1008306431147>. Availability: <<https://doi.org/10.1023/A:1008306431147>>.
- JOSEPH, V. R., GUL, E., BA, S., 2015, "Maximum projection designs for computer experiments", *Biometrika*, v. 102, n. 2, pp. 371–380.
- KARIWALA, V., 2007, "Optimal measurement combination for local self-optimizing control", *Industrial and Engineering Chemistry Research*, v. 46, n. 11, pp. 3629–3634.
- KARIWALA, V., CAO, Y., JANARDHANAN, S., 2008, "Local self-optimizing control with average loss minimization", *Industrial and Engineering Chemistry Research*, v. 47, n. 4, pp. 1150–1158.
- KIM, I.-W., LIEBMAN, M. J., EDGAR, T. F., 1990, "Robust error-in-variables estimation using nonlinear programming techniques", *AIChE Journal*, v. 36, n. 7, pp. 985–993. doi: <<https://doi.org/10.1002/aic.690360703>>. Availability: <<https://aiche.onlinelibrary.wiley.com/doi/abs/10.1002/aic.690360703>>.
- KORDA, M., MEZIĆ, I., 2018, "Linear predictors for nonlinear dynamical systems: Koopman operator meets model predictive control", *Automatica*, v. 93, pp. 149–160. doi: <<https://doi.org/10.1016/j.automatica.2018.03.046>>. Availability: <<https://www.sciencedirect.com/science/article/pii/S000510981830133X>>.
- KORTMANN, M., UNBEHAUEN, H., 1987, "Identification Methods for Nonlinear {MISO} Systems", *Proceedings of the IFAC World Congress*, v. 20, n. 5, pp. 225–230.

- KRISHNAMOORTHY, D., FOSS, B., SKOGESTAD, S., 2018, "Steady-state real-time optimization using transient measurements", *Computers & Chemical Engineering*, v. 115, pp. 34–45. doi: <<https://doi.org/10.1016/j.compchemeng.2018.03.021>>. Availability: <<https://www.sciencedirect.com/science/article/pii/S0098135418302096>>.
- KUSHNER, H. J., 1964, "A New Method of Locating the Maximum Point of an Arbitrary Multipeak Curve in the Presence of Noise", *Journal of Basic Engineering*, v. 86, n. 1 (03), pp. 97–106. doi: <10.1115/1.3653121>. Availability: <<https://doi.org/10.1115/1.3653121>>.
- LAUTENSCHLAGER MORO, L. F., ODLOAK, D., 1995, "Constrained multivariable control of fluid catalytic cracking converters", *Journal of Process Control*, v. 5, n. 1, pp. 29–39. doi: <[https://doi.org/10.1016/0959-1524\(95\)95943-8](https://doi.org/10.1016/0959-1524(95)95943-8)>. Availability: <<https://www.sciencedirect.com/science/article/pii/0959152495959438>>.
- LEE, J. H., 2011, "Model predictive control: Review of the three decades of development", *International Journal of Control, Automation and Systems*, v. 9, n. 3, pp. 415 – 424.
- LEE, W., WEEKMAN, V. W., 1976, "Advanced control practice in the chemical process industry: A view from industry", *AIChE Journal*, v. 22, n. 1, pp. 27–38.
- LIN, J., CHEN, S., ROBERTS, P. D., 1988, "Modified Algorithm for Steady-State Integrated System Optimisation and Parameter Estimation", *IEE Proceedings D: Control Theory and Applications*, v. 135, n. 2, pp. 119–126.
- LIU, Z., YE SU, H., XIE, L., GU, Y., 2012, "Improved LQG benchmark for control performance assessment on ARMAX model process\*", *IFAC Proceedings Volumes*, v. 45, n. 15, pp. 314 – 319.
- LOPHAVEN, S., NIELSEN, H., SONDEGARD, J., 2000, *DACE: a Matlab Kriging Toolbox, Version 2.0*. Manual do software, Technical University of Denmark, Dinamarca.
- LÓPEZ, D. A. N., 2012, *Handling Uncertainties in Process Optimization*. Tese de D.Sc., Universidade de Valladolid, Valladolid, Espanha.
- MACIEJOWSKI, J., 2000, *Predictive Control with Constraints*. New York, Prentice Hall.

- MANSOUR, M., ELLIS, J. E., 2003, "Comparison of methods for estimating real process derivatives in on-line optimization", *Applied Mathematical Modelling*, v. 27, n. 4, pp. 275–291.
- MARCHETTI, A., CHACHUAT, B., BONVIN, D., 2010, "A dual modifier-adaptation approach for real-time optimization", *Journal of Process Control*, v. 20, n. 9, pp. 1027–1037. Availability: <<http://dx.doi.org/10.1016/j.jprocont.2010.06.006>>.
- MARCHETTI, A. G., 2009, *Modifier-Adaptation Methodology for Real-Time Optimization*. PhD Thesis, EPFL, Lausanne, Swiss.
- MARCHETTI, A., CHACHUAT, B., BONVIN, D., 2009, "Modifier-Adaptation Methodology for Real-Time Optimization", *Industrial & Engineering Chemistry Research*, v. 48, n. 13, pp. 6022–6033.
- MARCHETTI, A. G., FRANÇOIS, G., FAULWASSER, T., BONVIN, D., 2016, "Modifier Adaptation for Real-Time Optimization—Methods and Applications", *Processes*, v. 4, n. 4. doi: <10.3390/pr4040055>. Availability: <<https://www.mdpi.com/2227-9717/4/4/55>>.
- MATIAS, J., OLIVEIRA, J. P., LE ROUX, G. A., JÄSCHKE, J., 2022, "Steady-state real-time optimization using transient measurements on an experimental rig", *Journal of Process Control*, v. 115, pp. 181–196. doi: <<https://doi.org/10.1016/j.jprocont.2022.04.015>>. Availability: <<https://www.sciencedirect.com/science/article/pii/S0959152422000713>>.
- MATIAS, J. O., LE ROUX, G. A., 2018, "Real-time Optimization with persistent parameter adaptation using online parameter estimation", *Journal of Process Control*, v. 68, pp. 195 – 204. doi: <<https://doi.org/10.1016/j.jprocont.2018.05.009>>. Availability: <<http://www.sciencedirect.com/science/article/pii/S0959152418301124>>.
- MATIAS, J. O., LE ROUX, G. A., 2020, "Plantwide optimization via real-time optimization with persistent parameter adaptation", *Journal of Process Control*, v. 92, pp. 62–78. doi: <<https://doi.org/10.1016/j.jprocont.2020.05.006>>. Availability: <<https://www.sciencedirect.com/science/article/pii/S0959152420302134>>.
- MAYNE, D. Q., 2014, "Model predictive control: Recent developments and future promise", *Automatica*, v. 50, n. 12, pp. 2967–2986. doi:

<<https://doi.org/10.1016/j.automatica.2014.10.128>>. Availability: <<https://www.sciencedirect.com/science/article/pii/S0005109814005160>>.

MAYNE, D., RAWLINGS, J., RAO, C., SCOKAERT, P., 2000, "Constrained model predictive control: Stability and optimality", *Automatica*, v. 36, n. 6, pp. 789 – 814.

MCBRIDE, K., SUNDMACHER, K., 2019, "Overview of Surrogate Modeling in Chemical Process Engineering", *Chemie Ingenieur Technik*, v. 91, n. 3, pp. 228–239. doi: <<https://doi.org/10.1002/cite.201800091>>. Availability: <<https://onlinelibrary.wiley.com/doi/abs/10.1002/cite.201800091>>.

MCKAY, M. D., BECKMAN, R. J., CONOVER, W. J., 1979, "A Comparison of Three Methods for Selecting Value of Input Variables in the Analysis of Output from a Computer Code", *Technometrics*, v. 21, n. 2, pp. 239–245.

MELO JR, P., PINTO, J., 2008, *Introdução à Modelagem Matemática e Dinâmica Não-Linear de Processos Químicos*. Notas de Aula, Escola Piloto Virtual Giulio Massarani.

MENDOZA, D. F., GRACIANO, J. E. A., DOS SANTOS LIPORACE, F., LE ROUX, G. A. C., 2016, "Assessing the reliability of different real-time optimization methodologies", *The Canadian Journal of Chemical Engineering*, v. 94, n. 3, pp. 485–497. doi: <<https://doi.org/10.1002/cjce.22402>>. Availability: <<https://onlinelibrary.wiley.com/doi/abs/10.1002/cjce.22402>>.

MICHALOPOULOS, J., PAPADOKONSTADAKIS, S., ARAMPATZIS, G., LYGEROS, A., 2001, "Modelling of an industrial fluid catalytic cracking unit using neural networks", *Chemical Engineering Research & Design*, v. 79, n. A2, pp. 137–142.

MIYOSHI, S. C., NUNES, M., SALLES, A., SECCHI, A. R., DE SOUZA, M. B., BRANDÃO, A. L., 2018, "Nonlinear model predictive control application for gas-lift based oil production". In: Friedl, A., Klemeš, J. J., Radl, S., Varbanov, P. S., Wallek, T. (Eds.), *28th European Symposium on Computer Aided Process Engineering*, v. 43, *Computer Aided Chemical Engineering*, Elsevier, pp. 1177–1182. Availability: <<https://www.sciencedirect.com/science/article/pii/B97804444642356502059>>.

- MOČKUS, J., 1975, "On bayesian methods for seeking the extremum". In: Marchuk, G. I. (Ed.), *Optimization Techniques IFIP Technical Conference Novosibirsk, July 1–7, 1974*, pp. 400–404, Berlin, Heidelberg. Springer Berlin Heidelberg. ISBN: 978-3-540-37497-8.
- MORARI, M., H. LEE, J., 1999, "Model predictive control: past, present and future", *Computers & Chemical Engineering*, v. 23, n. 4, pp. 667–682. doi: <[https://doi.org/10.1016/S0098-1354\(98\)00301-9](https://doi.org/10.1016/S0098-1354(98)00301-9)>. Availability: <<https://www.sciencedirect.com/science/article/pii/S0098135498003019>>.
- MORARI, M., ARKUN, Y., STEPHANOPOULOS, G., 1980, "Studies in the synthesis of control structures for chemical processes: Part I: Formulation of the problem. Process decomposition and the classification of the control tasks. Analysis of the optimizing control structures", *AIChE Journal*, v. 26, n. 2, pp. 220–232.
- MORSHEDI, A., CUTLER, C., SKROVANEK, T., 1985, "Optimal Solution of DMC with linear programming techniques", *American Control Conference*, pp. 199–208.
- MUSKE, K. R., RAWLINGS, J. B., 1993, "Model predictive control with linear models", *AIChE Journal*, v. 39, n. 2, pp. 262–287.
- NARASIMHAN, S., JORDACHE, C., 1999, *Data Reconciliation and Gross Error Detection*. 1 ed. Burlington, Gulf Professional Publishing.
- NARASINGAM, A., SON, S. H., KWON, J. S.-I., 2022, "Data-driven feedback stabilisation of nonlinear systems: Koopman-based model predictive control", *International Journal of Control*, v. 0, n. 0, pp. 1–12. doi: <10.1080/00207179.2021.2013541>. Availability: <<https://doi.org/10.1080/00207179.2021.2013541>>.
- NARENDRA, K., GALLMAN, P., 1966, "An Iterative Method for the Identification of Nonlinear Systems Using a Hammerstein Model", *IEEE Transactions on Automatic Control*, v. 11, n. 3, pp. 546–550.
- NASCIMENTO, C. A. O., GIUDICI, R., GUARDANI, R., 2000, "Neuronal Network Approach for Optimization of Industrial Chemical Processes", *Computers & Chemical Engineering*, v. 24, pp. 2303–2314.
- NAYSMITH, M. R., DOUGLAS, P. L., 1995, "Review of Real Time Optimization in the Chemical Process Industries", *Developments in Chemical Engineering and Mineral Processing*, v. 3, n. 2, pp. 67–87.

- NELDER, J., MEAD, R., 1965, "A simplex method for function minimization", *Computer Journal*, v. 7, n. 4, pp. 308–313.
- ODLOAK, D., 2004, "Extended robust model predictive control", *AIChE Journal*, v. 50, n. 8, pp. 1824–1836.
- OLIVEIRA-SILVA, E., DE PRADA, C., NAVIA, D., 2021, "Economic MPC with Modifier Adaptation using Transient Measurements". In: Türkay, M., Gani, R. (Eds.), *31st European Symposium on Computer Aided Process Engineering*, v. 50, *Computer Aided Chemical Engineering*, Elsevier, pp. 1253–1258. Availability: <<https://www.sciencedirect.com/science/article/pii/B9780323885065501935>>.
- PALMER, K., REALFF, M., 2002a, "Optimization and validation of steady-state flowsheet simulation metamodels", *Chemical Engineering Research and Design*, v. 80, n. 7, pp. 773–782.
- PALMER, K., REALFF, M., 2002b, "Metamodeling Approach To Optimization", *Chemical Engineering Research and Design*, v. 80, n. October.
- PANNOCCHIA, G., 2018, "An economic MPC formulation with offset-free asymptotic performance", *IFAC-PapersOnLine*, v. 51, n. 18, pp. 393–398. doi: <<https://doi.org/10.1016/j.ifacol.2018.09.332>>. Availability: <<https://www.sciencedirect.com/science/article/pii/S2405896318320159>>. 10th IFAC Symposium on Advanced Control of Chemical Processes ADCHEM 2018.
- PORFÍRIO, C., ODLOAK, D., 2011, "Optimizing model predictive control of an industrial distillation column", *Control Engineering Practice*, v. 19, n. 10, pp. 1137 – 1146.
- QIN, S. J., BADGWELL, T., 2003, "A survey of industrial model predictive control technology", *Control Engineering Practice*, v. 11, n. 7, pp. 733–764.
- QUACHIO, R., GARCIA, C., 2019, "MPC relevant identification method for Hammerstein and Wiener models", *Journal of Process Control*, v. 80, pp. 78–88. doi: <<https://doi.org/10.1016/j.jprocont.2019.01.011>>. Availability: <<https://www.sciencedirect.com/science/article/pii/S0959152419300496>>.
- QUELHAS, A. D., DE JESUS, N. J. C., PINTO, J. C., 2013, "Common vulnerabilities of RTO implementations in real chemical processes", *The Canadian Journal of Chemical Engineering*, v. 91, n. 4, pp. 652–668. doi:

<<https://doi.org/10.1002/cjce.21738>>. Availability: <<https://onlinelibrary.wiley.com/doi/abs/10.1002/cjce.21738>>.

RASMUSSEN, C. E., 2006, "Gaussian processes for machine learning". MIT Press.

RAWLINGS, J. B., ANGELI, D., BATES, C. N., 2012, "Fundamentals of economic model predictive control". In: *2012 IEEE 51st IEEE Conference on Decision and Control (CDC)*, pp. 3851–3861.

REGIS, R. G., 2016, "Multi-objective constrained black-box optimization using radial basis function surrogates", *Journal of Computational Science*, v. 16, pp. 140–155. doi: <<https://doi.org/10.1016/j.jocs.2016.05.013>>. Availability: <<https://www.sciencedirect.com/science/article/pii/S1877750316300904>>.

RIBEIRO, L., SECCHI, A. R., 2019, "A Methodology to Obtain Analytical Models that Reduce the Computational Complexity Faced in Real Time Implementation of NMPC Controllers", *Brazilian Journal of Chemical Engineering*, v. 36, n. 3, pp. 1255–1277. doi: <[dx.doi.org/10.1590/0104-6632.20190363s20180457](https://doi.org/10.1590/0104-6632.20190363s20180457)>.

RICHALET, J., RAULT, A., TESTUD, J., PAPON, J., 1978, "Model predictive heuristic control: Applications to industrial processes", *Automatica*, v. 14, n. 5, pp. 413 – 428.

ROBERTS, P. D., 1979, "An algorithm for steady-state system optimization and parameter estimation", *International Journal of Systems Science*, v. 10, n. September 2014, pp. 719–734.

RODRÍGUEZ, J., RENAUD, J., WATSON, L., 1998, "Convergence of trust region augmented Lagrangian methods using variable fidelity approximation data", *Structural Optimization*, v. 15, n. 3, pp. 141– 156. doi: <<https://doi.org/10.1007/BF01203525>>.

ROTAVA, O., ZANIN, A., 2005, "Multivariable control and real-time optimization – an industrial practical view", *Hydrocarbon Processing*, v. 84, pp. 61–71.

SACKS, J., SCHILLER, S., WELCH, W., 1989, "Designs for Computer Experiments", *Technometrics*, v. 31, n. 1, pp. 41–47.

- SANTNER, T., WILLIAMS, B., NOTZ, W., 2003, *The Design and Analysis of Computer Experiments*. Springer series in statistics. 1 ed. USA, Springer. ISBN: 9780387954202,0-387-95420-1.
- SANTOS, J. E. W., TRIERWEILER, J. O., FARENZENA, M., 2021, "Model Update Based on Transient Measurements for Model Predictive Control and Hybrid Real-Time Optimization", *Industrial & Engineering Chemistry Research*, v. 60, n. 7, pp. 3056–3065. doi: <10.1021/acs.iecr.1c00212>. Availability: <<https://doi.org/10.1021/acs.iecr.1c00212>>.
- SCHONLAU, M., 2015, *Computer Experiments and Global Optimization*. Tese de D.Sc., Univeristy of Waterloo, Waterloo, Ontario, Canada.
- SCHULTZ, E. S., 2015, *A importância do ponto de operação nas técnicas de Self-Optimizing Control*. Dissertação de mestrado, Universidade Federal do Rio Grande do Sul, Porto Alegre, Rio Grande do Sul, Brasil.
- SHI-SHANG, J., BABU, J., HIRO, M., 1987, "On-line Optimization of Constrained Multivariable Chemical Processes", *AIChE Journal*, v. 33, n. 1, pp. 26 – 35.
- SIMON, D., 2006, *Optimal State Estimation: Kalman, H Infinity, and Nonlinear Approaches*. USA, Wiley-Interscience. ISBN: 0471708585.
- SINGHAL, M., MARCHETTI, A. G., FAULWASSER, T., BONVIN, D., 2016, "Real-Time Optimization Based on Adaptation of Surrogate Models", *IFAC-PapersOnLine*, v. 49, n. 7, pp. 412–417.
- SKOGESTAD, S., 2000a, "Self-Optimizing Control: A Distillation Case Study", *IFAC Proceedings Volumes*, v. 33, n. 10, pp. 977–982.
- SKOGESTAD, S., 2000b, "Plantwide control: The search for the self-optimizing control structure", *Journal of Process Control*, v. 10, n. 5, pp. 487–507.
- SON, S. H., NARASINGAM, A., KWON, J. S.-I., 2020. "Handling plant-model mismatch in Koopman Lyapunov-based model predictive control via offset-free control framework". doi: <10.48550/ARXIV.2010.07239>. Availability: <<https://arxiv.org/abs/2010.07239>>.
- SRINIVASAN, B., BONVIN, D., 2007, "Real-time optimization of batch processes by tracking the necessary conditions of optimality", *Industrial and Engineering Chemistry Research*, v. 46, n. 2, pp. 492–504.

- SRINIVASAN, B., BONVIN, D., VISSER, E., PALANKI, S., 2003a, "Dynamic optimization of batch processes", *Computers & Chemical Engineering*, v. 27, n. 1, pp. 27–44.
- SRINIVASAN, B., BONVIN, D., VISSER, E., PALANKI, S., 2003b, "Dynamic optimization of batch processes", *Computers & Chemical Engineering*, v. 27, n. 1, pp. 27–44.
- SRINIVASAN, B., BIEGLER, L. T., BONVIN, D., 2008, "Tracking the necessary conditions of optimality with changing set of active constraints using a barrier-penalty function", *Computers and Chemical Engineering*, v. 32, n. 3, pp. 572–579.
- SUN, M., CHACHUAT, B., PISTIKOPOULOS, E. N., 2016, "Design of multi-parametric NCO tracking controllers for linear dynamic systems", *Computers and Chemical Engineering*, v. 92, pp. 64–77.
- TATJEWSKI, P., 2007, *Advanced control of industrial processes: structures and algorithms*. London, Springer.
- TATJEWSKI, P., BRDYŚ, M. A., DUDA, J., 2001, "Optimizing control of uncertain plants with constrained feedback controlled outputs", *International Journal of Control*, v. 74, n. 15, pp. 1510–1526.
- TATJEWSKI, P., 2002, "Iterative optimizing set-point control - The basic principle redesigned", *IFAC Proceedings Volumes (IFAC-PapersOnline)*, v. 15, n. 1, pp. 49–54.
- TELLINGHUISEN, J., 2001, "Statistical Error Propagation", *The Journal of Physical Chemistry A*, v. 105, n. 15, pp. 3917–3921. doi: <10.1021/jp003484u>. Availability: <<https://doi.org/10.1021/jp003484u>>.
- TERRY, P. A., HIMMELBLAU, D. M., 1993, "Data Rectification and Gross Error Detection in a Steady-State Process via Artificial Neural Networks", *Industrial and Engineering Chemistry Research*, v. 32, n. 12, pp. 3020–3028.
- THOMPSON, M. L., KRAMER, M. A., 1994, "Modeling chemical processes using prior knowledge and neural networks", *AIChE Journal*, v. 40, n. 8, pp. 1328–1340.
- TÖTTERMAN, S., TOIVONEN, H. T., 2009, "Support vector method for identification of Wiener models", *Journal of Process Control*, v. 19, n. 7, pp. 1174–1181. doi: <<https://doi.org/10.1016/j.jprocont.2009>>.

03.003>. Availability: <<https://www.sciencedirect.com/science/article/pii/S0959152409000407>>.

UENO, T., RHONE, T. D., HOU, Z., MIZOGUCHI, T., TSUDA, K., 2016, "COMBO: An efficient Bayesian optimization library for materials science", *Materials Discovery*, v. 4, pp. 18 – 21. doi: <<https://doi.org/10.1016/j.md.2016.04.001>>. Availability: <<http://www.sciencedirect.com/science/article/pii/S2352924516300035>>.

VACCARI, M., PANNOCCHIA, G., 2017, "A Modifier-Adaptation Strategy towards Offset-Free Economic MPC", *Processes*, v. 5, n. 1. doi: <10.3390/pr5010002>. Availability: <<https://www.mdpi.com/2227-9717/5/1/2>>.

VACCARI, M., PANNOCCHIA, G., 2018, "Implementation of an economic MPC with robustly optimal steady-state behavior", *IFAC-PapersOnLine*, v. 51, n. 20, pp. 92–97. doi: <<https://doi.org/10.1016/j.ifacol.2018.10.180>>. Availability: <<https://www.sciencedirect.com/science/article/pii/S2405896318326521>>. 6th IFAC Conference on Nonlinear Model Predictive Control NMPC 2018.

VACCARI, M., PELAGAGGE, F., BONVIN, D., PANNOCCHIA, G., 2020, "Estimation technique for offset-free economic MPC based on modifier adaptation", *IFAC-PapersOnLine*, v. 53, n. 2, pp. 11251–11256. doi: <<https://doi.org/10.1016/j.ifacol.2020.12.357>>. Availability: <<https://www.sciencedirect.com/science/article/pii/S2405896320306418>>. 21st IFAC World Congress.

VACCARI, M., BONVIN, D., PELAGAGGE, F., PANNOCCHIA, G., 2021, "Offset-Free Economic MPC Based on Modifier Adaptation: Investigation of Several Gradient-Estimation Techniques", *Processes*, v. 9, n. 5. doi: <10.3390/pr9050901>. Availability: <<https://www.mdpi.com/2227-9717/9/5/901>>.

VALKÓ, P., VAJDA, S., 1987, "An extended Marquardt-type procedure for fitting error-in-variables models", *Computers and Chemical Engineering*, v. 11, n. 1, pp. 37–43. doi: <[https://doi.org/10.1016/0098-1354\(87\)80004-2](https://doi.org/10.1016/0098-1354(87)80004-2)>. Availability: <<https://www.sciencedirect.com/science/article/pii/0098135487800042>>.

VALLURU, J., PATWARDHAN, S. C., 2019, "An Integrated Frequent RTO and Adaptive Nonlinear MPC Scheme Based on Simultaneous Bayesian

- State and Parameter Estimation”, *Industrial & Engineering Chemistry Research*, v. 58, n. 18 (May), pp. 7561–7578. doi: <10.1021/acs.iecr.8b05327>. Availability: <<https://doi.org/10.1021/acs.iecr.8b05327>>.
- VALLURU, J., PUROHIT, J. L., PATWARDHAN, S. C., MAHAJANI, S. M., 2015, “Adaptive Optimizing Control of an Ideal Reactive Distillation Column”, *IFAC-PapersOnLine*, v. 48, n. 8, pp. 489–494. doi: <<https://doi.org/10.1016/j.ifacol.2015.09.015>>. Availability: <<https://www.sciencedirect.com/science/article/pii/S2405896315010964>>. 9th IFAC Symposium on Advanced Control of Chemical Processes AD-CHEM 2015.
- WANG, H., VAN STEIN, B., EMMERICH, M., BACK, T., 2017, “A new acquisition function for Bayesian optimization based on the moment-generating function”. In: *2017 IEEE International Conference on Systems, Man, and Cybernetics (SMC)*, pp. 507–512.
- WANG, J.-S., CHEN, Y.-C., 2008, “A Hammerstein-Wiener recurrent neural network with universal approximation capability”. In: *2008 IEEE International Conference on Systems, Man and Cybernetics*, pp. 1832–1837.
- WELCH, W. J., SACKS, J., 1991, “A System for quality improvement via computer experiments”, *Communications in Statistics - Theory and Methods*, v. 20, n. 2, pp. 477–495.
- WENZEL, S., GAO, W., ENGELL, S., 2015, “Handling disturbances in modifier adaptation with quadratic approximation”, *IFAC-PapersOnLine*, v. 28, n. 25, pp. 132–137.
- WIGGINS, S., 2003, “Introduction to Applied Nonlinear Dynamical Systems and Chaos”. In: Mardsen, J. E., Sirovich, L., Antman, S. S. (Eds.), *Introduction to Applied Nonlinear Dynamical Systems and Chaos*, 2 ed., cap. 1, New York, USA, Springer-Verlag New York.
- WILLIAMS, T. J., OTTO, R. E., 1960, “A generalized chemical processing model for the investigation of computer control”, *AIEE Transaction*, v. 79, n. 5, pp. 458–473.
- WILSON, J. T., HUTTER, F., DEISENROTH, M. P., 2018. “Maximizing acquisition functions for Bayesian optimization”. doi: <10.48550/ARXIV.1805.10196>. Availability: <<https://arxiv.org/abs/1805.10196>>.

- WÜRTH, L., HANNEMANN, R., MARQUARDT, W., 2011, "A two-layer architecture for economically optimal process control and operation", *Journal of Process Control*, v. 21, n. 3, pp. 311–321. doi: <<https://doi.org/10.1016/j.jprocont.2010.12.008>>. Availability: <<https://www.sciencedirect.com/science/article/pii/S0959152410002428>>. Thomas McAvoy Festschrift.
- WU, C. F. J., 2017, *Space-Filling Designs*. Notas de aula da disciplina isye 8813 - special topics in data science, Georgia Institute of Technology, Atlanta.
- WU, Z., TRAN, A., RINCON, D., CHRISTOFIDES, P. D., 2019a, "Machine learning-based predictive control of nonlinear processes. Part I: Theory", *AIChE Journal*, v. 65, n. 11, pp. e16729. doi: <<https://doi.org/10.1002/aic.16729>>. Availability: <<https://aiche.onlinelibrary.wiley.com/doi/abs/10.1002/aic.16729>>.
- WU, Z., TRAN, A., RINCON, D., CHRISTOFIDES, P. D., 2019b, "Machine-learning-based predictive control of nonlinear processes. Part II: Computational implementation", *AIChE Journal*, v. 65, n. 11, pp. e16734. doi: <<https://doi.org/10.1002/aic.16734>>. Availability: <<https://aiche.onlinelibrary.wiley.com/doi/abs/10.1002/aic.16734>>.
- XIE, W., BONIS, I., THEODOROPOULOS, C., 2012, "Linear MPC based on data-driven Artificial Neural Networks for large-scale nonlinear distributed parameter systems". In: Bogle, I. D. L., Fairweather, M. (Eds.), *22nd European Symposium on Computer Aided Process Engineering*, v. 30, *Computer Aided Chemical Engineering*, Elsevier, pp. 1212 – 1216.
- YING, C. M., VOORAKARANAM, S., JOSEPH, B., 1998, "Analysis and performance of the LP-MPC and QP-MPC cascade control system", *Proceedings of the American Control Conference*, v. 2, n. 7, pp. 806–810.
- YOUSFI, C., TOURNIER, R., 1991, "Steady State Optimization Inside Model Predictive Control". In: *1991 American Control Conference*, pp. 1866–1870, June.
- YUAN, Z., CHEN, B., SIN, G., GANI, R., 2012, "State-of-the-Art and Progress in the Optimization-based Simultaneous Design and Control for Chemical Process", *Process Systems Engineering*, v. 58, n. 6, pp. 1640–1659.
- ZANIN, A. C., DE GOUVÊA, M. T., ODLOAK, D., 2000, "Industrial implementation of a real-time optimization strategy for maximizing production

of LPG in a FCC unit", *Computers and Chemical Engineering*, v. 24, n. 2-7, pp. 525–531.

ZANIN, A., TVRZSKA DE GOUVEA, M., ODLOAK, D., 2002, "Integrating real-time optimization into the model predictive controller of the FCC system", *Control Engineering Practice*, v. 10, pp. 819–831.

ZHANG, H., ROBERTS, P. D., 1990, "On-line steady-state optimisation of nonlinear constrained process with slow dynamics", *Transactions of The Institute of Measurement and Control*, v. 12, n. 5, pp. 251–261.

ZHANG, H., ROBERTS, P. D., 1991, "Integrated system optimization and parameter estimation using a general form of steady-state model", *Int. J. Systems Sci.*, v. 22, n. 10, pp. 1679–1693.

ZHANG, Y., FORBES, J. F., 2008, "Performance Analysis of Perturbation-Based Methods for Real-Time Optimization", *The Canadian Journal of Chemical Engineering*, v. 84, n. 2, pp. 209–218.

ZHANG, Z., WU, Z., RINCON, D., CHRISTOFIDES, P. D., 2019, "Real-Time Optimization and Control of Nonlinear Processes Using Machine Learning", *Mathematics*, v. 7, n. 10. doi: <10.3390/math7100890>. Availability: <<https://www.mdpi.com/2227-7390/7/10/890>>.

ZHILINSKAS, A. G., 1975, "Single-step Bayesian search method for an extremum of functions of a single variable", *Cybernetics*, v. 11, n. 1 (Jan), pp. 160–166. doi: <10.1007/BF01069961>. Availability: <<https://doi.org/10.1007/BF01069961>>.